

The exploration of CD44 as a mediator of a drug resistant phenotype in ER+ breast cancer

A thesis submitted for the degree of Philosophiae
Doctor in Cardiff University

by

Rebecca Bellerby

March 2015

Cardiff School of Pharmacy and Pharmaceutical Sciences
Cardiff University

Abstract

The majority of breast cancers express the oestrogen receptor and are potentially amenable to endocrine therapy, however the clinical effectiveness of these agents is limited by the phenomenon of acquired resistance which is associated with disease relapse and poor prognosis. It has been previously demonstrated that the CD44 receptor is overexpressed in acquired tamoxifen resistance where it associates with an enhanced migratory phenotype, however little is known regarding the effects of CD44 splice variants in this context. This thesis aimed to explore the role of CD44 variant isoforms in a model of ER+ breast cancer derived tamoxifen-resistance (Tam-R cells) and expand these explorations into an additional model of acquired fulvestrant-resistance (Fas-R cells).

Multiple CD44 isoforms were found to be upregulated in resistance although a differential expression profile was observed between Tam-R and Fas-R cells. Inhibition of global CD44 expression in both endocrine resistant models led to a loss in their migratory, proliferative and invasive capacity and attenuated their responses to the CD44 ligand, hyaluronan. Overexpression of CD44v6 in endocrine sensitive MCF-7 cells induced EGFR pathway activation leading to enhanced cellular invasion, and attenuated response to fulvestrant. Accordingly, CD44v6 suppression in Tam-R cells resulted in a loss of EGFR pathway signalling and reduced invasion. Preliminary clinical analysis revealed that co-expression of CD44v6 and EGFR associated with a trend for worsened outcome in ER+ breast cancer patients treated with tamoxifen.

These data suggest that upregulation of CD44v6 may contribute to an aggressive phenotype in tamoxifen resistant cells through a mechanism involving the EGFR. Future use of CD44v6 and EGFR as biomarkers may have potential therapeutic value to predict a cohort of ER+ breast cancer patients which relapse earlier on tamoxifen and may thus require more aggressive treatment strategies.

Acknowledgements

First and foremost I would like to thank my supervisor Dr Stephen Hiscox for giving me the opportunity to undertake this PhD and for his support, encouragement and guidance. I would also like to thank Dr Julia Gee for her professional guidance and valuable support.

I am extremely grateful to Cardiff University and In The Pink Charity for their generous funding, constant support and kindness. Thank you for providing me with the opportunity to conduct this research.

I would also like to express my deepest gratitude to all research technician staff and students associated with the Breast Cancer Molecular Pharmacology Group for their guidance, support and friendship. A special thanks goes to Christopher Smith, Sue Kyme, Richard McClelland and Lynne Farrow for their professional guidance and lab assistance in this project.

My warmest thanks also goes to other members of the Welsh School of Pharmacy whose friendship, support, advice and technical assistance has immeasurably helped and enriched my PhD experience. A special mention of gratitude goes to Dr Jenny Wymant for her kindness, generosity and encouragement and Sophie Emery for her friendship and support.

Lastly, I would like to offer the biggest thanks to my family without whom it would not have been possible to complete this PhD.

Table of Contents

Abstract.....	i
Acknowledgements.....	ii
Declaration.....	iii
Table of contents.....	iv
List of Tables and Figures.....	ix
List of Publications and Presentations	xvi
Abbreviations.....	xvii
1. Introduction.....	1
1.1 Breast cancer and risk factors.....	1
1.1.1 Oestrogen-independent action of ER	2
1.2. Oestrogen receptors	3
1.2.1 Mechanisms of ER action	6
1.2.1.1 Genomic action of ER.....	6
1.2.1.2 ERE-independent action of ER	7
1.2.1.3 Oestrogen-independent action of ER	8
1.2.1.4 Non-genomic ER action.....	8
1.3 Molecular and clinical subtypes of breast cancer.....	12
1.4. Endocrine therapies	13
1.4.1 SERMs and tamoxifen	14
1.4.2 Aromatase inhibitors.....	16
1.4.3 SERDs and fulvestrant	17
1.5 Therapeutic resistance in ER+ breast cancer	19
1.5.1 ER and resistance	20
1.5.2 Coregulatory protein availability and cell cycle apoptosis regulators	20
1.5.3 Crosstalk with receptor tyrosine kinases and their downstream signalling pathways.....	22
1.6 CD44	25
1.6.1 CD44 gene structure	25
1.6.2 CD44 protein structure	28
1.6.3 Post-translational modifications of the CD44 protein	35
1.6.4 CD44 variant expression and its role in pathology	37
1.6.5 Therapeutic targeting of CD44 in breast cancer.....	40

1.7 Aims and objectives	42
2. Materials and methods	44
2.1 Materials and reagents	44
2.2 Cell culture	48
2.2.1 In vitro cell models of endocrine sensitive and endocrine resistant breast cancer	48
2.2.2 Routine maintenance of in vitro cell models	50
2.2.2.1 Cell passaging.....	50
2.2.2.2 Setting up cells for experimental analysis	51
2.2.3 Cell treatments.....	51
2.3 Microarray analysis.....	52
2.4 Kaplan-Meier plotter analysis.....	54
2.5 Reverse-transcription polymerase chain reaction (RT-PCR).....	55
2.5.1 RNA extraction	55
2.5.2 Reverse transcription.....	56
2.5.3 Oligonucleotide primer design.....	57
2.5.4 RT-PCR analysis	58
2.6 Western blotting analysis	59
2.6.1 Cell lysis.....	59
2.6.2 Bio-Rad Detergent Compatible protein assay.....	60
2.6.3 Preparation of sample for SDS-PAGE.....	61
2.6.4 SDS-PAGE analysis.....	61
2.6.5 Western blot transfer	63
2.6.6 Immunoprobing of Western blots	64
2.6.7 Primary antibody stripping of nitrocellulose membranes.....	65
2.7 Immunocytochemistry	68
2.7.1 Analysis of immunocytochemistry and immunohistochemistry staining using H- scoring.....	69
2.8 Immunofluorescence	69
2.9 Boyden Chamber migration assay	70
2.10 Boyden Chamber invasion assay.....	71
2.11 Coulter Counter proliferation assay.....	73
2.12 Genetic manipulation of CD44 expression	73
2.12.1 siRNA-mediated CD44 suppression	73

2.12.2 CD44 siRNA transfection protocol	75
2.12.3 Transformation of plasmid DNA	76
2.12.3.1 Recovery of plasmid DNA from filter paper.....	77
2.12.3.2 Transformation procedure.....	77
2.12.3.3 Harvesting bacterial cells for collection and purification of plasmid DNA	78
2.12.4 DNA sequencing of plasmid constructs	81
2.12.5 CD44 transient transfection protocol	82
2.13 Statistical analysis	83
3. Characterisation of CD44 isoform expression in endocrine resistant breast cancer cell models versus their endocrine sensitive counterpart	84
3.1 Introduction	84
3.1.1 Objectives.....	86
3.2 Results.....	87
3.2.1 Analysis of hyaladherin family member gene expression in cell models of acquired endocrine resistance compared to their endocrine sensitive counterpart....	87
3.2.2 Validation of microarray data by RT-PCR analysis	93
3.2.3 Protein expression of CD44 and RHAMM in endocrine resistant cells versus their endocrine sensitive counterpart.....	96
3.2.3.1 Western blotting	96
3.2.3.2 Immunostaining analysis.....	99
3.3 Discussion.....	105
3.3.1 Summary	112
4. CD44 overexpression in endocrine resistant breast cancer models augments their aggressive phenotype and sensitivity to HA	114
4.1 Introduction	114
4.1.1 Objectives.....	117
4.2 Results.....	118
4.2.1 Exogenous HA stimulation enhanced the aggressive phenotype of Tam-R and Fas-R cells and modulated receptor tyrosine kinase signalling	118
4.2.2 CD44 suppression reduced endogenous migration, invasion and proliferation..	125
4.2.3 Endogenous HA synthesis and metabolism does not contribute to the aggressive phenotype of Tam-R and Fas-R cells	135
4.3 Discussion.....	139
4.3.1 Summary	145

5. Exploration of RHAMM as a mediator of the aggressive phenotype of endocrine resistant breast cancer cells	146
5.1 Introduction	146
5.1.1 Objectives.....	148
5.2 Results.....	149
5.2.1 RHAMM suppression inhibited the endogenous and HA-stimulated proliferation of Tam-R cells.....	149
5.2.2 RHAMM suppression augments cellular signalling in Tam-R and Fas-R cells	154
5.3 Discussion.....	159
5.3.1 Summary	163
6. CD44 variants differentially modulate the aggressive phenotype of breast cancer cells	164
6.1 Introduction	164
6.1.1 Objectives.....	166
6.2 Results.....	168
6.2.1 Optimisation of CD44v3 and CD44v6 overexpression in MCF-7 cells.....	168
6.2.2 CD44v6, but not CD44v3, overexpression enhanced the invasive capacity of MCF-7 cells and attenuated their sensitivity to fulvestrant.....	178
6.2.3 CD44v6 overexpression in MCF-7 cells enhanced EGFR pathway activity.....	184
6.2.4 CD44v6 overexpression in MCF-7 cells enhanced cellular invasion via EGFR activation and subsequent downstream signalling responses	189
6.2.5 CD44v6 suppression attenuated growth and and invasive capacity of Tam-R cells and enhanced their cellular migration.....	192
6.2.6 CD44 is associated with an increased duration of response to endocrine therapy in ER+ breast cancer.....	203
6.2.6.1 CD44v6 and EGFR co-expression is associated with a worsened outcome in a small exploratory patient series of tamoxifen-treated ER+ breast cancer patients....	205
6.3 Discussion.....	212
6.3.1 Summary	222
7. General Discussion	224
7.1 Future work.....	234
7.2 Conclusions	236
8. References	238
9. Appendices	285
Appendix A. Charcoal stripping procedure for 100 ml FCS.....	285

Appendix B. Jetset gene probes.....	285
Appendix C. CD44 gene sequence	286
Appendix D. HMMR gene sequence	291
Appendix E. Densitometry analysis using ImageJ software.....	294
Appendix F. (3-Aminopropyl)triethoxysilane-coating of coverslips.....	295
Appendix G. Total cell fluorescence analysis using ImageJ software	296
Appendix H. CD44 plasmid construct map	297
Appendix I. CD44 sequencing results.....	298
Appendix J. Optimisation of high and medium molecular weight HA stimulation across MCF-7, Tam-R and Fas-R cells.....	306
Appendix K. Densitometry analysis for CD44 isoform and RHAMM expression in Tam-R and Fas-R cells treated with global CD44 siRNA.....	307
Appendix L. Densitometry analysis for CD44 isoform expression in Tam-R and Fas-R cells treated with global RHAMM siRNA.....	308
Appendix M. Conserved domains in the CD44v3 sequence	309
Appendix N. Construction of alternative transfection controls.....	312
Appendix O. Densitometry analysis for CD44 isoform and RHAMM expression in MCF-7 cells treated with CD44v3 and CD44v3 Δ cyt plasmid DNA	313
Appendix P. Densitometry analysis for CD44 isoform and RHAMM expression in MCF-7 cells treated with CD44v6 and CD44v6 Δ cyt plasmid DNA	314
Appendix Q. Densitometry analysis for CD44 isoform and RHAMM expression in Tam-R and Fas-R cells treated with CD44v6 siRNA.....	315
Appendix R. Immunohistochemical analysis of CD44v6 expression in clinical breast cancer	316
Appendix S. Construction of alternative transfection controls.....	318
Appendix T. The effect of endocrine treatment upon CD44 expression in MCF-7 cells..	329

List of Figures and Tables

Figure 1.1. A schematic diagram of the human ER α and ER β receptors adapted from Kumar et al. 2011	5
Figure 1.2. Mechanisms of ER action, adapted from Cui et al. 2013.....	11
Figure 1.3. Structure of CD44 pre-mRNA transcripts, adapted from Ponta et al. 2003.....	27
Figure 1.4. CD44 protein structure, adapted from Ponta et al. 2003.....	28
Figure 1.5. A proposed model for HA-stimulated CD44-mediated signalling during tumour progression, adapted from Bourguignon et al. 2008.....	34
Table 2.1. A list of the materials and reagents used within this project and their source of purchase.....	48
Table 2.2. Key molecular features and characteristics of the cell models used in this project, adapted from Neve et al. 2006.....	50
Table 2.3. A list of the cell treatments used within this project along with their corresponding source of purchase and diluents used for storage.....	53
Table 2.4. A list of each target gene with their corresponding forward and reverse primer sequences, reaction conditions used for RT-PCR analysis and expected product size.....	58
Table 2.5. Thermocycle programme conditions required for RT-PCR amplification	59
Table 2.6. Bio-Rad Detergent Compatible protein assay.....	60
Table 2.7. The volume of BSA stock (1.45 mg/ml) and lysis buffer solution required for the final BSA concentration to generate a standard curve for a Bio-Rad Detergent Compatible protein assay.....	61
Table 2.8. The volume of substrate required to produce one electrophoresis gel with an 8 % resolving gel and a 4 % stacking gel	63
Figure 2.1. A diagram to show the assembly of a Western blot transfer apparatus. NC-membrane represents the nitrocellulose membrane.....	64
Table 2.9. A list of the primary antibodies used for Western blot analysis in this project with their corresponding dilution, host species, incubation conditions, predicted molecular weight (mw) and source of purchase	67
Table 2.10. A list of the target siRNA and source of purchase for all siRNAs used within this project.....	75
Table 2.11. The volumes required for the transfection of 35 mm dishes at a working solution of 100 nM. All volumes are in μ l.....	76
Table 2.12. A list of the components purchased within the endotoxin-free plasmid maxiprep kit (10) QIAGEN, Manchester, UK) detailing their composition, storage temperature and function.....	81

Table 2.13. A list of each primer sent to the CBS for DNA sequencing analysis of the plasmid constructs with their corresponding sequence and source of purchase.....	82
Table 3.1. A list of probe set ID's for each gene assessed using the GeneSifter programme with their corresponding performance across an array of parameters and detection call....	90
Figure 3.1. A heatmap profile displaying changes in gene expression for all hyaladherins analysed and the log ₂ intensity plots for the Jetset probe of each gene with the average normalised gene expression (+/- SEM) across 3 independent experiments	91
Table 3.2. The fold change values in gene expression of the Jetset probe for each gene analysed by affymetrix.....	92
Figure 3.2. Representative RT-PCR images from 3 independent experiments showing CD44 isoform expression in MCF-7, Tam-R and Fas-R cells with β -actin loading control.....	94
Figure 3.3. Densitometry graph for CD44 isoform expression detected in MCF-7, Tam-R and Fas-R cells by RT-PCR analysis and normalised to β -actin	95
Figure 3.4. Representative Western blot images from 3 independent experiments showing CD44 isoform and RHAMM expression in MCF-7, Tam-R and Fas-R cells with a GAPDH loading control.....	97
Figure 3.5. Densitometry graph showing CD44 isoform and RHAMM expression detected in MCF-7, Tam-R and Fas-R cells by Western blotting analysis and normalised to GAPDH	98
Figure 3.6. Representative images from 3 independent experiments showing CD44 isoform and RHAMM expression by immunocytochemical analysis (x20 magnification)	100
Figure 3.7. Membrane and cytoplasmic H-score assessment of CD44 isoform and RHAMM expression in MCF-7, Tam-R and Fas-R cells by immunocytochemical analysis.....	101
Figure 3.8. Representative images from 3 independent experiments showing CD44 isoform and RHAMM expression by immunofluorescence analysis (x63 magnification).....	103
Figure 3.9. Total cell fluorescence analysis of CD44 and RHAMM expression in MCF-7, Tam-R and Fas-R cells by immunofluorescence analysis	104
Figure 3.10. A diagram to represent the level of CD44 isoform expression and presence of splice variants in endocrine resistant Tam-R and Fas-R cells compared to their endocrine sensitive counterpart MCF-7 cells according to the characterisation results in Chapter 3....	108
Table 3.3. A table to show significant differences observed in CD44 isoform expression between all cell models across several detection techniques.....	111
Figure 4.1. The endogenous migratory, invasive and proliferative responses of MCF-7, Tam-R and Fas-R cells were determined using Boyden Chamber (migration and invasion) and Coulter Counter (proliferation) assays.....	119
Figure 4.2. The migratory, invasive and proliferative responses of MCF-7, Tam-R and Fas-R cells upon HA stimulation (215 kDa, 0 – 400 μ g/ml) were determined using Boyden Chamber (migration and invasion) and Coulter Counter (proliferation) assays	121
Figure 4.3. Representative Western blotting images from 3 independent experiments showing HER2, EGFR and ERK1/2 activation in Tam-R and Fas-R cells in response to dose-	

dependent HA stimulation (215 kDa, 0 – 400 µg/ml) for 10 minutes with β-actin as a loading control.....	123
Figure 4.4. Densitometry graph for HER2, EGFR and ERK1/2 activation across the cell models in response to HA stimulation (215 kDa, 0 – 400 µg/ml) were determined using Boyden Chamber (migration and invasion) and Coulter Counter (proliferation) assays	124
Figure 4.5. Representative Western blotting images and densitometry graphs from 3 independent experiments showing CD44 isoform and RHAMM expression in Tam-R and Fas-R cells after treatment with global CD44 siRNA for 24 – 144 hours post-transfection in comparison to the untreated and NT-siRNA treated control samples.....	126
Figure 4.6. Representative images from 3 independent experiments showing CD44 global expression from immunocytochemistry analysis (x20 magnification) in Tam-R and Fas-R cells after CD44 siRNA treatment for 24 – 144 hours post-transfection in comparison to the untreated and NT-siRNA treated control samples.....	127
Figure 4.7. Measurement of endogenous and HA-stimulated behavioural responses of Tam-R cells after global CD44 suppression	128
Figure 4.8. Measurement of endogenous and HA-stimulated behavioural responses of Fas-R cells after global CD44 suppression	129
Figure 4.9. Representative Western blotting images from 3 independent experiments showing HER2, EGFR, c-Met, FAK, AKT, Src and ERK1/2 activation in Tam-R cells after 48 hour treatment with global CD44 siRNA in the presence (215 kDa, 100 µg/ml HA, 10 minutes) or absence of HA	131
Figure 4.10. Densitometry graphs showing CD44 expression and HER2, EGFR, c-Met, FAK, AKT, Src and ERK1/2 activation in Tam-R cells after 48 hour treatment with global CD44 siRNA in the presence (215 kDa, 100 µg/ml HA, 10 minutes) or absence of HA, before cell lysis and detection by Western blotting analysis.....	132
Figure 4.11. Representative Western blotting images from 3 independent experiments showing HER2, EGFR, c-Met, FAK, AKT, Src and ERK1/2 activation in Fas-R cells after 48 hour treatment with global CD44 siRNA in the presence (215 kDa, 100 µg/ml HA, 10 minutes) or absence of HA	133
Figure 4.12. Densitometry graphs showing CD44 expression and HER2, EGFR, c-Met, FAK, AKT, Src and ERK1/2 activation in Fas-R cells after 48 hour treatment with global CD44 siRNA in the presence (215 kDa, 100 µg/ml HA, 10 minutes) or absence of HA, before cell lysis and detection by Western blotting analysis.....	134
Figure 4.13. Heatmap profile analysis displaying changes in gene expression of all HAS and HYAL genes analysed and their corresponding log ₂ intensity plots with the average normalised gene expression (+/- SEM) across 3 independent experiments	137
Table 4.1. A list of probe set ID's for each gene assessed using the GeneSifter programme, their performance scores across an array of parameters and corresponding detection calls	138

Table 4.2 The fold change values in gene expression of the Jetset probes for each gene analysed by affymetrix.....	138
Figure 5.1. Representative Western blotting images and densitometry graphs from 3 independent experiments showing RHAMM and CD44 isoform expression in Tam-R and Fas-R cells after treatment with global RHAMM siRNA for 24 – 144 hours post-transfection in comparison to the untreated and NT-siRNA treated control samples.....	150
Figure 5.2. Representative images from 3 independent experiments showing global RHAMM expression from immunocytochemistry analysis (x20 magnification) in Tam-R and Fas-R cells after RHAMM siRNA treatment for 24 – 144 hours post-transfection in comparison to the untreated and NT-siRNA treated control samples.....	151
Figure 5.3. Measurement of endogenous and HA-stimulated behavioural responses of Tam-R cells after global RHAMM suppression.....	152
Figure 5.4. Measurement of endogenous and HA-stimulated behavioural responses of Fas-R cells after global RHAMM suppression.....	153
Figure 5.5. Representative Western blotting images from 3 independent experiments showing HER2, EGFR, c-Met, FAK, AKT, Src and ERK1/2 activation in Tam-R cells after 48 hour treatment with global RHAMM siRNA in the presence (215 kDa, 100 µg/ml HA, 10 minutes) or absence of HA.....	155
Figure 5.6. Densitometry graphs showing RHAMM expression and HER2, EGFR, c-Met, FAK, AKT, Src and ERK1/2 activation in Tam-R cells after 48 hour treatment with global RHAMM siRNA in the presence (215 kDa, 100 µg/ml HA, 10 minutes) or absence of HA, before cell lysis and detection by Western blotting analysis.....	156
Figure 5.7. Representative Western blotting images from 3 independent experiments showing HER2, EGFR, c-Met, FAK, AKT, Src and ERK1/2 activation in Fas-R cells after 48 hour treatment with global RHAMM siRNA in the presence (10 minute treatment, 100 µg/ml HA) or absence of HA.....	157
Figure 5.8. Densitometry graphs showing RHAMM expression and HER2, EGFR, c-Met, FAK, AKT, Src and ERK1/2 activation in Fas-R cells after 48 hour treatment with global RHAMM siRNA in the presence (215 kDa, 100 µg/ml HA, 10 minutes) or absence of HA, before cell lysis and detection by Western blotting analysis.....	158
Figure 6.1. Representative Western blotting images from 3 independent experiments showing CD44v3 and CD44v3Δcyt protein expression levels in MCF-7 cells 24 – 144 hours post-transfection compared to the untreated and lipid-only treated control samples.....	171
Figure 6.2. Representative Western blotting images from 3 independent experiments showing CD44v6 and CD44v6Δcyt protein expression levels in MCF-7 cells 24 – 144 hours post-transfection compared to the untreated and lipid-only treated control samples.....	172
Figure 6.3. Representative images from 3 independent experiments showing CD44v3Δcyt, CD44v3, CD44v6Δcyt and CD44v6 expression from immunocytochemical analysis (x20 magnification) in MCF-7 cells 24 – 144 hours post-transfection compared to the untreated and lipid-only treated control samples.....	174

Figure 6.4. Representative images from 3 independent experiments showing CD44v3 and CD44v6 expression from immunocytochemical analysis (x20 magnification) in endogenous MCF-7, Tam-R and Fas-R cells and MCF-7 cells after 72 hour transfection.	175
Figure 6.5. Representative images from 3 independent experiments showing CD44v3Δcyt and CD44v3 expression from immunofluorescence analysis (x63 magnification) in MCF-7 cells 72 hours post-transfection compared to the untreated and lipid-only treated control samples	176
Figure 6.6. Representative images from 3 independent experiments showing CD44v6Δcyt and CD44v6 expression from immunofluorescence analysis (x63 magnification) in MCF-7 cells 72 hours post-transfection compared to the untreated and lipid-only treated control samples.....	178
Figure 6.7. Measurement of endogenous and HA-stimulated cell behavioural responses of MCF-7 cells overexpressing CD44v3 proteins.....	179
Figure 6.8. Measurement of endogenous and HA-stimulated cell behavioural responses of MCF-7 cells overexpressing CD44v6 proteins.....	180
Figure 6.9. Measurement of the growth response of MCF-7 cells overexpressing proteins in the presence of tamoxifen.....	182
Figure 6.10. Measurement of the growth response of MCF-7 cells overexpressing proteins in the presence of fulvestrant.....	183
Figure 6.11. Representative Western blotting images from 3 independent experiments showing HER2, EGFR, c-Met, FAK, Src, AKT and ERK1/2 activation in MCF-7 cells after 48 hour transfection with CD44v3 and CD44v3Δcyt plasmid DNA in the presence (10 minute treatment, 100 µg/ml) or absence of HA.....	185
Figure 6.12. Densitometry graphs showing CD44v3 and CD44v3Δcyt expression and HER2, EGFR, c-Met, FAK, AKT, Src and ERK1/2 activation in MCF-7 cells after 48 hour treatment with CD44v3 and CD44v3Δcyt plasmid DNA in the presence (215 kDa, 100 µg/ml HA, 10 minutes) or absence of HA, before cell lysis and detection by Western blotting analysis.....	186
Figure 6.13. Representative Western blotting images from 3 independent experiments showing HER2, EGFR, c-Met, FAK, Src, AKT and ERK1/2 activation in MCF-7 cells after 48 hour transfection with CD44v6 and CD44v6Δcyt plasmid DNA in the presence (10 minute treatment, 100 µg/ml) or absence of HA.....	187
Figure 6.14. Densitometry graphs showing CD44v6 and CD44v6Δcyt expression and HER2, EGFR, c-Met, FAK, AKT, Src and ERK1/2 activation in MCF-7 cells after 48 hour treatment with CD44v6 and CD44v6Δcyt plasmid DNA in the presence (215 kDa, 100 µg/ml HA, 10 minutes) or absence of HA, before cell lysis and detection by Western blotting analysis.....	188
Figure 6.15. Measurement of endogenous cell invasion in MCF-7 cells overexpressing CD44v6 and CD44v6Δcyt proteins in the presence and absence of gefitinib	190
Figure 6.16. Representative Western blotting images from 3 independent experiments showing EGFR, AKT and ERK1/2 activation in MCF-7 cells after 48 hour transfection with	

CD44v6 and CD44v6 Δ cyt plasmid DNA in the presence (5 minute treatment, 1 μ M) or absence of the EGFR inhibitor, gefitinib	191
Figure 6.17. Representative Western blotting images from 3 independent experiments showing CD44 and RHAMM protein expression in Tam-R and Fas-R cells after treatment with CD44v6 siRNA for 24 – 144 hours in comparison to the untreated and NT-siRNA treated controls	193
Figure 6.18. Representative images from 3 independent experiments from immunocytochemical analysis (x40 magnification) in Tam-R and Fas-R cells after treatment with CD44v6 siRNA for 24 – 144 hours post-transfection in comparison to the untreated and NT-siRNA treated control cells.....	194
Figure 6.19. Measurement of endogenous and HA-stimulated cell behavioural responses of Tam-R cells upon CD44v6 suppression	196
Figure 6.20. Measurement of endogenous and HA-stimulated cell behavioural responses of Fas-R cells upon CD44v6 suppression.....	197
Figure 6.21. Representative Western blotting images from 3 independent experiments showing HER2, EGFR, c-Met, FAK, Src, AKT and ERK1/2 activation in Tam-R cells after 48 hour transfection with NT-siRNA and CD44v6 siRNA in the presence (10 minute treatment, 100 μ g/ml) or absence of HA.....	199
Figure 6.22. Densitometry graphs showing CD44v6 expression and HER2, EGFR, c-Met, FAK, AKT, Src and ERK1/2 activation in Tam-R cells after 48 hour treatment with CD44v6 siRNA in the presence (215 kDa, 100 μ g/ml HA, 10 minutes) or absence of HA, before cell lysis and detection by Western blotting analysis.....	200
Figure 6.23. Representative Western blotting images from 3 independent experiments showing HER2, EGFR, c-Met, FAK, Src, AKT and ERK1/2 activation in Fas-R cells after 48 hour transfection with NT-siRNA and CD44v6 siRNA in the presence (10 minute treatment, 100 μ g/ml) or absence of HA.....	201
Figure 6.24. Densitometry graphs showing CD44v6 expression and HER2, EGFR, c-Met, FAK, AKT, Src and ERK1/2 activation in Fas-R cells after 48 hour treatment with CD44v6 siRNA in the presence (215 kDa, 100 μ g/ml HA, 10 minutes) or absence of HA, before cell lysis and detection by Western blotting analysis	202
Figure 6.25. Kaplan Meier curves generated by KM Plotter to display the association between CD44 mRNA expression and relapse-free survival (RFS) in ER+ breast cancer treated with any endocrine therapy (n = 1190) or confined to tamoxifen treatment (n = 615)	204
Figure 6.26. Representative images from TMA cores with high (left) and low (right) CD44v6 immunostaining from the Nottingham immunohistochemical clinical series (x40 magnification)	207
Table 6.1. The number of patients and associated percentage frequency for the 4 CD44v6 and EGFR tumour phenotypes in 140 ER+ tamoxifen-treated primary breast cancer patients from the TMA series	207

Figure 6.27. Investigation of high versus low CD44v6 membrane staining upon the impact of disease-free interval (DFI) in a small exploratory series of ER+ breast cancer patients treated with tamoxifen (n=140)	208
Figure 6.28. Investigation of high versus low CD44v6 membrane staining upon the impact of overall survival (OS) in a small exploratory series of ER+ breast cancer patients treated with tamoxifen (n = 140).....	209
Figure 6.29. Investigation of CD44v6 and EGFR co-expression upon the impact of disease-free interval (DFI) in a small exploratory series of ER+ breast cancer patients treated with tamoxifen (n = 140).....	210
Figure 6.30. Investigation of CD44v6 and EGFR co-expression upon the impact of overall survival (OS) in a small exploratory series of ER+ breast cancer patients treated with tamoxifen (n = 140).....	211
Figure 6.31. A proposed mechanism for CD44v6-mediated EGFR activation leading to enhanced cellular invasion and growth.....	217
Figure 9.1.The human CD44 mRNA sequence obtained by NCBI	288
Table 9.1. A list of the exon number, corresponding standard/variant exon number and their predicted colour and base pair size (as shown in Figure 9.1) for each exon in the human CD44 mRNA sequence obtained from the NCBI.....	289
Table 9.2. A list of the CD44 primers used in this project with their corresponding forward and reverse sequences and colour in which they are shown in the above human CD44 mRNA sequence (Figure 9.1).....	290
Table 9.3. A list of the target siRNAs and corresponding RNA and DNA sequences for each siRNA used in this project	290
Figure 9.2.The human HMMR (RHAMM) mRNA sequence obtained by NCBI	292
Table 9.4. A list of the exon number and corresponding base pair size for each exon in the human HMMR (RHAMM) gene.....	293
Table 9.5. The HMMR primer used in this project with its corresponding forward and reverse sequence and the colour in which it is highlighted in the above mRNA sequence	293
Figure 9.3. The plasmid construct map for the CD44v3, CD44v3Δcyt, CD44v6 and CD44v6Δcyt constructs obtained from Dr Ursula Gunthert, Basal University, Switzerland	297
Figure 9.4. The DNA sequencing results performed by the CBS and analysed using the software programmes Chromas Lite and Expassy for the CD44v3 plasmid construct	299
Figure 9.5. The DNA sequencing results performed by the CBS and analysed using the software programmes Chromas Lite and Expassy for the CD44v3 Δcyt plasmid construct..	301
Figure 9.6. The DNA sequencing results performed by the CBS and analysed using the software programmes Chromas Lite and Expassy for the CD44v6 plasmid construct	303
Figure 9.7. The DNA sequencing results performed by the CBS and analysed using the software programmes Chromas Lite and Expassy for the CD44v6Δcyt plasmid construct ..	305

Figure 9.8. Representative Western blot images 3 independent experiments showing HER2, EGFR and ERK1/2 activation in MCF-7, Tam-R and Fas-R cells in response to dose-dependent high molecular weight HA stimulation (>500 kDa, 0 – 400 µg/ml) for 10 minutes.....	306
Figure 9.10. Densitometry graphs showing CD44v3, CD44v6, CD44v10 and RHAMM expression in Tam-R and Fas-R cells after 24 – 144 hour treatment with global CD44 siRNA before cell lysis and detection by Western blotting analysis.....	307
Figure 9.11. Densitometry graphs showing CD44 Std, CD44v3, CD44v6 and CD44v10 expression in Tam-R and Fas-R cells after 24 – 144 hour treatment with global RHAMM siRNA before cell lysis and detection by Western blotting analysis.	308
Figure 9.12. Densitometry graphs showing CD44v6, CD44v10 and RHAMM expression in MCF-7 cells after 24 – 144 hour treatment with CD44v3 or CD44v3 Δ cyt plasmid DNA before cell lysis and detection by Western blotting analysis.	313
Figure 9.13. Densitometry graphs showing CD44v6, CD44v10 and RHAMM expression in MCF-7 cells after 24 – 144 hour treatment with CD44v3 or CD44v3 Δ cyt plasmid DNA before cell lysis and detection by Western blotting analysis.	314
Figure 9.14. Densitometry graphs showing CD44v3, CD44v6, CD44v10 and RHAMM expression in Tam-R and Fas-R cells after 24 – 144 hour treatment with CD44v6 siRNA before cell lysis and detection by Western blotting analysis.....	315
Table 9.6. A list of the components purchased with the QIAquick Gel Extraction Kit (QIAGEN, Manchester, UK) detailing their composition, storage temperature and function.....	321
Figure 9.15. The DNA sequencing results as performed by the CBS and analysed using the software programmes Chromas Lite and Expassy for the Empty Vector plasmid construct..	323
Figure 9.16. A map of the p-EGFP-N1 plasmid vector used for transfection of MCF-7 cells.	324
Figure 9.17. Western blotting images showing CD44 isoform expression and RHAMM expression in MCF-7 cells after 24 – 72 hour transfection with the EV or GFP plasmid DNA compared to the untreated and lipid-treated control (n = 1).....	326
Figure 9.18. Immunofluorescence images showing CD44 Std expression in MCF-7 cells after 72 hour transfection with the EV, GFP or CD44v6 plasmid DNA compared to the untreated and lipid-only treated controls (x63 magnification) (n = 1).....	327
Figure 9.19. Western blotting images showing CD44 expression and EGFR and ERK1/2 activation in MCF-7 cells after 72 hour transfection with the EV, GFP or CD44v6 plasmid DNA compared to the untreated or lipid-only treated control cells.....	328
Figure 9.12. Measurement of endogenous and HA-stimulated cellular migration in MCF-7 cells transfected with EV, GFP or CD44v6 plasmid DNA.....	328
Figure 9.21. Effect of short-term endocrine treatment on CD44 expression in MCF-7 cells	330

List of Publications and Presentations

Publications

Bellerby R, Smith C, Farrow L, Kyme S, Gee J, Gunthert U, Ellis I, Barrett-Lee P, Hiscox S. 2015. **Overexpression of specific CD44 isoforms is associated with aggressive cell features in acquired endocrine resistance.** *In process of publication.*

Hiscox S, Baruha B, Smith C, Bellerby R, Goddard L, Jordan N, Poghosyan Z, Nicholson RI, Barrett-Lee P, Gee J. 2012. **Overexpression of CD44 accompanies acquired tamoxifen resistance in MCF-7 cells and augments their sensitivity to the stromal factors, heregulin and hyaluronan.** *BMC Cancer.* 12 (458) pp. 1471 – 2407.

Presentations

R, Bellerby, C, Smith, Susan Kyme, Lynne Farrow, Ursula Gunthert, Julia Gee, Stephen Hiscox.

Overexpression of CD44 specific variants mediates endocrine insensitivity and invasion in breast cancer cells.

American Association for Cancer Research (AACR) Symposium, San Diego, California, April 2014.

Rebecca Bellerby, Chris Smith, Peter Barrett-Lee, Julia Gee, Stephen Hiscox. **Overexpression of CD44 accompanies endocrine resistance and sensitises breast cancer cells to the migratory-promoting action of hyaluronan.**

BACR Special Meeting. Tumour Microenvironment – Basic science to novel therapies. Bristol, United Kingdom, July 2013.

Rebecca Bellerby, Chris Smith, Peter Barrett-Lee, Julia Gee, Stephen Hiscox. **Overexpression of CD44 accompanies endocrine resistance and sensitises breast cancer cells to the migratory-promoting action of hyaluronan**

34th EORTC PAMM Winter Meeting. The British Association of Cancer Research (BACR), Cardiff, United Kingdom, January 2013.

Abbreviations

AF	Activating function
AI	Aromatase Inhibitor
AIB1	Amplified in breast 1
AKT	v-akt murine thymoma viral oncogene homolog
ANOVA	Analysis of variance
AP-1	Activator protein 1
APS	Ammonium persulphate
ATAC	Anastrozole or Tamoxifen Alone in Combination
ATTC	American Type Cell Collections
BCL/XL	B-cell lymphoma/extra large
BLAST	Basic Local Alignment Search Tool
bp	Base pair
BRCA1	Breast cancer type 1 susceptibility protein
BRCA2	Breast cancer type 2 susceptibility protein
BCMPG	Breast Cancer Molecular Pharmacology Group
CAM	Cell adhesion molecules
cAMP	Cyclic adenosine monophosphate
CBS	Central Biotechnology Services
CD24	Cluster of differentiation 24
CD44	Cluster of differentiation 44
c-Met	c-Met proto-oncogene (hepatocyte growth factor receptor)
CSC	Cancer stem cell
DBD	DNA binding domain
DFI	Disease free interval
DNA	Deoxyribonucleic acid
dNTPs	Deoxynucleotide triphosphates
DPX	Mixture of Distyrene, a plasticizer and xylene
DTT	Dithiothreitol
E2	Oestrogen/oestrodial

ECL	Enhanced chemoluminescence
EGFR	Epidermal growth factor receptor
EGF	Epidermal growth factor
EMT	Epithelial-mesenchymal transition
ER	Oestrogen receptor
ERE	Oestrogen response elements
ERK	Extracellular-signal-regulated kinases
ERM	Ezrin, moesin, radixin proteins
EtBr	Ethidium bromide
EU	European Union
Fas-R	Fulvestrant resistant cell line derived from MCF-7 cells
FCS	Foetal calf serum
FDA	Food and Drug Administration
FGF	Fibroblast growth factor receptor
GAG	Glycosaminoglycans
GFP	Green fluorescent protein
GTPases	Guanosine-5'-triphosphate
HA	Hyaluronan/hyaluronic acid
HAS1	Hyaluronan synthase 1
HAS2	Hyaluronan synthase 2
HAS3	Hyaluronan synthase 3
HDAC	Histone deacetylase
HER2	Human epidermal growth factor receptor 2
HER3	Human epidermal growth factor receptor 3
HER4	Human epidermal growth factor receptor 4
HGF/SF	Hepatocyte growth factor/scatter factor
HMMR	Hyaluronan mediated motility receptor (RHAMM)
HR	Hazard ratio
HRT	Hormone replacement therapy
HYAL1	Hyaluronidase 1
HYAL2	Hyaluronidase 2

HYAL3	Hyaluronidase 3
ICAM	Intracellular adhesion molecule 1
ICC	Immunocytochemistry
IF	Immunofluorescence
IGF	Insulin-like growth factor
IGF1R	Insulin growth factor 1 receptor
IHC	Immunohistochemistry
kDa	Kilodaltons
LBD	Ligand binding domain
LYVE-1	Lymphatic vessel endothelial hyaluronan acid receptor 1
MAPK	Mitogen-activated protein kinases
MAS 5.0	Affymetrix Microarray Suite 5
MCF-7	Michigan Cancer Foundation 7
MgCl ₂	Magnesium chloride
mRNA	Messenger RNA
miRNA	Micro RNA
MMLV	Molony-murine leukemia virus
MMP	Matrix metalloproteinase
mTOR	Mammalian target of rapamycin
MW	Molecular weight
NCBI	National Centre for Biotechnology Information
NCOA	Nuclear receptor coactivator
NCOR	Nuclear receptor corepressor
NF-κB	Nuclear factor kappa-light-chain enhancer of activated B cells
NR	Nuclear receptor
OS	Overall survival
PBS	Phosphate buffered saline
PCR	Polymerase chain reaction
PI3K	Phosphatidylinositide 3-kinases
PKA	Protein kinase A
PKC	Protein kinase C

PR	Progesterone receptor
PTM	Post-translation modifications
RFS	Relapse free survival
RNA	Ribonucleic acid
ROS	Reactive oxygen species
RPM	Revolutions per minute
RTK	Receptor tyrosine kinase
RT-PCR	Reverse transcription PCR
Ser118	Serine 118
Ser167	Serine 167
SD	Standard deviation
SDS-PAGE	Sodium-dodecyl-sulphate polyacrylamide gel electrophoresis
SEM	Standard error of the means
SERD	Selective oestrogen receptor down regulator
SERM	Selective oestrogen receptor modulator
SFCS	Charcoal stripped foetal calf serum
siRNA	Small interfering RNA
Src	Steroid receptor coactivator
SP-1	Specificity protein 1
STAB2	Stabilin 2
TAE	Tris base, acetic acid and EDTA
TDM-1	Trastuzumab emtansine
Tam-R	Tamoxifen resistant cell line derived from MCF-7 cells
TBST	Tris-Buffered Saline-Tween buffer solution
TGF β	Transforming growth factor beta 1
TL4	Toll-like receptor 4
VCAN	Versican
VEGF	Vascular endothelial growth factor
VEGFR2	Vascular endothelial growth factor receptor 2
WB	Western blotting
WRPMI	Phenol-red-free RPMI 1640

1. Introduction

1.1 Breast cancer and risk factors

Breast cancer is the second most common cancer among women worldwide and the second leading cause of cancer death among women (DeSantis et al. 2011). Breast cancer incidence and mortality varies significantly globally and in general a higher incidence rate is found within developed countries whilst a lower incidence rate is observed within developing countries (Parkin and Fernandez 2006). In the UK alone, approximately 50, 000 women and 350 men were diagnosed with invasive breast cancer in 2011 (Cancer Research UK statistics 2011). However, through intensified detection efforts and the introduction of screening programmes, mortality rates are now decreasing within high risk countries.

The majority of breast cancers are a result of sporadic mutations that result from an accumulation of uncorrected genetic changes in somatic genes. Therefore the large differences observed between incidence rates of breast cancer worldwide have stimulated the search to identify specific risk factors for breast cancer. Numerous breast cancer risk factors are now well-established and include: age (Slattery and Kerber 1993; Fraser and Shavlik 1997), ethnicity (Chlebowski et al. 2005), body mass index (Suzuki et al. 2009; Rohan et al. 2013), dietary factors (Bao et al. 2012; Link et al. 2013) cumulative exposure to endogenous and exogenous oestrogens and possibly progesterones (Clemons and Goss 2001) and family history of the disease (Claus et al. 1994; King et al. 2003). Further, history of benign breast cancer,

particularly atypical hyperplasia and dense breasts are also risk factors for breast cancer development (Dupont et al. 1993; Byrne et al. 1995; Marshall et al. 1997).

1.1.1 Oestrogen exposure

Endogenous and exogenous exposure to oestrogen in pre- and postmenopausal women are well-defined risk factors for breast cancer (Clemons and Goss 2001). Oestrogens increase cell proliferation which may decrease likelihood of DNA damage repair thus potentially leading to the accumulation of mutations (Preston-Martin et al. 1990; Pike et al. 1993a). Additional studies have suggested that oestrogens may also be directly genotoxic through their reactive metabolites however evidence for this mechanism remains limited (Liehr 2000; Yared et al. 2002).

Of crucial importance in breast cancer etiology is the timing of exposure to risk factors as early and late exposure may mediate different risks (Okasha et al. 2003). Although oestrogen exposure early in life may increase the risk of breast cancer onset, conversely, the reduction of these levels later in life may rapidly decrease risk of disease development. Factors that increase lifetime exposure to oestrogens include: early menarche (Ewertz and Duffy 1988; Hsieh et al. 1990), regular ovulation (Henderson et al. 1985; La Vecchia et al. 1985), late menopause (Alexander and Roberts et al. 1987; Hsieh et al. 1990), nulliparity or late age at first birth and lack of/or short term breast feeding (Ewertz et al. 1990; Negri et al. 1990). Alcohol consumption of a minimum of one drink per day also increases endogenous oestrogen levels which may further contribute to disease development (Harvey et al. 1986; Smith-Warner et al. 1998). Additionally, in postmenopausal women, obesity

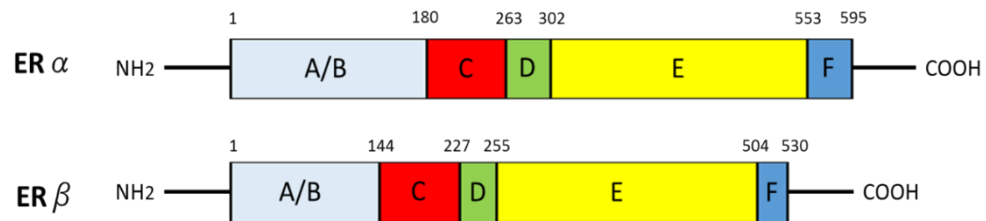
(Hunter et al. 1993; Huang et al. 1997; Morimoto et al. 2002) and long term use of hormone replacement therapy (HRT) (Lauritzen and Meier 1984; Hunt et al. 1990) are principle determinants of oestrogen exposure and have been linked to an increased risk of breast cancer. Other growth factors in addition to oestrogen, including insulin like growth factor 1 (IGF-1) and prolactin, are also thought to also contribute to breast cancer risk although the mechanisms underlying these associations are less well-defined (Hill et al. 1976; Clevenger et al. 2003; Renehan et al. 2004).

1.2 Oestrogen receptors

Oestrogens are steroid hormones that regulate cell growth and differentiation and play an important role in a variety of biological functions including reproduction, metabolism, homeostasis and brain function (Tsai and O'Malley 1994). Oestrogen exerts its biological effect on target tissues through binding to oestrogen receptors (ER) of which there are two main types, ER α and ER β (Walter et al. 1985; Mosselman et al. 1996). These receptors are members of the nuclear hormone receptor family which also include receptors for: androgens, thyroid hormones, progestins, glucocorticoids, retinoids and vitamin D (Tsai and O'Malley et al. 1994; Evans 1998). Numerous orphan receptors for which no ligands have been identified also belong to this family of receptors. ER α and ER β are modular proteins composed of six functionally distinct domains referred to as A – F and depicted in Figure 1.1 (Tsai and O'Malley 1994). Domain A/B is located within the amino-terminal domain of the protein and encodes a hormone-independent transcriptional activation function domain (AF1). The AF1 domain regulates transcription of oestrogen-responsive

genes independent of ligand binding and is alternatively activated through the phosphorylation of serine residues located within this region, particularly in response to ERK/MAPK action (Schwabe et al. 1993). Domain C encodes a highly conserved DNA binding domain (DBD) which is comprised of two functionally distinct zinc finger motifs. These motifs facilitate ER dimerization and bind specifically to oestrogen response elements (EREs) or ERE-like sequences (small palindromic DNA sequences) located within the 5' promoter region of target genes (Schwabe et al. 1993). Domain D is referred to as the hinge region as it separates the DBD from the ligand binding domain (LBD) of ER. This domain is required for binding to heat shock proteins in a resting state however upon activation, the flexibility conferred within the secondary structure of this domain is critical for ER dimerization (Kuiper et al. 1996). This region also contains a nuclear localisation signal which is exposed upon ligand activation (Kuiper et al. 1996). Domain E/F encodes the LBD and is situated at the carboxy-terminal region of the ER. The LBD is composed of 12 α helices which fold to form a compact three-layered helical core. This layered structure forms a hydrophobic pocket cavity which facilitates ligand binding to the ER. In a resting state, helix 12 extends away from the LBD core, however, upon ligand binding to the hydrophobic pocket, a conformational change is induced which leads to the repositioning of helix 12 over the core thus sealing the hydrophobic pocket; a prerequisite action for transcription initiation to occur (Wurtz et al. 1996; Brzozowski et al. 1997; Singh and Kumar 2005). This sealing mechanism creates a hydrophobic groove on the LBD which is recognised and bound to by coregulatory proteins which facilitate/inhibit gene transcription (Savkur and Burris 2004). This domain also contains a second

transcriptional activation functional domain (AF2) which is critical for transactivation in response to ligand binding (Kumar and Chambon 1988; Green and Chambon 1991).



AF1	DNA binding domain	Hinge domain	Ligand binding domain/AF2
A/B	C	D	E/F

Figure 1.1. A schematic diagram of the human ER α and ER β receptors adapted from Kumar et al. 2011. Each ER contains six functional domains denoted as A – F with the starting amino acid position for each domain shown above. The table describes the function of each domain region.

Whilst both AF1 and AF2 domains are capable of initiating transcription separately, it is thought that maximal transcriptional activity of ER is achieved through synergistic action of both domains and their activities (Tzuckerman et al. 1994). However, the differential modes of AF1 (ligand-independent) and AF2 (ligand-dependent) activation leads to the association of these domains with distinct coregulatory proteins thus the contribution of these activating function domains to gene transcription is cell type specific (Paech et al. 1997).

ER α and ER β receptors confer a high degree of homology between their DNA binding domains (approximately 96%) however display only a moderate level of homology between their ligand binding domains (approximately 53%) and a low level of homology between their hinge regions (approximately 36%) (Matthews and Gustafsson 2003; Singh and Kumar 2005). The major functional difference between these receptors is with respect to their AF1 domains. Whereas ER α exhibits a high

level of AF1-mediated transcriptional activity, this domain shows negligible activity in ER β (Hall and McDonnell 1999); this difference is suggested to be the major functional variation between the responses of these receptors to various ligands. Additional differences can be observed with respect to the expression patterns of these receptors. Whereas ER α is predominantly expressed in the breast, uterus and vagina, the majority of ER β expression is found within tissues of the central nervous system, cardiovascular system, immune system, gastrointestinal system, kidneys, lungs and bone, with low expression levels found within the breast (Couse et al. 1997; Kuiper et al. 1997). These differences in expression may explain the selective action of oestrogens between tissues.

Importantly, ER α and ER β appear to take on different roles within breast cancer biology. Approximately two thirds of breast cancers express the ER α , which has been shown to be the main mediator of oestrogen-induced proliferation (Matthews and Gustafsson 2003). In contrast, studies suggest that ER β may act as a tumour suppressor (Paruthiyil et al. 2004; Strom et al. 2004) however the prognostic value of ER β remains unclear. In light of ER α representing the dominant ER subtype in breast cancer, this protein will subsequently be referred to as ER throughout this project.

1.2.1 Mechanisms of ER action

1.2.1.1 Genomic action of ER

In the classical mechanism of ER action, oestrogen diffuses through the plasma membrane and associates with an ER bound to heat shock protein 90 (hsp90) in its resting state. The binding of oestrogen to the ER induces a conformational change

within the LBD causing the dissociation of hsp90 and the subsequent formation of a stable dimer complex (Cowley et al. 1997; Powell and Xu 2008). The oestrogen-ER dimer then undergoes nuclear translocation and binds to oestrogen receptor elements (EREs) (via the DBD) located in the promoter region of oestrogen responsive genes (Kumar and Chambon 1988). Once bound to DNA, the ER recruits coregulatory proteins (coactivators or corepressors) to the LBD which form a transcriptional complex leading to the activation or inhibition of gene transcription (Cowley et al. 1997; Kling et al. 2004). Coactivator proteins facilitate transcription through their intrinsic chromatin remodelling functions and through supporting linkage of ER to the basal transcription machinery (including activation of RNA polymerase II), whilst corepressors inhibit this process (McKenna and O'Malley 2001; Metivier et al. 2003). This mechanism is referred to as the classical mechanism of genomic ER action (Figure 1.2, pathway 1) and accounts for the majority of oestrogen-induced gene transcription.

1.2.1.2 ERE-independent action of ER

Evidence now exists which shows that ERs can regulate gene expression through various pathways separate from this classical genomic mechanism. O'loné et al. 2004 reported that approximately one third of genes regulated by the ER do not contain ERE/ERE-like sequences. This finding revealed a mechanism through which ERs are capable of regulating gene expression without directly binding to DNA in the promoter regions of their target genes. This is referred to as the ERE-independent genomic mechanism of ER action and is facilitated through the ability of ERs (bound to oestrogen and dimerized) to bind and modulate the function of other classes of

transcription factors (through protein-protein interactions in the nucleus) which in turn bind to their respective response elements within the DNA (depicted in Figure 1.2, pathway 2) (Gaub et al. 1990; Castro-Rivera et al. 2001). This phenomenon is referred to as 'transcriptional cross talk' and through this mechanism ERs are capable of regulating a vast array of oestrogen responsive genes that do not contain EREs (Gottlicher et al. 1998).

1.2.1.3 Oestrogen-independent action of ER

In addition to oestrogen, it is now known that the ER can be activated as a result of intracellular signalling molecules. For example various kinases, notably those downstream of EGFR and IGFR1, including MAPK (Tang et al. 2004) and protein kinase A (PKA) (Chen et al. 1999), can phosphorylate multiple serine residues within the ligand-independent AF1 domain of ER (Lannigan et al. 2003). Serine phosphorylation activates the ER in the absence of oestrogen and promotes ER dimerization (Chen et al. 1992), nuclear localisation (Lee and Bai et al. 2002), and subsequent transcription of oestrogen-responsive genes (Ali et al. 1993; Le Goff et al. 1994). This mechanism is referred to as the oestrogen-independent genomic mechanism of ER action (depicted in Figure 1.2, pathway 3). Additionally, growth factor signalling has been shown to directly activate coregulatory proteins of the ER thus providing an alternative influence on ER-mediated transcription (Osborne and Schiff et al. 2003).

1.2.1.4 Non-genomic ER action

Whilst it has been shown that oestrogen can mediate its effects through ER-regulated gene expression, other effects known to be facilitated by oestrogen occur rapidly

within cells and thus cannot be accounted for by ER-induced transcription and subsequent RNA and protein synthesis (Watters et al. 1997; Kelly and Levin 2001; Jakacka et al. 2002). This mode of ER function is termed the non-genomic mechanism of ER action and is mediated through oestrogen activation of a proportion of ERs which localise to the plasma membrane (membrane-associated ER) and the subsequent stimulation of multiple protein kinase interactions (Norfleet et al. 1999; Abraham et al. 2004; Guerra et al. 2004). Various signalling molecules are activated through oestrogen binding to membrane-associated ERs including: cAMP (Watters and Dorsa 1998), MAPK (Wade and Dorsa 2003), PI3K (Alexaki et al. 2004), protein kinases A and C (Qiu et al. 2003) and src kinase (Pawlak et al. 2005). These activated molecules induce downstream signalling pathways which modulate the phosphorylation status of multiple non-ER transcription factors leading to initiation of gene transcription (Figure 1.2, pathway 4) (Watters and Dorsa 1998; Hennessy et al. 2005). Conversely, these signalling pathways can also phosphorylate nuclear ER and influence coregulatory protein binding thus regulating its own transcription (Kow and Pfaff 2004; Vasudevan et al. 2004) (Figure 1.2, pathway 4). This non-genomic mode of ER action provides a further mechanism through which ERs can regulate the expression of genes which both contain EREs and those which do not, thus further diversifying the array of ER-mediated cellular functions.

Taken together, it is now apparent that ER regulation of gene expression is a multifactorial process involving both its genomic and non-genomic actions which may often converge at response elements in the promoters of target genes. However the final output of gene expression is dependent upon numerous cell-specific factors

including: the combination of transcription factors recruited to a specific gene promoter, the availability of coregulatory proteins and signal transduction elements, the cellular localisation of ERs and the nature of extracellular stimuli. These variable elements can be highly cell type specific, thus oestrogens may utilise numerous signalling pathways to induce distinct gene expression responses dependent upon the specific cellular context.

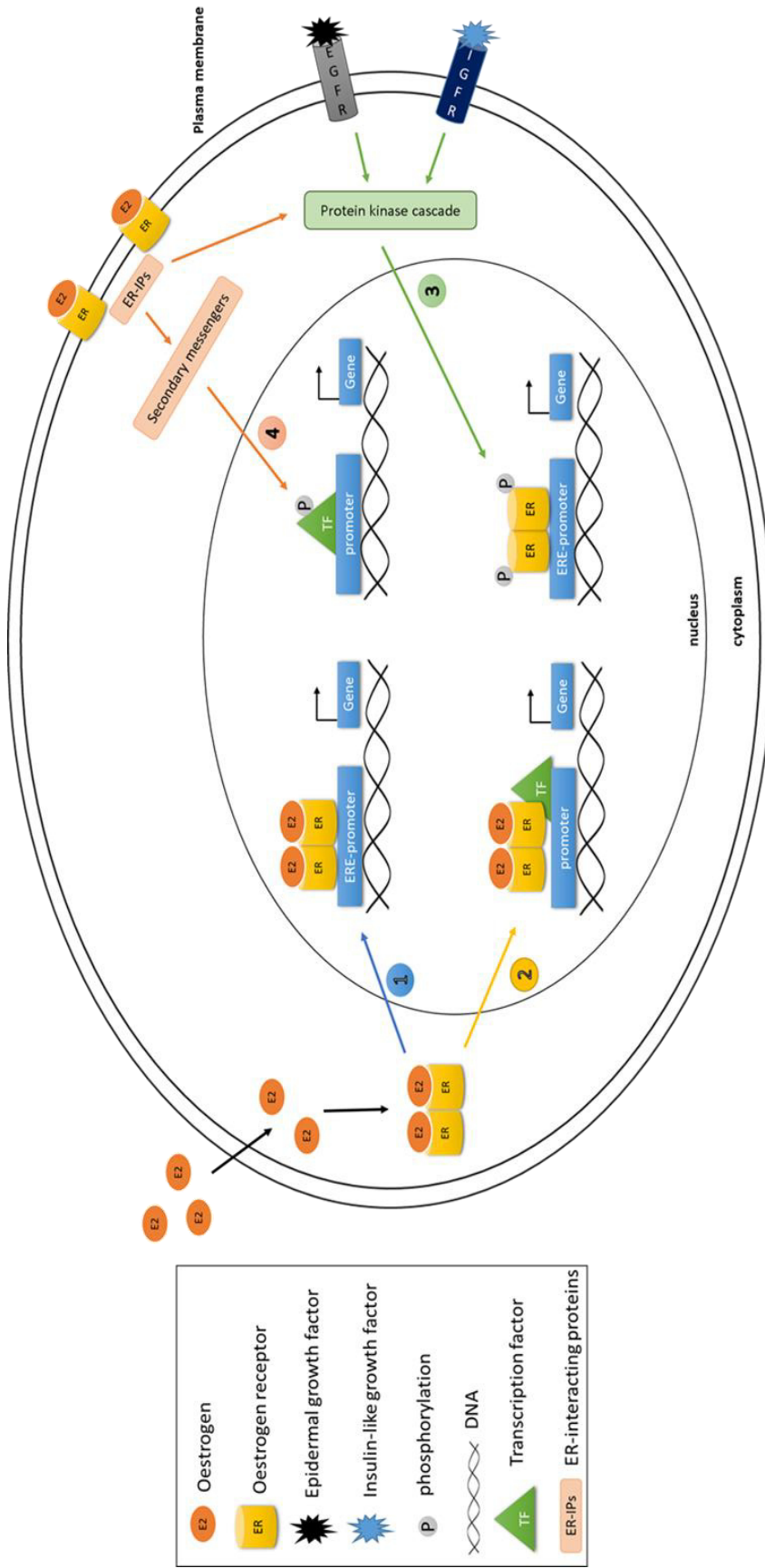


Figure 1.2. Mechanisms of ER action, adapted from Cui et al. 2013. Pathway 1. Classical mechanism of ER action. E2-ER dimer binds to ERE promoter regions of target genes to facilitate gene transcription. Pathway 2. ERE-independent ER action: E2-ER dimer binds to alternative classes of transcription factors to regulate transcription of genes which do not contain EREs. Pathway 3. Oestrogen-independent ER action: Phosphorylation of ER and/or activation of coregulatory proteins by various kinases downstream of growth factor receptor signalling leads to ER activation and subsequent binding to ERE promoter regions of target genes to facilitate gene transcription. Pathway 4. Non-genomic ER action. E2 activation of membrane-associated ER stimulates multiple protein kinase interactions which lead to phosphorylation of non-ER transcription factors and can also promote nuclear ER phosphorylation and ER coregulatory protein activation influencing both non-ERE and ER gene transcription.

1.3 Molecular and clinical subtypes of breast cancer

Breast cancer is characterised by its clinical and molecular heterogeneity. In the clinical setting breast cancer can be classified according to its hormone receptor (ER and/or PR) or human epidermal growth factor 2 receptor (HER2/ErbB2) status which indicates prognosis and directs for specific treatment options. Breast cancers displaying a positive hormone receptor status (approximately 70 – 75 % of patients are ER+) are more likely to respond to endocrine therapies which specifically target the ER (and indirectly the PR, as this is regulated by ER activity) (Cancer Genome Atlas Network, 2012). In tumours presenting as HER2+ (approximately 20 – 25 % of patients) treatments that target the HER2 receptor are used (Spector and Blackwell 2009; Dawood et al. 2010). At present there is no available targeted therapy in widespread use for tumours classified as ‘triple negative’ (do not display ER, PR or HER2 and represent 5 – 10 % of patients). Consequently, patients presenting with triple negative breast cancer have the poorest prognosis (Crown et al. 2012).

Over the past decade microarray profiling studies have further classified breast cancer into subtypes defined by a large number of genes and associated with different clinical outcomes. Each subtype displays a characteristic gene expression pattern thought to be partly dependent upon cellular origin. These molecular subtypes include: basal-like, normal-like, HER2-overexpressing, luminal A and luminal B (Sorlie et al. 2001; Perou et al. 2000; Sotiriou et al. 2003). The basal-like molecular subtype predominantly represent ER-/PR-/HER2- (triple negative) breast tumours whereas the HER2-overexpressing subtype represents HER2+ breast tumours (Creighton 2012). Normal-like, luminal A and luminal B molecular subtypes

all represent ER+ breast tumours however the significantly worse prognosis associated with diagnosis of luminal B breast cancer (highly proliferative ER+ ± HER2+) suggests that ER+ breast cancers may be made up of at least two distinct diseases with differing biology (Sorlie et al. 2001; Dawood et al. 2010).

1.4 Endocrine therapies

Since approximately 75 % of breast cancers diagnosed in postmenopausal women express the ER and/or PR they are likely to be stimulated to proliferate via the action of oestrogens (Anderson et al. 2002). Of these, approximately 80 % are ER+/HER2- (Harvey et al. 1999) and may benefit from endocrine treatment, whilst the other 20 % are ER+/HER2+ and show a greater response to HER2 targeted therapies (Brufsky et al. 2005; Spector and Blackwell 2009). Several types of endocrine therapies are available for the treatment of ER+ (HER2-) breast cancer in postmenopausal women which are designed to interfere with oestrogen/ER signalling and thus subsequently inhibit cell growth; these agents are routinely employed in a sequential manner. Endocrine therapies have been proven to be invaluable agents for adjuvant therapy following surgery in early ER+ breast cancer patients and can lead to extended survival rates or even act as a curative (Jordan and Ford 2011). These agents are also utilised in the advanced (metastatic) stage of ER+ breast cancer where they have been shown to inhibit tumour growth (Joensuu et al. 2005). Further, in the neoadjuvant setting, endocrine therapy has been shown to be effective in tumour reduction thus allowing for more conservative breast surgery (Olson et al. 2009).

1.4.1 SERMs and tamoxifen

Selective oestrogen receptor modulators (SERMs) are a class of endocrine therapeutic agents designed for the prevention and treatment of diseases including breast cancer and osteoporosis (Jordan 2004). Unlike oestrogens (which act as uniform agonists) and anti-oestrogens (which act as uniform antagonists), SERMs display an unusual tissue pharmacology in which they act as agonists and/or antagonists in a tissue-dependent manner (Wegner and Grady 1999; Muchmore 2000). The most widely used SERM to date is tamoxifen, a non-steroidal triphenylethylene that exhibits antagonist action in the breast (Fisher et al. 1998). It has been reported that tamoxifen displays ER agonist action in the bone, liver and cardiovascular system and antagonist action in the brain and breast whilst mixed agonist and antagonist action of tamoxifen can be observed within the uterus (Fisher et al. 1994). Therefore, this distinct mechanism of action is ideal for the treatment of breast cancer where tamoxifen can function as an antagonist in the breast whilst simultaneously exerting the beneficial effects of oestrogen within the hearts and bones of patients.

Tamoxifen competes with oestrogen for ER binding, however once bound, the bulky side chains of tamoxifen prevent the repositioning of helix 12 in the LBD which is necessary to seal the hydrophobic pocket and facilitate transcription (Brzozwski et al. 1997). Therefore, binding of tamoxifen to the ER prevents the recruitment of coactivator proteins to the LBD and inhibits AF2 driven gene transcription; however the activity of the AF1 domains remains unaffected (MacGregor-Shafer et al. 2000). In the breast, where ER activity is predominantly mediated by AF2-driven gene

transcription, tamoxifen functions as an antagonist (Metzger et al. 1995), however in the bone and uterus, where ER activity is mediated primarily through the AF1 domain, tamoxifen exhibits agonist activity (Tzukerman et al. 1994; McDonnell et al. 1995). Tamoxifen binding to ER can also favour the recruitment of corepressors to this complex which further contributes to the suppression of its agonist activity (Lavinsky et al. 1998; Shang and Brown 2002). Therefore it is postulated that altered availability/recruitment of coregulatory proteins to the tamoxifen-ER complex may also contribute to the specificity of tamoxifen function in different tissues (Schiff et al. 2003; Lonard et al. 2004; Shao et al. 2004). Interestingly, tamoxifen treatment can also lead to the induction of oestrogen responsive genes through association of tamoxifen-bound ER with cell surface signalling proteins (e.g. HER2) in the breast. This suggests that tamoxifen can facilitate the non-genomic activities of the ER thus leading to the promotion of agonist activity on a molecular level whilst functioning overall in these tissues as an antagonist of ER signalling (Chen et al. 1996).

In 1999, tamoxifen became the first drug to be approved by the US Food and Drug Administration (FDA) for the prevention of breast cancer and until relatively recently was given as the first line of treatment to pre- and postmenopausal women (Michaud et al. 2001) and men (Giordano et al. 2005) with metastatic ER+ breast cancer and in the adjuvant setting after surgery. An important question still to be answered however is that of defining the most appropriate treatment time for patients to receive the most benefit from this drug. Evidence has shown that adjuvant tamoxifen treatment over a 5 year period can suppress breast cancer recurrence and decrease incidence of contralateral breast tumours by 50% (EBCTCG 2011). Moreover,

beneficial effects from this agent remain for 5 years following treatment cessation (EBCTGG 1998). However, long term tamoxifen treatment has been associated with an increased incidence of thromboembolism, cataracts and endometrial cancer within breast cancer patients (EBCTGG 1998) and healthy women (Fisher et al. 1998) participating in chemopreventative trials. More recently, studies have also shown that tamoxifen treatment alternated with an aromatase inhibitor over a 5 year period can lead to benefits of a more extended time frame (Rao et al. 2012; Davies 2013).

1.4.2 Aromatase Inhibitors

Tamoxifen treatment as a first line therapy for ER+ breast cancer patients has been succeeded by aromatase inhibitors (AIs): endocrine agents which inhibit the synthesis of oestrogen in the body (Brodie et al. 2003). AIs have been shown to achieve more than 95 % inhibition of aromatase activity (an enzyme which converts androgens to oestrogen) and reduce circulating oestrogens to almost undetectable levels in postmenopausal ER+ breast cancer patients (Geisler et al. 1996). These endocrine agents have fewer side effects in comparison to tamoxifen. Following findings from the ATAC ('Arimidex', Tamoxifen, Alone or in Combination) trial, the AI anastrozole, was found to be superior to tamoxifen as first line treatment in the adjuvant setting of early disease for ER+ postmenopausal women (5 year treatment) (Baum et al. 2003; Howell et al. 2005). Therefore tamoxifen is now used as a second-line therapy following disease progression from AIs in hormone-dependent breast cancer.

1.4.3 SERDs and fulvestrant

Due to the failure of tamoxifen and other SERMs to eradicate total oestrogen agonist activity within breast cancer patients, a search for pure anti-oestrogens with a high potency led to the discovery of an additional class of drugs; selective oestrogen receptor downregulators (SERDs). The most effective SERD discovered to date is fulvestrant (trade name faslodex). Fulvestrant is a steroidal 7α -alkylsulfinyl analogue of oestradiol and functions as a pure antagonist of the ER (Wakeling 2000). This SERD is structurally distinct from the non-steroidal SERMs and exhibits a higher affinity for the ER compared with tamoxifen (89 % versus 2.5 % of the binding affinity of oestradiol respectively) (Wakeling et al. 1991). In comparison to tamoxifen, fulvestrant exerts additional effects on the ER leading to a more effective inhibition of oestrogen action. Fulvestrant also competes with oestrogen for ER binding, however once bound, the long side chains of fulvestrant severely alter ER conformation such that ER dimerization is inhibited (Fawell et al. 1990; Nicholson et al. 1995). This interaction leads to the formation of a highly unstable complex which impairs ER shuttling from the cytoplasm to the nucleus thus reducing nuclear localisation of ER (Dauvois et al. 1993). Fulvestrant-ER complexes that may enter the nucleus are additionally functionally redundant as, unlike tamoxifen, fulvestrant binding impairs both AF1 and AF2 transcriptional activating domains. Furthermore, the formation of highly labile fulvestrant-ER complexes results in their rapid degradation from the cytoplasm (Nicholson et al. 1995). In summary, fulvestrant binds to, blocks and causes accelerated degradation of ERs leading to abrogation of ER expression, gene transcription and signalling (Osborne et al. 1995; Wakeling et al.

1995). Thus in contrast to alternative anti-oestrogens, fulvestrant shows full antagonist activity of the ER and has no known oestrogen agonist activity (Wardley 2002).

Despite the greater efficacy of fulvestrant to abrogate ER expression and signalling in breast cancer cells as compared to tamoxifen and AIs (Nicholson et al. 1995; Pink and Jordan 1996) this anti-hormone remains a second line therapy where these agents have failed. However, utilisation of therapies in this sequential manner may be beneficial to patients as fulvestrant has been shown to remain active within tamoxifen-resistant patients and does not confer cross-resistance with other anti-oestrogens (DeFriend et al. 1994; Osborne et al. 1994). Furthermore, studies have suggested that HER2 status also does not preclude a response to fulvestrant; which is beneficial as HER2 is a limiting factor for tamoxifen treatment and may ultimately lead to acquired tamoxifen-resistance (Nicholson et al. 2004). To this end, in May 2002, the U.S Food and Drug Association (FDA) approved the use of fulvestrant for the treatment of hormone receptor positive metastatic breast cancer in postmenopausal women with disease progression following endocrine therapy. Further, in March 2004, the European Union licenced the use of fulvestrant for the treatment of postmenopausal women with advanced breast cancer for disease relapse on or after endocrine therapy or disease progression with anti-oestrogen treatment. Research suggests that fulvestrant is at least as effective as the most widely used AI, anastrozole, in patients that have progressed from adjuvant or first-line tamoxifen therapy (Howell et al. 2002; Osborne et al. 2002; Robertson et al. 2003) whilst others suggest the value of fulvestrant treatment after AI failure (Ingle

et al. 2004; Perey et al. 2004). However, some evidence suggests that fulvestrant may produce better results upon earlier administration in the treatment sequence (Howell et al. 2002; Steger et al. 2005). To this means, fulvestrant is now also being trialled in the first line clinical setting for advanced ER+ breast cancer disease with results revealing that fulvestrant may be at least as effective as anastrozole in this setting (Robertson et al. 2009). Overall, fulvestrant remains an ideal agent for combination treatment with other endocrine treatments and/or novel agents through its unique mechanism of function, good tolerability profile and lack of cross-resistance.

1.5 Therapeutic resistance in ER+ breast cancer

Whilst endocrine therapies have proven successful for the treatment of ER+ breast cancer, de novo or acquired resistance to these therapies remains a significant problem. In the setting of metastatic disease, it has been reported that only approximately 30 % of breast tumours display objective regression with initial endocrine therapy with an additional 20 % exhibiting a prolonged stable disease (Osborne and Schiff 2003). Acquisition of endocrine resistance to these therapies leads to disease progression, formation of a more aggressive cancer and worsened prognosis for breast cancer patients and further treatment options for relapsed patients remains limited. For the provision of better therapeutic options for these patients it is imperative to understand the mechanisms through which cells develop resistance. In recent years several resistance mechanisms have been identified through which cells may overcome the growth suppressive effects of endocrine therapy. These mechanisms focus around three general categories: i) loss or altered

ER expression and/or function ii) differential availability of coregulatory proteins and cell-cycle regulators and iii) modulated growth factor receptor signalling, leading to a shift from genomic to non-genomic ER activity. However it has now become evident that multiple mechanisms exist which combine to orchestrate the acquisition of, and sustained, endocrine resistance (Massarweh et al. 2008).

1.5.1 ER and resistance

At present, the ER remains the most powerful biomarker for the prediction of patient response to endocrine therapy, thus, alterations in ER expression may affect endocrine sensitivity. Loss of ER expression occurs in approximately 20 % of breast cancer patients treated with endocrine therapy (Gutierrez et al. 2005). ER expression is not thought to be controlled at the genomic level, instead it is thought to be predominantly regulated by epigenetic modifications and post-translational mechanisms (Giacinti et al. 2006). Indeed, ER mutations have been shown to occur in less than 1 % of ER+ breast cancers (Herynk and Fuqua 2004). Further complexity is added through the observation that the ER undergoes post-translational modifications (including phosphorylation, methylation and ubiquitination) which alter its interactions with coregulatory proteins thus influencing transcriptional activity and sensitivity to various endocrine therapies (Gururaj et al. 2006).

1.5.2 Coregulatory protein availability and cell cycle and apoptosis regulators

The ER regulates gene expression through interactions with coregulatory proteins that form complexes required for the initiation of transcription (McKenna et al. 1999). The presence of these proteins in the nucleus at rate-limiting levels can

significantly alter ER signalling and it has been observed that enhanced expression of ER coactivators and/or reduced expression of corepressors may negate the effects of endocrine therapy through influencing the balance of agonist versus antagonist activity of SERMs. Indeed, preclinical and clinical evidence suggests that enhanced expression of the ER coactivator AIB1/SRC3 is correlated with tamoxifen resistance (Osbourne and Schiff. 2003; Shou et al. 2004), whilst reduced expression of the co-repressor protein NCoR appears to be involved in tamoxifen-refractory tumours (Lavinsky et al. 1998). Additionally, increased levels of transcription factors such as NF κ B, AP1 and SP1, critical for ER-mediated signalling in the non-genomic pathway, have also been associated with endocrine resistance (Schiff et al. 2003; Osbourne and Schiff 2003). Therefore, the availability and altered function of coregulatory proteins has been shown to directly influence ER-mediated transcription and efficacy of endocrine therapy.

New evidence from preclinical and clinical studies suggests that the activity of cell cycle regulators and survival molecules contribute towards tumour sensitivity to endocrine therapies (Musgrove and Sunderland 2009). For example, overexpression of the cell cycle regulators MYC and cyclin D1 and E1 contribute to endocrine resistance through the activation of cyclin-dependent kinases that are critical for G1 phases or through negation of the inhibitory effects of the negative cell cycle regulators p21 and p27 (Butt et al. 2005). Indeed, studies have revealed that resistance to tamoxifen has been associated with decreased expression of the negative cell cycle regulators p21 and p27 along with inactivation of the tumour suppressor RB (Perez-Tenorio et al. 2006; Chu et al. 2008). Additionally, evidence

suggests that downregulated expression of pro-apoptotic proteins (e.g. caspase 9) and upregulated expression of anti-apoptotic proteins (e.g. BCL-XL) also facilitates acquisition of endocrine resistance (Kumar et al. 1996) through promoting cell survival. The activity of these cell cycle regulators and survival molecules can be modulated through receptor tyrosine kinase (RTK) and transcription factor signalling (Zhou et al. 2007); factors also influenced by endocrine treatment.

1.5.3 Cross-talk with receptor tyrosine kinases and their downstream signalling pathways

Preclinical and clinical evidence has also shown that RTKs can contribute to endocrine resistance. Indeed, studies have revealed a bidirectional cross-talk mechanism whereby membrane ER activates RTK signalling which in turn leads to phosphorylation of the ER and its coregulatory proteins (Shou et al. 2004). Phosphorylation of serine residues in the AF1 domain of the ER, particularly serine's 118 and 167, activate ER in a ligand-independent manner and lead to the transcription of oestrogen-sensitive genes thus forming a positive feedback loop (Bunone et al. 1996; Joel et al. 1998). This activation of ER in the presence of endocrine agents may switch the transcriptional programme from genomic to non-genomic pathway of ER action. Such signalling pathways implicated in reducing the efficacy of endocrine therapy include: the ErbB family of RTKs (Arpino et al. 2008), src (Morgan et al. 2009), ERK/MAPK (Britton et al. 2006), PI3/AKT (Campbell et al. 2001) and receptors for insulin/IGF, FGF and VEGF (Chakraborty et al. 2010). These pathways lead to the activation of various transcription factors which regulate the transcription of multiple genes either in combination with the ER or bypassing it. The

RTKs, EGFR and HER2, have been heavily implicated as prominent mediators of endocrine resistance in ER+ breast cancer (Konecny et al. 2003; De Laurentiis et al. 2005). Indeed, enhanced EGFR and/or HER2 expression has been found to become elevated in MCF-7 derived acquired tamoxifen-resistant (Tam-R) and fulvestrant-resistant (Fas-R) in vitro cell models compared to their wild-type MCF-7 cells. Studies have revealed that these endocrine resistant cell models show enhanced EGFR/HER2 heterodimerisation and activity leading to downstream activation of MAPK and PI3K/AKT signalling cascades which function to drive endocrine resistant cell growth (McClelland et al. 2001; Knowlden et al. 2003; Jordan et al. 2004; Nicholson et al. 2007). In Tam-R cells, hyperactivated EGFR/HER2 signalling has been shown to activate ER and its coregulatory proteins in a ligand-independent manner (Font de Marc and Brown 2000; Britton et al. 2006) and EGFR/MAPK signalling in these cells was shown to promote AF1 phosphorylation of the ER leading to enhanced agonist behaviour of tamoxifen and expression of oestrogen-regulated genes (Britton et al. 2006). Furthermore, immunohistochemical analysis of clinical breast cancer tissue revealed overexpression of EGFR, HER2 and MAPK in both de novo ER+ (and ER-) and acquired-tamoxifen resistant patients (Gee et al. 2005; Gutierrez et al. 2005). Additionally, in breast tumours resistant to fulvestrant, upregulation of HER2 and MAPK has been observed thus suggesting an involvement of this pathway in the acquisition of a resistant phenotype (Massarweh et al. 2006).

To this end, the use of specific blockers or inhibitors of RTK signalling has been a promising therapeutic approach in endocrine resistant breast cancer. Indeed, gefitinib (a selective inhibitor of EGFR) has been shown to restore the effects of

tamoxifen in HER2 overexpressing acquired tamoxifen-resistant MCF-7 cells, whilst trastuzumab (monoclonal antibody that blocks HER2) has been shown to inhibit growth of endocrine resistant ZR-75-1 cells (Shou et al. 2004). Furthermore, co-treatment of targeted therapies in conjunction with endocrine agents, e.g. tamoxifen, has also been shown to subvert the emergence of resistance in MCF-7 cells (Gee et al. 2003; Leary et al. 2010) and targeted therapies of downstream signalling kinases, MAPK and PI3K/AKT, have also been shown to inhibit growth of endocrine resistant cells (McClelland et al. 2001; Knowlden et al. 2003; Jordan et al. 2004).

Taken together, it is likely that multiple factors contribute to the acquisition of endocrine resistance in breast cancer, however a greater understanding of the mechanisms which drive this process is necessary to improve treatment options for patients. Progress is being made in this area through the identification of biomarkers of resistance and search for molecular targets through which to treat resistant disease in patients. Over the past few decades multiple proteins have been reported to be involved in the acquisition of endocrine resistance in breast cancer. One such protein is the cell surface receptor CD44 which has been implicated in the acquisition of tamoxifen resistance in an ER+ breast cancer cell model (Hiscox et al. 2012) and extensively found to become upregulated in numerous carcinomas where it is thought to contribute, in some instances, to disease progression (Ma et al. 2005; Misra et al. 2012; Saito et al. 2013; Shi et al. 2013; Todaro et al. 2014). CD44 will be subsequently reviewed in this project.

1.6 CD44

The CD44 protein belongs to a family of cell surface glycoproteins known as cell adhesion molecules (CAM) due to the strong bonds they form to specific ligands (Goodison et al. 1999). The CD44 family encompasses a polymorphic group of proteins which differ in size, glycosylation and function. Although CD44 is encoded by a single, highly conserved gene (Screaton et al. 1992; Rudzki and Jothy, 1997), the heterogeneity of CD44 proteins arise through the process of alternative splicing and post-translational modifications which may vary according to cell type and growth conditions (Jackson et al. 1992; Tolg et al. 1993). CD44 proteins are found present on the surface of most vertebrate cells and along with other members of the CAM family, are implicated in a diverse array of cellular functions including: cell to cell adhesions, cell to matrix adhesions, cell motility, growth, differentiation and signalling (Yu and Stamenkovic 1999; Mylona et al. 2006; Subramaniam et al. 2007; Cho et al. 2012; Montgomery et al. 2012; Bjorkland et al. 2013; Tsuneki and Mmadri 2014). Additionally, a large proportion of CD44-mediated functions are facilitated through binding to its principle ligand hyaluronan (HA) (Bartolazzi et al. 1994; Knudson et al. 2002; Hamilton et al. 2007; Bourguignon et al. 2012). Thus, CD44 belongs to a family of proteins linked by their shared ability to bind HA, termed hyaladherins.

1.6.1 CD44 gene structure

The human CD44 gene is located at the chromosomal locus 11p13 and is comprised of two groups of exons as denoted in Figure 1.3 (Goodfellow et al. 1982). The first

group are composed of exons 1 – 5 and 16 – 20. These constitutively expressed exons (termed standard exons) can be spliced together to form an isoform known as CD44 standard (CD44 Std). The second group comprise the exons 6 – 15 (termed variant exons 1 – 10). These variant exons may be alternatively spliced individually, or in combinations, and included with the constitutively expressed standard exons at the insertion site between exons 5 and 16; this process allows for the formation of a vast array of CD44 isoforms with differing exon compositions (Dougherty et al. 1991; Hoffman et al. 1991; Tolg et al. 1993). Additional complexity arises through the alternative splicing of standard CD44 exons or use of cryptic splice sites (Screaton et al. 1992; Ermack et al. 1996). However, unlike mice, the human CD44 gene contains a stop codon in exon 6 (variant 1) within the seventeenth amino acid and thus is not usually included within processed transcripts (Screaton et al. 1993).

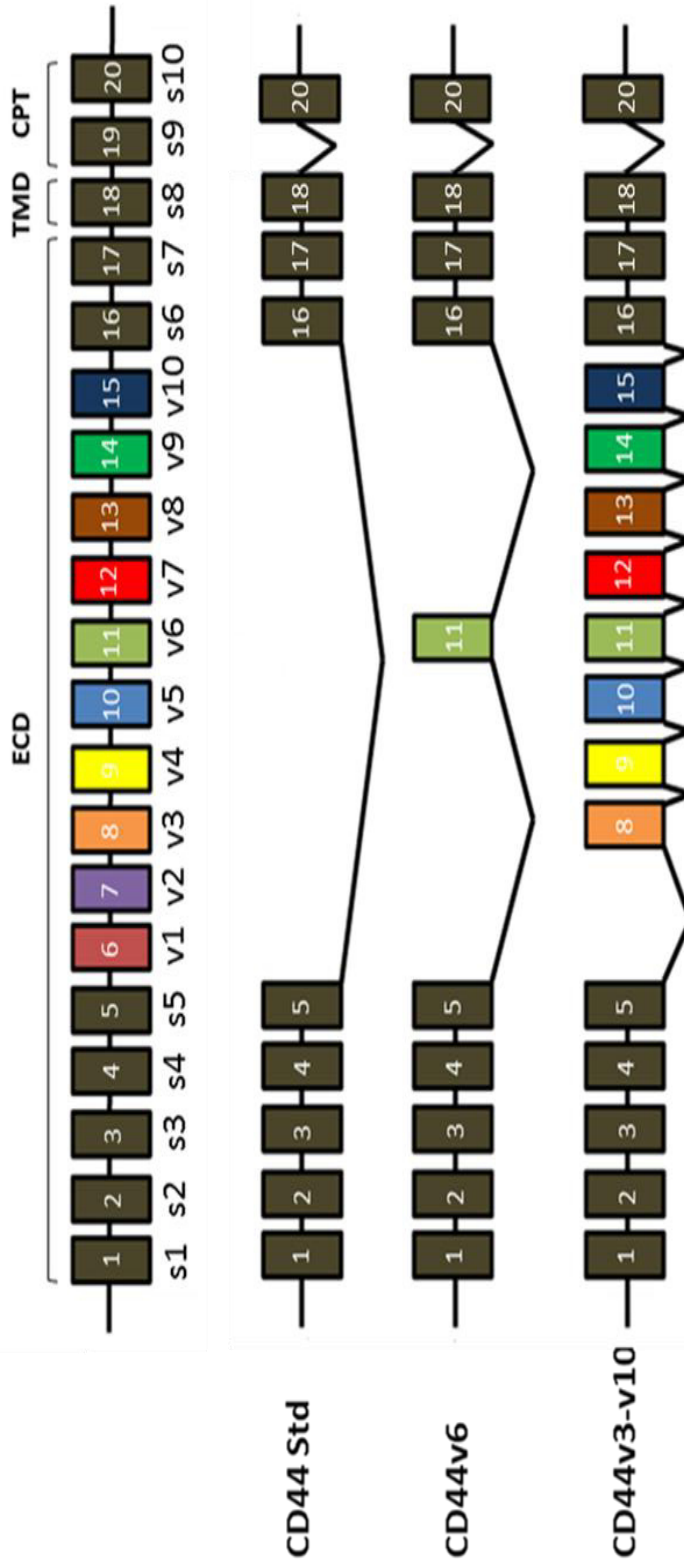
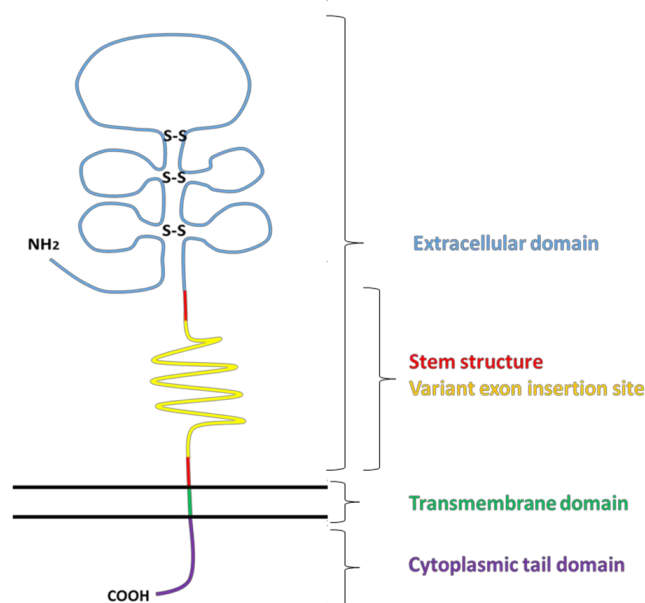


Figure 1.3. Structure of CD44 pre-mRNA transcripts adapted from Ponta et al. 2003. The CD44 gene is encoded by 20 exons. Standard exons are constitutively expressed and composed of exons 1 – 5 and 16 – 20 (denoted as s1 – 5 and s16 - 20). Standard exons can become spliced together to form a transcript which encodes the CD44 standard isoform (CD44 Std). The variant exons are composed of exons 6 – 15 (denoted as v1 – 10) and may be alternatively spliced individually (e.g. CD44v6, containing the variant 6 exon only) or in combinations (e.g. CD44v3-v10, containing variants exons 3 – 10) and included with the constitutively expressed standard exons to produce multiple CD44 isoforms. CD44 exon 6 (variant 1) and exon 19 (standard 9) are not usually included within processed transcripts. Abbreviations represent: EC: Extracellular domain, TMD: transmembrane domain, CPT: cytoplasmic domain, s: standard exon, v: variant exon.

1.6.2 CD44 protein structure

The CD44 protein structure is comprised of three domains; an N-terminal extracellular domain, a transmembrane domain and a C-terminal cytoplasmic domain (Figure 1.4) (Bosworth et al. 1991).



	Extracellular domain	Stem structure	Transmembrane domain	Cytoplasmic domain
Exon	Standard exons: 1 - 4	Standard exons: 5, 15, 16, 17 Variant exons: 2 - 10	Standard exon: 18	Standard exons: 18 (3 amino acids), 19 (usually excluded), 20
Binding motifs/ attachment sites	HA binding site (90 amino acid link module, standard exons 2 - 3)	Heparan sulphate (variant exon 3) Chondroitin sulphate (standard exons: 5, 15, 16 and 17) variant exon 10 GAG consensus motifs		ERM Merlin Ankyrin
Post-translational modifications	N-linked glycosylation O-linked glycosylation Chondroitin sulphate Tyrosine sulphate Keratin sulphate Sialic residues		Acetylation (cys286)	Acetylation (cys295) Phosphorylation (ser291 and 325)

Figure 1.4. CD44 protein structure adapted from Ponta et al. 2003. A schematic diagram to show the 3 structural domains of CD44 including: i) the N-terminal extracellular domain folded into a globular tertiary structure, which includes the stem structure containing the insertion site for individual or combinations of variant exons 2 – 10, ii) the highly conserved hydrophobic transmembrane domain and iii) the C-terminus cytoplasmic domain. The table lists the exon number(s), binding motifs/attachment sites and post-translation modifications attributed to each domain. Abbreviations represent: NH₂ (amino terminus), COOH (carboxy-terminus), S-S (disulphide bond formed between 2 cysteine residues).

The extracellular domain of CD44 can be divided into two regions: conserved and non-conserved. The largely conserved (85 %) N-terminal domain is encoded by exons 1 – 4 and forms a globular tertiary structure through the formation of disulphide bonds between three pairs of cysteine residues (Goodison et al. 1999) (Figure 1.4). Exon 1 encodes an N-terminal signal sequence whilst exons 2 – 3 comprise a stretch of 90 amino acids which contain the binding site for HA and other glycosaminoglycans (GAGs); this domain is termed the 'link module' (Aruffo et al. 1990; Culty et al. 1990; Naor et al. 1997). This domain also contains the conserved cysteine residues which form interchain disulphide bonds which are required for the stability of the domain and correct folding into the globular tertiary structure of this protein (Kohda et al. 1996; Banjeri et al. 1998; Day and Sheehan 2001). The less conserved N-terminal region (approximately 35 – 50 %) is the membrane proximal stem domain and is encoded partly by exon 5 and exons 16 and 17 (Goodison et al. 1999). This stem structure (46 amino acids in length) separates the N-terminal domain from the plasma membrane. This domain contains numerous carbohydrate modifications and putative proteolytic cleavage sites and is thought to form a stem structure due to heavy glycosylation (Screaton et al. 1992; Okamoto et al. 1999). The stem structure may be expanded (by up to 381 amino acids in humans, or 423 amino acids in mice) to contain individual or combinations of variant exons through the previously mentioned process of alternative splicing (Jackson et al. 1992) (Figure 1.4). This domain also contains various binding sites for alternative CD44 ligands including: chondroitin sulphate (exons: 5, 15, 16 and 17) (Knutson et al. 1996; Kawashima et al. 2000; Fujimoto et al. 2001; Murai et al. 2004), heparan sulphate (exon 8) (Bennet et

al. 1995; Jackson et al. 1995; Jones et al. 2000), collagen (Carter and Wayner 1988), laminin (Ishii et al. 1993; Hibino et al. 2004), fibronectin (Jalkanen and Jalkanen 1992) and osteopontin (Weber et al. 1996; Pietras et al. 2014) and is capable of forming complexes with various growth factors, cytokines, matrix-metalloproteinases and non-protein/protein integral membrane receptors (Bennet et al. 1995; Lammich et al. 2002; Murakami et al. 2003).

The transmembrane region is encoded by exon 18 and comprises 23 hydrophobic amino acids and a cysteine residue and shows 100 % conservation between species (Figure 1.4) (Isacke et al. 1994); Lesley and Hyman 1998). The functional significance of this highly conserved transmembrane region has not yet been fully elucidated. However, studies have suggested a role for this domain within CD44 oligomerisation and incorporation into lipid rafts for the stabilisation and regulation of CD44 ligand associations and subsequent downstream signalling and initiation of migration (Neame et al. 1995; Perschl et al. 1995; Thankamony and Knudson 2006; Donatello et al. 2012; Babina et al. 2014). Additional studies hypothesise a role for this domain in efficient ligand binding (Lesley et al. 1992; Thomas et al. 1992) however this is disputed (Lesley et al. 2000; Gal et al. 2003; Perschl et al. 2005).

The cytoplasmic region of CD44 is highly conserved and is encoded partially by exon 18 (3 amino acids) and by exons 19 and 20 (Figure 1.4) (Goodison et al. 1999). However exon 19 is usually excluded from the majority of CD44 transcripts as inclusion of this exon results in a short-tail variant of CD44 through the use of an alternative translation stop codon (Goldstein et al. 1989; Goldstein and Butcher. 1990; Jiang et al. 2001). Indeed, Jiang et al. 2002 revealed that inclusion of exon 19

in chondrocytes led to subsequent inhibition of HA endocytosis suggesting a possible role for this truncated isoform as a dominant negative regulator of HA internalisation. The cytoplasmic tail contains motifs for the cytoskeletal linker proteins ezrin, radixin, moesin (ERM) (Tsukita et al. 1994; Yonemura et al. 1994) and ankyrin (Bourguignon et al. 1986; Kalomiris et al. 1988). These proteins are found to localise to membrane ruffles, filopodia, microvilli and cleavage furrow and are implicated within cytoskeletal and membrane remodelling, regulation of cell shape and migration and may act as a scaffold for signalling events (Bretscher et al. 1997; Hiscox and Jiang 1999; Yonemura et al. 1999). Phosphorylation of the CD44 cytoplasmic tail by intracellular signalling components (including calmodulin-dependent protein kinase (CAMKII) and Rho-kinase (ROK)) enhance interactions between CD44 proteins and cytoskeletal linkers ERM and ankyrin, respectively, which regulate cell motility processes through facilitating indirect binding of CD44 to the actin cytoskeleton (as the CD44 gene itself does not encode actin binding motifs) (Zohar et al. 2000; Legg et al. 2002; Bourguignon et al. 2003; Donatello et al. 2012) shown in Figure 1.5. Furthermore the cytoplasmic tail plays an important role in subdomain localisation and in response to ligand binding can transduce intracellular signalling events leading to subsequent modulation of gene expression. As with all major classes of adhesion receptors, the CD44 molecule lacks intrinsic kinase activity therefore interactions with other proteins are required for the modulation of signalling within cells (Taher et al. 1996). Indeed, many intracellular signalling components have been reported to complex with the CD44 cytoplasmic tail including the Rho family of GTPases (and their exchange factors and adaptor molecules) (Oliferenko et al. 2000; Bourguignon

et al. 2003) and members of the src family of non-receptor tyrosine kinases (Llangumaran et al. 1998; Bourguignon et al. 2001). Numerous studies have shown that HA binding to CD44 stimulates Rho-guanine nucleotide exchange factors (RhoGEFs) (including p115RhoGEF and leukemia-associated RhoGEF (LARG)) which act as GDP/GTP exchange proteins for the Rho subfamily of GTPases, including RhoA. HA binding to CD44 stimulates RhoGEF/LARG mediated activation of RhoA which subsequently interacts with and activates downstream signalling components phospholipase C ϵ (PLC ϵ) and ROK (Bourguignon et al. 2004; Bourguignon et al. 2006). Interactions between RhoA and PLC ϵ promote inositol trisphosphate (IP $_3$) production and calcium (Ca $^{2+}$) mobilisation leading to CamKII activation and subsequent phosphorylation of the cytoskeletal protein filamin, resulting in cellular migration/invasion (Bourguignon et al. 2006) (Figure 1.5). Conversely, RhoA activation of ROK leads to the subsequent phosphorylation of several signalling proteins including Na $^+$ /H $^+$ exchanger 1 (NHE1), Grb-2 associated binder 1 (Gab-1) and myosin-phosphatase which contribute to enhanced cellular survival, growth, migration and invasion (Bourguignon et al. 2003; Bourguignon et al. 2004; Bourguignon et al. 2006) (depicted in Figure 1.5). Furthermore, Src has been shown to directly bind to the CD44 cytoplasmic tail leading to PKC activation and subsequent stimulation of the Ras-MEK-ERK signalling pathway resulting in enhanced cellular survival/growth (Bourguignon et al. 2001; Bourguignon et al. 2010) (Figure 1.5). Additionally, CD44 proteins are subject to proteolytic cleavage in the cytoplasmic domain (Okamoto et al. 2001; Lammich et al. 2002; Murakami et al. 2003). Extracellular domain cleavage of CD44 (by proteases) triggers subsequent

intracellular cleavage and the resultant fragment is translocated to the nucleus where it mediates the transcription of a variety of genes, including CD44 itself (Okamoto et al. 2001; Murakami et al. 2003).

In summary, CD44 proteins can contribute to multiple cellular functions through i) co-receptor formation with integral membrane proteins, ii) binding of growth factors, cytokines and MMPs, iii) incorporation into lipid rafts, iv) transduction of intracellular signalling through interactions with proteins via the cytoplasmic tail, v) cytoskeletal remodelling through indirect binding to the cytoskeleton and vi) transduction of gene expression through proteolytic cleavage. These interactions facilitate a highly diverse array of CD44-mediated functions.

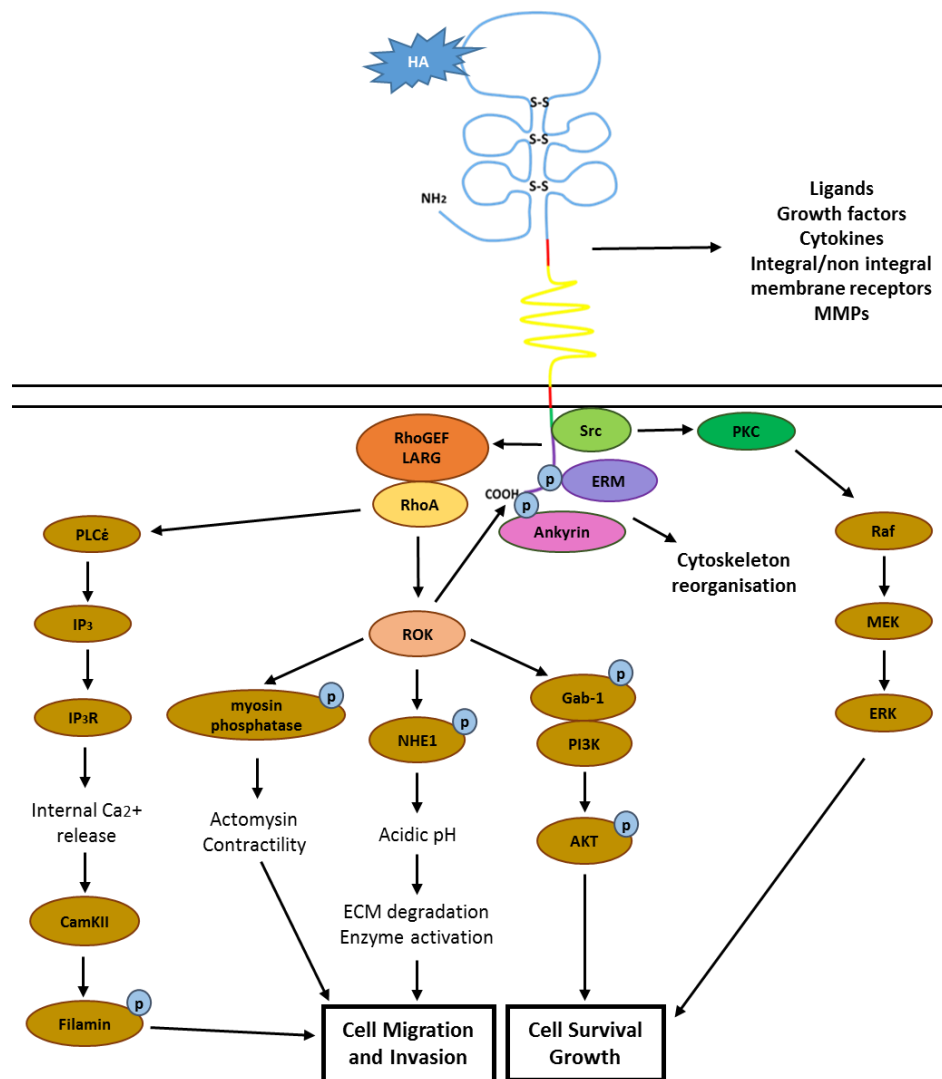


Figure 1.5. A proposed model for HA-stimulated CD44-mediated signalling during tumour progression, adapted from Bourguignon et al. 2009. HA binding to CD44 stimulates RhoGEF/LARG mediated activation of RhoA in a GTP-dependent manner which subsequently interacts with, and activates, downstream signalling components PLC ϵ and ROK. Interactions between RhoA and PLC ϵ promotes IP $_3$ production and Ca $^{2+}$ mobilisation leading to CamKII activation and subsequent phosphorylation of the cytoskeletal protein filamin, resulting in cellular migration/invasion. RhoA-activated ROK phosphorylates several signalling proteins including: i) myosin phosphatase leading to actomyosin mediated membrane motility, ii) NHE-1 leading to intracellular acidification and acidic ECM conditions resulting in cysteine proteinase-mediated matrix degradation and cellular migration/invasion and iii) Gab-1 leading to PI3K-AKT pathway activation and subsequently enhanced cell survival and growth. Furthermore, ROK phosphorylates the CD44 cytoplasmic tail leading to enhanced interaction with the cytoskeletal protein ankyrin resulting in cytoskeleton reorganisation. Phosphorylation of an alternative site in the CD44 cytoplasmic tail leads to interaction with the cytoskeletal linker proteins ERM also resulting in cytoskeleton reorganisation. The cytoplasmic domain of CD44 can also directly bind to Src leading to PKC activation and stimulation of the Raf-MEK-ERK signalling pathway resulting in enhanced cell survival and growth. Additionally, the extracellular region of CD44 can interact with numerous ligands, growth factors, cytokines, MMPs and integral/non-integral membrane receptors thus contributing towards the activation of numerous alternative cellular signalling pathways.

1.6.3 Post-translational modifications of the CD44 protein

The calculated theoretical mass of the standard CD44 isoform (comprised of 363 amino acids) is 37 kDa however its apparent mass (determined by gel electrophoresis) is approximately 80 kDa (Stamenkovic et al. 1989; Goodison et al. 1999). Moreover, the observed mass of the largest CD44 isoform (containing all CD44 variant exons and termed 'epican') can be over 200 kDa; with other CD44 variant isoforms falling within this size range (Goodison et al. 1999). The differences between the theoretical and observed mass of CD44 isoforms are due to extensive post-translational modifications which tend to be cell specific. Such modifications of CD44 may occur within the N-terminal domain which harbours: (i) a minimum of seven conserved consensus N-glycosylation sites (Bartolazzi et al. 1996; English et al. 1998), (ii) chondroitin- (Knutson et al. 1996) tyrosine- (Sleeman et al. 1998) and keratin sulphate attachment sites (Bennet et al. 1995) (iii) O-linked glycosylation sites (Lesley et al. 1995) and (v) sialic residues located on the standard extracellular region (Goodison et al. 1999) (shown in Figure 1.4). The splice variant exons also have the potential for various post-translational modifications including extra sites for N- and O-linked glycosylation, GAG consensus motifs and attachment sites for heparan sulphate on exon 8 (variant 3) and chondroitin sulphate on exon 15 (variant 10) (Jackson et al. 1995; Jones et al. 2000; Fujimoto et al. 2001; Murai et al. 2004) (Figure 1.4).

Post-translational modifications have also been shown to occur within the transmembrane and cytoplasmic domains of the CD44 molecule. Bourguignon et al. 1991 revealed that CD44 can be reversibly palmitoylated at the acylation sites

cysteine 286 and 295 in the transmembrane and cytoplasmic domain respectively (Figure 1.4). The functional significance of this post-translational modification has been suggested to enhance the interactions between CD44 and the cytoskeletal protein ankyrin (Bourguignon et al. 1991) and play a role in the partitioning of CD44 into lipid rafts (Thankamony et al. 2006; Babina et al. 2014). Additionally, the cytoplasmic tail of CD44 contains two phosphorylation sites at serine 235 and 291 (Neame and Isacke 1992) and 4 other potential phosphorylation sites (Figure 1.4). Studies have revealed a functional importance of these post-translational modifications in HA-stimulated migration. Indeed, Legg et al. 2002 revealed that protein kinase C (PKC) mediates phosphorylation switching between serine 235 and serine 291 on the CD44 molecule. Complete dephosphorylation of CD44 at position serine 235 followed by phosphorylation of serine 291 by PKC causes dissociation of ezrin from the molecule; these events are essential for the regulation of CD44 interactions with ERM proteins and subsequent cytoskeleton modulation (Legg et al. 2002).

Clearly the CD44 molecule has the potential to be extensively modified following translation. The degree of glycosylation, acetylation and phosphorylation can alter the ligand binding characteristics of the protein and may thus account for altered functions observed between CD44 family members. Therefore incorporation of different combinations of CD44 exons into the CD44 protein can lead to the formation of multiple isoforms with distinct post-translational modifications, thus adding a further level of complexity to understanding CD44 functions.

1.6.4 CD44 variant expression and its pathological roles

CD44 proteins do not exhibit uniform expression within tissues. Whereas the standard CD44 isoform (CD44 Std) has been shown to be ubiquitously expressed in the majority of vertebrate tissues (Terpe et al. 1994; Mackay et al. 1994), the larger CD44 variant isoforms exhibit a more restricted expression pattern and are predominantly located in cells of a stressed/diseased state e.g. during wound repair (Oksala et al. 1995; Huebener et al. 2008), inflammatory diseases (Pure and Cuff 2001; Teder et al. 2002) and cancer cells (Gunthert et al. 1991; Foekens et al. 1999; Lopez et al. 2005; Louderbough et al. 2011). Further, CD44 variant expression changes during distinct stages of maturation (Zoller et al. 1997). Although most hematopoietic and epithelial cells display a CD44 variant positive phenotype during embryonic development and lymphocyte maturation and activation (Weber et al, 1996), adult CD44 variant expression is confined predominantly to the skin (Haggerty et al. 1992; Tuhkanen et al. 1997), squamous and epithelia and ductal parts of the glands (Gansauge et al. 1995) and proliferating cells of epithelial tissues (Mackay et al. 1994). Various cell types have been identified which do not appear to express any of the CD44 isoforms amongst which include: hepatocytes, pancreatic acinar cells, adrenal glands, striated muscle, astrocytes and epithelium of the stromal intestine (Terpe et al. 1994; Mackay et al. 1994).

CD44 proteins have been shown to mediate a diverse array of physiological cellular and tissue functions including: embryonic development (Sherman et al. 1996; Wainwright et al. 1996), haematopoiesis (Lewinsohn et al. 1990; Rossbach et al. 1996), lymphocyte homing (Goldstein et al. 1989; Stamenkovic et al. 1989) and

migration (Bourguignon et al. 2001; Subramaniam et al. 2007; Donatello et al. 2012), leucocyte activation (Huet et al. 1989), effector functions and activation induced cell death (AICD) (McKallip et al. 2002), angiogenesis (Griffioen et al. 1997; Cao et al. 2006) and cell adhesion (Aruffo et al. 1990; Bjorklund et al. 2013) and neoplasia (Gunthurt et al. 1991; Bartolazzi et al. 1994; Cho et al. 2012; Montgomery et al. 2012). Surprisingly, despite the well-defined role for CD44 in many physiological processes, CD44 null mice remain viable and develop normally showing only mild phenotypic abnormalities (Schmits et al. 1997; Protin et al. 1999) potentially suggesting a compensatory mechanism for loss of CD44. However, the effects of CD44 deletion in response to wound repair (Huebener et al. 2008), inflammatory diseases (Pure and Cuff et al. 2001; Teder et al. 2002) and tumour prone mice/tumour progression (Gunthurt et al. 1991; Foekens et al. 1999; Lopez et al. 2005; Louderbough et al. 2011) are prominent, suggesting that the main role of CD44 may be in response to environmental insult and disease progression.

A large body of evidence has been gathered to support the finding of aberrant CD44 variant expression in cancer; however this area remains largely controversial due to contradictory findings. Indeed, multiple studies have established a role for CD44 variants (and in some instances upregulated expression of CD44 Std) in tumour progression and correlation with poor prognosis in many cancers including: breast carcinomas (Kalish et al. 1999; Herrera-Gayol and Jothy 1999a; Ma et al. 2005; Afify et al. 2009; Yae et al. 2012), colorectal carcinomas (Kuniyasa et al. 2002; Misra et al. 2011; Saito et al. 2013), pancreatic cancer (Takada et al. 1994; Gotoda et al. 1998), ovarian cancer (Jaggupilli and Elkord 2012; Shi et al. 2013) and cancers of the prostate

(Hao et al. 2010; Ni et al. 2014; Tei et al. 2014) and brain (Marzese et al. 2014). However, conversely, the absence of CD44 expression (including variant proteins) has been shown to confer poorer prognosis in prostate cancer (Aaltomaa et al. 2001; Gupta et al. 2013) and neuroblastomas (Shtivelman and Bishop 1991; Favrot et al. 1993).

Further, in recent years, CD44 has been established as a marker of cancer stem cells (CSCs) (in combination with other markers) in multiple carcinomas including: breast (CD44+/CD24-) (Al-Hajj et al. 2003; Honeth et al. 2008; Idowu et al. 2012), pancreas (CD44+/CD133+ or CD44+/CD24+) (Li et al. 2007; Soner et al. 2014), prostate (CD44+/CD133+) (Collins et al. 2005; Hurt et al. 2008; Lui et al. 2011), colon (CD44+/CD133+) (Du et al. 2008; Sahlberg et al. 2014), and gallbladder (CD44+/CD133+/CD24-) (Shi et al. 2010; Yin et al. 2011) where it has been reported to be associated with metastasis, chemo- and/or radioresistance, disease relapse and poor prognosis. However, whilst CD44 has been widely identified as a CSC marker in multiple organs, it remains unclear which isoforms of CD44 are specifically associated with the stem cell phenotype. Recent studies have shown that in particular, the presence of the CD44v6 isoform has been suggested to be a marker of CSCs in breast (Synder et al. 2009), pancreatic (Gaviraghi et al. 2011; Wang et al. 2013), prostate (Ni et al. 2014), colorectal (Todaro et al. 2014), bladder (Yang and Chang 2008) and tongue (Yanamoto et al. 2014) where it has been shown to contribute to tumour development and aggressive phenotype.

Overall these studies suggest a substantial role for CD44 as a marker of tumour initiating cancer stem cells and as a protein involved in multiple processes critical for

tumour progression behaviours, however results remain contradictory. Therefore additional analyses are required to further substantiate the role of individual isoforms within these processes and divulge the mechanisms through which these proteins may contribute to disease progression.

1.6.5 Therapeutic targetting of CD44 in cancer

In light of its strong association with disease progression and poor prognosis in many cancer types including breast cancer, CD44 could present as an attractive therapeutic target. Multiple groups have investigated the value of CD44 as a therapeutic target in numerous cancers through the use of various techniques including: monoclonal antibodies against CD44 proteins (Seiter et al. 1993; Koppe et al. 2004; Tijink et al. 2006), mimic peptides, miRNA therapies (Liu et al. 2011) or tumour specific nanocarriers/shRNA nanoparticles (Misra et al. 2009; Qian et al. 2013). Whilst these approaches have been met with some success in multiple cancers including pancreatic (Qian et al. 2013), colon (Misra et al. 2009) and prostate (Liu et al. 2011) their effectiveness in breast cancer remains limited. These limited successes may be due to the development of therapies designed to target total CD44 proteins and may suggest a requirement for more specified targetting of individual CD44 variant isoforms.

To reduce the off target effects of chemotherapeutic drugs in normal non-cancerous cells, researchers are investigating approaches in which to exploit the HA-binding properties of CD44 as a mechanism of localising drugs to specific sites and through which they can be endocytosed by cancer cells. HA is the principle ligand of CD44 and

is often found in abundance within the breast tumour stroma where it is correlated with poor prognosis (Auvinen et al. 2000; Auvinen et al. 2013). Recent studies have shown that these approaches have been met with some success in breast cancer cells highly expressing CD44 proteins (Ganesh et al. 2013; Yang et al. 2013) however more research is required before these treatments can be taken to clinical trials.

However in recent years, studies have tended to focus upon CD44 targetting in the context of CSCs, defined by their CD44⁺/CD24⁻ expression in breast cancer cells amongst other markers. This has been met with some success as Diessner et al. 2014 revealed that targetting breast CSCs with the new antibody drug conjugate T-DM1 (comprised of the potent chemotherapeutic agent, DM1, coupled with the HER2 targetted antibody, trastuzumab) led to the depletion of a pre-existing subset of CD44⁺/CD24⁻ stem cells and efficiently suppressed colony formation across a panel of breast cancer cell lines and primary tumours. Furthermore, therapies which act to induce differentiation of stem cells have shown that knockdown of CD44 in breast CSCs sensitised them to the anti-tumour drug doxorubicin and inhibited the 'stemness' and differentiation properties of these cells (Pham et al. 2011). Whilst Ginestier et al. 2009 revealed that modulation of retinoid signalling may be sufficient to induce differentiation of breast CSCs. Additionally, multiple pathways are known to play a fundamental role in the maintenance and regulation of stem cells, of which, the Notch signalling pathway has been well-established. Studies aiming to target this pathway have been met with success including McGowan et al. 2011 which revealed that inhibition of Notch1 signalling significantly reduced the CD44⁺/CD24^{-/low} subpopulation in a breast cancer cell line whilst also lowering the incidence of

metastases to the brain. In support of this, Harrison et al. 2010 revealed that inhibition of Notch4 mediated signalling decreased CSC populations in breast cancer cells whilst simultaneously inhibiting tumour initiation.

Taken together, these studies reveal promising results for CD44 proteins as candidates of novel therapeutic strategies for breast cancer. Therefore it is hoped that with the advent of breast CSC targetted therapies, specific targetting of CD44 variant isoforms and exploitation of the HA binding capacity of CD44 proteins, better therapies may become available in the future for the treatment of CD44+ breast cancer and patients who experience disease progression from endocrine-, chemo- and radio- therapies.

1.7 Aims and Objectives

CD44 expression has been extensively shown to become upregulated in numerous carcinomas where it correlates with an enhanced metastatic phenotype (Ma et al. 2005; Afify et al. 2009; Saito et al. 2013; Shi et al. 2013; Ni et al. 2014) however these findings are controversial due to contradictory results. One aspect of CD44 that may account for variability between studies is the extensive alternative splicing attributed to this molecule which may lead to the production of novel CD44 isoforms with enhanced migratory/invasive functions. At present there is no substantial data surrounding the role of CD44 variant isoforms in clinical endocrine resistance, however previous work by the Breast Cancer Molecular Pharmacology Group (BCMPG) showed elevated total CD44 expression in a model of acquired tamoxifen resistance which associated with an increase in their migratory capacity (Hiscox et al.

2012). Therefore, the overall goals of this thesis were to characterise CD44 variant isoform expression across cell models of acquired tamoxifen-resistance and further extend these studies into a model of fulvestrant-resistant breast cancer to explore the hypothesis that upregulation of specific CD44 isoforms in endocrine resistant breast cancer promote an aggressive phenotype. To achieve this, a number of objectives were decided:

1. To characterise CD44 isoform expression in endocrine sensitive and endocrine resistant breast cancer cells.
2. To determine whether CD44-overexpressing resistant cells were sensitised to their principle ligand, HA, leading to enhanced activation of receptor tyrosine kinases and augmented cellular behaviours.
3. To validate a potential link between CD44 and an adverse cellular phenotype in resistance by exploring the effects of CD44 suppression in endocrine resistant cells and investigating specific CD44 isoform overexpression upon the phenotype of endocrine sensitive cells.
4. To define a mechanism through which CD44 specific isoforms promote aggressive cellular behaviours.

2. Materials and Methods

2.1 Materials and reagents

The materials and reagents used for experimental procedures in this project and their source of purchase are listed in Table 2.1.

Materials/Reagents	Supplier
2-propanol (isopropanol)	Sigma-Aldrich, Poole, Dorset, UK
Acetic acid, glacial	Sigma-Aldrich, Poole, Dorset, UK
Acrylamide/bis-acrylamide (30 % solution, 29:1 ratio)	Sigma-Aldrich, Poole, Dorset, UK
Activated charcoal	Sigma-Aldrich, Poole, Dorset, UK
Agarose	Bioline Ltd, London UK
Alexa Fluor 488 conjugated secondary antibody (anti-rabbit)	Life Technologies, Inc. UK
Alexa Fluor 594 conjugated secondary antibody (anti-mouse)	Life Technologies, Inc. UK
Ammonium Persulphate (APS)	Sigma-Aldrich, Poole, Dorset, UK
Amphotericin B (Fungizone)	Invitrogen, Paisley, UK
Ampicillin	Sigma-Aldrich, Poole, Dorset, UK
Anti-mouse IgG HRP-linked antibody	Cell Signaling Technology, UK
Anti-rabbit IgG HRP-linked antibody	Cell Signaling Technology, UK
Antibiotics: Penicillin/Streptomycin	Life Technologies, Inc. UK
Aprotinin	Sigma-Aldrich, Poole, Dorset, UK
BamHI	New England Biolabs Inc, Ipswich, UK
BglIII restriction endonuclease	New England Biolabs Inc, Ipswich, UK
Bijou vials – sterile (5 ml)	Bibby Sterilin Ltd, Stone, UK
Bio-Rad Dc Protein Assay	Bio-Rad Laboratories Ltd, Herts, UK
Bovine serum albumin (BSA)	Sigma-Aldrich, Poole, Dorset, UK
Bromophenol Blue (BPB)	BDH Chemicals Ltd, Poole, UK
RPMI 1640 (containing Glutamine (200 mM) phenol-red-free RPMI 1640	Life Technologies Inc, UK
Sterile cell culture Corning plasticware (flasks, Petri-dishes, 24-, 48- and 96-well plates)	ThermoFisher Scientific, Leicestershire, UK
Cell scrapes	Greiner Bio-One Ltd, Gloucestershire, UK

Chemiluminescent Supersignal West HRP Substrate (Pico, Dura, Femto)	Pierce and Warriner Ltd, Chesire, UK
Chloroform	Sigma-Aldrich, Poole, Dorset, UK
Corning Standard Transwell inserts (6.5 mm diameter, 8 µm pore size)	Fisher Scientific, Leicestershire, UK
Coulter Counter counting cups and lids	Sarstedt AG and Co., Numbrecht, Germany
Crystal Violet	Sigma-Aldrich, Poole, Dorset, UK
Dako diaminobenzidine (DAB)/substrate chromogen system solution	Dako Ltd, Cambridgeshire, UK
Dako Envision+ system-HRP labelled polymer anti-mouse,	Dako Ltd, Cambridgeshire, UK
Dextran from <i>Leuconostoc spp.</i>	Sigma-Aldrich, Poole, Dorset, UK
DharmaFECT 1 Transfection Reagent	Thermo Scientific Dharmacon, GE Healthcare, UK
Disposable cuvettes	Fisher Scientific UK Ltd, Loughborough, UK
Di-thiothreitol (DTT)	Sigma-Aldrich, Poole, Dorset, UK
Deoxyribonucleotides (dNTPs)	Invitrogen, Paisley, UK
DPX mountant (06522)	Sigma-Aldrich, Poole, Dorset, UK
Dulbecco's Phosphate Buffered Saline	Sigma-Aldrich, Poole, Dorset, UK
Ethidium Bromide (EtBr)	Sigma-Aldrich, Poole, Dorset, UK
Ethylene diamine tetraacetic acid (EDTA)	Sigma-Aldrich, Poole, Dorset, UK
Ethylene glycol-bis(2-aminoethylether)-N,N,N',N'-tetraacetic acid (EGTA)	Sigma-Aldrich, Poole, Dorset, UK
Falcon tubes – sterile (15 ml and 50 ml)	Sarstedt AG and Co, Numbrecht, Germany
Fibronectin (from human plasma; 1 mg/ml in 0.05 TBS. pH 7.5)	Sigma-Aldrich, Poole, Dorset, UK
Filter paper (Grade 3)	Whatman, Maidstone, UK
Foetal calf serum (FCS)	Life Technologies Inc, UK
Formaldehyde solution	Sigma-Aldrich, Poole, Dorset, UK
FuGENE 6 transfection reagent	Promega, Southampton, UK
Gefitinib	Gift from Astrazeneca, UK
General laboratory glass and plastic ware	Fisher Scientific UK Ltd, Loughborough, UK
Glacial Acetic Acid	Fisher Scientific UK Ltd, Loughborough, UK
Glass coverslips (thickness no. 2, 22 mm ²)	BDH Chemicals Ltd, Poole, Dorset, UK
Glass slides (1.0 – 1.2 mm thickness)	Fisher Scientific UK Ltd, Loughborough, UK
Glycerol	Fisher Scientific UK Ltd, Loughborough, UK
Glycine	Sigma-Aldrich, Poole, Dorset, UK

Hydrochloric acid (HCl; 5M)	Fisher Scientific UK Ltd, Loughborough, UK
Hyperladder™ I and Hyperladder™ IV	Bioline Ltd, London, UK
Isoton II azide-free balanced electrolyte solution	Beckman Coulter Ltd, High Wycombe, UK
Kodak MXB Autoradiography film (blue sensitive; 18 cm x 24 cm)	Genetic Research Instrumentation (GRI), Rayne, UK
Lennox L Agar	Sigma-Aldrich, Poole, Dorset, UK
LB broth EZmix™ powder dust	Sigma-Aldrich, Poole, Dorset, UK
Leupeptin	Sigma-Aldrich, Poole, Dorset, UK
L-glutamine	Life Technologies Inc, UK
Liquid DAB ⁺ substrate chromogen substrate	DAKO, Cambridgeshire, UK
Lower buffer for SDS-PAGE Gels (Tris 1.5 M, pH 8.8)	Bio-Rad Laboratories Ltd, Hertfordshire, UK
Magnesium Chloride (MgCl ₂)	Sigma-Aldrich, Poole, Dorset, UK
Matrigel™ Basement Membrane Matrix	BD Biosciences, Oxford, UK
Max Efficiency DH5α™ <i>E.coli</i> competent cells	Life Technologies Inc, U
Methyl green (M8884)	Sigma-Aldrich, Poole, Dorset, UK
Micro-centrifuge tubes (0.5 and 1.5 ml)	Elkay Laboratory Products, Basingstoke, UK
Mineral oil PCR reagent	Sigma-Aldrich, Poole, Dorset, UK
Molony-murine leukemia virus (MMLV) reverse transcriptase enzyme	Promega, Southampton, UK
NEBuffer 3	New England Biolabs Inc, Ipswich, UK
N,N,N',N'-tetramethylene-diamine (TEMED)	Sigma-Aldrich, Poole, Dorset, UK
Nitrocellulose transfer membrane (Protran B85; 0.45 μm pore size)	Thermo Fisher Scientific, Leicestershire, UK
Normal goat serum (10 %)	Sigma-Aldrich, Poole, Dorset, UK
PCR Buffer (10X) without MgCl ₂	Sigma-Aldrich, Poole, Dorset, UK
Phenol	Sigma-Aldrich, Poole, Dorset, UK
Phenylarsine oxide	Sigma-Aldrich, Poole, Dorset, UK
Phenylmethylsulfonyl fluoride (PMFS)	Sigma-Aldrich, Poole, Dorset, UK
Phosphate buffered saline – sterile (PBS)	Life Technologies Inc, UK
Pipette tips	Greiner Bio-One Ltd, Gloucestershire, UK
Polyoxyethylene-sorbitan monolaurate (Tween 20)	Sigma-Aldrich, Poole, Dorset, UK
Ponceau S solution	Sigma-Aldrich, Poole, Dorset, UK
Potassium Chloride (KCl)	Sigma-Aldrich, Poole, Dorset, UK
Potassium di-hydrogen orthophosphate (KH ₂ PO ₄)	Fisher Scientific UK Ltd, Loughborough UK
Precision Plus Protein™ All Blue Standards (10 – 250 kDa)	Bio-Rad Laboratories Ltd, Hertfordshire, UK

Protein Assay Reagent A	Bio-Rad Laboratories Ltd, Hertfordshire, UK
Protein Assay Reagent B	Bio-Rad Laboratories Ltd, Hertfordshire, UK
Protein Assay Reagent C	Bio-Rad Laboratories Ltd, Hertfordshire, UK
pUC19 vector	Life Technologies Inc, UK
Random Hexamers (RH)	Amersham, Little Chalfont, UK
Recombinant RNasin Ribonuclease Inhibitor	Promega, Southampton, UK
Restore™ Western blot Stripping Buffer	
RNase-free H ₂ O	Sigma-Aldrich, Poole, Dorset, UK
Serological pipettes – sterile, disposable (5 ml, 10 ml, 15 ml)	Sigma-Aldrich, Poole, Dorset, UK
siRNA buffer (5X)	Thermo Fisher Scientific, Leicestershire, UK
Super Optimal broth with Catabolic repression (SOC) media	Life Technologies Inc, UK
Sodium Azide	Sigma-Aldrich, Poole, Dorset, UK
Sodium Chloride (NaCl)	Sigma-Aldrich, Poole, Dorset, UK
Sodium dodecyl sulphate (SDS)	Sigma-Aldrich, Poole, Dorset, UK
Sodium Fluoride (NaF)	Sigma-Aldrich, Poole, Dorset, UK
Sodium hydroxide (NaOH; 5M)	Fisher Scientific UK Ltd, Loughborough, UK
Sodium Molybdate (Na ₂ M ₁₀ O ₄)	Sigma-Aldrich, Poole, Dorset, UK
Sodium Orthovanadate (Na ₃ VO ₄)	Sigma-Aldrich, Poole, Dorset, UK
Solvents (acetone, chloroform, ethanol, formaldehyde, isopropanol, methanol)	Fisher Scientific UK Ltd, Loughborough, UK
Sucrose	Sigma-Aldrich, Poole, Dorset, UK
Syringe filters – sterile (0.2 µm)	Corning Inc, Corning, New York, USA
Syringe needles – sterile (BD Microbalance™ 3/25G x 5/8)	Becton Dickenson (BD) UK Ltd, Oxford, UK
Syringe needles – sterile (Sherwood Medical Monoject; 21G x 1 ₁ / ₂)	Sherwood Davis and Geck, Gosport, Hampshire, UK
Sucrose	Fisher Scientific UK Ltd, Loughborough, UK
T4 DNA ligase	New England Biolabs Inc, Ipswich, UK
T4 DNA ligase reaction buffer 10X	New England Biolabs Inc, Ipswich, UK
Taq DNA polymerase (BioTaq™; 5 U/µl)	Bioline Ltd, London, UK
Test tubes – sterile (5 mls)	Fisher Scientific UK Ltd, Loughborough, UK
TRI Reagent	Sigma-Aldrich, Poole, Dorset, UK
Tris HCl	Sigma-Aldrich, Poole, Dorset, UK

Tris-EDTA buffer solution (100X)	Sigma-Aldrich, Poole, Dorset, UK
Triton X-100	Sigma-Aldrich, Poole, Dorset, UK
Trizma (Tris) base	Sigma-Aldrich, Poole, Dorset, UK
Trypsin/EDTA 10x solution	Life Technologies Inc, UK
TWEEN20	Sigma-Aldrich, Poole, Dorset, UK
Universal containers – sterile (30 ml)	Greiner Bio-One Ltd, Gloucestershire, UK
Upper Buffer for SDS-PAGE gels (Tris 0.5 M, pH 6.8)	Bio-Rad Laboratories Ltd, Inc, Hertfordshire, UK
VectorShield hard-set mounting medium containing DAPI nuclear stain	Vector Laboratories, Inc, Peterborough Ukk
Western Blocking Reagent	Roche Diagnostics, Mannheim, Germany
Whatman qualitative filter paper, Grade 4 (diameter, 125 mm)	Sigma-Aldrich, Poole, Dorset, UK
X-ray film developer solution (X-O-dev)	X-O- graph Imaging System, Tetbury, UK
X-ray film fixative solution (X-O-fix)	X-O- graph Imaging System, Tetbury, UK

Table 2.1. A list of the materials and reagents used within this project and their source of purchase.

2.2 Cell culture

2.2.1 In vitro cell models of endocrine sensitive and endocrine resistant breast cancer

To model a hormone sensitive ER+ breast cancer, MCF-7 (Michigan Cancer Foundation-7) wild type cells (a gift from AstraZeneca Pharmaceuticals (Macclesfield, Cheshire, UK) and obtained from American Type Cell Collections (ATCC) Number HTB-22™) were maintained as a monolayer culture in vitro. The routine maintenance media used to culture MCF-7 cells was composed of: phenol-red pH indicator (RPMI-medium 1640) media containing glutamine (200 mM) and supplemented with 5 % (v/v) foetal calf serum (FCS) and 1 % antibiotics (Fungizone (2.5 µg/ml) and penicillin (100 IU/ml)/streptomycin (100 µg/ml)). For experimental comparison between cell lines, MCF-7 cells were transferred into experimental media composed of: phenol-

red-free pH indicator 1640 media (WRPMI) and supplemented with 5 % (v/v) charcoal-stripped foetal calf serum (SFCS), 2 % (v/v) L-Glutamine (200 mM) and 1 % antibiotics (Fungizone (2.5 µg/ml) and penicillin (100 UI/ml)/streptomycin (100 µg/ml)).

In vitro cell models of acquired-resistance to the endocrine agents, 4-hydroxytamoxifen (tamoxifen) and fulvestrant (trade name faslodex), were previously created by the Breast Cancer Molecular Pharmacology Group (BCMPG) through culturing MCF-7 cells in the presence of tamoxifen (100 nM) or fulvestrant (100 nM) respectively, for 6 months. Upon acquisition of endocrine resistance (as determined by the ability of the cells to grow in the presence of the endocrine agent) these cells were then maintained for a further 3 months to develop a stable resistant phenotype which could then be used for routine culture. MCF-7 cells which have acquired resistance to the endocrine agent tamoxifen are denoted as Tam-R cells. MCF-7 cells which have acquired resistance to the endocrine agent fulvestrant are denoted as Fas-R cells. Both the Tam-R and Fas-R cell lines used within these experimental studies are models of early acquired endocrine resistance and have been cultured for 18 months in their respective endocrine agent. Tam-R and Fas-R cells were routinely maintained in phenol-red-free pH indicator (WRPMI-medium 1640) supplemented with 5 % (v/v) charcoal-stripped foetal calf serum (SFCS), 2 % (v/v) L-Glutamine (200 mM), 1 % antibiotics (Fungizone (2.5 µg/ml) and penicillin (100 UI/ml)/streptomycin (100 µg/ml)) and 4-hydroxytamoxifen (100 nM) or fulvestrant (100 nM) respectively. The key molecular features and characteristics of all cell models used in this project are described in Table 2.2.

Cell Line	Molecular Subtype	ER status	PR status	Original source of cells	Tumour type
MCF-7	Luminal	+	+	Pleural effusion	Invasive ductal carcinoma
Tam-R	Luminal	+	+	Pleural effusion	Invasive ductal carcinoma
Fas-R	Luminal	-	-	Pleural effusion	Invasive ductal carcinoma

Table 2.2. Key molecular features and characteristics of the cell models used in this project (adapted from Neve et al., 2006).

2.2.2 Routine maintenance of in vitro cell models

For routine maintenance and experimental studies, all cell lines were grown under sterile conditions in a 37 °C/5 % CO₂ incubator (Sanyo MCO-17AIC incubators, Sanyo Gallenkamp, Loughborough, UK). Cell culture was carried out under sterile conditions in an MDH Class II laminar-flow safety cabinet (Bioquell UK Ltd, Andover, UK) and all equipment and consumables were either purchased sterile for single use or sterilised at 119 °C in a Denley BA825 autoclave (Thermoquest Ltd, Basingstoke, UK).

2.2.2.1 Cell passaging

Growth of the cell lines was visually assessed using a phase-contrast microscope (Nikon Eclipse TE200n, Nikon Ltd, Kingston-upon-Thames, UK). At 70 – 80 % confluency, cell lines were passaged through the aspiration of culture media and addition of 0.05 % trypsin (with 0.02% EDTA) to each flask. The flasks were then returned to the incubator for 3 – 5 minutes to allow complete cell detachment from the flask walls. The trypsin suspension containing the detached cells was then transferred to a universal tube where it was combined with an equal volume of routine maintenance media, the suspension was then centrifuged for 5 minutes at 1000 rpm (Mistral 3000i centrifuge, Sanyo Gallenkamp, Loughborough, UK). After

centrifugation, the supernatant was discarded and the pellet was resuspended in 10 ml of maintenance media and mixed gently. A 1:10 dilution of cell suspension to maintenance media was then dispensed into a clean flask and returned to the incubator. Flasks were subsequently replaced with fresh maintenance media every 3 days until harvesting for experimentation or further passaging was required. Cell lines were passaged in total for no more than 25 times and then discarded. Cell line stocks were stored in liquid nitrogen and thawed as necessary.

2.2.2.2 Setting up cells for experimental analysis

For experimental analysis, cells underwent the primary trypsin/EDTA dispersion, centrifugation and re-suspension steps as described above and were then passed through a sterile 25G syringe needle to obtain a single cell suspension. 100 µl of this cell suspension was added to 10 ml Isoton II solution and cells were counted using a Coulter Counter™ Multisizer (Beckman Coulter Ltd, High Wycombe, UK). Once cell number was determined, the appropriate volume of cells was combined with experimental media and seeded into sterile dishes at the required density.

2.2.3 Cell treatments

Cell lines were subjected to various treatments for experimental procedures in this project. Table 2.3 lists the treatment types along with their corresponding diluent and source of purchase. Details of the concentration and duration of these treatments are displayed in the figure legends throughout the results chapters.

Treatment	Diluent	Source
Tamoxifen	Ethanol	Sigma-Aldrich, UK
Faslodex	Ethanol	AstraZeneca, UK
Oestradiol	Ethanol	AstraZeneca, UK
Charcoal Stripped FCS	-	In-house (Appendix A)
Gefitinib	Ethanol	AstraZeneca, UK
Epidermal Growth Factor (EGF)	PBS containing 0.1% BSA	Sigma-Aldrich, UK
Hyaluronan	RPMI/WRPMI	R&D Systems, UK

Table 2.3. A list of the cell treatments used within this project along with their corresponding source of the purchase and diluents used for storage.

2.3 Microarray analysis

Prior to this project, RNA samples from all cell models routinely maintained by the BCMPG cell culture staff were obtained in triplicate and sent to the Cardiff University Central Biotechnology Services (CBS) to be microarrayed and gene expression analysis using the resultant data was used as a focus of this project. Initial assessments were performed on samples of the cell models by the CBS to determine the quality (analysis of degradation or contamination) of RNA and once satisfied these samples were run on Affymetrix Human Genome U133A gene chips containing approximately 23, 000 gene probes. The Affymetrix suite 5.0 programme used for microarray analysis provides powerful algorithms that analyse the data and generate appropriate analysis output files for subsequent analysis. The triplicate raw data obtained from microarraying was then uploaded onto the online bioinformatics software programme GeneSifter (<https://login.genesifter.net/>) where median normalisation across all datasets and log transformation was performed. Log₂ intensity plots were also generated by this programme to visualise gene expression changes across the models and fold change calculations for each gene were

performed. In some instances, the Affymetrix U133A gene chips contained more than one gene probe for each gene therefore particular importance was placed on the 'Jetset' gene probe. Jetset is an online software programme created by the Technical University of Denmark which allocates each gene probe used for affymetrix analysis with a score (ranging from 0 – 1) determined by their performance across three parameters: i) specificity of the probe to bind to the target sequence, ii) ability of the probe to detect as many splice isoforms of the target gene as possible to estimate overall gene expression and iii) the degradation resistance of each probe (robust score). This tool then combines these scores to determine the best overall performing probe (on a scale of 0 – 1, with a score closer to 1 showing the best performance) for a given gene which is termed the 'Jetset' probe and identifies the most reliable profile in the array for the gene of interest (see Appendix B for further information) (Li et al. 2011). Expression 'call' for all gene probes assessed by microarraying was also analysed using the GeneSifter programme via the 'detection call' algorithm to determine the reliability of transcript expression. A detection call of 'absent' suggests unreliable or low/no detection of gene expression whilst 'present' suggests existing/reliable gene expression across the cells and 'mixed' represents partial detection of gene expression. In this project, for each gene analysed, GeneSifter was used to create a heatmap expression profile and corresponding log₂ intensity plot for each Jetset probe along with their fold change values. Statistical significance was determined by ANOVA analysis with Tukey post-hoc testing and significance was set at $p < 0.05$. In this project, data created from microarraying and subsequent online analysis was used to explore the endogenous

gene expression of CD44, HMMR, LYVE-1, TL4, STAB2, ICAM-1, VCAN, HAS1, HAS2, HYAL1, HYAL2 and HYAL3 across MCF-7, Tam-R and Fas-R cells. All microarray and subsequent statistical analysis was performed by the CBS and the BCMPG statistician Lynne Farrow respectively.

2.4 Kaplan Meier plotter analysis

The Kaplan Meier (KM) plotter is a publically available online database tool (<http://kmplot.com/analysis/>) which was used in this project to assess the relationship between the expression levels of CD44 and clinical outcome with endocrine therapy. The KM plotter interrogates Affymetrix microarray chip-derived mRNA expression data accumulated from breast cancer patients prior to therapy in relation to survival outcome measures (Györfy et al. 2010). The database utilises this information to derive survival plots which are used to relate gene expression levels to clinical outcome by splitting patients into two groups based on various quantile expression of the proposed gene and integrating this data simultaneously with clinical data (Györfy et al. 2010). In this project, KM survival curves were generated to examine the clinical relevance of CD44 gene expression in an ER+ breast cancer patient cohort where any endocrine treatment (n=1190) or tamoxifen treatment alone (n=615) was known with up to 20 year follow up, to determine the relationship between CD44 and overall survival (OS) and relapse-free survival (RFS). All analyses were generated using the Jetset Affymetrix CD44 gene probe (212063_at) and output was displayed as KM survival curves with associated Hazard ratio (HR) and significance value (log rank $p < 0.05$).

2.5 Reverse transcription polymerase chain reaction (RT-PCR) analysis

2.5.1 RNA extraction

MCF-7, Tam-R and Fas-R cells were seeded into 150 mm dishes at a density of 3.4×10^6 cells/dish and cultured until 70 – 80 % confluency. Media from the dishes was removed and cells were washed twice with 10 ml tissue culture grade PBS (1X). 1 ml TRI Reagent/10 cm² surface area was added to each dish and gently rocked for 1 minute to ensure complete coverage. Cell lysates were then collected using a sterile disposable cell scraper, transferred into a 1.5 ml eppendorf tube and equilibrated for 5 minutes at room temperature. 200 µl Chloroform/1 ml TRI Reagent was added to the lysates followed by brief vortexing (20 seconds) and incubation at room temperature for 10 minutes. Lysates were then placed into a pre-cooled centrifuge (Labofuge 400R centrifuge, Heraeus, Germany) and spun for 15 minutes at 4 °C, 12, 000 rpm. After centrifugation, the lysate separates into 3 phases; the upper aqueous phase containing the RNA, the middle layer containing the DNA and the lower phenolic phase containing proteins. The upper aqueous phase of each supernatant was carefully removed without disturbing the interface to avoid genomic DNA contamination and transferred to a clean 1.5 ml eppendorf tube. 500 µl isopropanol was added to each tube and briefly vortexed before incubation at room temperature for 10 minutes to precipitate the RNA. The samples were then returned to the centrifuge and spun at 12, 000 rpm, 4 °C for 15 minutes. The supernatant was removed from the tubes and the RNA pellet was washed in 1 ml 75 % ethanol. Samples were then briefly vortexed and centrifuged at 7, 500 rpm, 4 °C for 5 minutes. Ethanol was discarded from the tubes and the RNA pellets were air dried for 5

minutes and re-dissolved in 20 μ l RNase-free distilled water. RNA concentration (μ g/ml) and purity was quantified by diluting 1 μ l RNA in 499 μ l RNase-free water and absorbance was measured at 260 nm (A_{260}) on a spectrophotometer (Cecil CE2041, Cambridge UK) based on the following formula: $RNA = A_{260} \times 40 \times \text{dilution factor}$. A ratio of 1.8 – 2.0 represented pure preparations of RNA. RNA integrity was assessed via gel electrophoresis for each sample. Intact RNA would lead to the formation of two bands identifying the 18S and 28S ribosomal RNA with a smear in between denoting mRNA of different sizes. Intact RNA was observed in all samples examined in this project. Samples were stored at -80°C .

2.5.2 Reverse transcription

This procedure converts isolated RNA molecules into their complementary DNA (cDNA) which is required for RT-PCR experiments. For each reverse transcription reaction, 1 μ g RNA (diluted to a total volume of 7 μ l in sterile RNase-free water) was added to 11.5 μ l master mix solution in an sterile eppendorf tube on ice comprising of: 5 μ l dNTPs (2.5 mM), 2 μ l 10 x PCR buffer (10 mM Tris-HCl, pH 8.3, 50 mM NH_4 , 0.001 % w.v gelatin), 2 μ l Dithiothreitol (DTT), (0.1 M), 2 μ l random hexamers (100 μ M), 0.5 μ l MgCl_2 (50 mM). Samples were then denatured at 95°C for 5 minutes in a PTC-100 thermocycler (MJ Research Ltd, USA) and rested on ice for 5 minutes. The samples were then pulse spun in a microfuge (Biofuge, Heraeus, Germany) and returned to ice. To each reaction, 1 μ l Molony-murine leukemia virus (MMLV) (200U/ μ l) reverse transcriptase enzyme and 0.5 μ l commercial RNase inhibitor RNasinTM (40U/ μ l) was added to give a final volume of 20 μ l. Samples were then transferred to the thermocycler and reverse transcribed using the following

parameters: annealing at 22 °C for 10 minutes, reverse transcriptase extension at 42 °C for 40 minutes, denaturation at 95 °C for 5 minutes. The resultant cDNA was then stored at - 20 °C.

2.5.3 Oligonucleotide primer design

The oligonucleotide primers used for RT-PCR analysis were designed using the Invitrogen OligoPerfect™ Designer software (<http://tools.lifetechnologies.com/content.cfm?pageid=9716>) using the CD44 (Appendix C) and HMMR (Appendix D) gene sequences obtained from the National Centre for Biotechnology Information (NCBI) online database (<http://www.ncbi.nlm.nih.gov/>). This programme allowed the consideration of product size, melting temperature and likelihood of undesirable primer-dimer formation between the primer pairs. Table 2.4 lists the target gene along with the corresponding designed forward and reverse primer sequences, parameters required for the RT-PCR reaction and expected product sizes. Once primer pairs were selected, these sequences were inputted into the online bioinformatics programme Basic Local Alignment Search Tools (BLAST) (<http://blast.ncbi.nlm.nih.gov/>) which allowed similarity comparison of the primer sequences to other DNA sequences across the human genome. BLAST analysis confirmed the high level of specificity of these primers to the gene of interest for all primer pairs used within this project.

Gene	Forward Sequence	Reverse Sequence	RT-PCR reaction	Expected product size
CD44 Std	5'-GACACATATTGC TTCAATGCTTCAGC-3'	5'-GATGCCAAGATGAT CAGCCATTCTGGAAT-3'	61 °C 30 cycles	482 – 1496 bp
CD44v3	5'-CGTCTTCAAAT ACCATCTCAGC-3'	5' TCATCATCAA TGCCTGATCC-3'	60 °C 29 cycles	100 bp
CD44v6	5'-CAACGGAAGA AACAGCTACCC-3'	5' CCTGTTGTCG AATGGGAGTC-3'	61 °C 30 cycles	100 bp
CD44v10	5'-GGAATGATGTCA CAGGTGGA-3'	5'-AAGGTCCTGCT TTCCTTCGT-3'	57 °C 29 cycles	109 bp
HMMR	5'-TGCAGCTCAG GAACAGCTAA-3'	5'-GCTGACAGCGG AGTTTTGAT-3'	60 °C 29 cycles	149 bp
β-actin	5'-GGAGCAATGATC TTGATCTT-3'	5'-CCTTCCTGGGCA TGGAGTCCT-3'	55 °C 27 cycles	204 bp

Table 2.4. A list of each target gene along with their corresponding forward and reverse primer sequences, reaction conditions used for RT-PCR analysis and expected product size.

2.5.4 RT-PCR analysis

RT-PCR reactions were performed in 0.5 ml sterile eppendorf tubes containing a total volume of 25 µl consisting of 0.5 µl cDNA and 24.5 µl master mix solution for each sample. The master mix was prepared on ice and contained: 2 µl dNTPs (2.5 mM), 2.5 µl 10X PCR buffer (10 mM Tris-HCl pH 8.3, 50 mM KCl, 1.5 mM MgCl₂ and 0.001 % w/v gelatin), 0.625 µl forward primer (20 µM), 0.625 µl reverse primer (20 µM), 0.2 µl Taq DNA polymerase (5 U/µl) and 18.6 µl sterile RNase free water. For each RT-PCR reaction, an eppendorf containing the master mix solution without the cDNA was used as a negative control. The reaction mixture was briefly vortexed and a drop of sterile mineral oil was placed on top of the solution to prevent evaporation during the reaction. The samples were then placed into a PTC-100 thermocycler (MJ Research Ltd, Massachusetts, USA). Table 2.5 reveals the thermocycle parameters performed for RT-PCR detection and describes the optimal conditions required for

the detection of each target gene. To visualise the results of the RT-PCR, the samples were electrophoresed on a 2 % agar gel (2 g agar, 100 ml 1X Tris Acetate (TAE) buffer (20 ml 50X TAE buffer (242g Tris, 57.1 ml glacial acetic acid, 100 ml 0.5 EDTA, 1 L distilled water, pH 8.3) diluted in 1 L distilled water), 1 µl ethidium bromide). The set agar gels were placed into a Mini-Sub Cell GT electrophoretic tank (Bio-Rad Laboratories Ltd, Hertfordshire, UK) filled with 1 X TAE buffer. To 9 µl RT-PCR product was added 5 µl loading buffer (6 g sucrose, 2 mg bromophenol blue, 10 ml distilled water) and pipetted into the wells of the 2 % agar gel and 5 µl hyperladder IV was used as a marker. The electrophoresis reaction was allowed to run for 1 hour at 75 volts constant. RT-PCR products were visualised and photographed using a Bio-Rad GS-690 Imaging Densitometer (Bio-Rad Laboratories Ltd, Hertfordshire, UK). Qualitative quantitation of RNA bands was performed using densitometry analysis (ImageJ software programme) (Appendix E).

Phase	Step	Temperature (°C)	Duration	Cycle Number
1	denaturing annealing extension	95 dependent on target gene 72	2 minutes 1 minute 2 minutes	1 x
2	denaturing annealing extension	94 dependent on target gene 72	1 minute 30 seconds 1 minute	dependent on target gene
3	denaturation	94	1 minute	1 x
4	final extension	60	7 minutes	1 x

Table 2.5. Thermocycle program conditions required for RT-PCR amplification.

2.6 Western Blotting analysis

2.6.1 Cell lysis

For cell lysis, protease inhibitors were added immediately before use to the required volume of lysis buffer (0.61 g TRIS base (50 mM), 0.19 g EGTA (5 mM), 0.875 g NaCl (150 mM), 1 ml 1 % TritonX-100 (diluted in 1X PBS), 100 ml distilled water, pH 7.6) on ice (Table 2.6). Cells were then removed from the incubator, placed onto ice and briefly washed 3 times with PBS (1X) ensuring thorough drainage on the final wash. A sufficient volume of lysis buffer (dependent on cell container volume and cell density) to cover the surface of the culture dish was added and the cell material was collected using a disposable cell scraper and transferred into a 1.5 ml eppendorf. The cell lysate was incubated on ice for 5 minutes before centrifugation at 12, 000 rpm, 4 °C for 15 minutes to remove insoluble cell debris. The resultant supernatant was then transferred to a clean eppendorf and stored at – 20 °C.

Inhibitor	1 ml Lysis Buffer	Final Concentration
Sodium Orthovanadate (100 mM)	20 µl	2 mM
Sodium Fluoride (2.5 M)	20 µl	50 mM
Phenylmethylsulfonyl (100 mM)	10 µl	1 mM
Sodium molybdate (1M)	10 µl	10 mM
Phenylarsine (20 mM)	1 µl	20 µM
Leupeptin (5 mg/ml)	2 µl	10 µg/ml
Aprotinin (2 mg/ml)	4 µl	8 µg/ml

Table 2.6. The volume of protease inhibitors required for 1 ml Lysis Buffer for cell lysis.

2.6.2 Bio-Rad Detergent Compatible protein assay

The concentration of total soluble protein contained within the collected cell lysates was determined using a Bio-Rad colorimetric Detergent Compatible (DC™) protein assay which is a modified version of the Lowry protein assay (Lowry et al. 1951;

Peterson 1977). A standard curve was prepared in duplicate using 1.45 mg/ml BSA stock diluted in lysis buffer (described in Table 2.7). To each 1 ml cuvette was added, 5 μ l cell lysate diluted in 45 μ l of lysis buffer. 250 μ l Protein Assay Reagent A (containing 5 μ l Protein Assay Reagent S) was then added to each cuvette followed by 2 ml Protein Assay Reagent B. The contents of the cuvettes were thoroughly mixed by pipetting and allowed to incubate for 5 minutes. The absorbance of the standard curve and cell lysate samples was then measured at 750 nm using a spectrophotometer (Cecil CE2041 Spectrophotometer, Cecil Instruments, Cambridge, UK) to obtain the total amount of protein contained within each lysate.

BSA Concentration	BSA Stock (1.45 mg/ml)	Lysis Buffer Solution
0 mg/ml	0 μ l	50 μ l
0.247 mg/ml	8.5 μ l	41.5 μ l
0.508 mg/ml	17.5 μ l	32.5 μ l
0.754 mg/ml	26 μ l	24 μ l
1.0 mg/ml	34.5 μ l	15.5 μ l
1.45 mg/ml	50 μ l	0 μ l

Table 2.7. The volume of BSA stock (1.45 mg/ml) and lysis buffer solution required for the final BSA concentration to generate a standard curve for a Bio-Rad Detergent Compatible protein assay.

2.6.3 Preparation of samples for SDS-PAGE

To prepare samples for SDS-PAGE, 3x Laemmli loading buffer (400 μ l distilled water, 3 ml SDS (20 %), 3 ml Glycerol, 3.6 ml TRIS base (0.5 M), 2 mg bromophenol blue, 24 mg/ml dithiothreitol (DTT)) was added to each lysate. The volume of loading buffer added to each sample was calculated as 50 % of the total cell lysate volume. The lysates were then placed into a heating block for denaturation (Techne DRI-Block DB.2, Bibby Scientific Limited, Staffordshire, UK) and boiled at 100 °C for 5 minutes. Samples were briefly centrifuged for 5 seconds and stored at - 20°C.

2.6.4 SDS-PAGE analysis

Each gel for SDS-PAGE analysis was prepared as follows: 2 x 1.5 mm glass plates were cleaned with 70 % ethanol and placed into a casting stand (Bio-Rad Laboratories Ltd, Hertfordshire, UK). An 8 % resolving gel was prepared (Table 2.8) and poured between glass plates until $\frac{3}{4}$ full and overlaid with distilled water to prevent evaporation and produce a sharp interface between the resolving gel and stacking gel. Once set, the overlaying water was removed and a 4 % stacking gel was then prepared (Table 2.8) and poured on top of the resolving gel. A 10 or 15 well (1.5 mm) moulding comb (Bio-Rad Laboratories Ltd, Hertfordshire, UK) was then inserted into the stacking gel. The set gel/glass plate cassette was then assembled into the inner chamber of the electrophoresis unit as per manufacturer's instructions (Bio-Rad Mini-Protean III apparatus power pack, Bio-Rad Laboratories Ltd, Hertfordshire, UK) and the inner and outer reservoir of the tank was filled with SDS-PAGE 1X running buffer (3.03 g TRIS Base, 14.4 g glycine, 1 g SDS in 1 L distilled water, pH 8.3). 5 μ l protein molecular weight marker (Precision Plus Protein™ All Blue Standards (10 – 250 kDa)) was loaded into the first lane of the gel followed by 20 - 40 μ g of cell lysate into the proceeding wells. Electrophoresis was performed at 120 volts constant current for approximately 90 minutes or until the marker reached the bottom of the gel.

Substrate	8 % Resolving Gel	4 % Stacking Gel
Distilled water	4.6 ml	3.05 ml
Lower buffer (1.5 M Tris pH 8.8)	2.5 ml	-
upper buffer (0.5 M Tris pH 6.6)	-	1.25 ml
30 % acrylamide/bis Acrylamide (29:1)	2.7 ml	650 μ l
10 % SDS (in distilled water)	100 μ l	50 μ l
10 % APS (in distilled water)	100 μ l	25 μ l
TEMED	10 μ l	3 μ l

Table 2.8. The volume of substrates required to produce one electrophoresis gel with an 8 % resolving gel and a 4 % stacking gel.

2.6.5 Western Blotting transfer

Proteins separated by SDS-PAGE were transferred onto a protran B85 nitrocellulose membrane (0.45 μ m pore size) using a Bio-Rad Protean III Mini Trans Blot apparatus (Bio-Rad Laboratories Ltd, Hertfordshire, UK). For each gel, a Western blot transfer cassette was assembled by placing a Teflon sponge fibre pad onto the side of the negative electrode followed by two filter papers, a nitrocellulose membrane cut to the size of the gel, SDS-PAGE electrophoresis gel, two filter papers and a Teflon sponge fibre pad (depicted in Figure 2.1). All components were pre-soaked in transfer buffer before assembly (800 ml distilled water, 3.03 g TRIS base, 14.4 g glycine, 200 ml methanol). The cassette was then inserted into the Trans Blot module with the gel positioned nearest to the negative electrode. The module was then placed into a tank containing transfer buffer along with an ice block and a magnetic stirrer to maintain an even temperature and ion distribution. The transfer process was performed at 100 volts constant current for 60 minutes for sufficient protein transfer.

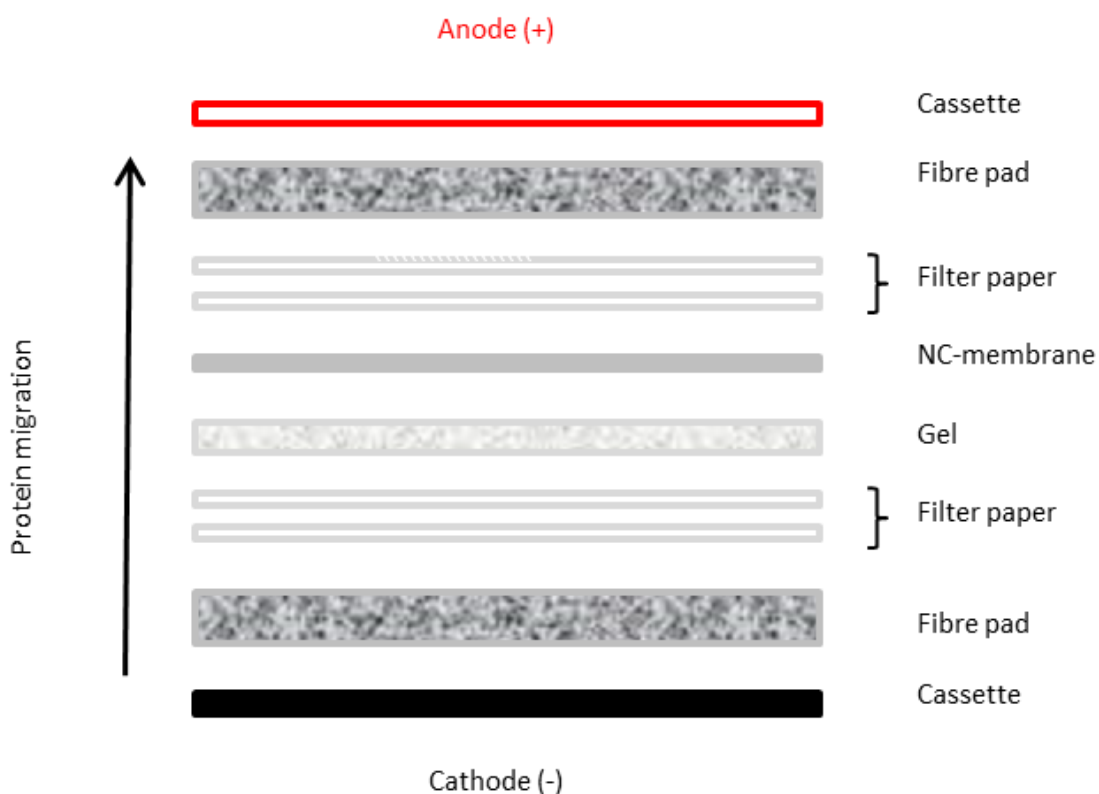


Figure 2.1. A diagram to show the assembly of a Western blotting transfer apparatus. NC-membrane represents the nitrocellulose membrane.

2.6.6 Immunoprobing of Western blots

The nitrocellulose membrane onto which the proteins were transferred was then removed from the transfer apparatus and washed briefly with 10 ml 1X Tris-Buffered Saline-Tween (TBS-Tween) (1.2 g TRIS Base, 8.7 g NaCl, 50 µl Tween20, pH 7.6 in 1 L distilled water). To assess the efficiency of protein transfer and loading, the membrane was briefly incubated in 10 ml Ponceau S solution (475 ml distilled water, 25 ml acetic acid, 0.5 g Ponceau S powder) to stain the proteins. The membrane was subsequently washed with 1X TBS-Tween until the Ponceau S stain was completely removed. A blocking step was performed using 25 ml/membrane of 5 % non-fat dried

dry skimmed milk (Marvel) in 1X TBS-Tween (w/v) for 1 hour at room temperature on a rocking platform. The nitrocellulose membrane was then incubated on a roller bed at 4° C overnight or for 1 hour at room temperature with the appropriate primary antibody solution (9.5 ml 1X TBS-Tween, 500 µl Western blotting reagent, 100 µl sodium azide (1M) and diluted primary antibody). The dilution for each primary antibody used in this project is listed in Table 2.9 along with the corresponding antibody host species, incubation conditions, predicted molecular weight and source of purchase. Following incubation, the nitrocellulose membrane underwent 3 x 5 minute washes with 1X TBS-Tween before incubation with a 1:10, 000 dilution of secondary antibody solution (0.1 g marvel dry skimmed milk, 10 ml 1X TBS-Tween, 1 µl anti-mouse/anti-rabbit IgG HRP-secondary antibody) at room temperature for 1 hour. Following incubation, the membrane underwent 4 x 5 minute washes with 1X TBS-Tween. Chemiluminescence was then performed using the appropriate luminol/peroxide based enhanced chemiluminescent (ECL) reagent (SuperSignal™ West Pico (high sensitivity), Supersignal™ West Dura (medium sensitivity) or Supersignal™ West Femto (low sensitivity)). The membrane was placed into a clean light-proof cassette and sufficient ECL reagent (prepared according to manufacturer's instructions) to cover the blot (100 – 250 µl) was pipetted onto the membrane. X-ray films were exposed to the membranes for different lengths of time to obtain the optimal signal emitted from the protein of interest bound to the membrane. The X-ray films were then developed using an X-O-graph compact X2 X-ray developer (Konica Minolta SRX-101A, Photon Imaging Systems Ltd, Wiltshire, UK).

X-ray films were scanned and quantitation of protein bands was performed using densitometry analysis (ImageJ software) (Appendix E).

2.6.7 Primary antibody stripping of nitrocellulose membranes

For detection of proteins on the same nitrocellulose membrane with a similar/identical molecular weight (e.g. phospho- and total proteins) the membrane was stripped of primary and secondary antibodies before being re-probed. After the initial immunoblotting procedure was completed, the nitrocellulose membranes underwent 2 x 5 minute washes in 1X TBS-Tween, followed by 2 x 5 minute washes in distilled water. The membranes were then immersed in 10 ml Restore™ Western blot Stripping Buffer (Thermo Fisher Scientific, UK) and incubated on a rocker for 10 minutes at room temperature, followed by 2 x 5 minute washes in 1X TBS-Tween. To ensure the primary antibody had been completely removed, the membrane was re-probed with secondary antibody (as described above) and underwent immuno-detection. If no signal was emitted from the membrane using the appropriate ECL-chemiluminescent reagent, it was assumed that the stripping protocol was successful. Nitrocellulose membranes were then probed with alternative primary and secondary antibodies and immuno-detection was carried out as described above.

Antibody	Host species	Incubation conditions	Dilution	MW (kDa)	Source of Purchase
CD44 Standard (Clone 156-3C11)	Mouse	O/N 4 °C	1:1000	80	Fisher Scientific, UK
anti-CD44v3 (Clone VFF-327)	Mouse	O/N 4 °C	1:1000	85 – 250	R&D Systems, UK
anti-CD44v6 (Clone 2F10)	Mouse	O/N 4 °C	1:1000	85 - 250	R&D Systems, UK
anti-CD44v10 (Clone VFF-14)	Mouse	O/N 4 °C	1:1000	90 - 250	Thermo Fisher Scientific, UK
anti-RHAMM/CD168	Rabbit	O/N 4 °C	1:1000	25 - 85	Abcam, UK
phospho-HER2/ErbB2 (Y1248)	Rabbit	O/N 4 °C	1:1000	185	CST, UK
Total HER/ErbB2	Rabbit	O/N 4 °C	1:1000	185	CST, UK
phospho-EGFR (Y1068)	Rabbit	O/N 4 °C	1:1000	175	CST, UK
Total EGFR	Rabbit	O/N 4 °C	1:1000	175	CST, UK
phospho-c-Met (Y1234/1235)	Rabbit	O/N 4 °C	1:1000	145	CST, UK
Total c-Met	Rabbit	O/N 4 °C	1:1000	145	CST, UK
phospho-FAK (Y397)	Rabbit	O/N 4 °C	1:1000	125	CST, UK
Total FAK	Rabbit	O/N 4 °C	1:1000	125	CST, UK
phospho-AKT (S473)	Rabbit	O/N 4 °C	1:1000	60	CST, UK
Total AKT	Rabbit	O/N 4 °C	1:1000	60	CST, UK
Phospho-Src (Y416),	Rabbit	O/N 4 °C	1:1000	60	CST, UK
Total Src	Rabbit	O/N 4 °C	1:1000	60	CST, UK
phospho-ERK1/2 (T202/Y204)	Rabbit	O/N 4 °C	1:1000	42,44	CST, UK
Total ERK1/2	Rabbit	O/N 4 °C	1:1000	42,44	CST, UK
β-actin	Mouse	1 hr RT	1:20000	45	CST, UK
GAPDH	Mouse	1 hr RT	1:15000	37	CST, UK

Table 2.9. A list of primary antibodies used for Western blotting analysis in this project with their corresponding dilution, host species, incubation conditions, predicted molecular weight (MW) (kDa) and source of purchase. The abbreviations represent Cell Signalling Technology, UK. (CST, UK), overnight (O/N) and room temperature (RT).

2.7 Immunocytochemistry

Log phase cells were seeded into 35 mm dishes containing Tespa-coated (Appendix F) glass coverslips at a density of 2×10^5 cells/dish and allowed to grow to 70 – 80 % confluency. After incubation the media was removed from the dishes and cells were fixed in 1 ml 2.5 % phenol formal saline (0.25g phenol dissolved in 10 ml formal saline solution (1.8 g NaCl, 20 ml formaldehyde, 180 ml tap water)) for 5 minutes. Cells were then washed with 1 ml 100 % ethanol for 5 minutes followed by 2 x 5 minute washes in 1 ml 0.02 % PBS/Tween (100 μ l Tween20 diluted in 500 ml PBS (0.1 M)). To each coverslip, 50 μ l primary antibody diluted in 1 % BSA/PBS (CD44 Std: 1/1200, CD44v3 (1/40), CD44v6 (1/40), CD44v10 (1/50), RHAMM (1/50)) was added for 60 minutes. Cells were then washed with 0.02 % PBS/Tween for 2 x 5 minutes. Secondary antibody detection was performed by adding 50 μ l/coverslip Dako mouse EnVision (Dako Envision+ system-HRP labelled polymer anti-mouse) for 30 minutes. Cells were then washed with 1 ml 0.02 % PBS/Tween for 2 x 5 minutes. Cells were then incubated with 50 μ l/coverslip Dako 2,3-diaminobenzidine (DAB)/substrate chromogen system solution for 8 minutes followed by 3 x 5 minute washes in 1 ml distilled water. Counterstaining was performed using 1 ml/dish 0.05 % methyl green (dissolved in water) for 10 minutes followed by 3 x 5 minute washes in distilled water. The coverslips were then dried in a heating and drying oven (Kelvitron^R t, Heraeus, Thermo Scientific, UK) for 1 hour and mounted onto glass microscope slides (1.0 – 1.2 mm) using di-butylphthalatexylene (DPX) mountant (a mixture of Distyrene, a plasticizer, and xylene).

2.7.1 Analysis of immunocytochemical and immunohistochemical staining using H-

Scoring

Cells were analysed using a light microscope (Olympus BH-2) at x10 magnification and photographs were taken at x20/x40 magnification. A modified histochemical score (H-score) method was used for semi-quantitative analysis of both the intensity and percentage positivity immunostaining of cells. For H-score evaluation, 6 fields of view/sample were analysed. To assess plasma membrane and cytoplasmic intensity, a score of 0 – 3 was given for each sample corresponding to negative (0), weak (1), moderate (2) and strong (3) immunostaining. The percentage plasma membrane and cytoplasmic immunostaining positivity was also estimated. Together these values were used to derive a total H-score value for each sample using the following formula: (% at 0) x 0 + (% at 1) x 1 + (% at 2) x 2 + (% at 3) x 3 to give an overall score ranging from 0 – 300. H-score evaluation has been successfully used for immunocytochemical and immunohistochemical analysis and TMA evaluation as seen in Rimm et al. 2001, Ginestier et al. 2002 and Callaby et al. 2003.

2.8 Immunofluorescence

Log phase cells were seeded into 35 mm dishes containing glass coverslips at a density of 2×10^5 /dish and allowed to grow until cells reached 70 – 80 % confluency. After incubation the media was removed and the cells were fixed in 1 ml 3.7 % formaldehyde (diluted in 0.01 M PBS) for 10 minutes. Cells were then briefly washed 3 times with 1 ml PBS (0.01 M). Permeabilisation was performed using 200 μ l/coverslip 0.2 % Triton-X 100 (diluted in 0.01 M PBS) for 8 minutes. Cells were then

briefly washed 3 times with 1 ml 0.01 M PBS. Blocking was performed using 200 μ l/coverlip 10 % normal goat serum (diluted in 1 % BSA in 0.01 M PBS solution) for 20 minutes. The washing step was repeated with PBS. Primary antibody detection was performed using 200 μ l/coverlip of appropriate antibody (1:100 dilution with 1 % BSA in 0.01 M PBS solution) for 30 minutes. The wash step with PBS was then repeated. Secondary antibody detection was performed using 200 μ l/coverlip Alexa Fluor 488 (anti-mouse) or 594 (anti-rabbit) conjugated secondary antibodies (1:1000 dilution in 1 % BSA in 0.1 M PBS solution) for 30 minutes. The wash step with PBS was repeated. Coverslips were drained and mounted onto slides using DAPI-containing Vectashield mountant. The cells were analysed using a fluorescent microscope (Leica DMil, Leica Microsystems Ltd, Milton Keynes, UK) at x63 magnification. For analysis, 6 fields of view/coverlip were photographed and cell immunofluorescence was quantitated using a previously published approach (Burgess et al. 2010, Gavet and Pines 2010 and Potapova et al. 2011), details of which are described in Appendix G.

2.9 Boyden Chamber migration assay

In vitro cell migration was measured using 24 well plates containing Corning Standard Transwell porous polycarbonate inserts (6.5 mm, 8 μ m pore size). Before use, the underside of each polycarbonate membrane was coated with 300 μ l fibronectin (10 μ l/ml) diluted in 1X tissue culture grade PBS (PBS) and incubated at 37 °C for 2 hours. Following coating, insert membranes were washed twice with PBS and allowed to air dry. 600 μ l of the appropriate experimental media (\pm treatments) was placed into the lower chamber of each well and air-dried inserts were placed into the wells taking care to avoid air bubble formation. Cells were then trypsinised and resuspended in

experimental media at 2×10^5 cells/ml and 200 μ l cell suspension was placed into the upper chamber of each insert to obtain a cell density of 40,000 cells/insert. Transwell plates were then returned to the incubator for 24 hours to allow cells to migrate to the underside of the membrane. Following incubation, the transwell plates were removed from the incubator and media contained in the upper chamber of the insert was removed using a pipette. Any cells remaining on the upper surface of the membrane (non-migratory cells) was removed by gentle swabbing using a cotton bud. Inserts were then placed into wells containing 600 μ l 3.7 % formaldehyde diluted in PBS for 10 minutes to fix cells that had migrated to the underside of the membrane. Following fixation, inserts were removed and washed twice with PBS (1X). Inserts were then added to wells containing 600 μ l 0.5 % crystal violet for 30 minutes to stain fixed cells for viewing under the microscope. Following staining, inserts were washed twice with PBS and allowed to air dry. Upon analysis using a light microscope (Olympus BH-2) at X20 objective, 6 fields of view/insert were assessed to obtain the average cell number count for each insert. Each determination represents the average of 3 individual experiments, each performed in duplicate.

2.10 Boyden Chamber invasion assay

In vitro cell invasion was measured using 24 well plates containing Corning Standard Transwell porous polycarbonate inserts (6.5 mm, 8 μ m pore size). Insert membranes were coated on their upper surface with 50 μ l Matrigel (9.6 mg/ml) (diluted in WRPMI (1:3)) and incubated at 37°C for 2 hours. 600 μ l of the appropriate experimental media (\pm treatments) was placed into the lower chamber of each well and air-dried inserts were placed into the wells taking care to avoid air bubble

formation. Cells were then trypsinised and resuspended in experimental media at 2×10^5 cells/ml and 200 μ l cell suspension was placed into the upper chamber of each insert to obtain a cell density of 50,000 cells/insert. Transwell plates were then returned to the incubator and cells were allowed to invade to the underside of the membrane for 3 days. Following incubation, the transwell plates were removed from the incubator and media contained in the upper chamber of the insert was removed using a pipette. The Matrigel and any remaining (non-invasive) cells was then removed from the upper surface of the membrane using a cotton bud by gentle swabbing. Inserts were then placed into wells containing 600 μ l 3.7 % formaldehyde in PBS (1X) for 10 minutes to fix cells that had invaded to the underside of the membrane. Following fixation, inserts were removed and washed twice with PBS (1X) and allowed to air dry for 1 hour. The membrane from each insert was then excised using a scalpel blade and placed cell side up onto a glass microscope slide (1.0 – 1.2 mm) containing a drop of DAPI-containing Vectashield hardset mountant. An additional drop of the Vectashield mountant was then added to the top of the insert and overlaid with a glass coverslip. The slides were allowed to set at room temperature and stored at 4 °C. For quantification of the number of cells that had invaded to the underside of each membrane, the slides were analysed using a fluorescent microscope (Leica DMil, Leica Microsystems Ltd, Milton Keynes, UK) and cell nuclei counts and photographs were taken from 6 fields of view at X63 magnification. Each determination represents the average of 3 individual experiments.

2.11 Coulter Counter proliferation assay

Log phase cells were harvested and seeded into a 24 well plate at a density of 1×10^6 cells/plate and returned to the incubator for 24 hours. Following incubation the media was removed and replaced with 1 ml/well experimental media (\pm treatments) and returned to the incubator for the required incubation time. The media was replaced every 3 days. After the treatment time had elapsed the media was removed and 1 ml trypsin was added to each well and incubated until cells were in suspension. To each well 1 x 3 ml Isoton was added and drawn into a sterile 25G 5 ml syringe to separate cells into a single cell suspension and this solution was added to 6 ml Isoton. The 10 ml Isoton cell suspension was counted twice on a Coulter counter (Coulter™ Multisizer II (Beckam Coulter UK, Ltd, High Wycombe, UK) according to manufacturer's instructions. The average count was multiplied by 20 to calculate cells/well.

2.12 Genetic Manipulation of CD44 expression

In this project, CD44 expression was manipulated in endocrine resistant and sensitive cell models by siRNA knockdown or transfection respectively in order to determine the role of CD44 in cellular behaviours.

2.12.1 siRNA-mediated CD44 suppression

Global CD44 expression was suppressed in endocrine resistant cells using a pool of CD44 siRNAs supplied by Dharmacon. Similarly, RHAMM expression was suppressed using a pool of RHAMM siRNAs obtained from Santa Cruz Biotechnology. For specific knockdown of CD44v6, an siRNA sequence was designed using the Invitrogen online

stealth RNAi™ siRNA design tool, BLOCK-iT™ RNAi Designer (<http://rnaidesigner.lifetechnologies.com/rnaiexpress/>) from the gene sequence encoding the CD44v6 exon obtained from the online NCBI database (Appendix C). This programme allowed the consideration of GC content and knockdown probability as calculated by the online tool for each sequence generated. Once the siRNA sequence was selected, the corresponding DNA sequence was inputted into the online bioinformatics programme BLAST which compared sequence similarity to other DNA sequences across the human genome. BLAST analysis confirmed the high level of specificity for the CD44 and CD44v6 siRNA sequences used within this project (listed in Table 2.10) to their respective gene target, however RHAMM specificity could not be determined as these sequences were not supplied. For additional confirmation, the gene sequences for CD44 and CD44v6 obtained from the NCBI online database were used to verify siRNA sequence target specificity (Appendix C). Target siRNA, their corresponding RNA sequences and source of purchase for all siRNAs used within this project are detailed in Table 2.10.

Target siRNA	RNA sequences	Source
CD44 (total)	GAAUUAACCUGCCGCUU CAAGUGGACUCAACGGAGA CGAAGAAGGUGUGGGCAGA GAUCAACAGUGGCAAUGGA	ON-TARGETplus SMARTpool Human CD44) Thermo scientific Dharmacon, Leicestershire, UK
CD44v6	CAGAUGGCAUGAGGGGAUUCGCCAA	BLOCK-iT™ RNAi Designer, Invitrogen™, Life Technologies, UK
RHAMM	siRNA pool sequences not supplied	RHAMM siRNA Santa Cruz Biotechnology, Inc. Heidelberg, Germany
NT-siRNA (control)	UGGUUUACAUGUCGACUAA UGGUUUACAUGUUGUGUGA UGGUUUACAUGUUUUCUGA UGGUUUACAUGUUUCCUA	ON-TARGETplus control pool Non-Targeting Pool, Thermo scientific Dharmacon, Leicestershire, UK

Table 2.10. A list of target siRNA, RNA sequences and source of purchase for all siRNAs used within this project.

2.12.2 CD44 siRNA transfection protocol

Log phase cells were seeded into 35 mm dishes (2×10^5 cells density) in experimental media without the presence of antibiotics and returned to the incubator until 50 % cell confluency was reached. To achieve a working solution of 100 nM, siRNA stock solution was diluted to 2 μ M using 1 x siRNA buffer (5 x siRNA buffer diluted in sterile RNase free water). Table 2.11 lists the 3 control arms that were used for each siRNA experiment: control (cells grown in experimental media), lipid-only (cells incubated with lipid transfection reagent only (DharmaFECT 1 Transfection Reagent)) and non-targeting (NT)-siRNA (negative control siRNA, described in Table 2.10). The constituents for each sample were assembled into 2 sterile eppendorf tubes (A and B) according to Table 2.11, mixed by gentle pipetting and incubated at room temperature for 5 minutes. The eppendorfs (A and B) for each sample were then combined, mixed by gentle pipetting and incubated at room temperature for 20

minutes. Each sample was then diluted 1:5 in warmed media (WRPMI containing 5% SFCS, 2 % glutamine, no antibiotics). Experimental media was removed from the 35 mm dishes and replaced with 1 ml siRNA control or transfection media. Dishes were gently rocked to ensure even coverage of transfection media and returned to the incubator for 48 hours to allow sufficient siRNA protein knockdown before harvesting the cells for experimental purposes.

100 nM working Solution	Control		Lipid-only		NT-siRNA		Target-specific siRNA	
	A	B	A	B	A	B	A	B
Eppendorf WRPMI	100	100	100	98.4	50	98.4	50	98.4
2 μM siRNA	-	-	-	-	50	-	50	-
Dharmafect #1	-	-	-	1.6		1.6		1.6
Total Volume	200		200		200		200	

Table 2.11. The volumes required for the transfection of 35 mm dishes at a working solution of 100 nM. All volumes are in μ l.

2.12.3 Transformation of plasmid DNA

To determine the role of CD44 in endocrine sensitive MCF-7 cells that express low levels of endogenous CD44, a transfection-based method was used. Plasmid DNA constructs containing CD44v3 and CD44v6 isoforms and their cytoplasmic tail truncation mutation counterparts (denoted as CD44v3 Δ cyt and CD44v6 Δ cyt respectively) were a kind gift from Dr Ursula Gunthert (Basel University, Switzerland). Each plasmid construct is fused with an EGFP-tag at the carboxy terminus and contained in a p-PGKT-T7/2 vector (plasmid map shown in Appendix H). Previous use of these plasmids are found in the 2006 and 2007 publications by Mielgo et al.

2.12.3.1 Recovering plasmid DNA from filter paper

Plasmid DNA constructs were sent embedded onto filter papers. To extract the plasmid DNA, each filter paper was placed into a 1.5 mm sterile eppendorf tube and immersed in 100 μ l TE buffer (10 mM Tris, 1 mM EDTA), briefly vortexed and incubated at room temperature for 15 minutes. 1 - 10 μ l of this solution was then removed from the eppendorf and added to 100 μ l DH5 α competent *E.coli* cells. The remainder of the plasmid DNA/TE buffer solution was stored at -20 °C as a permanent archive.

2.12.3.2 Transformation procedure

DH5 α *E.coli* cells were thawed on wet ice. Once thawed, 100 μ l DH5 α cells were placed into the required number of 17 x 100 mm polypropylene tubes on ice and gently mixed. Any unused DH5 α cells were refrozen in a dry ice/ethanol bath for 5 minutes before returning to -70 °C for storage. To determine transformation efficiency, a control of 5 μ l stock pUC19 solution (0.01 μ g/ml) was added to a polypropylene tube containing 100 μ l DH5 α *E.coli* cells and the tube was mixed by gentle tapping. 1 – 10 ng of plasmid DNA/TE solution was added to a polypropylene tube containing 100 μ l DH5 α cells and the tube was mixed by gentle tapping. The tube was then allowed to incubate on ice for 30 minutes. The DH5 α cells were heat shocked in a 42 °C water bath (Grant W14, Grant Instruments, UK) for 45 seconds to allow entrance of the plasmid and immediately placed onto ice for 2 minutes to reclose the cell walls. 900 μ l room temperature Super Optimal broth with Catabolite repression (SOC media, nutrient rich bacterial growth medium for maximal

transformation efficiency of *E.coli* cells) was then added to each polypropylene tube and the tubes were incubated for 1 hour with vigorous shaking, 37 °C, 225 rpm (Gallenkamp cooled orbital incubator, Sanyo, UK). Following incubation, the control pUC19 and experimental plasmid were each diluted 1:100 with SOC media. 100 µl of each of these diluted media was then spread onto individual LB agar plates containing 100 µg/ml ampicillin and the plates were incubated upside down overnight at 37 °C. After the overnight incubation a single colony from each plate was selected and inoculated in a starter culture containing 2 ml warm LB media with 100 µg/ml ampicillin. The starter cultures were contained in a vessel of at least 4 times the volume of the culture and incubated with vigorous shaking for 8 hours at 37 °C, 300 rpm (Gallenkamp cooled orbital incubator, Sanyo, UK). Following incubation, the starter culture was diluted 1:1000 into selective warm LB medium containing 100 µg/ml ampicillin. The cultures were contained in a vessel of at least 4 times the volume of the culture and incubated with vigorous shaking for 14 hours at 37 °C, 300 rpm (Gallenkamp cooled orbital incubator, Sanyo, UK).

2.12.3.3 Harvesting bacterial cells for collection and purification of plasmid DNA

The bacterial cells were then harvested and purified using an Endotoxin Free Plasmid Maxiprep Kit (10) (QIAGEN Ltd, Manchester, UK #12632), all equipment and reagents used for this process were enclosed within the kit upon purchase. Table 2.12 lists all reagents used with their corresponding composition, storage temperature and function. After the 14 hour incubation, bacterial cells were transferred into a sterile container and centrifuged at 6000 rpm for 15 minutes, 4 °C (Sorvall RC5B PLUS, Thermo Scientific, UK). The bacterial pellets were then resuspended in 10 ml pre-

chilled (4 °C) Buffer P1 (containing RNase and pre-mixed with LyseBlue reagent) by pipetting until no cell clumps remained. 10 ml Buffer P2 was then added to the solution and mixed thoroughly by vigorously inverting the sealed tube 4 – 6 times and then incubated at room temperature for 5 minutes. 10 ml pre-chilled (4 °C) Buffer P3 was then added to the lysate and mixed immediately and thoroughly by vigorously inverting the sealed tube 4 – 6 times. The lysate was then immediately poured into the barrel of the QIAfilter Cartridge (with the cap screwed onto the outlet nozzle and placed in a convenient tube) and incubated at room temperature for 10 minutes ensuring the cartridge was not agitated during this incubation period. The cap from the QIAfilter cartridge outlet nozzle was then removed, the plunger was gently inserted into the cartridge and the cell lysate was filtered into a 50 ml sterile falcon tube recovering approximately 25 µl of the lysate. 2.5 ml of Buffer ER was then applied to the filtered lysate, mixed by inversion 10 times and incubated on ice for 30 minutes. During the incubation period, a QIAGEN-tip 500 column was equilibrated by applying 10 ml Buffer QBT and the column was allowed to empty by gravity flow. After incubation, the filtered lysate was then applied to the equilibrated QIAGEN-tip 500 column and allowed to enter the resin by gravity flow. The QIAGEN-tip 500 column was then washed twice with 30 ml Buffer QC and allowed to empty by gravity flow. The DNA attached to the column was then eluted with 15 ml Buffer QN and collected in a 30 ml endotoxin/pyrogen-free tube. The DNA was then precipitated by adding 10.5 ml (0.7 volumes diluted with RNase free water) room-temperature isopropanol to the eluted DNA, mixed and centrifuged immediately at 9000 rpm for 30 minutes, 4°C. The supernatant was then carefully decanted at room temperature

and the resultant DNA pellet was washed with 5 ml endotoxin-free room temperature 70 % ethanol and centrifuged at 9, 000 rpm for 10 minutes. The supernatant was carefully decanted without disturbing the DNA pellet and allowed to air dry for 5 – 10 minutes. The DNA pellet was then re-dissolved in 100 µl of endotoxin-free Buffer TE without pipetting the DNA up and down to avoid shearing. The DNA yield was then determined by UV spectrophotometry at 260 nm and quantitative analysis on a 2 % agarose gel. DNA concentration (µg/ml) and purity was quantified using the DNA_{260/280} programme on the spectrophotometer where A₂₆₀ readings should lie between 0.1 and 1. To measure DNA concentration, 1 ml 1X TNE buffer (100 µl 10X TNE buffer in 900 µl RNase free water) was placed into a glass cuvette and used as a blank. 2 µl DNA sample was added to 1 ml 1X TNE buffer and placed into the glass cuvette, the absorbance was measured at 260 nm (A₂₆₀) on the spectrophotometer (Cecil CE2041, Cambridge UK). DNA concentration was calculated using the following formula: DNA = A₂₆₀ x 50 x dilution factor. DNA integrity was also assessed via gel electrophoresis for each sample. Samples were stored at -20 ° C.

Component	Composition	Storage (°C)	Function
Buffer P1	50 mM Tris HCl pH 8 100 mM EDTA 100 µg/ml RNase A	2 - 8	Resuspension buffer
Buffer P2	200 mM NaOH 1 % SDS (w/v)	15 - 25	Lysis buffer
Buffer P3	3 M potassium acetate pH 5.5	2 - 8	Neutralisation buffer
Buffer ER	Not disclosed	15 - 25	Endotoxin removal buffer
Buffer QBT	750 mM NaCl 50 mM MOPS pH 7 15 % isopropanol (v/v) 0.15 % triton-X-100	15 - 25	Equilibration buffer
Buffer QC	1 M NaCl 50 mM MOPS pH 7 15 % isopropanol (v/v)	15 - 25	Wash buffer (removes excess salt residues/contaminants)
Buffer QN	1.6 mM NaCl 50 mM MOPS pH 7 15 % isopropanol (v/v)	15 - 25	Elution buffer
Isopropanol	70 % isopropanol 30 % sterile water	15 - 25	Precipitates DNA Removes excess salts
Ethanol	70 % ethanol 30 % endotoxin-free water	15 - 25	Removes excess salts
TE buffer	10 mM Tris Cl pH 8 1 mM EDTA	15 - 25	Solubilised DNA Protects from DNA degradation

Table 2.12. A list of the components purchased with the Endotoxin-Free Plasmid Maxiprep kit (10) (QIAGEN, Manchester, UK) detailing their composition, storage temperature and function.

2.12.4 DNA sequencing of plasmid constructs

The successful transformation of the plasmid constructs was verified by DNA sequencing. The plasmid constructs and corresponding primers were transferred on dry ice to the CBS where they underwent a clean-up procedure and DNA sequencing analysis. To obtain an accurate read, each CD44 plasmid construct underwent a sequence reaction with 3 primers including: T7 promoter primer, CD44 Std forward primer and CD44v3/CD44v6 primer (dependent on plasmid construct). Table 2.13

lists each primer used for DNA sequence and their corresponding sequence, concentration and source of purchase. The sequencing results files were then analysed using the Chromas Lite software programme (<http://technelysium.com.au/>) and the DNA sequences for each plasmid construct are shown in Appendix I. To determine whether any changes in DNA base pair sequence resulted in amino acid changes in the protein structure, the DNA sequence obtained for each plasmid was uploaded onto the online protein translation tool ExPasy (<http://web.expasy.org/translate/>) and the results are shown in Appendix I).

Primer	Sequence	Source of Purchase
T7 promoter	5'-TAATACGACTCAC TATAGGG-3'	Integrated DNA Technologies, Belgium
CD44 Std	5'-GACACATATTGC TTCAATGCTTCAGC-3'	Life Technologies Inc, UK
CD44v3	5'-CGTCTTCAAAT ACCATCTCAGC-3'	Life Technologies Inc, UK
CD44v6	5'-CAACGGAAGA AACAGCTACCC-3'	Life Technologies Inc, UK

Table 2.13. A list of each primer sent to the CBS for DNA sequencing analysis of the plasmid constructs along with their corresponding sequence and source of purchase.

2.12.5 CD44 transient transfection protocol

MCF-7 cells were seeded (2×10^5 cells density) into 35 mm dishes in RPMI with 5 % FCS (no antibiotics) and incubated at 37 °C until cells reached 50 % cell confluency. For transfection of one 35 mm dish, 117.5 µl pre-warmed RPMI was combined with 7.5 µl FuGENE 6 transfection reagent, mixed by pipetting and incubated for 5 minutes at room temperature. 100 ng plasmid DNA was added to each eppendorf (3:1 FuGENE 6:DNA), mixed by gentle pipetting and incubated for 15 minutes at room temperature. 125 µl transfection solution was then added to 1.5 ml RPMI with 5 %

FCS (no antibiotics) and placed into a 35 mm dish. Dishes were rocked gently to ensure even coverage of transfection media and returned to the incubator for 48 hours before harvesting to allow optimal transfection to occur.

2.13 Statistical analysis

In the results chapters, all data from 3 independent experiments are shown or representative images/immunoblots are presented. Statistical analysis of the results were carried out where data allowed. Where replicates were performed, quantitative data are presented as standard error of the means (SEM). For comparison between two groups, paired/unpaired student's t-tests were performed. For comparisons between 3 or more groups, a one-way ANOVA was carried out with Tukey post-hoc analysis. Significance was determined as $p < 0.05$.

3. Characterisation of CD44 isoform expression in endocrine resistant breast cancer cell models versus their endocrine sensitive counterpart

3.1 Introduction

Whilst a large body of evidence has been gathered to support a role for CD44 as a significant factor in tumour progression, this area remains controversial due to contradictory findings and a lack of clear association between CD44 expression and clinical outcome. Indeed, CD44 has been heavily implicated as a contributor towards the metastatic phenotype of numerous carcinomas including breast, pancreatic and ovarian, however, whilst some studies report that elevated CD44 expression correlates with poor prognosis in these carcinomas (Takada et al. 1994; Looi et al. 2006; Li et al. 2008a; Huh et al. 2009; Klingbeil et al. 2010; Auvinen et al. 2014) others suggest that the presence of CD44 associates with a favourable outcome (Sillanpaa et al. 2003; Diaz et al. 2005; Lopez et al. 2005; Al-Maghrabi et al. 2012; Takahara et al. 2012). Furthermore, reports have suggested that both overexpression (Lokeschwar et al. 1995; Hao et al. 2012) and loss (Verkaik et al. 2000; Kito et al. 2001) of CD44 is associated with advanced progression and metastasis of prostate cancer.

One aspect which makes CD44 difficult to study and undoubtedly contributes to variability between studies is the extensive alternative splicing attributed to this molecule. Thus a possible explanation for these discrepancies may lie in the fact that a high proportion of studies have analysed total CD44 expression and not taken into account the differential expression of specific CD44 variant isoforms. For example, it has been extensively established that individual CD44 exons have the potential for

the addition of specific post-translational modifications thus conferring differential affiliation for membrane receptor binding and ligand sensitivity (Jalkanen et al. 1988; Bennet et al. 1995; Hasenauer et al. 2013). Therefore, the incorporation of specific exons into the CD44 molecule via alternative splicing may lead to novel cell functions through association of these molecules with, and subsequent activation of, various growth factor receptors and their downstream targets. Indeed, alternative splicing, a phenomenon known to be upregulated in cancer cells, allows for the formation of an extensive array of CD44 isoforms, each with a potentially distinct function with regards to their role in cancer development (Goldstein and Butcher 1990; Stamenkovic et al. 1991; Screaton et al. 1992).

With relation to the characterisation and function of specific CD44 isoforms in breast cancer, this area remains largely unstudied, however multiple reports present convincing evidence for the role of several individual isoforms in breast cancer progression (Cheng et al. 2006; Lian et al. 2006; Afify et al. 2009; Lida et al. 2014), although these reports have also been contradictory. Olsson et al. 2011 published findings indicating that individual CD44 isoform expression may be associated with specific breast cancer characteristics and molecular subtypes and may also contribute to specific oncogenic signalling pathways. In addition, previous studies by the BCMPG (Hiscox et al. 2012) suggested a role for CD44 expression in acquired tamoxifen-resistance where it correlated with an enhanced migratory phenotype. However, given the lack of knowledge regarding the role of individual CD44 isoforms in cancer, particularly within the context of acquired endocrine resistance, this was explored further in this project.

To begin these studies, it was first necessary to characterise CD44 variant isoform expression in endocrine sensitive MCF-7 cells along with two endocrine resistant cell models, a tamoxifen-resistant (Tam-R) and fulvestrant-resistant (Fas-R) cell line, both derived from MCF-7 cells (see Materials and Methods 2.2.1). For the purpose of this project, it was decided to focus on CD44 Std, CD44v3, CD44v6 and CD44v10 as these isoforms have previously been identified as markers of poor prognosis and related to tumour progression functions in breast cancer (Kalish et al. 1999; Herrera-Gayol and Jothy 1999; Bourguignon et al. 2008; Afify et al. 2009; Lida et al. 2014; Fahe et al. 2014). An important aspect of CD44-mediated function is its ability to bind to its principle ligand HA, an extracellular matrix component abundantly expressed in breast carcinomas and correlated with poor outcome (Auvinen et al. 2000; Auvinen et al. 2014). Therefore, in addition to CD44, alternative members of the HA-binding family (hyaladherins) which have been implicated in breast cancer progression were also investigated to evaluate their contribution to the endocrine resistant phenotype of Tam-R and Fas-R cells.

3.1.1 Objectives

1. To explore the expression of CD44 variant isoforms and additional hyaladherin family members across endocrine sensitive and endocrine resistant cell models at gene level using an existing microarray database.
2. To validate microarray gene expression data by RT-PCR analysis.
3. To determine hyaladherin expression and cellular localisation at protein level by Western blotting, immunocytochemistry and immunofluorescence analysis.

3.2 Results

3.2.1. Analysis of hyaladherin family member gene expression in cells models of acquired endocrine resistance compared to their endocrine sensitive counterpart

Of the multiple hyaladherins identified to date, several have been implicated in breast cancer progression including: RHAMM (HMMR) (Wang et al. 1998; Hamilton et al. 2007; Maxwell et al. 2011), lymphatic vessel endothelial hyaluronan acid receptor 1 (LYVE-1) (Bono et al. 2004), Stabilin 2 (STAB2) (Hirose et al. 2012), Toll-like receptor 4 (TL4) (Yang et al. 2010; Yang et al. 2013) versican (VCAN) (Du et al. 2013) and intracellular adhesion molecule 1 (ICAM-1) (Rosette et al. 2005; Guo et al. 2014). Therefore the gene expression of these hyaladherins, along with CD44, were assessed using affymetrix analysis.

Following the completion of microarray gene expression profiling of RNA samples from the cell models, the resultant triplicate expression data for each gene analysed was uploaded into the software analysis programme GeneSifter (see Materials and Methods 2.3). Using this programme, the raw data underwent median normalisation and log transformation which led to the construction of heatmap profiles and log₂ intensity plots for the visualisation of individual gene expression changes across the cell models. In some instances, the affymetrix U133A gene chips contained more than one probe set ID for each gene. Therefore upon analysis, particular importance was placed upon the best performing 'Jetset' probe for each gene which was determined by the online Jetset programme based upon the performance of each probe across three parameters (shown in Table 3.1). Figure 3.1 reveals the heatmap profile for

each gene probe assessed within this project along with log₂ intensity plots displaying the average normalised data (\pm SEM) for each Jetset probe (with their corresponding fold change values shown in Table 3.2). Heatmap analysis revealed that the expression of the majority of gene probes corresponding to LYVE-1, STAB2, TL4, ICAM-1 and VCAN in Tam-R and Fas-R cells were either reduced or unaltered compared to MCF-7 cells. Furthermore, the detection calls for each Jetset probe corresponding to these genes were absent in all cell lines and the log₂ expression values were below 0, indicative of absent/very low expression of these genes across all cell models. Statistical analysis to compare gene fold changes revealed that STAB2 expression was significantly reduced in Tam-R and Fas-R cells compared to MCF-7 cells (Table 3.2) however these data may be unreliable as the detection of this gene was determined as absent across these cells. No other statistically significant differences in fold changes for these gene probes were detected across all cell models.

In contrast, heatmap analysis revealed increased HMMR gene expression in Tam-R and Fas-R cells compared to MCF-7 cells (Figure 3.1). Detection calls revealed that HMMR was present in both endocrine resistant cell models but absent in MCF-7 cells (Table 3.1) which was confirmed by the log₂ expression values from the Jetset probe (Figure 3.1). Fold change analysis revealed substantially enhanced HMMR gene fold changes in both Tam-R and Fas-R cells compared to MCF-7 cells however these changes were not statistically significant (Table 3.2). Additionally, heatmap analysis revealed that the majority of gene probes corresponding to CD44 showed enhanced gene expression in Tam-R and Fas-R cells compared to MCF-7 cells. However, these

probes showed poor 'overall scores' (Table 3.1) and thus data for these genes may be unreliable. The Jetset probe for CD44 (indicated on row 5 of the heatmap profile) appeared as 'present' across all cell models suggesting that CD44 is expressed within these cells. Furthermore, log₂ expression and fold change analysis for the Jetset probe revealed enhanced CD44 expression in Fas-R cells, but not Tam-R cells, compared to MCF-7 cells and statistical testing revealed a significant increase in gene fold change in Fas-R cells compared to both MCF-7 and Tam-R cells (Table 3.2). Based on these data, CD44 and HMMR expression were explored further in these cell models.

Gene	Probe Set ID	Specificity Score	Cover Score	Robust Score	Overall Score	Detection Call (MCF-7/Tam-R/Fas-R)
HMMR	207165_at	1	1	0.8064	0.8064	A/P/P
CD44	209835_x_at	0.8182	0.8421	0.0037	0.0026	P/P/P
CD44	204489_s_at	0.9091	0.8947	0.115	0.0093	M/M/P
CD44	212014_x_at	0.8182	0.8421	0.0036	0.0025	P/P/P
CD44	212063_at	0.8182	0.8947	0.4285	0.3508	P/P/P
CD44	210916_s_at	0.8182	1	0.0005	0.0004	A/A/P
CD44	204490_s_at	0.9091	0.8947	0.0037	0.003	P/P/P
CD44	217523_at	-	1	-	-	A/A/P
HMMR	209709_s_at	0.901	1	0.4785	0.3896	A/P/P
LYVE-1	219059_s_at	0.9091	1	0.2277	0.2070	A/A/A
LYVE-1	220037_s_at	0.9091	1	0.0883	0.0803	A/A/A
TL4	221060_s_at	1	1	0.0285	0.0285	A/A/A
CD44	216056_at	-	1	-	-	A/A/A
STAB2	220114_s_at	0.8182	0.6666	0.4901	0.2673	A/A/A
ICAM-1	202637_s_at	0.9091	1	0.1809	0.1644	A/A/A
ICAM-1	202638_s_at	0.7277	1	0.4848	0.3566	A/A/A
ICAM-1	215485_s_at	1	1	0.0631	0.0631	A/A/A
VCAN	211571_s_at	0.7272	1	0.2021	0.0146	A/A/A
VCAN	204620_s_at	0.1818	1	0.0894	0.0732	A/A/A
VCAN	215646_s_at	1	1	0.0319	0.0319	A/A/A
VCAN	204619_s_at	0.9090	1	0.6459	0.5872	A/A/A
VCAN	221731_x_at	0.5454	1	0.1230	0.0671	M/A/M

Table 3.1. A list of the probe set IDs for each gene assessed using the GeneSifter programme with their corresponding performance across an array of parameters and detection call. Each probe appears in accordance to the sequence shown in the heatmap profile (Figure 3.1). Jetset probe identifies the probe set ID which scored the highest overall performance score for each gene and is indicated in bold. All parameters are assessed on a scale ranging from 0 – 1 with a score closer to 1 indicating a better performance. Detection call identifies whether the gene expression was determined as absent (A), present (P) or mixed (M) for each probe set ID in MCF-7, Tam-R and Fas-R cells respectively.

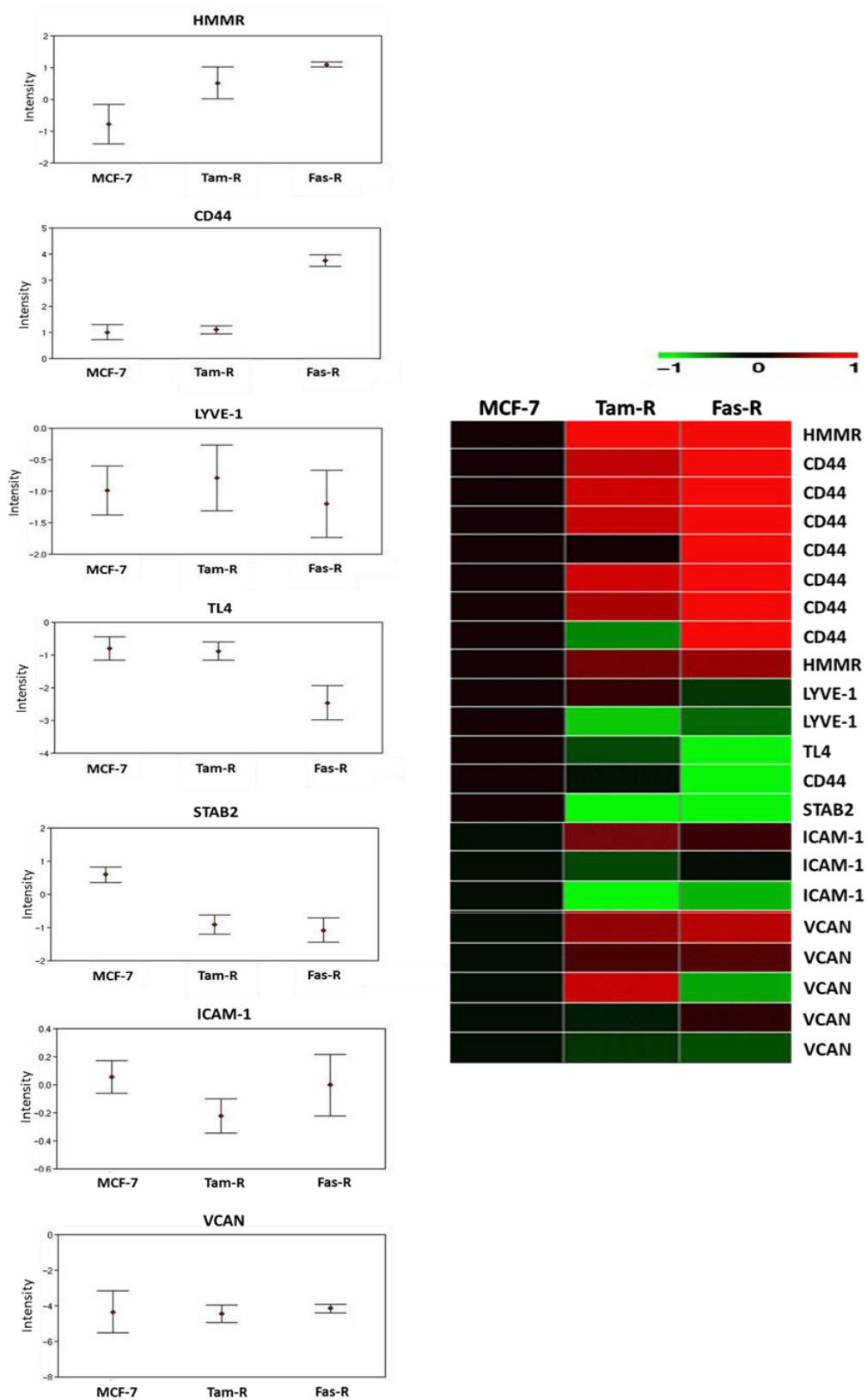


Figure 3.1. A heatmap profile displaying changes in gene expression for all hyaladherins analysed and the log2 intensity plots for the Jetset probe of each gene with the average normalised gene expression (\pm SEM) across 3 independent experiments.

Gene	MCF-7 versus Tam-R	MCF-7 versus Fas-R	Tam-R versus Fas-R
HMMR	2.45	3.64	1.48 F
CD44	1.06	<u>6.71</u>	<u>6.30 F</u>
LYVE-1	1.15	1.16	1.33 T
TL4	1.06	3.14	2.97 F
STAB2	<u>2.84</u>	<u>3.19</u>	1.12 F
ICAM-1	1.21	1.04	1.17 F
VCAN	1.08	1.14	1.23 T

Table 3.2. The fold change values in gene expression of the Jetset probes for each gene analysed by affymetrix. ANOVA testing with Tukey post-hoc analysis was performed to identify any significant changes in gene fold across all 3 cells models and significant changes are highlighted in bold and underlined. Green represents decreased fold changes, red indicates increased fold changes and black indicates no change in fold levels. CD44 gene fold change was significantly increased in Fas-R cells compared to MCF-7 cells ($p = 0.00038$) and Tam-R cells (p value = 0.00045). STAB2 gene fold changes were significantly decreased in Tam-R cells ($p = 0.0291$) and Fas-R cells ($p = 0.0186$) compared to MCF-7 cells. In the final column, fold change values relating to either Tam-R or Fas-R cells are indicated by 'T' or 'F' respectively.

3.2.2 Validation of microarray data by RT-PCR analysis

Whilst microarray analysis provided important insight into CD44 and HMMR gene expression across the cell models, this technique cannot distinguish between different splice variants of these genes. Therefore, to validate microarray results and further investigate the presence of different CD44 and HMMR splice variants across the cell lines, RT-PCR was performed on mRNA isolated from MCF-7, Tam-R and Fas-R cells using CD44 isoform and HMMR specific primers designed in-house. Primers designed for detection of CD44 Std and HMMR were situated in the domain common to all isoforms therefore use of these primers was anticipated to result in multiple PCR products. It should also be noted that primers used for detection of CD44v3, CD44v6 and CD44v10 detected any isoforms containing these exons. Figure 3.2 reveals the expression of multiple bands (200 – >1000 bp) using the CD44 Std primer across all cell models, however overall these bands showed stronger expression within Tam-R and Fas-R cells compared to MCF-7 cells. Figure 3.2 further reveals the upregulation of bands corresponding to the predicted base pair sizes of CD44v3 (100 bp) and CD44v6 (100 bp) in Tam-R and Fas-R cells compared to MCF-7 cells. The band corresponding to CD44v10 (109 bp) expression showed a modest increase in Fas-R cells compared to MCF-7 cells (Figure 3.2). No signal could be detected for HMMR across the cell models (Figure 3.2). Densitometry analysis revealed enhanced gene expression of CD44 Std and CD44v6-containing isoforms in Fas-R cells compared to MCF-7 cells (Figure 3.3).

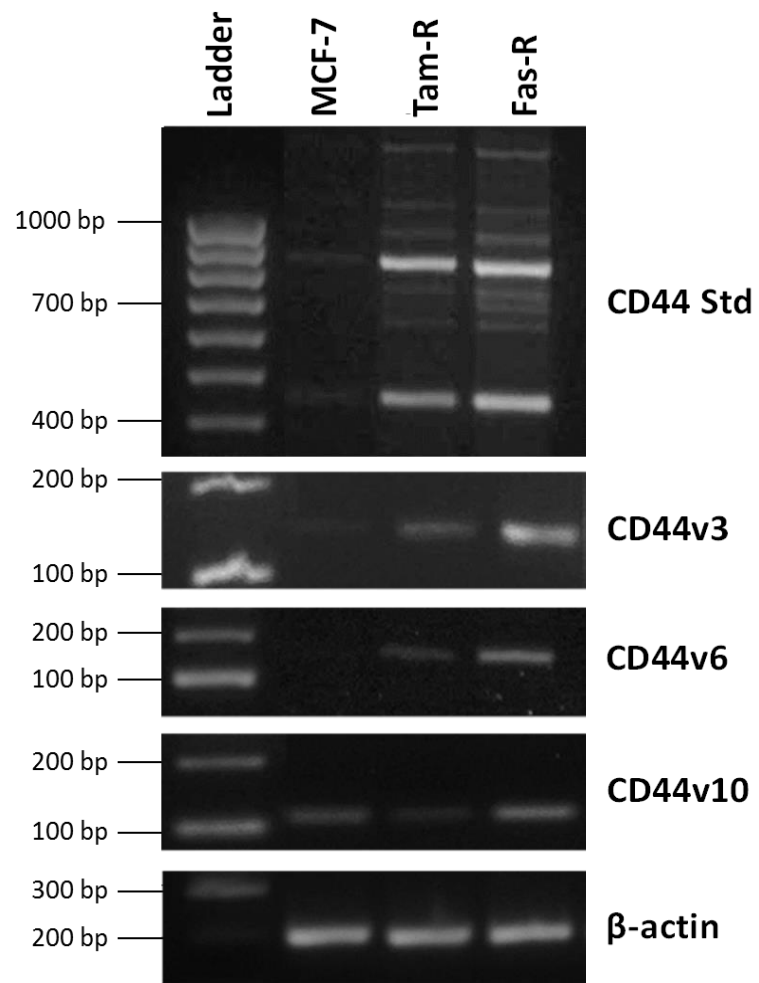


Figure 3.2. Representative RT-PCR images from 3 independent experiments showing CD44 isoform expression in MCF-7, Tam-R and Fas-R cells with β -actin loading control.

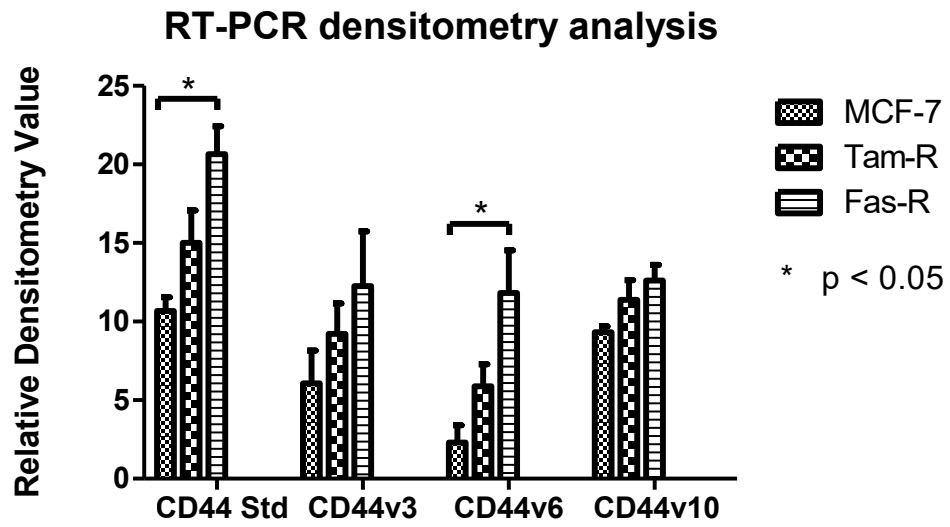


Figure 3.3. Densitometry graph for CD44 isoform expression detected in MCF-7, Tam-R and Fas-R cells by RT-PCR analysis normalised to β -actin. Error bars represent the average normalised data \pm SEM from 3 independent experiments and statistical analysis was performed using a one-way ANOVA with Tukey post-hoc testing to identify any significant changes across all 3 cell models. Significance was set at $p < 0.05$.

3.2.3 Protein expression of CD44 and RHAMM in endocrine resistant cells versus their endocrine sensitive counterparts

Given that CD44 isoform gene expression appeared to be elevated in resistant cell models versus their MCF-7 counterparts, the next step was to assess CD44 isoform expression at the protein level along with their cellular localisation patterns. Whilst HMMR was undetectable by RT-PCR analysis, microarray data revealed elevated expression of this gene across the endocrine resistant cell models compared to their endocrine sensitive counterpart, MCF-7 cells. Therefore HMMR (RHAMM) expression was also investigated at the protein level across the cell models.

3.2.3.1 Western blotting

Western blotting analysis revealed enhanced expression of an 80 kDa band corresponding to the hypothetical size of CD44 Std in Tam-R and Fas-R cells compared to MCF-7 cells; with the highest expression level observed in Fas-R cells (Figure 3.4). Further analysis revealed elevated expression of protein products corresponding to CD44v3 (85 kDa), CD44v6 (85 kDa) and CD44v10 (90 kDa) in Tam-R and Fas-R cells compared to MCF-7 cells (Figure 3.4). Interestingly, detection of CD44v6 and CD44v10 resulted in the presence of multiple bands (130 – 250 kDa) in the endocrine resistant cell lines that were not observed in MCF-7 cells (Figure 3.4). These are likely to be due to the presence of unidentified splice variants containing these exons and/or differences in glycosylation of these exons, also observed by other groups including Dougherty et al. 1991; Gansauge et al. 1995; Kuncova et al.

2005. Western blotting analysis also detected an 85 kDa band corresponding to a variant of RHAMM with a similar expression profile across all cell models (Figure 3.4).

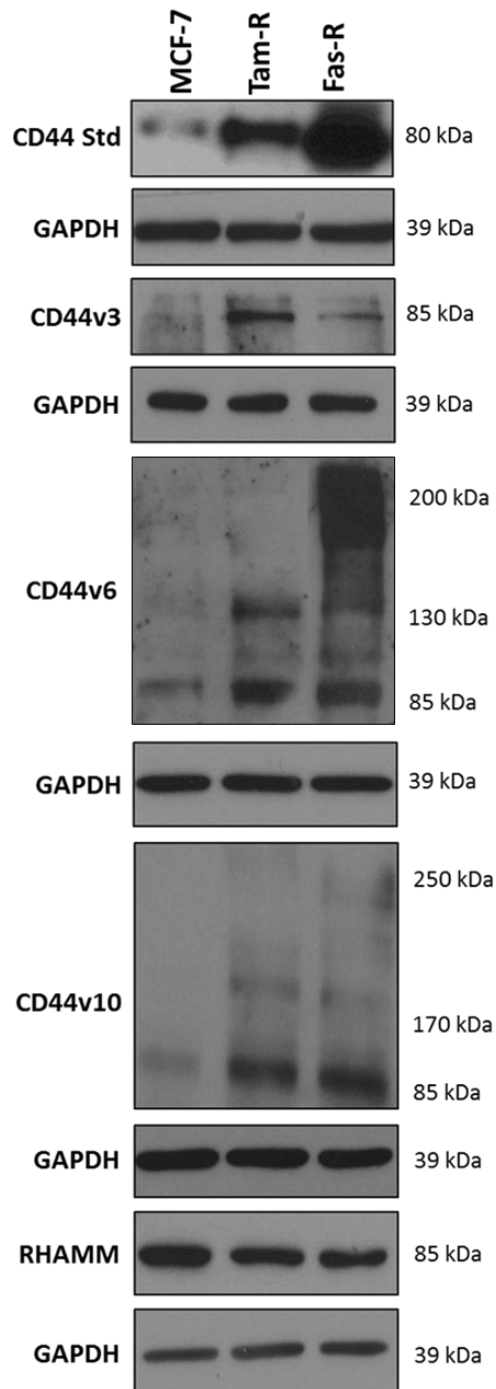


Figure 3.4. Representative Western blot images from 3 independent experiments showing CD44 isoform and RHAMM expression in MCF-7, Tam-R and Fas-R cells with a GAPDH loading control.

Densitometry analysis confirmed significantly elevated CD44 Std and CD44v6 protein expression in Fas-R cells compared to both MCF-7 and Tam-R cells and enhanced CD44v10 expression in Fas-R cells compared to MCF-7 cells (Figure 3.5). Furthermore, these analyses revealed increased CD44 Std and CD44v3 protein expression in Tam-R cells compared to MCF-7 cells (Figure 3.5).

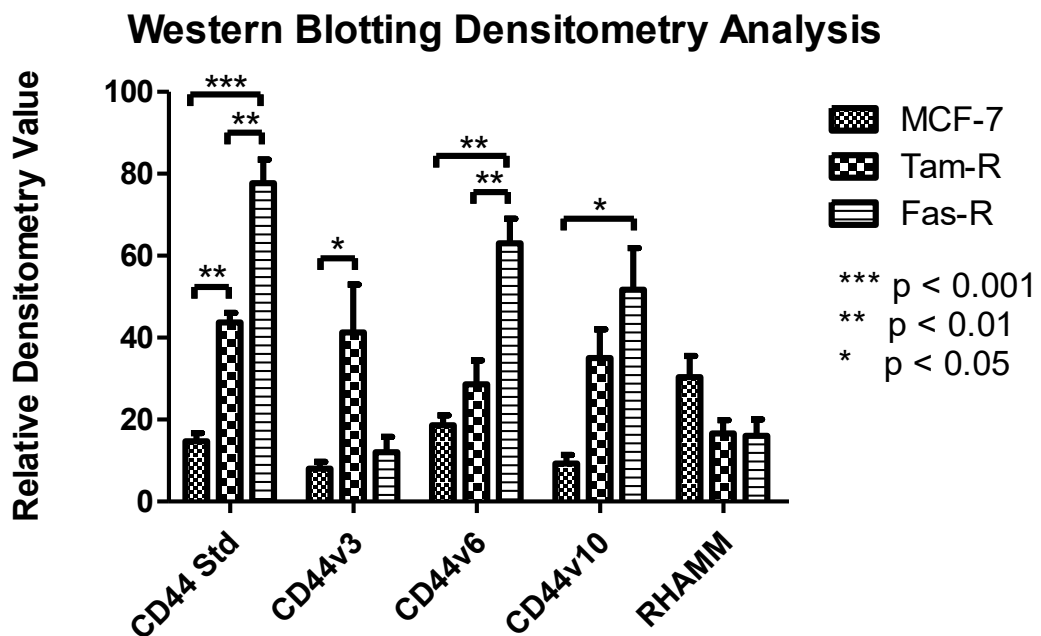


Figure 3.5. Densitometry graph showing CD44 isoform and RHAMM expression detected in MCF-7, Tam-R and Fas-R cells by Western blotting analysis normalised to GAPDH. Error bars represent the average normalised data \pm SEM from 3 independent experiments and statistical analysis was performed using a one-way ANOVA with Tukey post-hoc testing to identify any significant changes across all 3 cell models. Significance was set at $p < 0.05$.

3.2.3.2 Immunostaining analysis

Immunostaining approaches were used to quantify the expression and subcellular localisation pattern of CD44 and RHAMM proteins across all cell lines. These approaches detected all CD44 isoforms containing the specific variant exon.

Immunocytochemical analysis revealed intense staining of CD44 Std and CD44v6-containing isoforms in Tam-R and Fas-R cells versus MCF-7 cells, particularly at the cell surface (Figure 3.6). A similar trend for increased expression of CD44v3- and CD44v10-containing isoforms was observed in the resistant cell models compared to the endocrine sensitive MCF-7 cells although to a lesser degree than CD44 Std and CD44v6 proteins (Figure 3.7). Interestingly, CD44v3 and CD44v10 proteins showed predominant cytoplasmic localisation in the resistant cells (Figure 3.6). Upregulated protein expression of these isoforms in the resistant cells was further confirmed by quantitative assessment of immunostaining by H-score analysis (Figure 3.7). H-score quantitation suggested enhanced membrane staining of CD44 Std in Tam-R and Fas-R cells compared to MCF-7 cells, and increased CD44v6 expression in Fas-R cells, compared to MCF-7 and Tam-R cells (Figure 3.7). These analyses also revealed increased cytoplasmic CD44 Std, CD44v6 and CD44v10 protein expression in Fas-R cells compared to MCF-7 cells (Figure 3.7) and CD44v6 and CD44v10 expression was enhanced in Fas-R cells compared to Tam-R cells (Figure 3.7). Cytoplasmic expression of CD44v6 was increased in Tam-R cells compared to MCF-7 cells (Figure 3.7). Analysis of RHAMM showed decreased staining in Tam-R and Fas-R cells compared to MCF-7 cells and H-score analysis revealed reduced cytoplasmic RHAMM expression in Fas-R cells compared to MCF-7 cells (Figure 3.6 and 3.7 respectively).

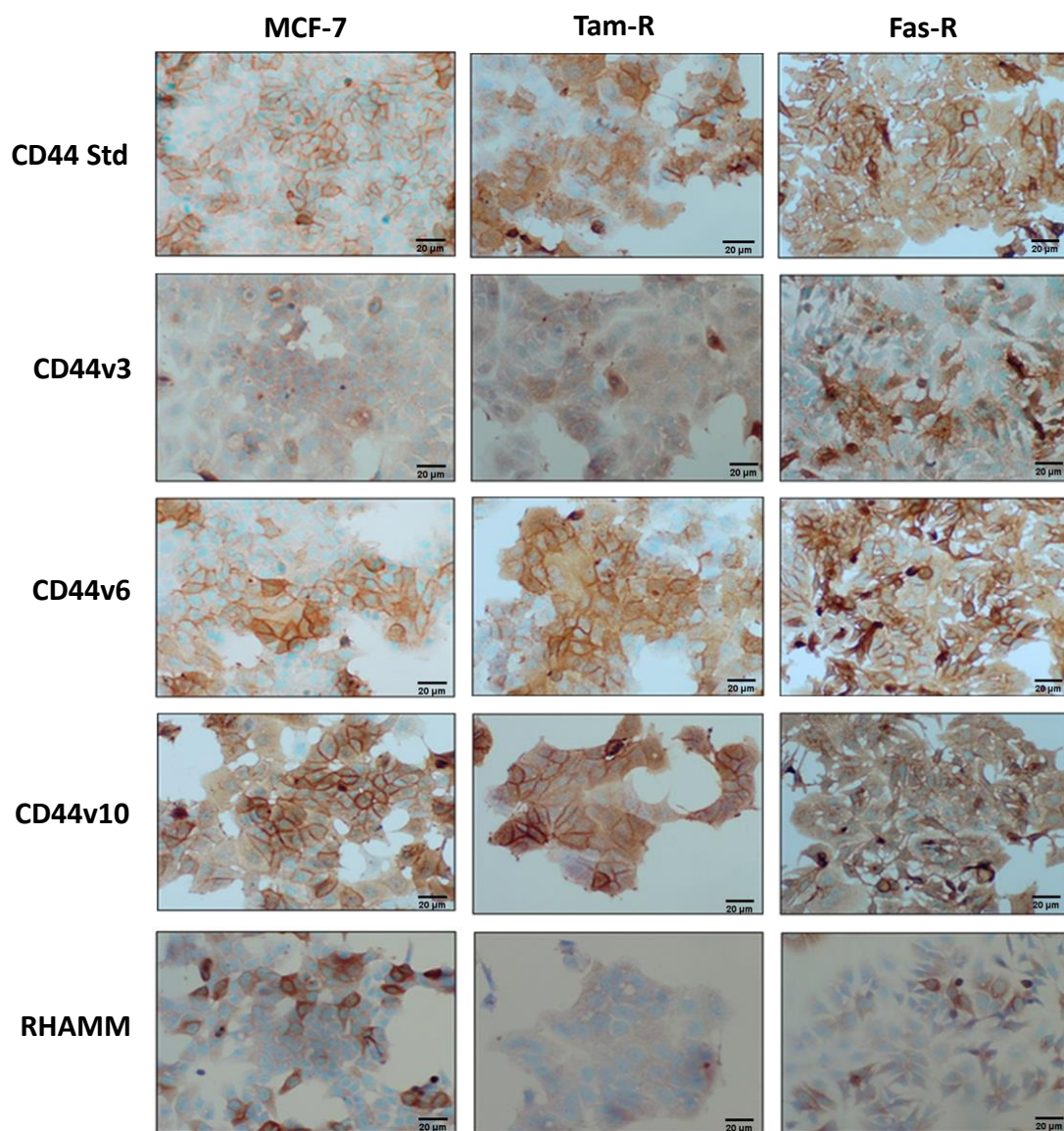
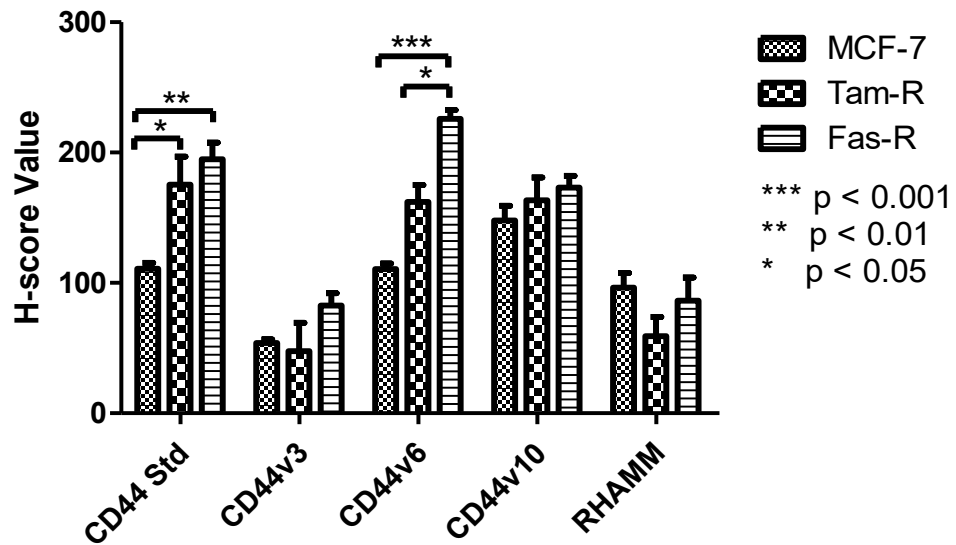


Figure 3.6. Representative images from 3 independent experiments showing CD44 isoform and RHAMM expression by immunocytochemical analysis (x20 magnification).

H-score quantification of CD44 membrane staining



H-score quantification of CD44 cytoplasmic staining

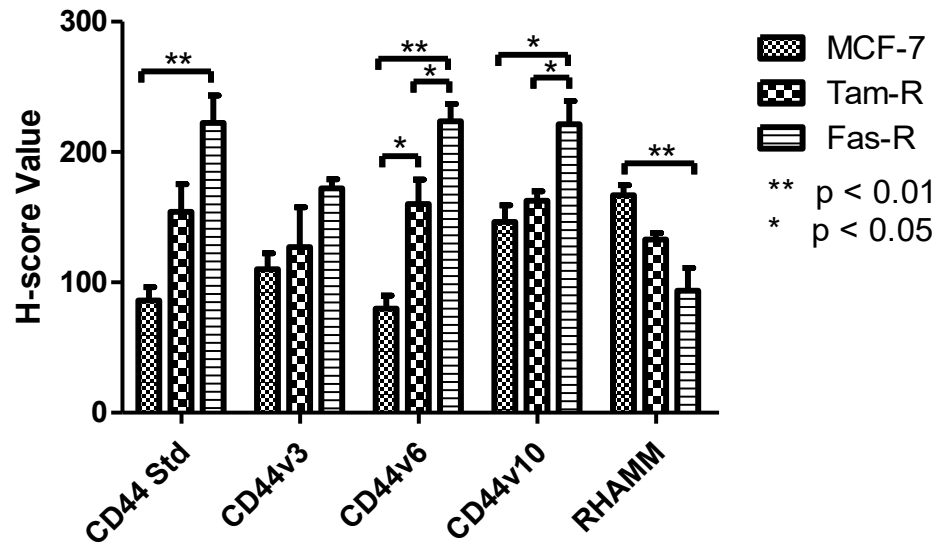


Figure 3.7. Membrane and cytoplasmic H-score assessment of CD44 isoform and RHAMM expression in MCF-7, Tam-R and Fas-R cells by immunocytochemistry analysis. Error bars represent the average normalised data \pm SEM from 3 independent experiments and statistical analysis was performed using a one-way ANOVA with Tukey post-hoc testing to identify any significant changes across all 3 cell models. Significance was set at $p < 0.05$.

To further validate CD44 and RHAMM expression, immunofluorescence microscopy was undertaken. This assessment also revealed intense staining of CD44 Std and CD44v6-containing isoforms in Tam-R and Fas-R cells compared to MCF-7 cells, with elevated staining observed on the plasma membrane (Figure 3.8). These data further revealed intense cytoplasmic staining of proteins corresponding to CD44v3- and CD44v10- containing isoforms in Tam-R cells compared to MCF-7 cells (Figure 3.8). Quantitative analysis using ImageJ to determine total cell fluorescence revealed enhanced staining of CD44 Std and CD44v6 in Fas-R cells compared to MCF-7 and Tam-R cells (Figure 3.9). Analysis of RHAMM revealed a heterogeneous staining pattern in MCF-7 and Fas-R cells, interestingly these proteins revealed cytoskeletal localisation across all cell models, an observation also shown by others (Assmann et al. 1999; Jiang et al. 2013) (Figure 3.8).

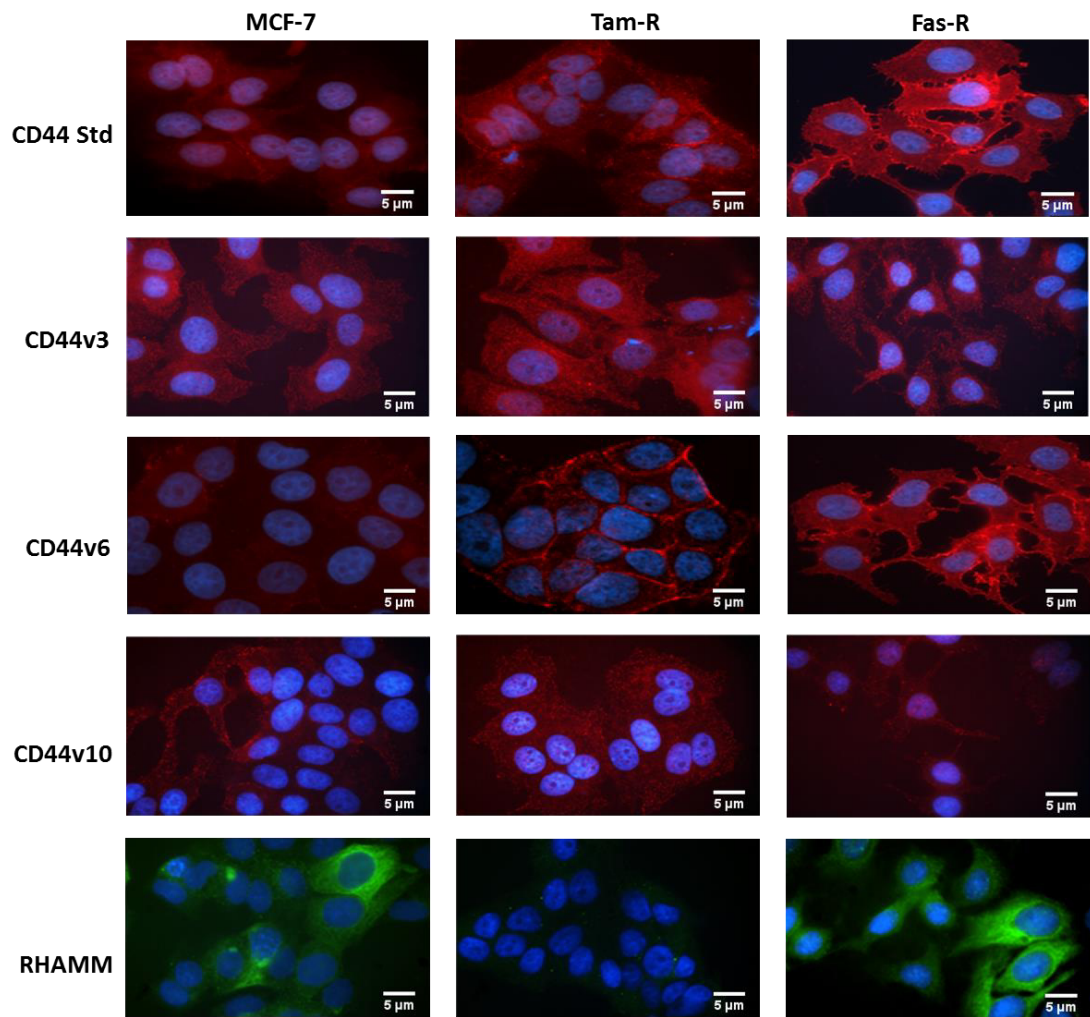


Figure 3.8. Representative images from 3 independent experiments showing CD44 isoform and RHAMM expression by immunofluorescence analysis (x63 magnification).

Quantitation of Immunofluorescence Staining

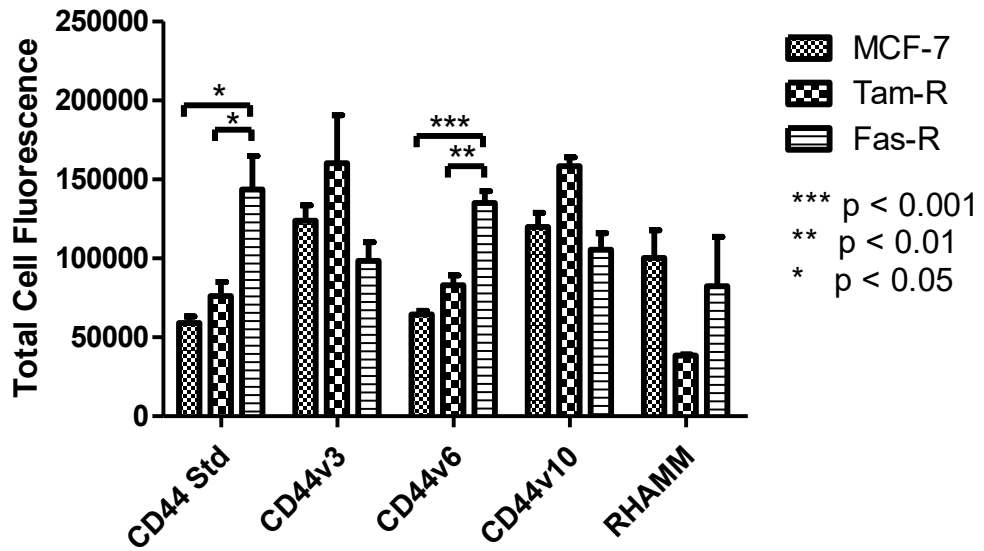


Figure 3.9. Total cell fluorescence analysis of CD44 isoform and RHAMM expression in MCF-7, Tam-R and Fas-R cells by immunofluorescence analysis. Error bars represent the average normalised data \pm SEM from 3 independent experiments and statistical analysis was performed using a one-way ANOVA with Tukey post-hoc testing to identify any significant changes across all 3 cell models. Significance was set at $p < 0.05$.

3.3 Discussion

The purpose of this chapter was to explore whether the expression of CD44 isoforms and alternative hyaladherin family members were altered in cell models of acquired endocrine resistance versus their endocrine sensitive counterparts. It has been well-established that deregulated CD44 expression contributes to the metastatic behaviour of numerous carcinomas (Klingbeil et al. 2010; Al-Maghrabi et al. 2012; Takahara et al. 2012; Hao et al. 2012), therefore the overall goal of this thesis was to explore the hypothesis that augmented CD44 isoform expression may confer an aggressive phenotype onto endocrine resistant cell models, potentially through enhanced growth factor pathway activation. Thus in order to elucidate the function of CD44 in the context of resistance, initial studies focussed around characterization of CD44 and related hyaladherin family members in endocrine sensitive and resistant breast cancer models.

Of the multiple hyaladherins identified to date, several have been reported to be implicated in various cancers including: CD44, HMMR, LYVE-1, TL4, STAB2, ICAM-1 and VCAN (Gao et al. 2006; Li et al. 2009; Hirose et al. 2012). In particular, CD44 (Afify et al. 2009; Ma et al. 2005; Lian et al. 2006), HMMR (Hamilton et al. 2007; Maxwell et al. 2011), LYVE-1 (Bono et al. 2004), TL4 (Yang et al. 2010; Yang et al. 2013), STAB2 (Hirose et al. 2012), VCAN (Du et al. 2013), and ICAM-1 (Rosette et al. 2005; Guo et al. 2014) have all been reported to be highly expressed in breast cancer where they have been shown to correlate with poor prognosis. However, with the exception of CD44 and HMMR, results obtained from affymetrix analysis did not suggest a role for these hyaladherin family members in endocrine resistance. It could be suggested that

downregulation, rather than overexpression, of specific hyaladherin genes may confer an aggressive phenotype in endocrine resistance through a tumour suppressor function, however no known tumour suppressor functions have been reported for the alternative hyaladherins assessed in this project. Despite microarray analysis revealing elevated gene expression of HMMR in both endocrine resistant cell models versus their MCF-7 counterpart, this effect was not statistically significant. Although HMMR gene expression was unable to be detected across the cell models by RT-PCR analysis, protein detection revealed a similar level of RHAMM expression across all cell models and staining appeared to show predominant cytoskeletal localisation. Thus together, these data could infer that RHAMM may not act as a major contributor towards the aggressive phenotype of these endocrine resistant cell models, however it could be argued that the presence of RHAMM in these cells alone is important to their aggressive phenotype.

In contrast, both affymetrix analysis and RT-PCR validation demonstrated elevated CD44 gene expression in endocrine resistance, however significant upregulation of CD44 splice variants was only observed for CD44 Std- and CD44v6-containing proteins in Fas-R cells compared to MCF-7 cells. Western blotting analysis confirmed upregulation of CD44 Std in both endocrine resistant cell models versus their endocrine sensitive MCF-7 counterpart. However these data revealed a differential expression profile of CD44 variants between Tam-R and Fas-R cells, with a significant upregulation of CD44v6 and CD44v10 proteins in Fas-R cells and enhanced CD44v3 in Tam-R cells, compared to MCF-7 cells (depicted in Figure 3.10). Interestingly, Western blotting data suggested the presence of multiple CD44v6- and CD44v10-

containing isoforms in the resistant cell models that were undetectable in MCF-7 cells, potentially suggesting that greater amounts of alternative splicing may occur in endocrine resistance. Indeed, aberrant splicing frequently occurs in carcinomas, although it remains unclear whether the production of abnormal transcripts is of functional importance to cancer cells or merely a by-product of transformation. However, growing evidence suggests that aberrant splicing contributes to the aggressive phenotype of cancer cells through the production of proteins with altered or novel functions (Xing et al. 2003; Hiller et al. 2005; Fackenthal and Godley 2008). Indeed numerous reports document upregulation of CD44 splice variants in aggressive carcinoma tissues compared to their normal tissues (Herrera-Gayol et al. 1999; Ni et al. 2002; Ma et al. 2005; Shi et al. 2013; Misra et al. 2012). These data may suggest that upregulation of CD44 splicing leading to the production of alternative CD44 variant isoforms, as observed within Tam-R and Fas-R cells, may contribute to the acquisition of an aggressive phenotype observed in resistant models since these CD44 isoforms may have altered pro-invasive/migratory functions.

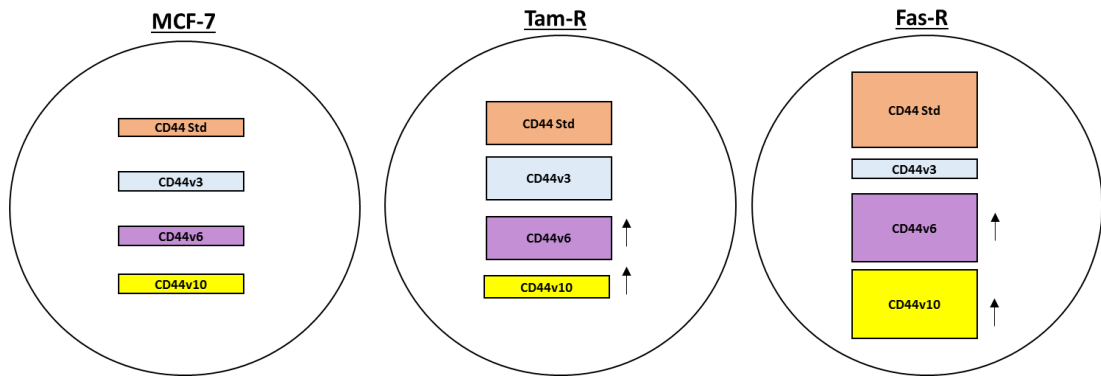


Figure 3.10. A diagram to represent the level of CD44 isoform expression and presence of splice variants in endocrine resistant Tam-R and Fas-R cells compared to their endocrine sensitive counterpart MCF-7 cells according to the characterisation results in Chapter 3. The size of each CD44 isoform represents its expression level across the cell lines with an increase in size corresponding to enhanced protein expression. The arrows represent the presence of multiple isoforms containing the specific exon in the cell models. In MCF-7 cells, the level of CD44 Std, CD44v3, CD44v6 and CD44v10 is low and multiple splice isoforms containing specific exons are not present in these cells. In Tam-R cells, CD44 Std, CD44v3 and CD44v6 protein expression becomes enhanced compared to MCF-7 cells and multiple splice variants containing variant exons 6 and 10 are present in these cells. In Fas-R cells, CD44 Std, CD44v6 and CD44v10 expression becomes upregulated compared to MCF-7 cells, and to a greater level compared to Tam-R cells, and multiple splice variants containing variant exons 6 and 10 are also present in these cells.

Immunostaining analysis confirmed upregulation of CD44 Std, CD44v6 and CD44v10 in Fas-R cells and revealed elevated expression of CD44 Std and CD44v6 proteins in Tam-R cells compared to their MCF-7 counterparts. Furthermore, these techniques revealed distinct subcellular localisation patterns of individual CD44 isoforms across cell models. Whereas CD44 Std- and CD44v6-containing isoforms appeared to localise to the membrane, CD44v3- and CD44v10-containing proteins showed predominant cytoplasmic staining in models of endocrine-resistance; and these expression patterns may allude to differential cellular functions. For example, whilst CD44 Std and CD44v6 isoforms may interact with extracellular factors at the cell surface (including extracellular matrix components, growth factor receptors and growth factors themselves), CD44v3 and CD44v10 isoforms may have more distinguished roles within intracellular signalling, receptor/ligand internalisation and cytoskeleton binding. Indeed, CD44 Std has been suggested to confer enhanced HA

binding through the accessibility of its extracellular HA-binding N-terminus and its expression has been tightly coupled with HER2 in cancer cells and found to be strongly expressed in HER2-enriched breast tumours (Bourguignon et al. 1997; Bao et al. 2011, Olsson et al. 2011). In support of this, Hiscox et al. 2012 reported that HA activation of CD44 led to dimerization with HER2 and subsequent downstream signalling resulting in promotion of aggressive cellular behaviours in Tam-R cells. Additionally, it has been reported that CD44v6 is required for the full activation of the membrane tyrosine kinase receptor c-Met (Orian-Rousseau et al. 2002; Hasenauer et al. 2013); a protein overexpressed in approximately 20 – 30 % of invasive basal breast cancers (Lengyel et al. 2005; Zagouri et al. 2013; Ho-Yen et al. 2014) and shown to be an independent predictor of poor clinical outcome (Ghoussoub et al. 1999; Camp et al. 1999; Gonzalez-Angulo et al. 2012). Further, Hiscox et al. 2006 reported that the c-Met receptor is overexpressed in Fas-R cells where it has been suggested to augment an aggressive cellular phenotype. These data may implicate a role for CD44v6 in the activation of the c-Met receptor in Fas-R cells where it may play a role in the initiation of signalling pathways leading to enhanced invasive behaviours. However unlike CD44 Std, the contribution of CD44v6 to HA-binding and ErbB receptor activation currently remains unknown.

Conversely, the CD44v10 exon has been shown to undergo extensive post-translational modifications within cells that subsequently prevents dimerization of CD44 molecules at the cell surface, an event known to promote high affinity HA-binding (Droll et al. 1995; Bourguignon et al. 1998). Therefore it is thought that CD44v10 proteins exhibit reduced capability of HA binding and may thus provide an

explanation for its predominant cytoplasmic localisation in endocrine resistant cells potentially through its enhanced turnover. Furthermore, CD44v3 and CD44v10 variant isoforms have been shown to be involved in enhanced cellular motility through interactions with cytoskeletal proteins, ROK and ankyrin (Bourguignon et al. 1999; Singleton and Bourguignon 2002; Singleton and Bourguignon 2004). Therefore, it may be suggested that within these cell models, the role of CD44v3- and CD44v10-containing proteins may predominantly involve cytoskeletal-mediated functions and may therefore support evidence for the cytoplasmic localisation of these proteins. Taken together, the intracellular localisation of CD44 isoforms containing variant exons 3 and 10 may be postulated to be a result of enhanced turnover and degradation, cytoskeletal binding, endosomal signalling, receptor/ligand endocytosis or cellular processing in the endoplasmic reticulum. Whilst numerous studies report cytoplasmic localisation of CD44 proteins, intracellular roles for variant isoforms have not yet been reported in literature.

Several approaches were undertaken to explore CD44 isoform expression across these cells models as discrepancies in antibody detection have previously been reported due to differences in immunostaining techniques which may alter or mask the access of antibodies to protein epitopes (Martegani et al. 1999; Louderbough et al. 2011). The analyses revealed a similar expression profile of CD44 isoforms across these techniques (Table 3.3) suggesting an accurate representation was gained across the cell models in Fas-R cells, however some variation was shown in Tam-R cells. A limitation to using immunostaining analysis for the detection of specific CD44 variants in this study was that antibodies detected any CD44 variant possessing the

specific exon and could not distinguish between different splice variants. This effect was overcome by Western blotting analysis which detected multiple bands potentially correlating to CD44 variant-containing isoforms, however the composition of these splice variants across the cell models remains undetermined. It must be noted that the CD44 Std antibody used in this study detected all CD44 isoforms present in the cell models and therefore was a representation of total CD44 expression. Given that CD44 Std and CD44v6 detection appeared to show similar expression profiles between all cell models, it may be suggested that the CD44 Std antibody mainly detected the CD44v6-containing proteins. Thus, the expression of the CD44 Std isoform alone may be difficult to interpret in this study. This thesis therefore highlights the importance of using a breadth of detection techniques to gain an accurate representation of CD44 isoform expression across models and may go some way to explain experimental discrepancies between studies.

	RT-PCR	WB	ICC (M)	ICC (C)	IF
MCF-7 v Tam-R	-	Std, v3	Std	v6	-
MCF-7 v Fas-R	Std, v6	Std, v6, v10	Std, v6	Std, v6, v10	Std, v6
Tam-R v Fas-R	-	Std, v6, v10	Std, v6	Std, v6, v10	Std, v6

Table 3.3. A table to show significant differences observed in CD44 isoform expression between all cell models across several detection techniques. Abbreviations represent: WB (Western blotting), ICC (M) (immunocytochemistry, membrane H-score), ICC (C) (immunocytochemistry, cytoplasm H-score), IF (immunofluorescence), Std (CD44 Std), v3 (CD44v3), v6 (CD44v6) and v10 (CD44v10).

Overall, the data demonstrated that the expression of specific CD44 splice variants was increased in endocrine resistant cell models versus their endocrine sensitive counterpart. Interestingly, analyses revealed a greater level of CD44 isoform expression in the ER- Fas-R cells, compared to ER+ Tam-R cells (Table 3.3), which

supports previous research suggesting that CD44 expression is inversely proportional to ER expression (Klingbeil et al. 2010; Montgomery et al. 2012), although suggests that this relationship is not absolute. Both Tam-R and Fas-R cells are known to display an aggressive, metastatic phenotype (Hiscox et al. 2011) mediated in part by altered growth factor signalling. A number of studies support a role for CD44 isoforms as contributors towards the aggressive cellular features that may ultimately promote tumour spread. For example, a pioneering study by Gunthurt et al. 1991 revealed that CD44v6 transfection into non-metastatic rat carcinomas converted them into metastatic cells and subsequent co-injection of anti-CD44v6 antibody suppressed this metastatic behaviour. Furthermore, Yae et al. 2012 showed that inoculation of the CD44 variant (v8-v10) isoform-expressing subpopulation of breast cancer cells into mice conferred metastatic potential and led to the formation of lung metastases which was accompanied by an expansion of stem-like cancer cells, an observation that was not seen in the CD44 variant-negative (CD44 Std) subpopulation. Indeed, it is generally considered that tumours expressing specific CD44 variants are more aggressive than those which display the CD44 Std protein alone. In support of this, Banky et al. 2012 reported that CD44 proteins containing variant exons 3 and 6 showed dominant expression compared to other CD44 variants across colorectal cancer cell lines and suggested that in a minority of tumour subclones these variants may act as 'metastasis genes' and drivers of the metastatic phenotype in these cells.

3.3.1 Summary

In this chapter it was demonstrated that CD44 variant isoforms are upregulated in acquired endocrine resistance, however a differential expression profile of CD44

isoforms was detected between the resistant cell models, with the greatest level of CD44 isoform expression found in Fas-R cells compared to their endocrine sensitive MCF-7 parental cells. Given that these resistant cells display an aggressive phenotype combined with the well-established roles for CD44 proteins in tumour progression behaviours, these observations may point to a role for CD44 isoforms in acquired endocrine resistance.

4. CD44 overexpression in endocrine resistant breast cancer models augments their aggressive phenotype and sensitisation to HA

4.1 Introduction

In the previous chapter, it was demonstrated that the expression of multiple CD44 isoforms are elevated within endocrine resistant cell models versus their endocrine sensitive counterpart. However the contribution of CD44 proteins to the aggressive resistant phenotype of these cells remains unclear. Many studies have shown a link between high levels of CD44 expression and enhanced metastatic behaviour in a number of cancer cell models, which is mirrored in the clinical setting (Lui et al. 2005; Lian et al. 2006; Harrison et al. 2006; Shi et al. 2013; Ni et al. 2014) however results remain contradictory. Whilst the full extent of CD44 contribution towards tumour progression remains to be elucidated, two key mechanisms underlying CD44 function appears to be mediated through binding to their principle ligand hyaluronan (HA), and associations with, and regulation of, receptor tyrosine kinases (RTKs) (Kim et al. 2008; Hiscox et al. 2012; Hasenauer et al. 2013).

HA is found in abundance within the tumour stroma of many carcinomas where its accumulation is often predictive of unfavourable prognosis (Anttila et al. 2000; Nykopp et al. 2010; Kultti et al. 2014). In particular, HA concentration in breast carcinomas has been shown to be an independent predictor of poor patient outcome (Auvinen et al. 2000; Auvinen et al. 2014). However the origins of HA in these tumours remains under debate and whilst numerous studies have shown that HA is produced by stromal cells stimulated by tumour cells (Anttila et al. 2000; Tammi et

al. 2008), others reveal evidence that carcinoma cells also synthesise HA (Kimata et al. 1983; Heldin et al. 1996; Simpson et al. 2002).

HA is synthesised within the inner face of the plasma membrane by HA synthases which produce different length HA polymers that are subsequently extruded into the tumour matrix or retained at the cell surface (Udabage et al. 2005a; Weigel and DeAngelis 2007). HA polymers that are released into the microenvironment contribute to the provision of structural integrity, tissue hydration and homeostasis of the tumour (Turley et al. 2002; Toole and Hascall 2002). Alternatively, HA retained at the cell surface may further aggravate tumourigenecity through binding to hyaladherins leading to the activation of signalling cascades, or become endocytosed (via a CD44-mediated mechanism), together resulting in the consequent induction of numerous cellular processes including angiogenesis, migration and differentiation (Tammi et al. 1998; Knudson et al. 2002; Evanko et al. 2007 Qhattal and Lui 2011). Indeed, CD44 proteins have been shown to be strongly expressed at sites of HA accumulation in breast cancer cells thus suggesting a link between enhanced HA levels, CD44 expression and poor patient survival (Udabage et al. 2005a, Auvinen et al. 2014). Furthermore, Hamilton et al. 2007 showed that the highly CD44-expressing invasive MDA-MB-231 breast cancer cell line produced higher levels of endogenous HA compared to the low CD44-expressing less invasive MCF-7 cell line. From these findings this group proposed that invasive breast cancer cells rely more upon endogenous HA production and establish an autocrine mechanism required for rapid rates of motility; a mechanism which less invasive cells lack.

Furthermore, CD44 activation of RTK signalling, which occurs endogenously or upon HA-activation, has been implicated towards the induction of the metastatic cascade in numerous carcinomas (Palyi-Krekk et al. 2008; Bao et al. 2011; Hasenauer et al. 2013). Indeed, several receptor tyrosine kinase (RTKs), including EGFR, HER2 and c-Met are commonly found to be expressed in invasive breast carcinomas where they correlate with an aggressive phenotype (Lengyel et al. 2005; Reis-Filho et al. 2006; Gravel et al. 2009; Dawood et al. 2010; Baek et al. 2011; Auvinen et al. 2013). Numerous studies have reported that CD44 proteins act as co-receptors for EGFR, HER2 and c-Met leading to the subsequent transduction of downstream signalling cascades and enhanced tumourigenic activity (Kim et al. 2008; Bao et al. 2011; Hatano et al. 2011; Hasenauer et al. 2013). Importantly, these RTKs have been implicated in the acquisition of tamoxifen- and/or fulvestrant-resistance (Knowlden et al. 2003; Britton et al. 2006; Hiscox et al. 2006) coinciding with upregulated CD44 expression.

Taken together, the fact that CD44, HA and RTKs have been shown to become elevated in invasive breast carcinomas (separately or in combination) and correlated with poor prognosis suggests that these factors may be a critical requirement for breast tumour progression. Therefore, the aims of this chapter were to investigate whether CD44 contributes to the aggressive phenotype of endocrine resistant breast cancer models by augmenting RTK activation and/or sensitising these cells to HA.

4.1.1 Objectives

1. To explore the effects of exogenous HA upon migration, invasion, growth and modulation of RTK signalling in endocrine sensitive versus endocrine resistant cell models.
2. To investigate whether CD44 contributes to the intrinsic aggressive nature of endocrine resistant cells by RTK activation and/or response to HA through global CD44 siRNA knockdown.
3. To determine whether endocrine resistant cells express the relevant machinery required for HA production at the gene level.

4.2 Results

4.2.1. Exogenous HA stimulation enhances the aggressive phenotype of Tam-R and Fas-R cells and modulates receptor tyrosine kinase signalling

To begin to explore whether upregulated CD44 expression may alter the aggressive phenotype of endocrine resistant cell models, it was first necessary to measure their endogenous cellular behaviours. Given that high levels of CD44 have been associated with metastatic behaviours of breast cancer cells (Afify et al. 2009; Montgomery et al. 2012; Babina et al. 2014), primary exploration was focused upon the basal level of cellular migration, invasion and proliferation across all cell models. Boyden chamber assays revealed that Fas-R cells exhibited a higher level of endogenous migration across fibronectin-coated membranes and enhanced proliferative capacity compared to MCF-7 cells (Figure 4.1). Further, these analyses revealed that both Tam-R and Fas-R cells exhibited enhanced endogenous invasive capacity through Matrigel compared to their endocrine sensitive counterpart (Figure 4.1).

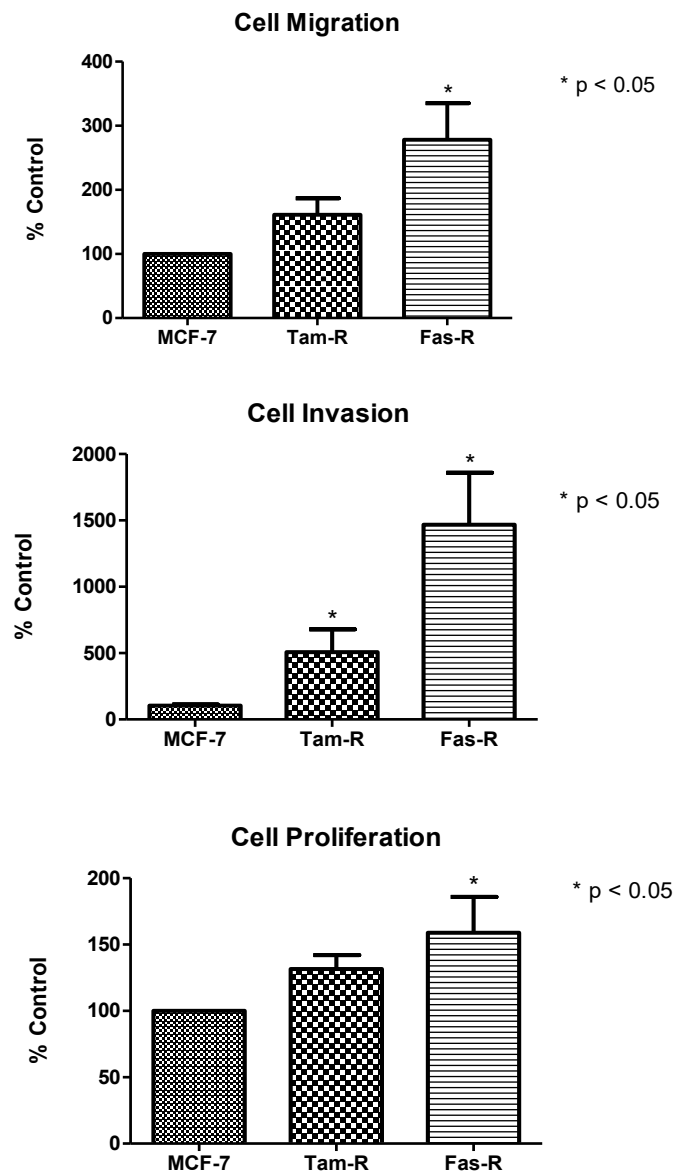


Figure 4.1. The endogenous migratory, invasive and proliferative responses of MCF-7, Tam-R and Fas-R cells were determined using Boyden Chamber (migration and invasion) and Coulter Counter (proliferation) assays. Error bars represent the average normalised data \pm SEM from 3 independent experiments. Statistical analysis was performed using a one-way ANOVA with Tukey post-hoc testing to identify any significant changes across all 3 cell models. Significance was set at $p < 0.05$.

Given that CD44 is the principle receptor for HA, an extracellular matrix component found in abundance in the tumour stroma and identified as an independent predictor of poor patient outcome (Auvinen et al. 2000; Auvinen et al. 2014), it was next explored whether the highly CD44-expressing endocrine resistant cell models were sensitised to HA, compared to their low CD44-expressing endocrine sensitive counterpart. As HA has been well documented to activate signalling cascades that induce cell migration, invasion and growth in breast tumours through CD44-mediated mechanisms (Bourguignon et al. 2002; Kung et al. 2012; Montgomery et al. 2012), the effect of exogenous HA stimulation upon these functions across the cell models was evaluated.

Optimisation procedures (Appendix J) revealed that medium molecular weight HA (215 kDa) induced the best signalling response across the cell models, an effect also observed by other groups (Hamilton et al. 2007; Montgomery et al. 2012; Ouhtit et al. 2013), and was therefore used for subsequent exogenous stimulation. MCF-7, Tam-R and Fas-R cells were treated with HA in a dose dependent manner for the times indicated and the resultant effects on cellular function were measured.

Boyden chamber assays revealed HA stimulation enhanced the migratory capacity of Tam-R and Fas-R cells compared to their MCF-7 counterpart; this effect was dose-dependent in Tam-R cells up to a concentration of 200 µg/ml HA (Figure 4.2). Boyden chamber invasion assays revealed a dose-dependent increase in Fas-R cell invasion compared to MCF-7 cells, this effect was not seen in Tam-R cells (Figure 4.2). Proliferation assays revealed enhanced growth of Fas-R cells in response to 100 µg/ml HA stimulation compared to MCF-7 cells (Figure 4.2).

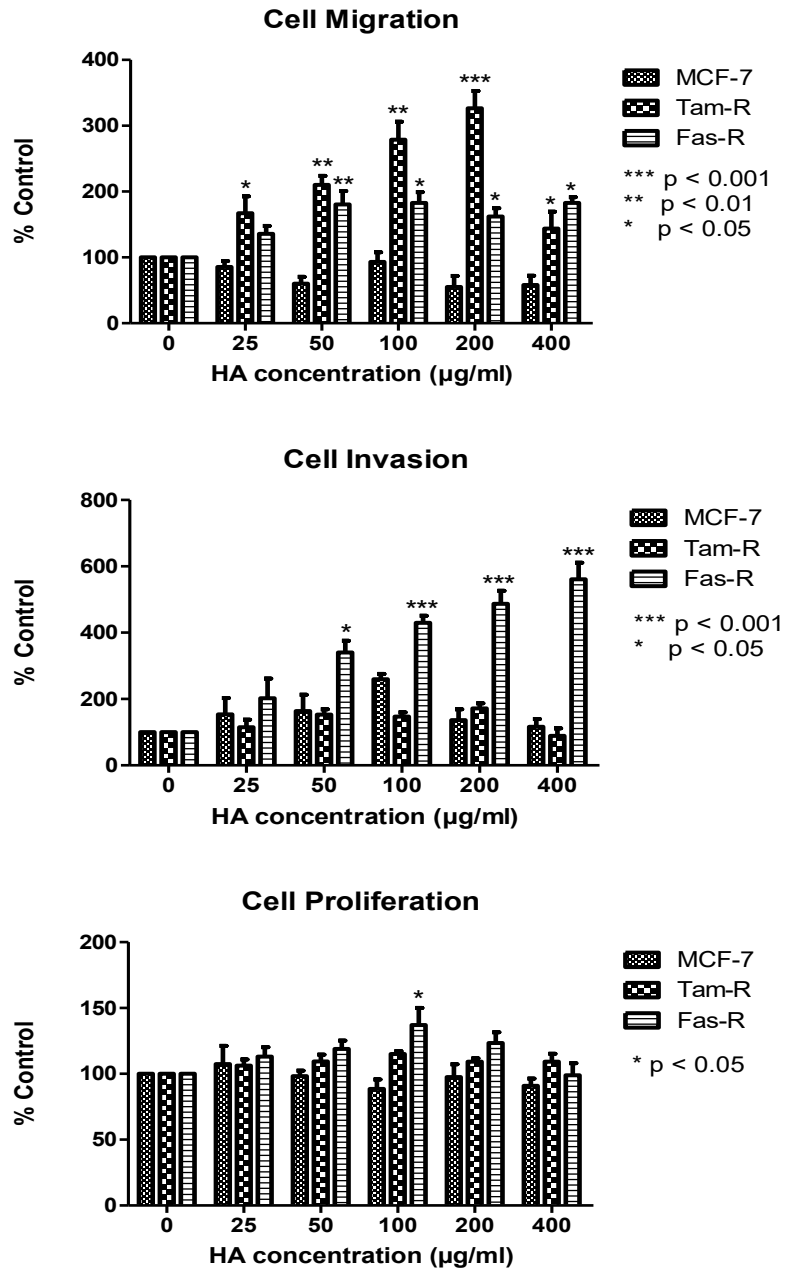


Figure 4.2. The migratory, invasive and proliferative responses of MCF-7, Tam-R and Fas-R cells upon HA stimulation (215 kDa, 0 – 400 µg/ml) were determined using Boyden Chamber (migration and invasion) and Coulter Counter (proliferation) assays. Error bars represent the average normalised data \pm SEM from 3 independent experiments and data is presented as the percentage of the untreated control. Statistical analysis was performed using a one-way ANOVA with Tukey post-hoc testing to identify any significant changes across all 3 cell models. Significance was set at $p < 0.05$.

Deregulation of receptor tyrosine kinase signalling has been heavily implicated in the acquisition of tamoxifen- and fulvestrant- resistance and previous studies from the Breast Cancer Molecular Pharmacology group (BCMPG) have shown that these cell models display enhanced EGFR and/or HER2 endogenous expression compared to their parental MCF-7 cells (McClelland et al. 2001; Knowlden et al. 2003; Hiscox et al. 2006). Thus, given that CD44 is known to activate these receptors upon HA binding (Bourguignon et al. 1997; Kim et al. 2008; Hatano et al. 2011), the effect of exogenous HA stimulation upon ErbB receptor activation across the cell models was next investigated. MCF-7, Tam-R and Fas-R cells were treated with HA in a dose dependent manner and the effects upon EGFR and HER2 activation and subsequent induction of the downstream effector, ERK1/2, was assessed across all cell models by Western blotting analysis.

The results revealed a dose-dependent increase in HER2 and EGFR activation up to 200 µg/ml and 400 µg/ml HA stimulation in Tam-R cells respectively (Figure 4.3). Densitometry analysis confirmed a significant increase in HER2 phosphorylation upon stimulation with 100 – 200 µg/ml HA in Tam-R cells in comparison to MCF-7 cells (Figure 4.4). Western blotting analysis revealed that Fas-R cells showed modestly enhanced HER2 and EGFR activation in response to HA stimulation and densitometry assessment revealed enhanced HER2 (200 µg/ml), but not EGFR activation, in these cells compared to MCF-7 cells (Figures 4.3 and 4.4). Western blotting analysis also revealed a dose dependent increase in ERK1/2 activation in Tam-R and Fas-R cells compared to MCF-7 cells (Figure 4.3). Densitometry assessment showed that this

effect was significant in Fas-R cells (50 – 400 $\mu\text{g/ml}$) and Tam-R cells (200 $\mu\text{g/ml}$) compared to MCF-7 cells (Figures 4.3 and 4.4).

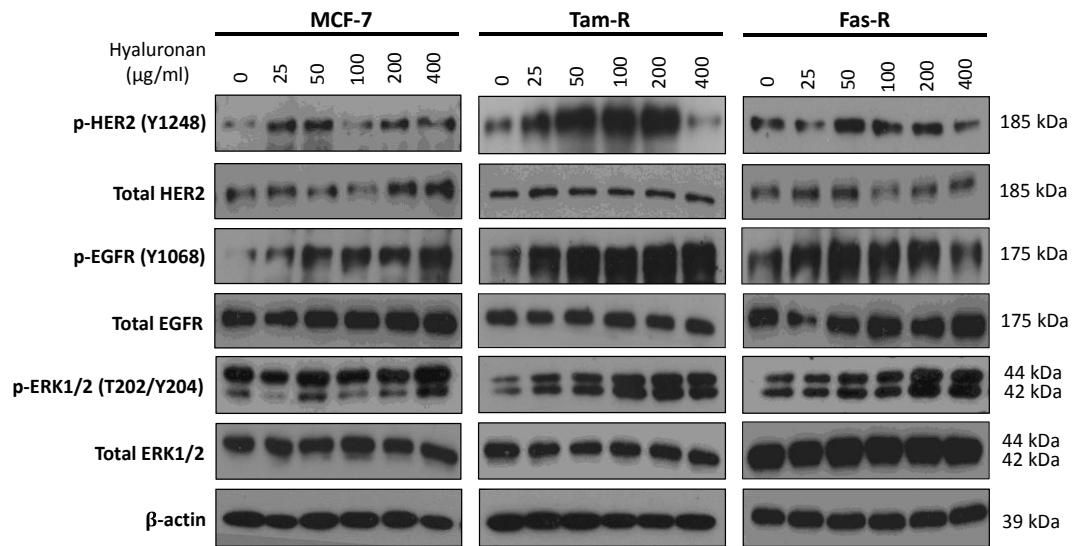


Figure 4.3. Representative Western blot images from 3 independent experiments showing HER2, EGFR and ERK1/2 activation in MCF-7, Tam-R and Fas-R cells in response to dose-dependent HA stimulation (215 kDa, 0 – 400 $\mu\text{g/ml}$) for 10 minutes with β actin as a loading control. Total protein levels were unchanged.

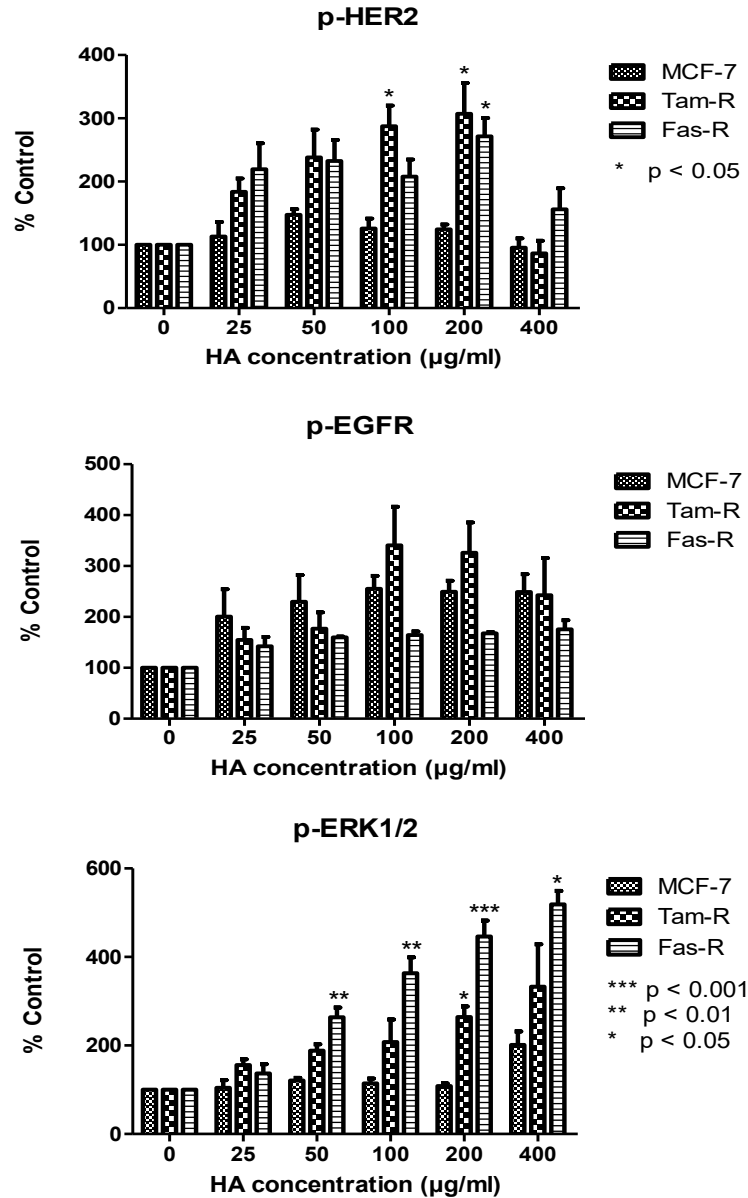


Figure 4.4. Densitometry graphs for HER2, EGFR and ERK1/2 activation across MCF-7, Tam-R and Fas-R cell models in response to dose dependent HA stimulation (215 kDa, 0 – 400 µg/ml) for 10 minutes before cell lysis and detection by Western blotting analysis. The data shows the relative protein levels in the cell lines expressed as a ratio of the active protein:total protein normalised to β-actin. Error bars represent the average normalised data ±SEM from 3 independent experiments and the data is presented as the percentage of the untreated control. Statistical analysis was performed using a one-way ANOVA with Tukey post-hoc testing to identify any significant changes across all 3 cell models.

4.2.2 CD44 suppression reduces endogenous migration, invasion and proliferation

in Tam-R and Fas-R cells

To explore whether CD44 proteins may play a role in the observed endogenous aggressive nature and HA-sensitised phenotype of the endocrine resistant cell models, an siRNA-based approach was used to suppress global CD44 expression and re-evaluate these behaviours. In this chapter it was also investigated whether RHAMM, an additional hyaladherin family member, previously shown to be expressed by endocrine resistant cell models and implicated in breast cancer (Hamilton et al. 2007; Veisoh et al. 2014), may play a role in any observed HA responses. For all subsequent experiments, 100 µg/ml HA was chosen for exogenous stimulation of resistant cell lines based upon previous data which showed that this concentration enhanced cellular behaviours in both Tam-R and Fas-R cells.

Optimisation experiments using Western blotting analysis and immunocytochemistry revealed that treatment of Tam-R and Fas-R cells with CD44 siRNA resulted in suppression of global CD44 protein expression compared to the non-targetting (NT) controls between 24 hours to 144 hours post-transfection (Figures 4.5 and 4.6 respectively). Densitometry analysis revealed a significant suppression of CD44 global expression (including CD44 Std (Figure 4.5) CD44v3, CD44v6 and CD44v10 (Appendix K)) between 48 hours – 144 hours post-transfection in Tam-R and Fas-R cells compared to the NT-siRNA control cells (however CD44v6 suppression was only significant in Tam-R cells between 72 – 144 hours), but did not alter RHAMM expression (Appendix K). Analysis of the functional effects of CD44 suppression in endocrine resistant cell lines revealed that Tam-R and Fas-R cells

treated with CD44-siRNA showed reduced endogenous and HA-stimulated migration, invasion and proliferation compared to the NT-siRNA control (Figure 4.7 and Figure 4.8 respectively).

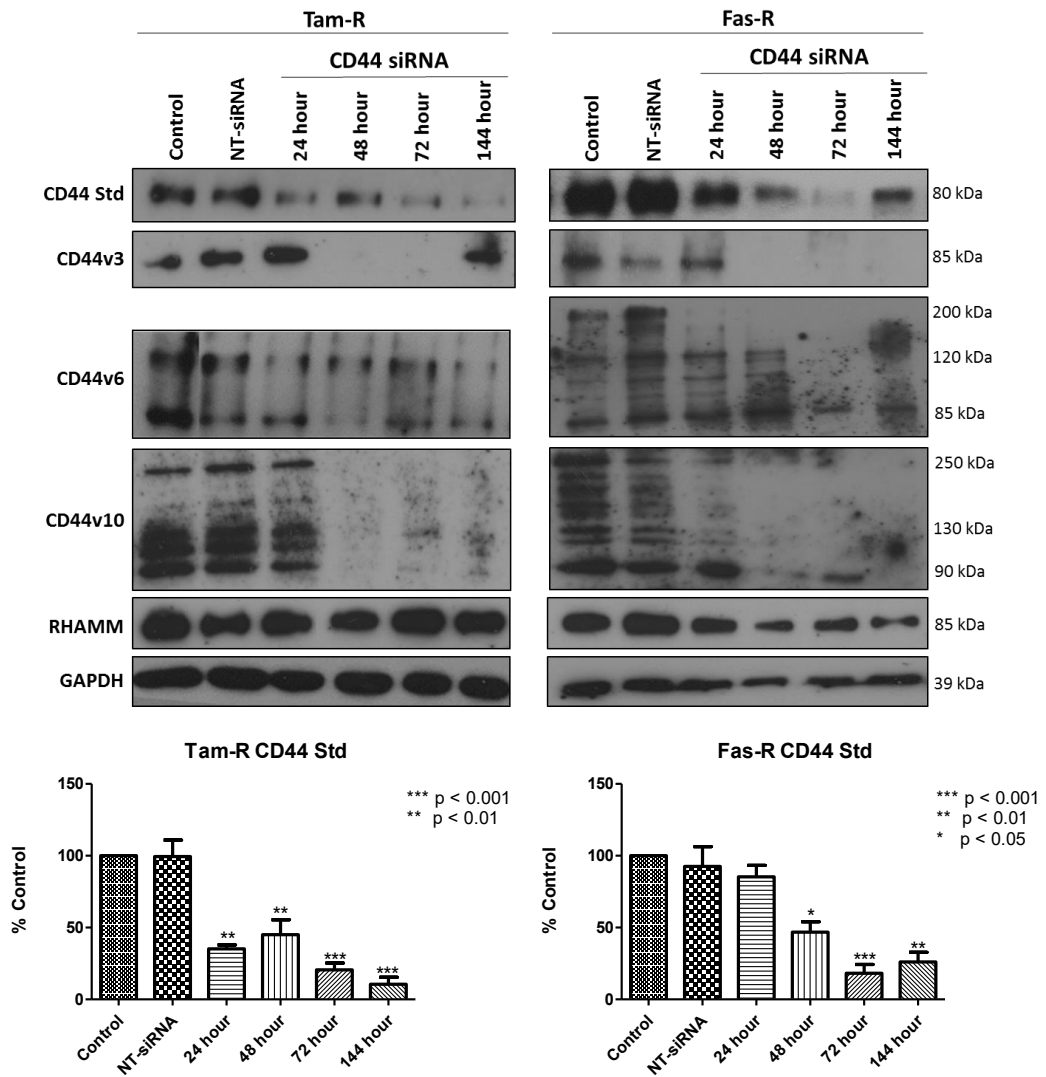


Figure 4.5. Representative Western blot images from 3 independent experiments showing CD44 isoform and RHAMM expression in Tam-R and Fas-R cells after treatment with global CD44 siRNA for 24 – 144 hours post-transfection in comparison to the untreated and NT-siRNA treated controls. GAPDH was used as a loading control. Densitometry graphs show CD44 Std expression in Tam-R and Fas-R cells between 24 – 144 hours post-transfection. Error bars represent the average normalised data \pm SEM from 3 independent experiments. Data is normalised to GAPDH and presented as the percentage of the untreated control. Statistical analysis was performed using an ANOVA test with tukey post-hoc analysis and values were compared to the NT-siRNA.

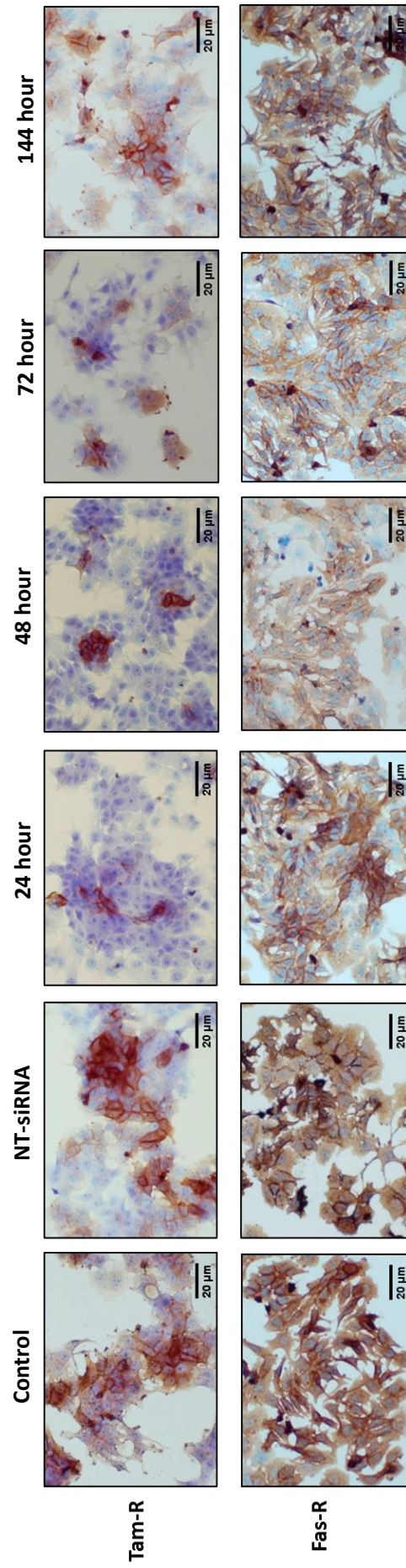


Figure 4.6. Representative images from 3 independent experiments showing CD44 global expression from immunocytochemistry analysis (x20 magnification) in Tam-R and Fas-R cells after treatment with CD44 siRNA for 24 – 144 hours post-transfection in comparison to the untreated and NT-siRNA control cells.

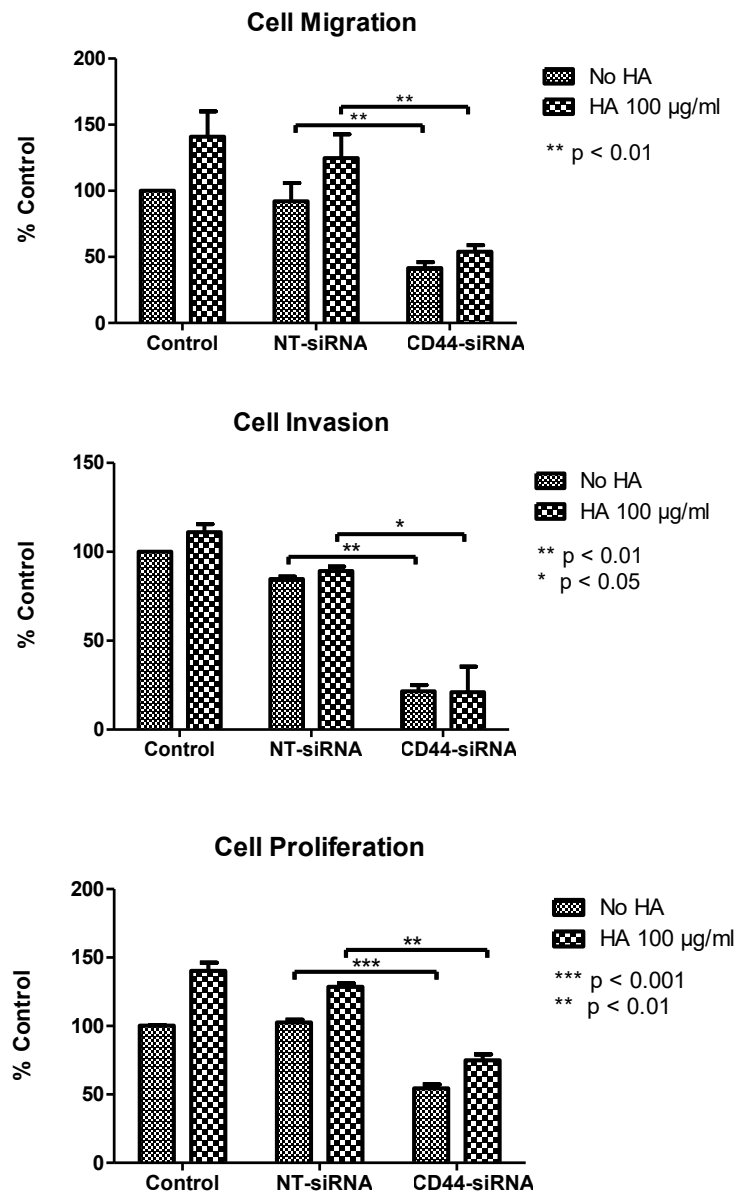


Figure 4.7. Measurement of endogenous and HA-stimulated behavioural responses of Tam-R cells after CD44 suppression. Tam-R cells were treated with NT- and CD44- siRNA for 48 hours prior to the assessment of migration, invasion (Boyden Chamber) and proliferation (Coulter Counter) assays in the presence (100 µg/ml) or absence of HA. Error bars represent the average normalised data \pm SEM from 3 independent experiments and the data is presented as the percentage of the untreated control. Statistical analysis was performed using an unpaired t-test and significance set at $p < 0.05$.

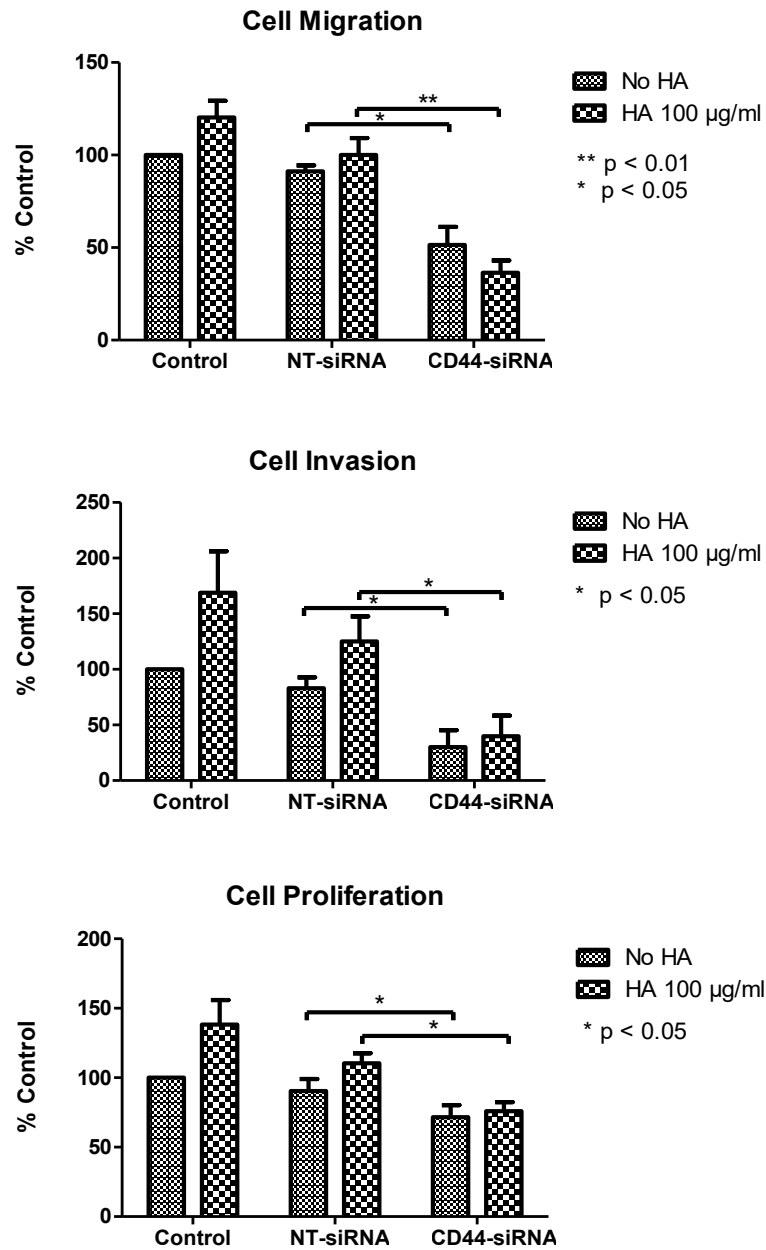


Figure 4.8. Measurement of endogenous and HA-stimulated behavioural responses of Fas-R cells after CD44 suppression. Fas-R cells were treated with NT- and CD44- siRNA for 48 hours prior to the assessment of migration, invasion (Boyden Chamber) and proliferation (Coulter Counter) in the presence (100 µg/ml) or absence of HA. Error bars represent the average normalised data \pm SEM from 3 independent experiments and the data is presented as the percentage of the untreated control. Statistical analysis was performed using an unpaired t-test and significance set at $p < 0.05$.

Since the data suggested a potential role for CD44 in HA-mediated EGFR, HER2 and ERK1/2 activation in endocrine resistant cell models, the next approach was to investigate the ability of HA to induce activation of these components in the absence of CD44, using siRNA. This approach additionally allowed the analysis of endogenous CD44-induced cellular signalling and c-Met, FAK, AKT and Src activation was also assessed as these proteins have additionally been substantially implicated in breast tumour progression behaviours and resistance to endocrine therapy (Hiscox et al. 2006; Tokunaga et al. 2006; Morgan et al. 2009; Hiscox et al. 2011; Elsberger et al. 2012; Raghav et al. 2012). Initially Western blotting analysis revealed a small increase in c-Met, FAK and AKT activation in Tam-R cells (Figure 4.9), and an increase in FAK and AKT activation in Fas-R cells (Figure 4.11), upon HA stimulation, suggesting an involvement of these proteins in the HA-induced behavioural responses of these cells. Upon CD44 suppression, Western blotting analysis further revealed a reduction in endogenous and HA-stimulated HER2, EGFR and ERK1/2 activation and HA-stimulated FAK and AKT signalling in Tam-R cells treated with CD44-siRNA compared to the NT-siRNA control (Figure 4.9) which were confirmed to be significantly reduced by densitometry analysis with the exception of HER2 (Figure 4.10). Comparatively, CD44 suppression in Fas-R cells led to a reduction in endogenous c-Met, FAK and AKT activation and HA-stimulated FAK activation compared to the NT-siRNA control (Figure 4.11), which was confirmed by densitometry analysis (Figure 4.12).

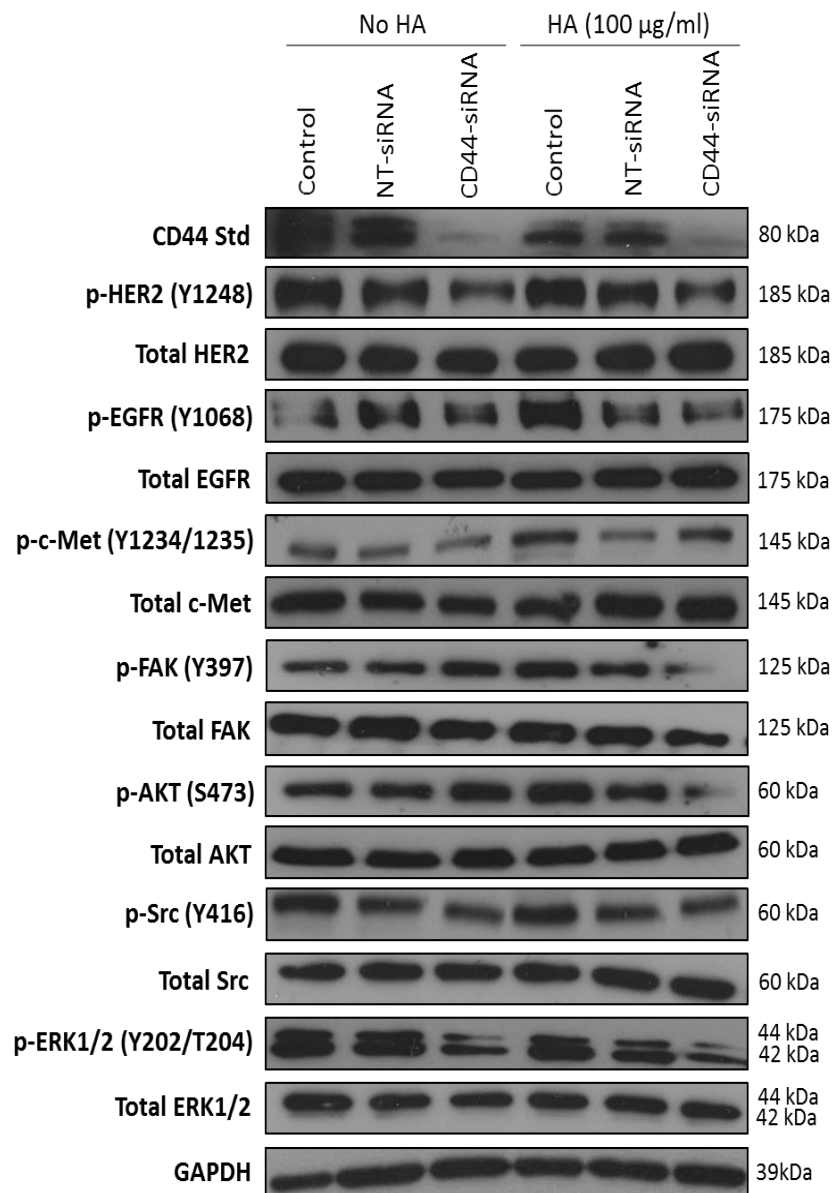


Figure 4.9. Representative Western blot images from 3 independent experiments showing HER2, EGFR, c-Met, FAK, AKT, Src and ERK1/2 activation in Tam-R cells after 48 hour treatment with global CD44 siRNA in the presence (215 kDa, 10 minutes, 100 µg/ml) or absence of HA. Total levels of each protein analysed were unchanged and GAPDH was used as a loading control.

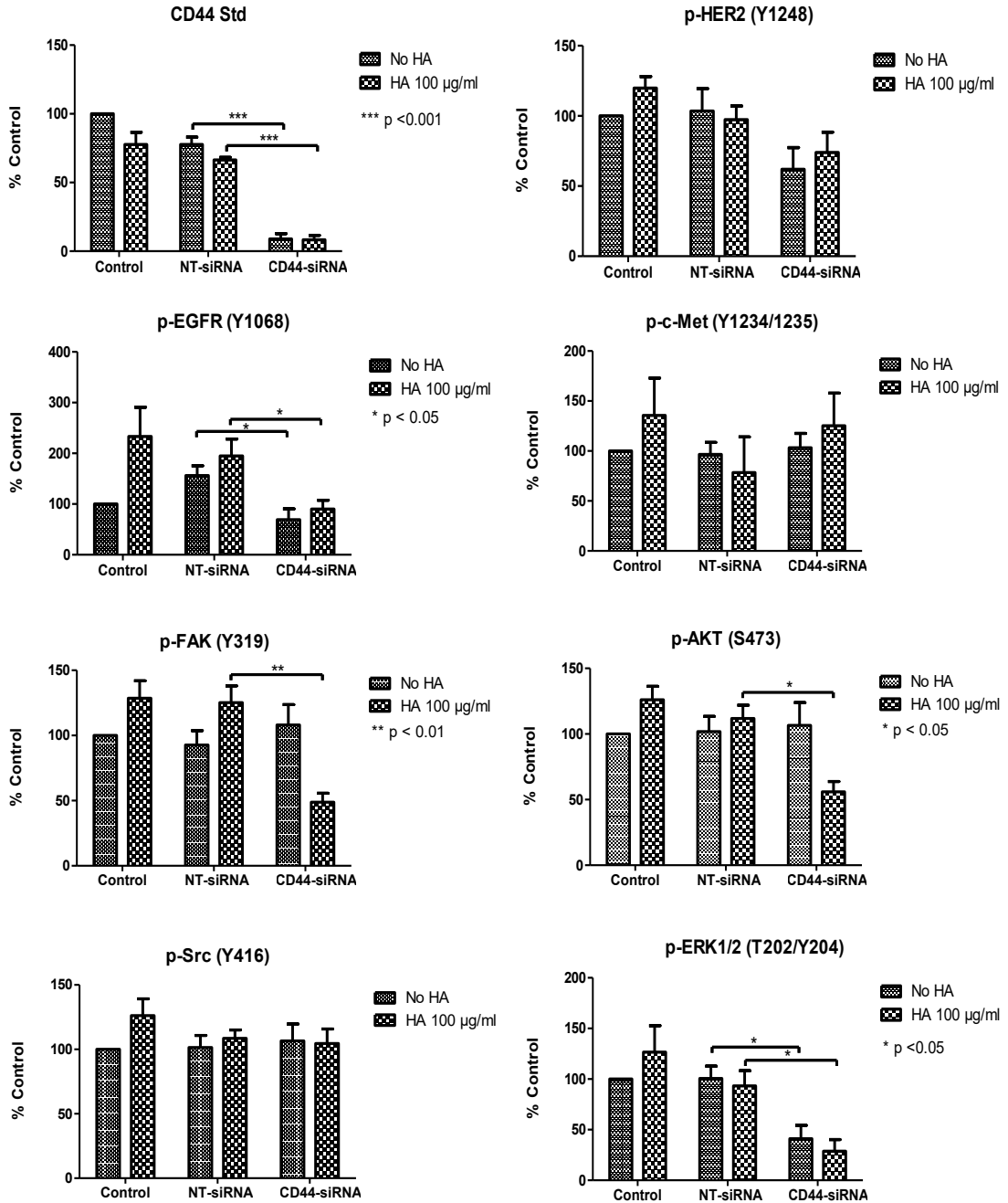


Figure 4.10. Densitometry graphs showing CD44 Std expression and HER2, EGFR, c-Met, FAK, AKT, Src and ERK1/2 activation in Tam-R cells after 48 hour treatment with global CD44 siRNA in the presence (215 kDa, 100 µg/ml, 10 minutes) or absence of HA, before cell lysis and detection by Western blotting analysis. The data shows the relative protein levels in the cell lines expressed as a ratio of the active protein:total protein normalised to GAPDH. Error bars represent the average normalised data \pm SEM from 3 independent experiments and the data is presented as the percentage of the untreated control. Statistical analysis was performed using an unpaired t-test and significance was set at $p < 0.05$.

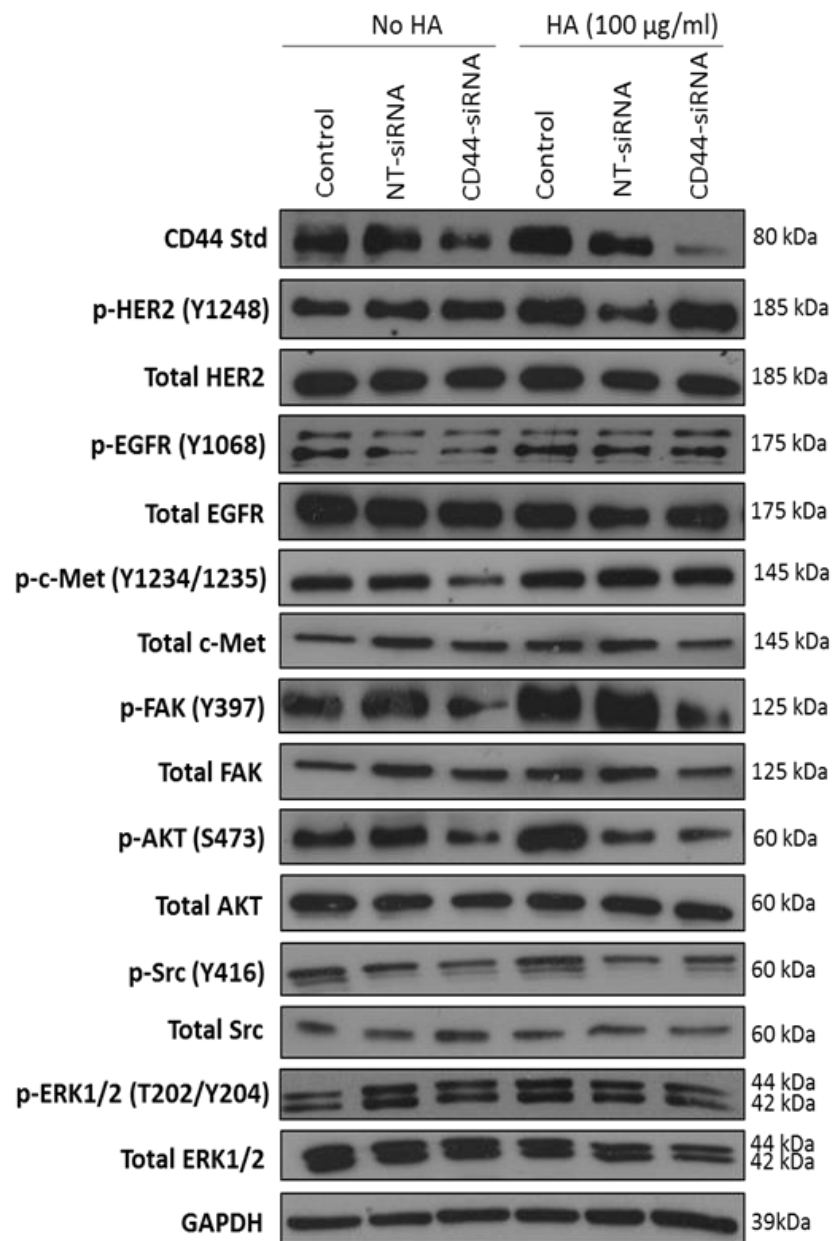


Figure 4.11. Representative Western blot images from 3 independent experiments showing HER2, EGFR, c-Met, FAK, AKT, Src and ERK1/2 activation in Fas-R cells after 48 hour treatment with global CD44 siRNA in the presence (215 kDa, 10 minutes, 100 µg/ml) or absence of HA. Total levels of each protein analysed were unchanged and GAPDH was used as a loading control.

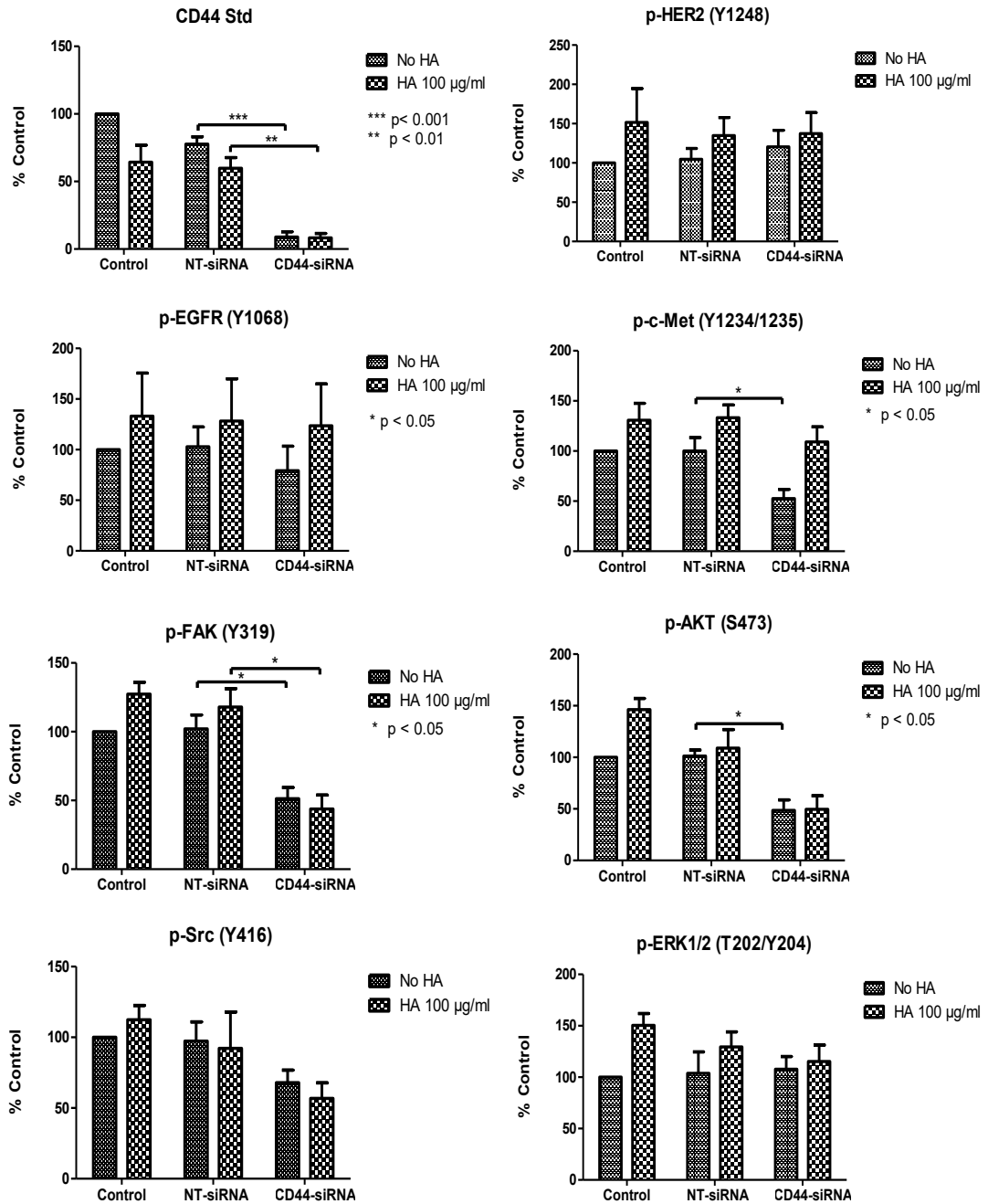


Figure 4.12. Densitometry graphs showing CD44 Std expression and HER2, EGFR, c-Met, FAK, AKT, Src and ERK1/2 activation in Fas-R cells after 48 hour treatment with global CD44 siRNA in the presence (215 kDa, 100 µg/ml, 10 minutes) or absence of HA, before cell lysis and detection by Western blotting analysis. The data shows the relative protein levels in the cell lines expressed as a ratio of the active protein:total protein normalised to GAPDH. Error bars represent the average normalised data \pm SEM from 3 independent experiments and the data is presented as the percentage of the untreated control. Statistical analysis was performed using an unpaired t-test and significance was set at $p < 0.05$.

4.2.3 Endogenous HA synthesis and metabolism does not contribute to the aggressive phenotype of Tam-R and Fas-R cells

Numerous studies have revealed correlations between high levels of HA synthases (HAS) and degradation enzymes (hyaluronidases (HYAL)) and enhanced breast cancer progression and poor patient prognosis (Udabage et al. 2005a; Tan et al. 2011; Auvinen et al. 2014). Given that the data implicated an important role for CD44 as a mediator of the highly migratory and invasive behaviour of endocrine resistant cell lines, it was hypothesised that this may be due to autocrine CD44 activation through HA synthesis (as previously reported by Hamilton et al. 2007). To begin to explore this, the gene expression of the HA synthases (HAS1/2/3) and hyaluronidases (HYAL1/2/3/SPAM1) was characterised across the cell models using affymetrix analysis.

Figure 4.13 reveals the heatmap profile for each gene probe assessed in this project with the corresponding log₂ intensity plots displaying the average normalised data (\pm SEM) and Table 4.1 lists the gene probe set IDs with their performance scores and detection calls. It should be noted that the HAS3 gene probe was not available on the U133A microarray gene chip and therefore subsequently could not be assessed within this study. Heatmap analysis revealed no change or reduced expression for all gene probes assessed in Tam-R and Fas-R cells compared to MCF-7 cells (Figure 4.13). Furthermore, the detection calls for each probe corresponding to HAS1, HAS2, HYAL1, HYAL3 and SPAM1 were absent in all cell lines and the log₂ expression values were below 0, indicative of very low/no expression of these genes across all cell models (Figure 4.13, Table 4.1). Conversely, log₂ intensity values for HYAL2 were

above 0 and the detection calls showed that this gene was present across all cell models (Figure 4.13, Table 4.1). Statistical analysis to compare gene fold changes across the cell models (shown in Table 4.2) revealed that HYAL2 gene expression was significantly reduced in Fas-R cells compared to MCF-7 cells. Further analysis revealed a significant suppression of HYAL1 gene expression in Tam-R cells versus MCF-7 cells, however, these data may be unreliable as the detection of this gene probe was determined as absent across these cells. Taken together, microarray analysis revealed a reduced expression of HYAL2 in Fas-R cells compared to their MCF-7 counterpart and suggests that HAS and HYAL gene expression is very low/absent across all the cell models. This data does not implicate these genes towards the aggressive phenotype of the endocrine resistant cells thus verification of gene expression by RT-PCR analysis would likely be unsuccessful. Based on these data, further exploration of HAS/HYAL gene expression was not undertaken.

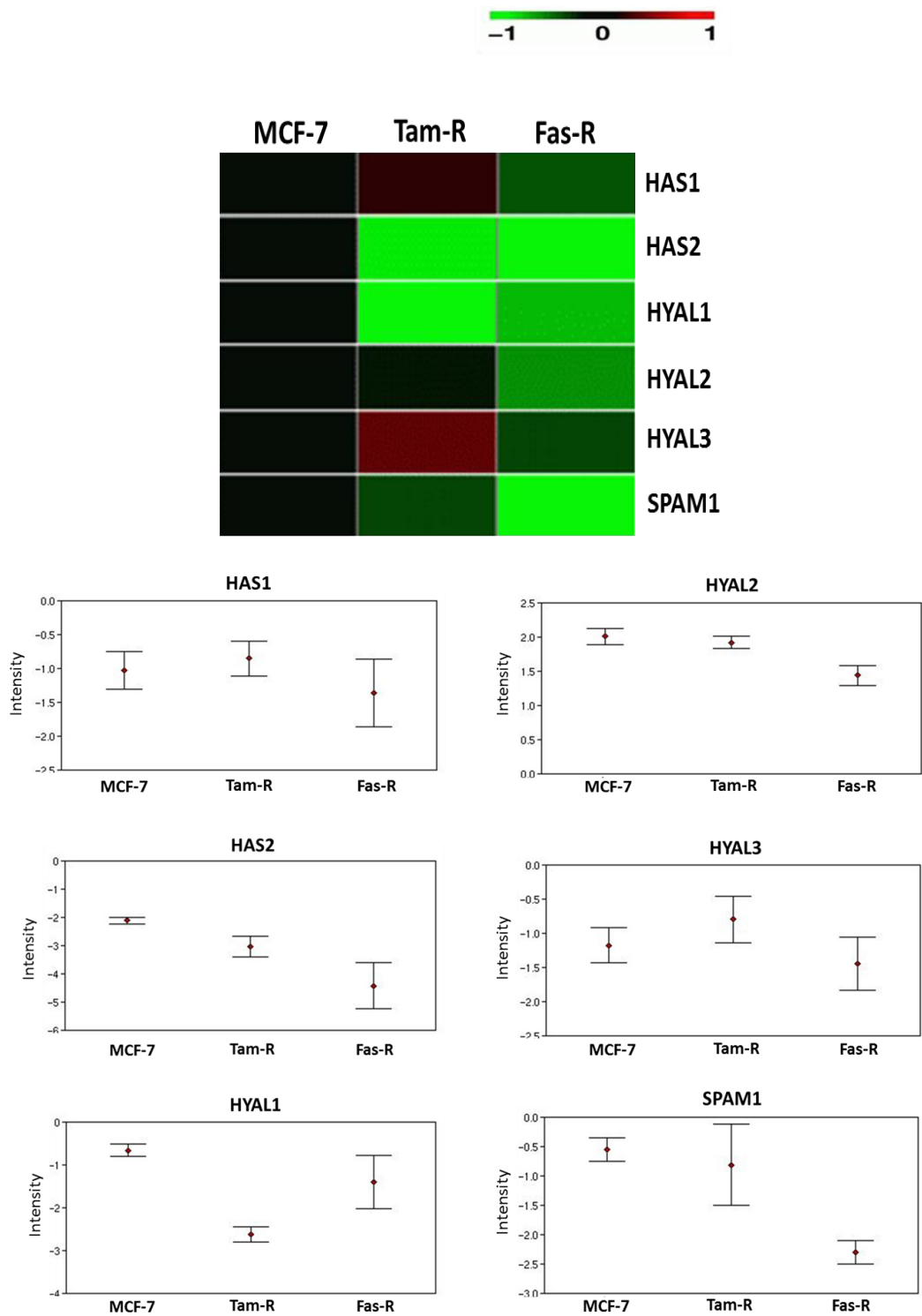


Figure 4.13. Heatmap profile displaying changes in gene expression of all HAS and HYAL genes analysed and their corresponding log₂ intensity plots with the average normalised gene expression (\pm SEM) across 3 independent experiments.

Gene	Probe Set ID	Specificity Score	Coverage Score	Robust Score	Overall Score	Detection Call
HAS1	207316_at	0.5454	1	0.6175	0.3368	A/A/A
HAS2	206432_at	0.5454	1	0.2974	0.1622	A/A/A
HYAL1	210619_s_at	0.7272	0.75	0.6002	0.3274	A/A/A
HYAL2	206855_s_at	1	1	0.5577	0.5577	P/P/P
HYAL3	211728_s_at	0.9090	1	0.5596	0.5987	A/A/A
SPAM1	210536_s_at	1	1	0.4357	0.4357	A/A/A

Table 4.1. A list of the probe set IDs for each gene assessed using the GeneSifter programme, their performance scores across an array of parameters and corresponding detection calls. All parameters are assessed on a scale ranging from 0 – 1 with a score closer to 1 indicating a better performance. Detection call identifies whether the gene expression was determined as absent (A), present (P) or mixed (M) for each probe set ID in MCF-7, Tam-R and Fas-R cells respectively.

Gene	MCF-7 versus Tam-R	MCF-7 versus Fas-R	Tam-R versus Fas-R
HAS1	1.13	<u>1.26</u>	1.42 F
HAS2	<u>1.90</u>	4.96	2.62 T
HYAL1	<u>3.90</u>	1.67	2.34 F
HYAL2	1.06	<u>1.49</u>	1.40 F
HYAL3	1.30	1.21	1.57 F
SPAM1	<u>1.20</u>	3.38	2.80 F

Table 4.2. The fold change values in gene expression for each gene analysed by affymetrix. ANOVA testing with Tukey post-hoc analysis was performed to identify any significant changes in gene fold expression across all 3 cells models and significant changes are highlighted in bold and underlined. Green represents decreased fold changes, red indicates increased fold changes and black represents no change. HYAL1 gene fold change was significantly decreased in Tam-R cells compared to MCF-7 cells ($p = 0.02554$) and HYAL2 gene fold change was significantly decreased in Fas-R cells compared to MCF-7 cells ($p = 0.036404$). In the final column, fold change values relating to either Tam-R or Fas-R cells are indicated by 'T' or 'F' respectively.

4.3 Discussion

This chapter set out to explore the consequence of CD44 overexpression for both the intrinsic and HA-stimulated phenotype of endocrine resistant cell models. In particular, the hypothesis that upregulated expression of CD44 proteins in Tam-R and Fas-R cells leads to HA-sensitisation and subsequently induced migratory, invasive and/or proliferative responses by RTK activation was explored.

The results primarily revealed that enhanced CD44 expression correlated with an increase in the endogenous aggressive phenotype of endocrine resistant cell models. Analysis showed an enhanced basal invasive capacity of Tam-R cells compared to MCF-7 cells, however Fas-R cells (which exhibit the highest level of CD44 expression) displayed an elevated migratory, invasive and proliferative capacity compared to their endocrine sensitive MCF-7 counterpart. This association was validated by global suppression of CD44 proteins which reduced the endogenous migratory, invasive and proliferative capacity of Tam-R and Fas-R cells. However, upon investigation of the signalling mechanisms through which CD44 proteins may mediate these events, differences in RTK activation and downstream signalling was observed between these resistant cell models. Indeed, the siRNA data suggested a role for CD44 proteins within the endogenous activation of the RTKs, EGFR and HER2, leading to downstream activation of ERK1/2 in Tam-R cells. These results were not surprising as EGFR and HER2 have been heavily implicated within the acquisition of tamoxifen resistance and high levels of endogenous HER2 and EGFR expression are exhibited in Tam-R cells (Knowlden et al. 2003; Hiscox et al. 2012). Furthermore, these data corroborate with other studies which have shown dimerization to occur between

CD44 and ErbB receptors in carcinoma cells (Bao et al. 2011; Hatano et al. 2011; Hiscox et al. 2012) and revealed a role for CD44-mediated activation of these RTKs leading to enhanced cellular motility (Wang et al. 2006; Kim et al. 2008). However, although previous data from the BCMPG revealed elevated levels of EGFR and HER2 in fulvestrant-resistant cells (McClelland et al. 2001; Gee et al. 2005), the contribution of these receptors to their aggressive phenotype remains to be elucidated and data here suggests that these receptors do not play a prominent role in CD44-mediated behaviours in these cells. However, previous studies by the Hiscox group (2006) revealed that c-Met is overexpressed in fulvestrant-resistance and CD44 global suppression data in this study revealed reduced endogenous c-Met activation in Fas-R cells, thus potentially suggesting a role for CD44-mediated c-Met activation in this cell line. In support of this, Orian-Rousseau et al. 2002 identified that CD44 is required for the full activation of the c-Met receptor and Hasenauer et al. 2013 published evidence for the requirement of CD44v6 in c-Met internalisation. In further support of an association between CD44 and c-Met, numerous clinical studies have revealed upregulation of both CD44 (Klingbeil et al. 2010; Montgomery et al. 2012) and c-Met (Garcia et al. 2007; Graveel et al. 2009; Ho-Yen et al. 2014) expression to be strongly correlated with the aggressive triple negative basal subtype of breast cancer and poor prognosis. Interestingly, an ER-negative, basal-like phenotype is also exhibited by Fas-R cells. Taken together, whilst our siRNA suppression data revealed an importance for CD44 proteins towards the aggressive phenotype of both endocrine resistant cell models, the signalling mechanisms through which they contribute to

these behaviours appear to be mediated through differential pathways, potentially due to variances in the bioavailability of specific co-receptors between these cells.

To explore whether enhanced CD44 protein expression sensitised endocrine resistant cells to HA, these cells were treated with exogenous HA and their behavioural responses were re-evaluated. The results revealed that HA stimulation led to an enhanced migratory response in Tam-R cells and elevated migration, invasion and growth responses in Fas-R cells, an effect not observed in MCF-7 cells. These results implicate CD44 proteins towards the augmentation of HA responses in the endocrine resistant cell models, particularly within Fas-R cells which exhibit the greatest level of CD44 expression compared to MCF-7 and Tam-R cells. As a further demonstration that CD44 was responsible for these HA-induced cellular behaviours, it was also observed that HA failed to elicit a response in endocrine resistant cells upon CD44 suppression by siRNA. These data are supported by findings from Hamilton et al. 2007 which revealed that the highly CD44- (and RHAMM-) expressing invasive MDA-MB-231 breast cancer cell line showed significantly enhanced motility in response to HA stimulation, which was not found in MCF-7 cells. Furthermore, Vieseh et al. 2014 revealed that the more malignant MDA-MB-231 and T4-2 breast cancer cells (high CD44 and RHAMM expression) showed enhanced total levels of HA binding and a greater degree of HA heterogeneity binding compared to MCF-7 and SKBr3 cells (low CD44 and RHAMM expression), and conversion of MDA-MB-231 cells to a less malignant phenotype reverted these HA binding capabilities. The data also suggested that CD44, and not the alternative hyaladherin RHAMM (also present within the endocrine resistant cells), mediated these effects as RHAMM expression

was not substantially impaired upon CD44 suppression. Taken together, the data corroborates with previously reported findings and suggests that enhanced HA binding capabilities in cells may act as a determinant towards the degree of their malignant behaviour; an effect likely to be the result of enhanced CD44 expression in the endocrine resistant cell models.

To determine the mechanisms through which HA stimulation may enhance the adverse cellular behaviour of these endocrine resistant cell models, the effect of exogenous HA induction upon ErbB activation was investigated. The results revealed enhanced HER2 and EGFR activation in Tam-R cells upon HA stimulation, an effect observed to a lesser degree in MCF-7 and Fas-R cells. Furthermore, these investigations revealed a dose dependent increase in HER2 activation in Tam-R cells upon HA stimulation which mirrored their migratory response, thus potentially implicating CD44 in the activation of HER2 and subsequently enhanced migration in these cells. These data were further verified through CD44 siRNA analyses which revealed that suppression of CD44 proteins reduced both migration and HER2 signalling upon HA stimulation in Tam-R cells. These data corroborate with published studies which implicate CD44 (particularly the standard isoform) in the activation of HER2-mediated signalling and subsequently enhanced tumour progression behaviours of cancer cells (Bourguignon et al. 1997; Palyi-Krekk et al. 2008; Bao et al. 2011). Furthermore, studies by Duru et al. 2012 showed that HER2+/CD44+ breast cancer stem cells exhibited a more aggressive phenotype and were found to be more frequently detected in recurrent tumours as compared to the HER2-/CD44+ subpopulation. These findings have also been observed in the clinical setting through

strong associations between the co-expression of CD44, HA and HER2 in breast cancer patients and poor prognosis (Baek et al. 2011; Auvinen et al. 2013).

The siRNA data also suggested an important role for CD44 proteins in the HA-induced invasive and growth capabilities of Tam-R cells; an effect which may involve downstream ErbB receptor signalling activation of FAK, AKT and ERK1/2 cascades. Indeed, numerous studies have reported a role for CD44-ErbB dimer complexes in enhanced cellular motility through the activation of various signalling molecules including those identified in this study (Wang and Bourguignon et al. 2006; Kim et al. 2008; Bao et al. 2011; Hatano et al. 2011). In Fas-R cells, HA also promoted a CD44-dependent increase in migration, invasion and proliferation although the mechanisms through which this occurs remains unclear. Western blotting data suggested an involvement of FAK, AKT and ERK1/2, however did not implicate the activation of these effectors downstream of the ErbB receptor signalling cascade.

As the data revealed an important role for HA towards the augmentation of adverse cellular behaviour in the resistant cells, the role of endogenous HA synthesis across all cell models was investigated. Whilst the majority of HA is thought to be produced by stromal cells in the tumour microenvironment, several studies have revealed that carcinoma cells themselves can also synthesise HA (Kimata et al. 1983; Heldin et al. 1996; Simpson et al. 2002) and numerous reports have shown a role for the enzymes responsible for HA synthesis and degradation in the development of a pro-metastatic environment and enhanced breast tumourigenesis (Li et al. 2007; Tan et al. 2011; Auvinen et al. 2014). Furthermore, Hamilton et al. 2007 revealed that the highly CD44-expressing invasive MDA-MB-231 breast cancer cell line produced higher levels

of endogenous HA compared to the low CD44-expressing, less invasive MCF-7 cell line. From these findings this group suggested that invasive breast cancer cells establish an autocrine HA-CD44 mechanism to promote cellular motility. In this context, HA production by breast cancer cells could involve an alteration in its synthesis and/or metabolism.

Whilst many reports have correlated high levels of HAS/HYAL gene expression with breast cancer progression and poor prognosis (Udabage et al. 2005a; Tan et al. 2011; Auvinen et al. 2014), the microarray data suggested that enzymes involved in HA synthesis or metabolism were not overexpressed in the endocrine resistant cell models. Whilst endogenous HA production by these cells through alternative measures such as an ELISA was not examined, it is unlikely that significant levels of HA synthesis occur in these cells due to the low/absent levels of these enzymes detected by microarray analysis. Whilst these results are in discordance with findings from Hamilton et al. 2007 and do not suggest that the aggressive endocrine resistant cells exhibit a greater reliance upon endogenous HA, it may be argued that upregulation of CD44 in these cells would sensitise them to HA present in the tumour microenvironment. Indeed, although Auvinen et al. 2014 found a wide expression of HAS enzymes in both stromal and carcinoma cells across 278 breast cancer cases, a stronger correlation of these enzymes with disease recurrence and poor prognosis was found in stromal cells. These studies suggested that enhanced HAS expression in stromal cells was a more robust marker for tumour progression compared with HAS in carcinoma cells. Whilst numerous reports present a convincing role for HAS/HYAL enzymes in tumour progression behaviours in multiple carcinomas, including breast

cancer, this area remains largely unstudied and results have been contradictory. Furthermore, understanding the role of HAS/HYAL enzymes in breast cancer cell models under cell culture conditions remains complicated as cells may exhibit reduced capabilities to synthesise HA in vitro, even when derived from HA-enriched tumours (Knudson et al. 1989). Taken together, the role of HAS/HYAL enzymes across the cell models in this project remains incompletely understood and requires further elucidation, however data may indicate a greater reliance of Tam-R and Fas-R cells upon HA production from the microenvironment for their subsequent utilisation and HA-induced activities.

4.3.1 Summary

In this chapter, an important role for CD44 proteins in both the basal and HA-stimulated adverse cellular phenotype of Tam-R and Fas-R cells has been shown. However due to the phenotypic differences between Tam-R (ER+) and Fas-R (ER-) cells and differential protein compositions, results suggest that CD44 proteins may activate alternative RTK signalling pathways in these cell lines to mediate distinct behavioural functions. Taken together, these data suggest that upregulation of CD44 proteins in endocrine resistance may enhance their aggressive phenotype through RTK activation and sensitivity to their principle ligand, HA.

5. Exploration of RHAMM as a mediator of the aggressive phenotype of endocrine resistant breast cancer cells

5.1 Introduction

In the previous chapter it was demonstrated that HA augmented the migratory, invasive and proliferative capacity of the endocrine resistant, but not endocrine sensitive, cells. Given that the endocrine resistant cell models both overexpress CD44, the major receptor for HA, and siRNA suppression of CD44 reduced the HA augmented cellular functions in these cells, it is likely that these effects are mediated through the CD44 receptor. However, initial characterisation studies also revealed the expression of an additional hyaladherin, RHAMM, in Tam-R and Fas-R cells, albeit at a level similar to that observed in their parental endocrine sensitive MCF-7 cell line, thus, the contribution of RHAMM to the endogenous and HA-induced cellular behaviours of the endocrine resistant cell models remains unclear. Given that several studies have revealed a link between RHAMM expression and enhanced metastasis and poor prognosis in breast cancers (Wang et al. 1998; Hamilton et al. 2011; Veiseh et al. 2014; Wang et al. 2014), it may be possible that RHAMM possesses tumour-promoting activity in endocrine resistant cells.

Similarly to CD44, RHAMM undergoes alternative splicing, however the biological roles of RHAMM are complex and it is one of the first proteins to be identified in which its intracellular and extracellular functions are distinct (Chivasa et al. 2006; Tjaslma et al. 2006). Intracellular full length RHAMM isoforms are cytoskeletal, centrosomal and nuclear proteins which mediate functions critical for mitotic spindle

integrity, progression through the cell cycle and cell division fidelity (Maxwell et al. 2003; Groen et al. 2004; Tolg et al. 2010). Conversely, truncated cell surface RHAMM isoforms are exported to the cell surface where they associate with integral non-protein/protein tyrosine kinase receptors to bind HA and mediate downstream signalling responses leading to enhanced cellular motility (Hamilton et al. 2007; Hatano et al. 2011; Park et al. 2012). At present the separate and coordinated functions of extracellular and intracellular RHAMM proteins remains to be elucidated (Chivasa et al. 2006; Tjaslma et al. 2006).

The oncogenic functions of RHAMM have been predominantly linked to its extracellular functions as a consequence of its HA-binding capacity. Indeed, RHAMM has been implicated in breast cancer progression through the activation of multiple signalling cascades which control the expression of cell cycle and motility genes including: ras (Hall et al. 1995), Src (Hall et al. 1996), and MAPK (Wang et al 1998). Since RHAMM proteins lack a membrane spanning domain, cell surface RHAMM partners with various integral membrane receptors to mediate these functions (Savani et al. 2001; Manzanares et al. 2007; Hatano et al. 2011; Park et al. 2012). Of these, the most extensively studied associations of RHAMM in breast cancer is with the CD44 receptor. Indeed, Veiseh et al. 2014 revealed that CD44 and RHAMM co-expression was found to be highest in aggressive triple negative subtypes of breast cancer cells which also exhibited the greatest degree of HA-binding; properties thought to contribute to the malignant phenotype. Furthermore, Hamilton et al. 2007 established a role for the formation of RHAMM-CD44 complexes at the cell surface of the highly invasive MDA-MB-231 breast cancer cell line towards the

promotion of an HA-induced autocrine motility mechanism in an ERK1/2 dependent manner. These studies, and observations from other groups, have raised the possibility that cell surface RHAMM may partner with CD44 to enhance its localisation at the cell surface and 'unleash' its pro-migratory and invasive functions (Tolg et al. 2006).

Taken together, numerous studies potentiate a role for RHAMM proteins within breast cancer oncogenesis particularly through their extracellular HA-binding capacity. As it was previously revealed that HA stimulation enhances the aggressive phenotype of the endocrine resistant cell models, the contribution of RHAMM to these HA-mediated behaviours was explored. As initial characterisation studies revealed that RHAMM proteins showed predominant cytoskeletal staining across all cell models, the role of RHAMM proteins towards the endogenous phenotype of the endocrine resistant cell models was also investigated.

5.1.1 Objectives

1. To investigate the contribution of RHAMM proteins towards the endogenous and HA-stimulated migratory, invasive and proliferative phenotype of endocrine resistant cell models by siRNA-mediated RHAMM suppression.
2. To determine whether RHAMM is involved in endogenous and HA-stimulated signalling activity across the cell models of endocrine resistance.

5.2 Results

5.2.1 RHAMM suppression inhibits proliferation of Tam-R cells

Numerous reports have shown that RHAMM proteins mediate migratory, invasive and proliferative behaviours in breast cancer cells (Hamilton et al. 2007; Heldin et al. 2013; Wang et al. 2014). Therefore, to investigate the contribution of RHAMM towards the aggressive phenotype of Tam-R and Fas-R cells, an siRNA based approach was used prior to the assessment of these behaviours in the presence (100 µg/ml) and absence of HA. Initial Western blotting and immunocytochemistry analysis revealed that treatment of both Tam-R and Fas-R cells with global RHAMM siRNA reduced RHAMM expression in comparison to the NT-siRNA control and untreated control samples between 24 – 144 hours post-transfection (Figures 5.1 and 5.2 respectively). Densitometry analysis revealed that RHAMM expression was significantly reduced between 72 - 144 hours post-transfection in Tam-R cells and between 48 – 144 hours post-transfection in Fas-R cells, compared to the NT-siRNA control cells (Figure 5.1). Densitometry analysis also confirmed that CD44 isoform expression was not significantly altered in Tam-R and Fas-R cells upon RHAMM suppression (Appendix L).

Analysis of the functional effects of RHAMM suppression in the endocrine resistant cells revealed no significant alterations in the migratory or invasive capacity of Tam-R or Fas-R cells (Figure 5.3 and Figure 5.4 respectively), however reduced the endogenous and HA-stimulated proliferation of Tam-R cells, but not Fas-R cells, compared to the NT-siRNA control (Figure 5.3 and Figure 5.4 respectively).

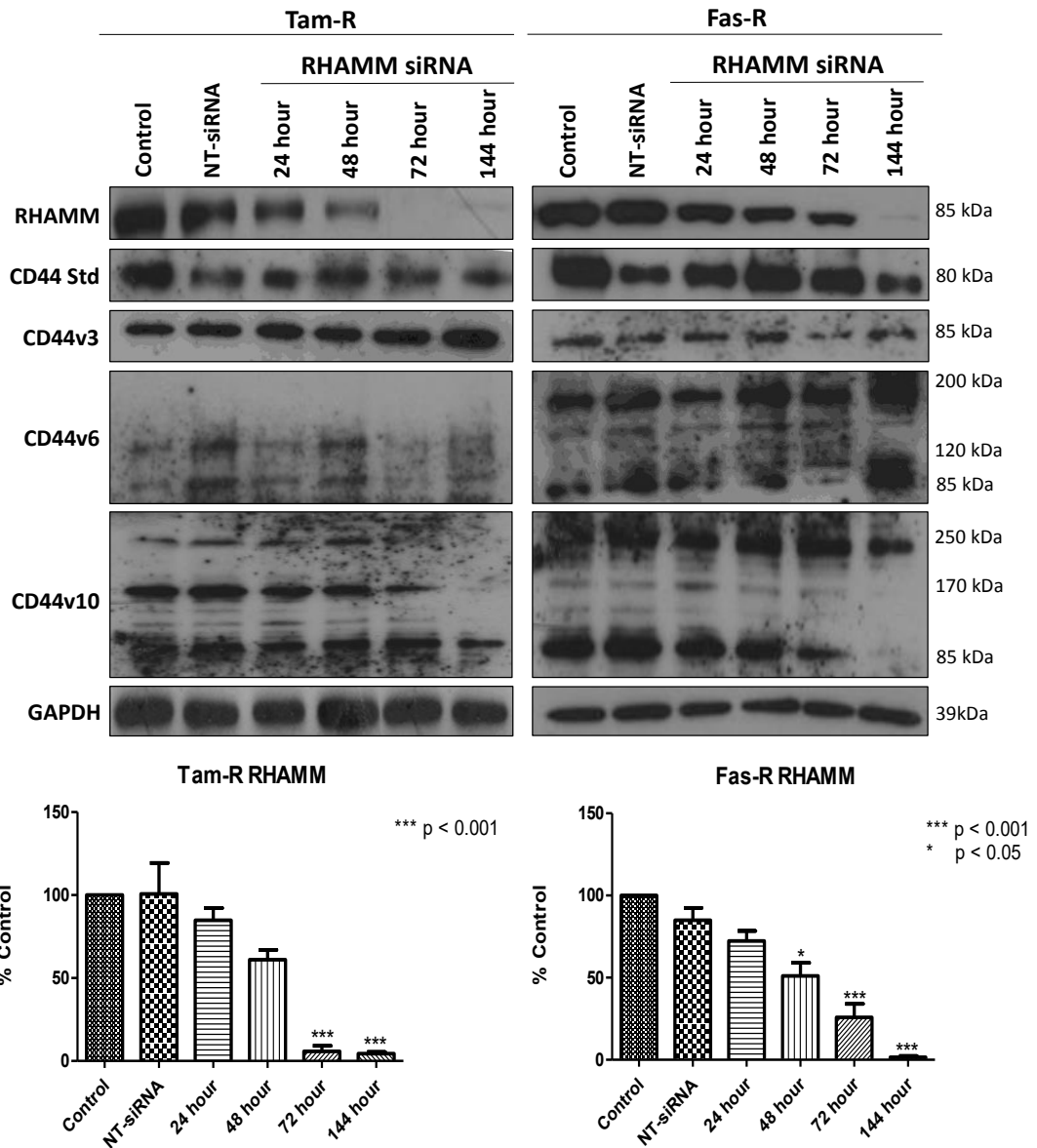


Figure 5.1. Representative Western blot images from 3 independent experiments showing RHAMM and CD44 isoform expression in Tam-R and Fas-R cells after treatment with global RHAMM siRNA between 24 – 144 hours post transfection in comparison to the untreated and NT-siRNA treated control. GAPDH was used as a loading control. Densitometry graphs show RHAMM expression in Tam-R and Fas-R cells between 24 – 144 hours post-transfection. Error bars represent the average normalised data \pm SEM from 3 independent experiments. The data is normalised to GAPDH and presented as the percentage of the untreated control. Statistical analysis was performed using an ANOVA test with tukey post-hoc analysis and values were compared to the NT-siRNA control sample. Significance was set at $p < 0.05$.

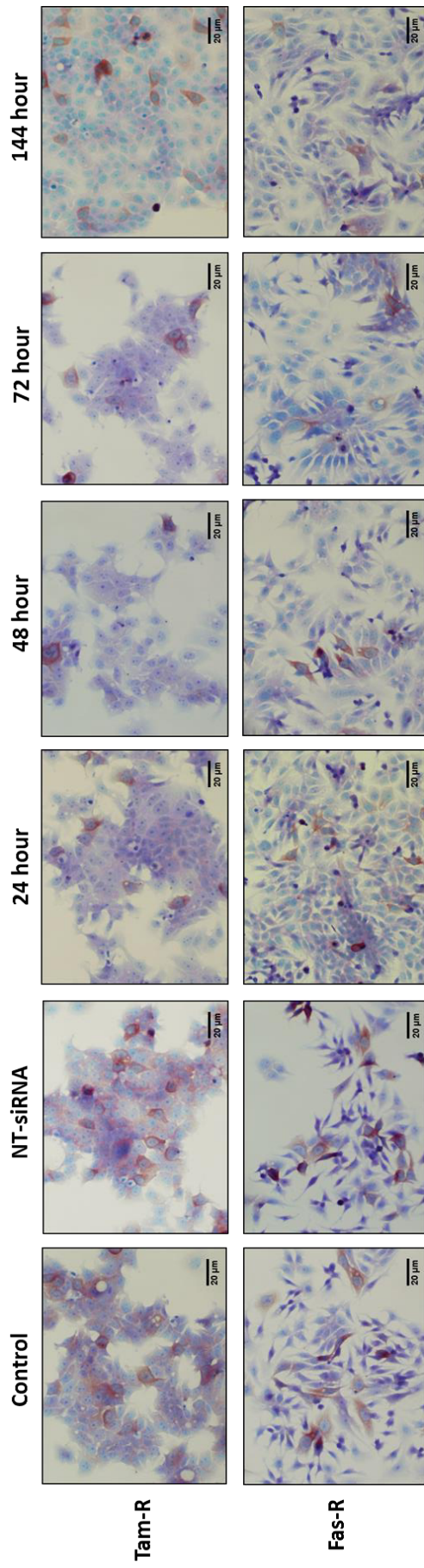


Figure 5.2. Representative images from 3 independent experiments showing global RHAMM expression from immunocytochemistry analysis (x20 magnification) in Tam-R and Fas-R cells after RHAMM siRNA treatment for 24 – 144 hours post-transfection in comparison to the untreated and NT-siRNA treated control samples.

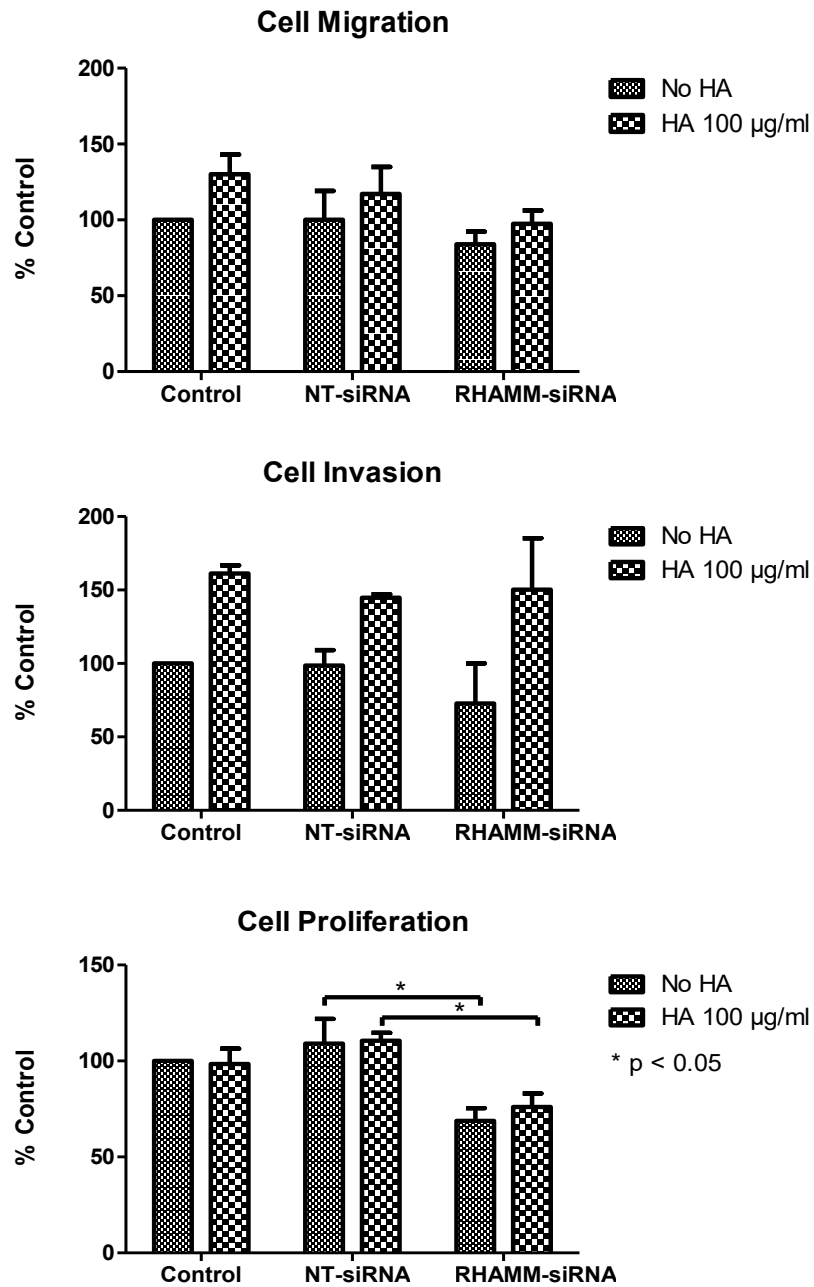


Figure 5.3. Measurement of endogenous and HA-stimulated cell behaviour of Tam-R cells after RHAMM suppression. Tam-R cells were treated with RHAMM siRNA for 48 hours prior to the assessment of migration, invasion (Boyden Chamber) and proliferation (Coulter Counter) in the presence (100 µg/ml) and absence of HA. Error bars represent the average normalised data \pm SEM from 3 independent experiments and the data is presented as the percentage of the untreated control. Statistical analysis was performed using an unpaired t-test and significance set at $p < 0.05$.

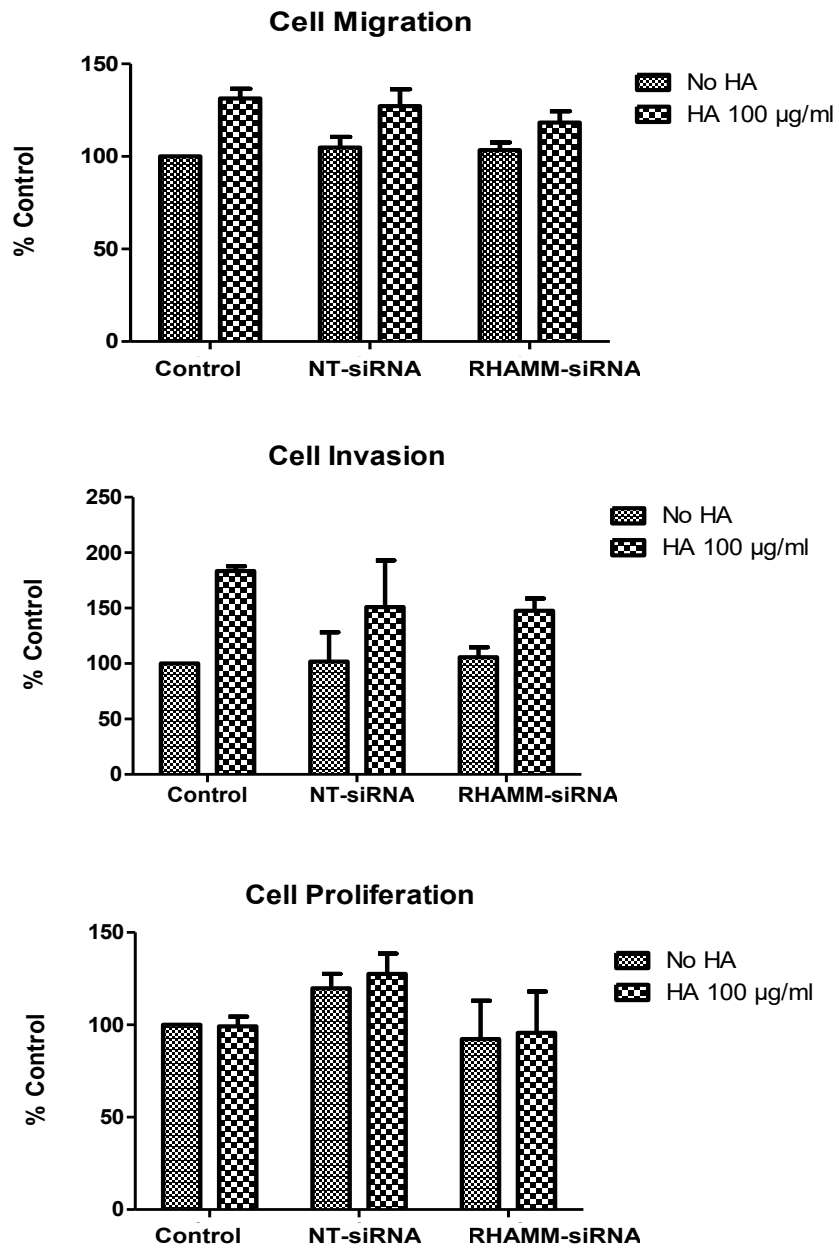


Figure 5.4. Measurement of endogenous and HA-stimulated cell behaviour of Fas-R cells after RHAMM suppression. Fas-R cells were treated with RHAMM siRNA for 48 hours prior to the assessment of migration, invasion (Boyden Chamber) and proliferation (Coulter Counter) in the presence (100 µg/ml) and absence of HA. Error bars represent the average normalised data \pm SEM from 3 independent experiments and the data is presented as the percentage of the untreated control. Statistical analysis was performed using an unpaired t-test and significance set at $p < 0.05$.

5.2.2 RHAMM suppression augments cellular signalling in Tam-R and Fas-R cells

Given that RHAMM suppression led to a reduction in the proliferation of Tam-R cells, the next step was to explore the hypothesis that RHAMM may act to control cell growth through activation of signalling pathways. The effect of RHAMM suppression upon Fas-R signalling was also investigated. To investigate this hypothesis, the effect of RHAMM suppression upon endogenous and HA-stimulated FAK, Src and ERK1/2 activation in the endocrine resistant cell models was explored; effectors known to be involved in RHAMM-mediated motility in breast cancer cells (Hall et al. 1994; Hall et al. 1996; Wang et al. 1998). Western blotting analysis revealed that RHAMM suppression led to a non-significant reduction in endogenous ERK1/2 activation in Tam-R cells and suppressed endogenous and HA-stimulated FAK activation in Fas-R cells, however Src activity was unaltered (Figures 5.5 - 5.8).

RHAMM binding to CD44 has been reported to impact upon the signalling competency of this receptor (Hatano et al. 2011; Park et al. 2012), therefore it was important to determine the role of RHAMM in CD44-mediated signalling. As previous studies in this thesis revealed a role for CD44 in the activation of ErbB receptors, c-Met and AKT in the endocrine resistant cell models, the modulation of these receptors upon RHAMM suppression was investigated. Western blotting analysis revealed a reduction in endogenous c-Met and AKT signalling and HA-induced c-Met and EGFR activation in Tam-R cells compared to the NT-siRNA control, confirmed by densitometry analysis (Figures 5.5 and 5.6). RHAMM suppression in Fas-R cells led to a non-significant decrease in endogenous c-Met activation and HA-stimulated EGFR and AKT signalling compared to the NT-siRNA control (Figures 5.7 and 5.8).

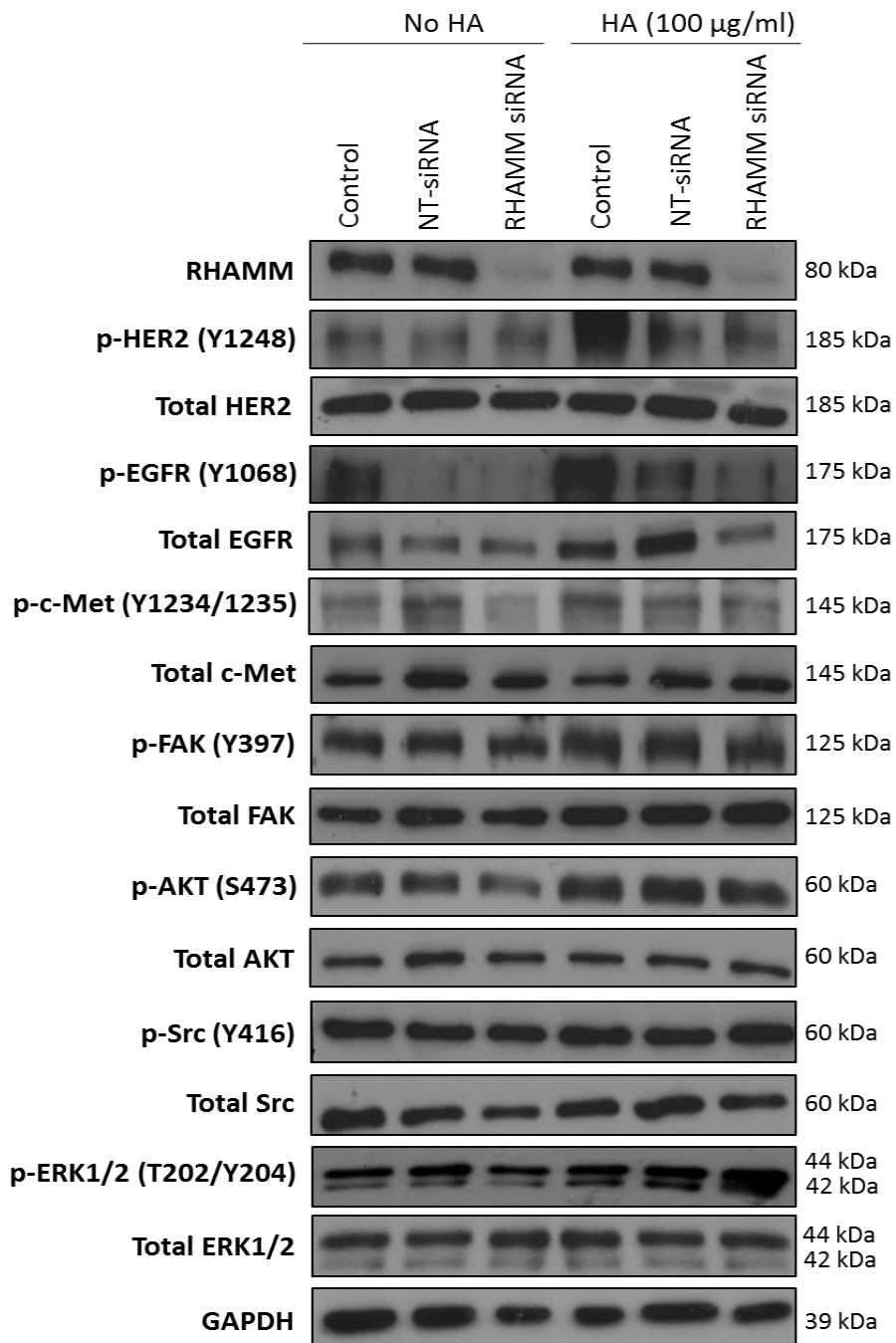


Figure 5.5. Representative Western blot images from 3 independent experiments showing HER2, EGFR, c-Met, FAK, AKT, Src and ERK1/2 activation in Tam-R cells treated with RHAMM siRNA for 48 hours in the presence (10 minute treatment, 100 µg/ml) and absence of HA. GAPDH was used as a loading control. Total levels of each protein analysed were unchanged.

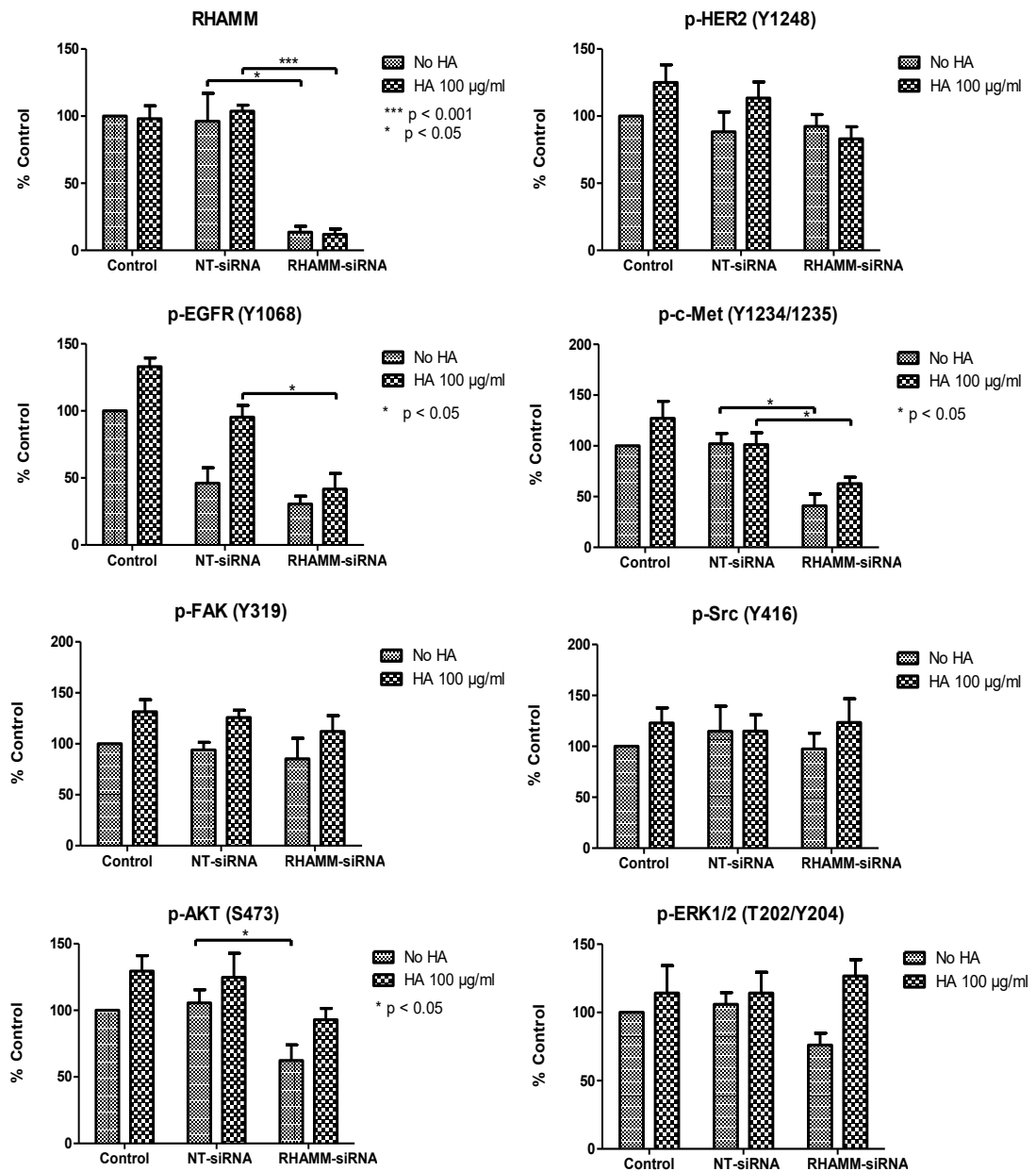


Figure 5.6. Densitometry graphs showing RHAMM expression and HER2, EGFR, c-Met, FAK, AKT, Src and ERK1/2 activation in Tam-R cells after 48 hour treatment with global RHAMM siRNA in the presence (215 kDa, 100 µg/ml, 10 minutes) of absence of HA, before cell lysis and detection by Western blotting analysis. The data shows the relative protein levels in the cell lines expressed as a ratio of the active protein:total protein normalised to GAPDH. Error bars represent the average normalised data \pm SEM from 3 independent experiments and the data is presented as the percentage of the untreated control. Statistical analysis was performed using an unpaired t-test and significance was set at $p < 0.05$.

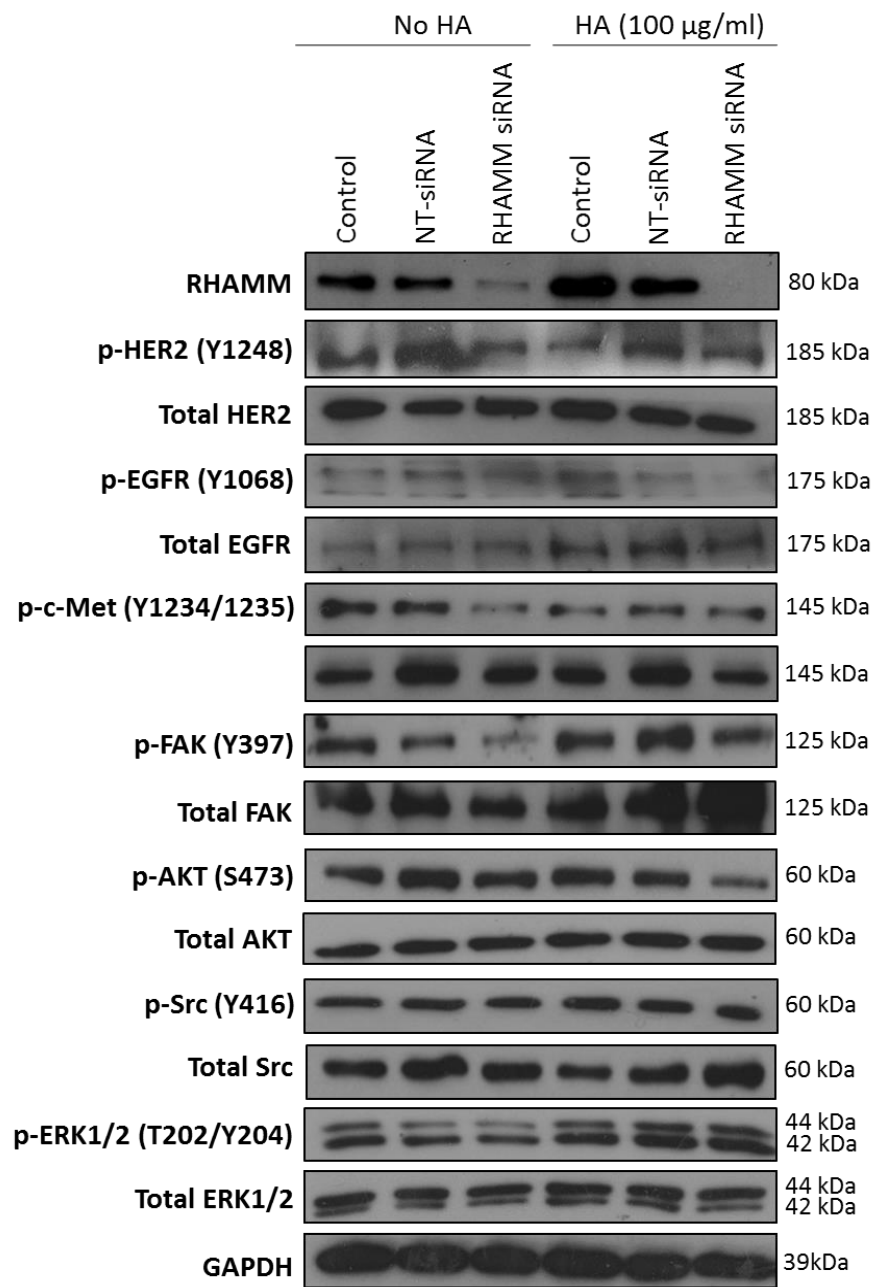


Figure 5.7. Representative Western blot images from 3 independent experiments showing HER2, EGFR, c-Met, FAK, AKT, Src and ERK1/2 activation in Fas-R cells treated with RHAMM siRNA for 48 hours in the presence (10 minute treatment, 100 μ g/ml) and absence of HA. GAPDH was used as a loading control. Total levels of each protein analysed were unchanged.

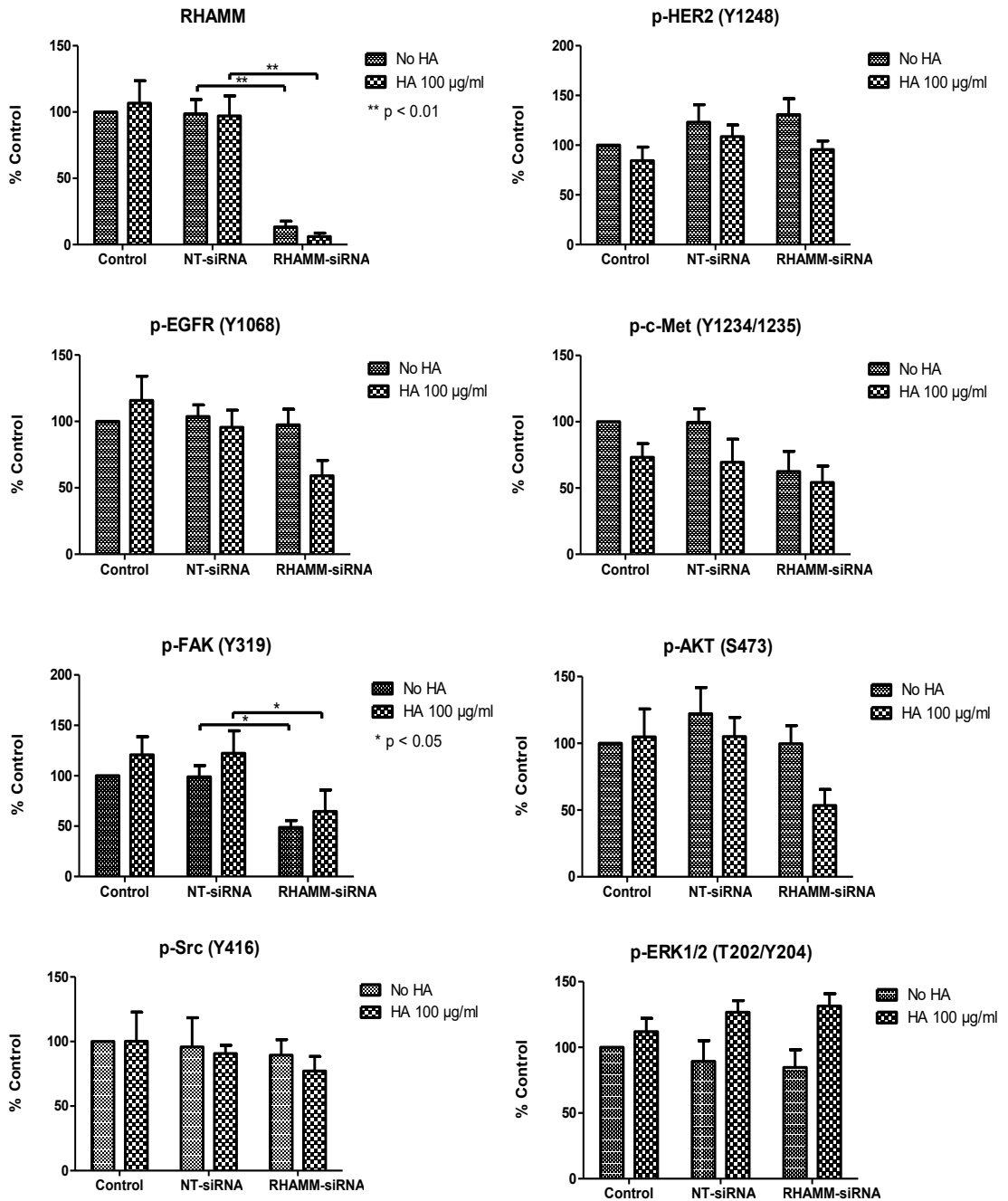


Figure 5.8. Densitometry graphs showing endogenous and HA-stimulated (215 kDa, 100 µg/ml, 10 minutes) RHAMM expression and HER2, EGFR, c-Met, FAK, AKT, Src and ERK1/2 activation in Fas-R cells before cell lysis and detection by Western blotting analysis. The data shows the relative protein levels in the cell lines expressed as a ratio of the active protein:total protein normalised to GAPDH. Error bars represent the average normalised data \pm SEM from 3 independent experiments and the data is presented as the percentage of the untreated control. Statistical analysis was performed using an unpaired t-test and significance was set at $p < 0.05$.

5.3 Discussion

This chapter set out to determine the contribution of the alternative hyaladherin RHAMM to endocrine resistance. Given that initial characterisation studies revealed the presence of RHAMM across our cell models and data revealed a role for HA in the augmentation of adverse cellular behaviours in both endocrine resistant cell models, together with numerous reports implicating RHAMM in breast tumour progression (Wang et al. 1998; Hamilton et al. 2007; Tolg et al. 2010), it was important to determine the contribution of RHAMM to these processes within the endocrine resistant cell models.

The findings revealed that suppression of RHAMM did not alter the basal or HA-stimulated behavioural functions of Fas-R cells and had only a modest impact upon EGFR, c-Met and AKT activation in these cells, however FAK activation was significantly suppressed in these cells. Furthermore, RHAMM suppression did not significantly impair the migratory or invasive function of Tam-R cells. Despite several reports linking RHAMM expression with breast cancer progression, RHAMM appears to be transforming only when overexpressed in these cells (Wang et al. 1998; Pujana et al. 2007) and high levels of RHAMM correlate with an aggressive phenotype (Hamilton et al. 2007; Vieseh et al. 2014). Given that the previous characterisation data revealed a similarly low level of RHAMM expression across all cell models, coupled with the data here, the inference is that RHAMM may not be a major contributor to the endocrine resistant phenotype.

However, an exception to this was observed in Tam-R cells where RHAMM inhibition impaired their basal and HA-stimulated proliferative capabilities potentially through a pathway involving c-Met and EGFR signalling respectively. Numerous studies document a role for RHAMM proteins towards the promotion of cellular motility in several carcinomas, however evidence remains limited in the context of breast cancer (Wang et al. 1998; Hamilton et al. 2007). It is thought that HA-induced RHAMM-mediated motility occurs through the cell surface activity of RHAMM proteins. However, as RHAMM proteins do not exhibit a membrane-spanning region, RHAMM must partner with various membrane receptors at the cell surface to mediate HA-induced signalling cascades. Numerous receptors have been characterised to partner with RHAMM, however the most extensively studied of these is with the CD44 and the CD44-EGFR complex (Tolg et al. 2006; Hatano et al. 2011; Nikitovic et al. 2013). Indeed, multiple studies have revealed that high expression levels of both CD44 and RHAMM proteins are restricted to highly aggressive breast cancer cell lines (Hamilton et al. 2007; Veisoh et al. 2014). These studies propose that RHAMM enhances CD44 localisation to the surface of invading breast cancer cells thereby promoting sustained CD44-mediated signalling and elevated cellular motility (Tolg et al. 2006; Hatano et al. 2011). Through this mechanism RHAMM is thought to activate the motogenic functions of CD44 proteins. Given that CD44 and EGFR expression is elevated in the highly motile Tam-R cells, in combination with data which reveals that suppression of both RHAMM and CD44 separately led to reduced HA-induced EGFR activation and cellular proliferation in these cells, it may be postulated that RHAMM plays a role in HA-stimulated CD44-

EGFR mediated cellular motility of Tam-R cells. In support of this hypothesis, Hamilton et al. 2007 revealed that RHAMM and CD44 form a complex at the cell surface of highly invasive breast cancer cells to coordinate enhanced cellular motility in an ERK1/2 dependent manner. However, this group suggested that the aggressive breast cancer cell lines, MDA-MB-231 and Ras-MCF10A, establish an autocrine mechanism to promote enhanced cellular motility through high rates of endogenous HA synthesis; a phenomenon which the affymetrix data in this thesis suggested may not be exhibited by Tam-R cells. Furthermore, this group revealed that RHAMM and CD44 were both highly expressed in MDA-MB-231 cells and the formation of RHAMM-CD44 complexes was mediated by the oncogenic cell surface 63 kDa RHAMM isoform; which was upregulated in these invasive cell lines compared to their less invasive counterparts. Here lies further discordance with the data from the initial Western blotting characterisation studies in this thesis which detected only the full length 85 kDa RHAMM isoform at low levels across all cell models (Chapter 3, Figure 3.4) with little/no membrane staining observed by immunostaining analysis (Chapter 3, Figures 3.6 and 3.8). Whilst it may be suggested that the 85 kDa RHAMM isoform expressed by Tam-R cells may contribute to HA-mediated cellular signalling, numerous reports suggest that these isoforms are predominantly localised intracellularly and found to be associated with microtubules and mitotic spindles (Assmann et al. 1999; Tolg et al. 2010; Ma et al. 2014), whereas the amino-terminal truncated 63 kDa isoform is primarily implicated in cell surface activity (Hoffmann et al. 1998; Ahrens et al. 2001; Zaman et al. 2005). Indeed, the previous immunostaining analyses in this thesis support these findings and revealed predominant RHAMM

cytoskeleton and microtubule staining across all cell models (see Chapter 3, Figure 3.6 and 3.8). Taken together, these data do not suggest a role for RHAMM in HA-mediated CD44-EGFR activation in Tam-R cells. However, for further investigation of RHAMM-CD44 complex activity in the endocrine resistant cell models, future studies could be undertaken using double siRNA knockdown to investigate whether an additive effect upon proliferation occurs upon suppression of both RHAMM and CD44 expression. Furthermore, utilisation of confocal microscopy to investigate RHAMM interactions with CD44 and EGFR at the cell surface of Tam-R cells could be analysed to explore the mechanisms through which RHAMM may contribute to cellular motility.

Whilst the extracellular functions of RHAMM are thought to be instrumental to the oncogenic effects of this protein, the mitotic spindle and centrosomal binding properties of RHAMM also have the potential to influence tumour progression. These centrosomal functions of RHAMM are critical for mitotic spindle integrity, progression through the cell cycle and cell division fidelity of breast cancer cells (Maxwell et al. 2003; Groen et al. 2004; Joukov et al. 2006). Furthermore, intracellular RHAMM has also been shown to regulate cell directionality, migration and facilitate cytoskeletal reorganisation (Smith et al. 2013; Chen et al. 2014). Indeed, the crucial role of RHAMM in these processes has been proven through overexpression and loss of function studies which reveal that, in both instances, deregulation of RHAMM expression results in the deformation of mitotic spindles (Maxwell et al. 2005; Tolg et al. 2010). Therefore, it could be postulated that loss of RHAMM expression in Tam-R cells may significantly impair cellular division processes

and cytoskeletal reorganisation leading to decreased cellular growth, and may suggest a minimal role for RHAMM proteins in HA-mediated activities in these cells; however the mechanism of this remains unclear.

5.3.1 Summary

In this chapter it has been shown that loss of RHAMM expression did not significantly alter the aggressive phenotype of Fas-R cells however impaired the proliferative capacity of Tam-R cells through an as-yet unknown mechanism. Whilst numerous studies have implicated a role for CD44-RHAMM complexes in breast cancer progression, these studies report that high expression levels of both hyaladherin receptors are required for enhanced cellular motility with particular importance placed upon the oncogenic amino-terminal truncated 63 kDa RHAMM protein; an isoform not detected across these cell models. Taken together, these data may not implicate RHAMM as a major contributor to acquired endocrine resistance and may infer a greater importance for CD44 proteins within the aggressive phenotype of these cells and as the principle receptor of HA-mediated signalling.

6. CD44 variants differentially modulate the aggressive phenotype of breast cancer cells

6.1 Introduction

In the previous chapters, it was demonstrated that loss of global CD44 expression impaired the aggressive phenotype of endocrine resistant cell models and attenuated their HA responses thus suggesting an important role for CD44 proteins in endocrine resistance. Whilst initial characterisation studies revealed elevated expression of multiple CD44 variants in endocrine resistant cell models compared to their endocrine sensitive counterpart, it remains unclear which of these may act as dominant contributors to the endocrine resistant phenotype. Numerous CD44 isoforms have been shown to become upregulated in multiple carcinomas, however a large proportion of in vitro studies have focused upon CD44v3 and CD44v6 isoform expression and their prominent roles as promoters of tumour migration, invasion and spread, which has also been observed in the clinical setting (Kuniyasa et al. 2002; Wang et al. 2007; Saito et al. 2013; Shi et al. 2013; Marzese et al. 2014).

In breast carcinomas, CD44v3 has been implicated in cytoskeletal-mediated cellular migration (Bourguignon et al 1998; Bourguignon et al. 1999) and in the clinical setting has been found to become upregulated in highly invasive tumours (Auvinen et al. 2005) and correlated with lymph node metastases (Kalish et al. 1999; Rys et al. 2003). CD44v6 expression has also been shown to become upregulated in primary breast carcinomas (Auvinen et al. 2005; Lian et al. 2006) and correlated with tumour size, lymph node metastases and patient survival (Ma et al. 2005; Lian et al. 2006; Yu et

al. 2010). However, whilst some studies suggest CD44v6 as an independent prognostic factor of breast cancer (Lian et al. 2006; Yu et al. 2010) others suggest this is not the case (Jansen et al. 1998; Ma et al. 2005). In recent years the presence of CD44v6 has also been suggested to be a marker of cancer stem cells (in combination with other proteins) in breast cancer (Synder et al. 2009) as well as numerous other carcinomas (Wang et al. 2013; Ni et al. 2014; Todaro et al. 2014). However controversy regarding the role of specific CD44 isoforms in breast cancer still remains a problem due to contradictory findings (Morris et al. 2001; Berner et al. 2003; Shah et al. 2010).

Whilst the HA-binding domain is common to all CD44 isoforms, thus conferring the potential for HA-mediated cellular responses, individual CD44 variants exhibit specific ligand and membrane receptor affinity which may also enhance their metastatic capacity. For example, the CD44 variant 3 exon contains the attachment site for the proteoglycan heparan sulphate (HPS) which is responsible for the presentation of several growth factors to their receptors (Bennet et al. 1995; Van der Voort et al. 1999). In this respect, CD44v3 isoforms have been shown to contribute to the malignant behaviour of cancer cells through HPS binding. Indeed, in colon cancer cells, HPS interaction with CD44v3 proteins has been shown to enhance tumour growth and invasion, in some instances in collaboration with the c-met receptor (Van der voort et al. 1999; Wielenga et al. 2000; Kuniyasa et al. 2001). Additionally, CD44v3-containing isoforms have been functionally linked to TGF β R1, MMP-9 and the cytoskeletal proteins ankyrin and Rho-kinase, resulting in the promotion of breast cancer invasion and metastasis through invadopodia formation

and enhanced degradation of the extracellular matrix (Bourguignon et al. 1998; Bourguignon et al. 1999; Bourguignon et al. 2002). Alternatively, CD44v6 has been reported to exhibit specific co-receptor function for the activation of the receptor tyrosine kinases, c-Met and VEGFR2 (Tremmel et al. 2009; Hasenaer et al. 2013; Elliot et al. 2014). Indeed, CD44v6 has been shown to be required for the full activation and internalisation of the c-Met receptor (Orian-Roussaeu et al. 2002; Hasenaer et al. 2013) and loss of CD44 correlates with c-Met haploinsufficiency in mouse models (Matkze et al. 2007). Therefore, it could be suggested that contradictory results involving CD44 isoforms in breast cancer may be due to the differential bio-availability of specific ligands/membrane co-receptors between tumours.

Given that CD44v3 and CD44v6 isoforms have been strongly implicated within breast cancer progression and elevated in models of endocrine resistance, the aims of this chapter were to explore the functional contribution of these specific variant isoforms to the endocrine resistant phenotype.

6.1.1 Objectives

1. To overexpress CD44v3 and CD44v6 isoforms in endocrine sensitive MCF-7 cells and investigate their subsequent effect upon the aggressive nature and/or response to HA in these cells.
2. To suppress specific CD44 isoform expression using targetted siRNA in endocrine resistant Tam-R and Fas-R cells and explore the resultant effect on cellular phenotype and response to HA along with changes in cell signalling.

3. To determine whether CD44 isoforms are linked to outcome on tamoxifen through immunohistochemical analysis of clinical samples and to perform survival analysis on publically available breast cancer datasets (KM plotter).

6.2 Results

6.2.1 Optimisation of CD44v3 and CD44v6 overexpression in MCF-7 cells

To begin to explore the functional contribution of CD44v3 and CD44v6 to endocrine resistant cell behaviour, a transfection-based approach was used to overexpress these isoforms in the endocrine sensitive MCF-7 cell model. Plasmid vectors containing DNA encoding full length human CD44v3 and CD44v6 were obtained from Dr Ursula Gunthert (Basal University, Switzerland). This group additionally provided the cytoplasmic tail truncated counterparts of CD44v3 and CD44v6 (missing the DNA sequence encoding the cytoplasmic tail domain, denoted as CD44v3 Δ cyt and CD44v6 Δ cyt respectively) to use as transfection controls, as loss of the cytoplasmic tail is reported to block CD44 cellular signalling and functional activities (Mielgo et al. 2007). All plasmid constructs contain an EGFP-tag fused at the carboxy-terminus end of the CD44 protein.

Plasmid DNA constructs were transformed and purified before being utilised for transfection into MCF-7 cells. To confirm the successful purification of plasmid DNA constructs, samples were initially sequenced (see Materials and Methods 2.12.4). The results confirmed the presence of the variant 3 and variant 6 exon in the CD44v3 and CD44v6 plasmid DNA construct respectively and further verified the truncation of the CD44 cytoplasmic tail sequence at the correct position in the CD44 Δ cyt samples (Appendix I). Sequencing analysis revealed a base pair mutation in the variant 3 exon of the CD44v3 and CD44v3 Δ cyt DNA constructs leading to an amino acid substitution (N239D), however subsequent investigations suggested that this

substitution is unlikely to alter CD44v3 function (shown in Appendix M and N) and evaluated in the discussion section below (6.3)). No other base pair mutations were detected across the plasmid DNA constructs.

Western blotting analysis using antibodies specific for CD44v3 and CD44v6 detection confirmed the successful transfection of plasmid constructs and showed upregulated expression of CD44v3, CD44v3 Δ cyt, CD44v6 and CD44v6 Δ cyt in MCF-7 cells between 48 - 144 hours post-transfection compared to the control cells which did not alter the expression of alternative CD44 variant isoforms (Figures 6.1 and 6.2). Densitometry analysis could not be performed on this overexpression data due to limitations by Western blotting analysis due to exposure issues, however analysis revealed that the expression of alternative isoforms were not altered upon CD44 overexpression in MCF-7 cells (Appendix O and P). Whilst RHAMM expression was modestly reduced in MCF-7 cells overexpressing CD44v3, CD44v6 and CD44v6 Δ cyt proteins, densitometry analysis revealed that this was not significant (Figure 6.1 and 6.2 and Appendix O and P). Whilst analysis revealed that CD44 variant overexpression in MCF-7 cells enhanced CD44 Std isoform expression (Figure 6.1 and 6.2) this is likely to be a result of the CD44 Std antibody recognising an epitope which is common to all CD44 isoforms.

An increase in the expected molecular weight of these proteins was observed due to the presence of a 27 kDa EGFP tag on each construct (Figure 6.1 and 6.2). The CD44 cytoplasmic tail (excluding exon 19 which is not present in the majority of CD44 transcripts (Goldstein and Butcher 1990; Jiang et al. 2001)) is encoded by 70 amino acids and has a molecular weight of approximately 7.8 kDa. Therefore CD44v3 Δ cyt

and CD44v6 Δ cyt isoforms were detected at 104 kDa in MCF-7 cells (a molecular weight of 7.8 kDa lower than their full length counterparts) (Figure 6.1 and 6.2). This observation has also been shown by other groups using CD44 cytoplasmic tail truncated mutants (Neame and Isacke 1993; Gal et al. 2003; Mielgo et al. 2007

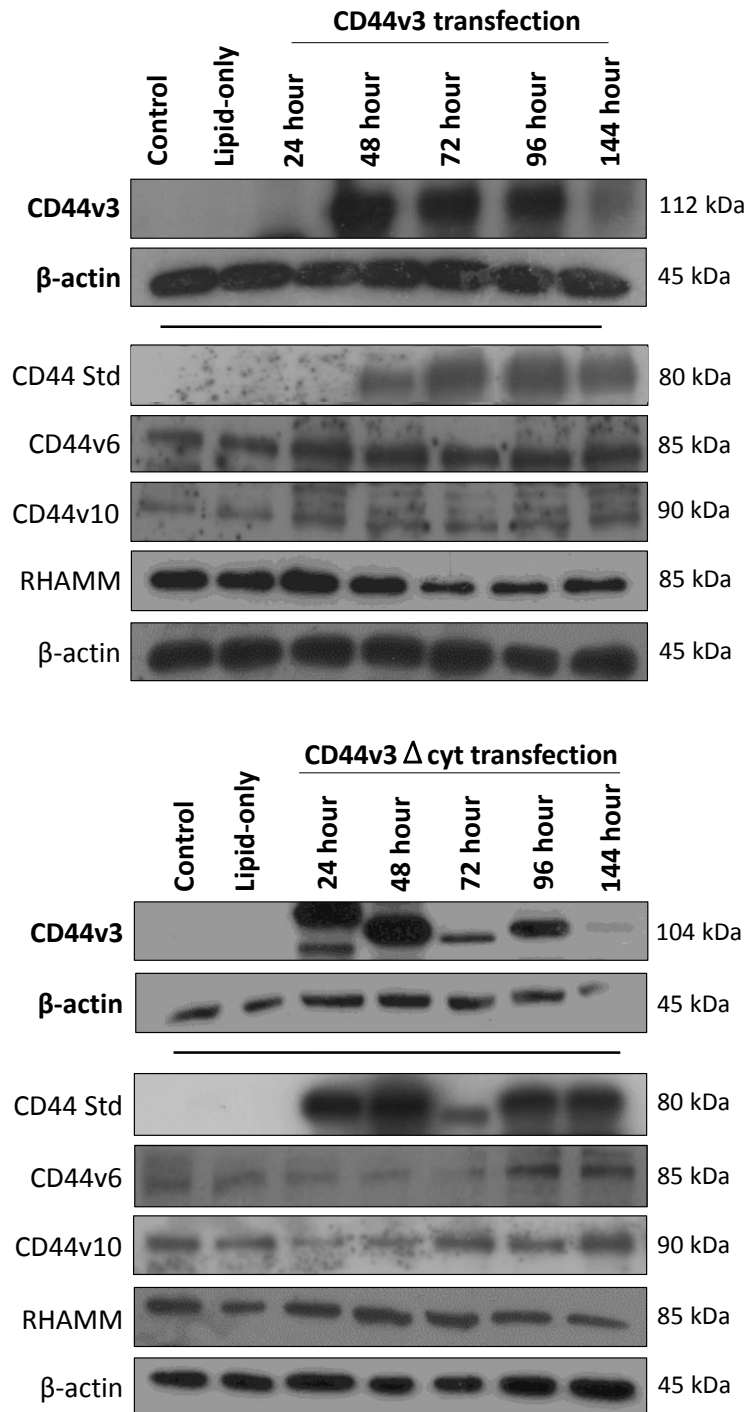


Figure 6.1. Representative Western blot images from 3 independent experiments showing CD44v3 and CD44v3Δcyt protein expression levels in MCF-7 cells 24 – 144 hours post-transfection compared to the untreated and lipid-only control samples. Protein expression levels of CD44 Std, CD44v6 and CD44v10 were unchanged however CD44v3 overexpression modestly reduced RHAMM expression. β-actin was used as a loading control.

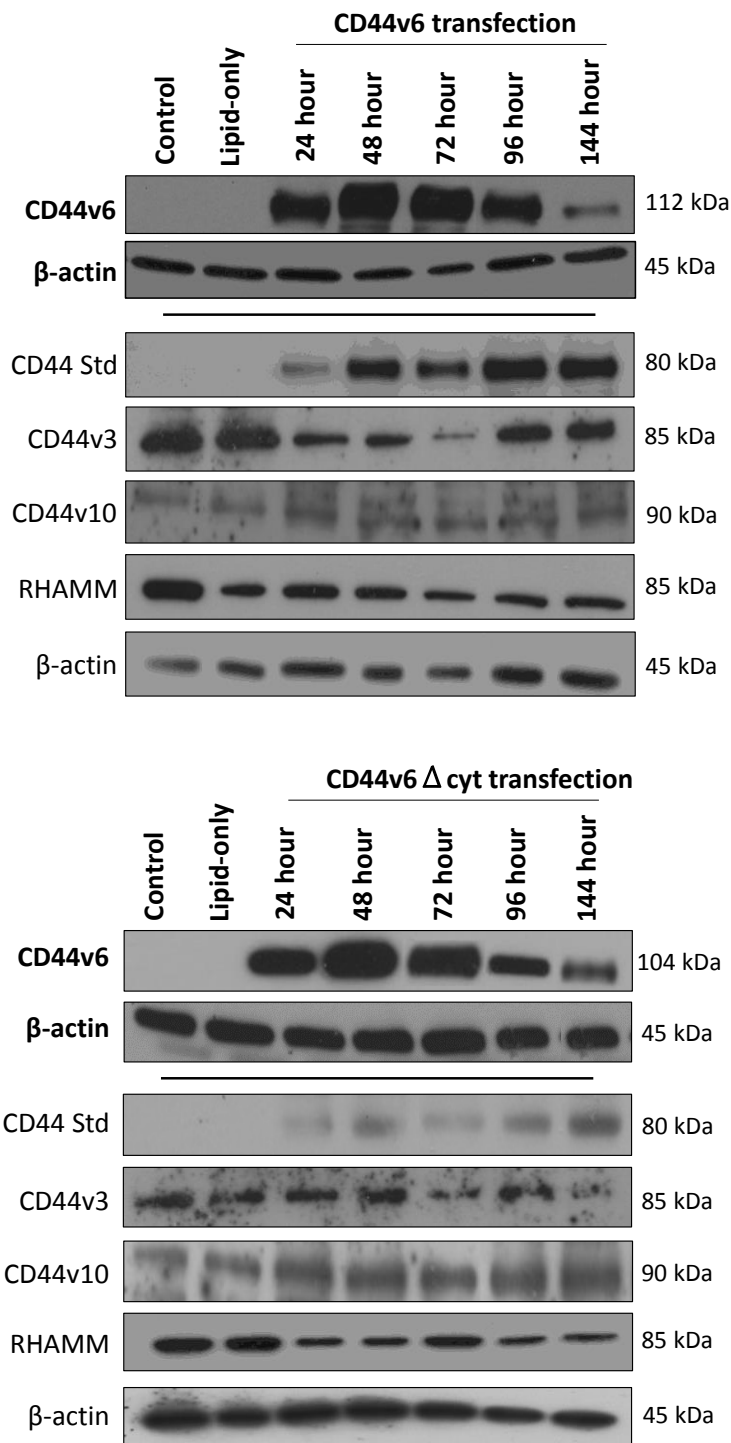


Figure 6.2. Representative Western blot images from 3 independent experiments showing CD44v6 and CD44v6 Δ cyt protein expression levels in MCF-7 cells 24 – 144 hours post-transfection compared to the untreated and lipid-only control samples. Protein expression levels of CD44 Std, CD44v3 and CD44v10 were unchanged however RHAMM expression was modestly reduced. β -actin was used as a loading control.

Immunostaining analysis was utilised to confirm the protein expression and localisation of CD44 variant constructs in transfected MCF-7 cells. Immunocytochemistry revealed the upregulation of CD44v3, CD44v3 Δ cyt, CD44v6 and CD44v6 Δ cyt proteins in MCF-7 cells 48 – 144 hours post transfection, compared to the control samples (Figure 6.3). These data also revealed that CD44v3 and CD44v6 isoforms overexpressed in MCF-7 cells showed similar localisation patterns to their endogenous control cells, whilst CD44v3 Δ cyt and CD44v6 Δ cyt isoforms were predominantly expressed in the cytoplasm, however limited membrane expression of these isoforms was also observed (Figure 6.3). Furthermore, Figure 6.4 reveals that transfection of MCF-7 cells with CD44v6 and CD44v6 Δ cyt led to a similar expression level as that observed for the endogenous levels of CD44v6-containing proteins in endocrine resistant Tam-R and Fas-R cell models. Conversely, CD44v3 and CD44v3 Δ cyt transfection in MCF-7 cells led to an enhanced expression of these proteins as compared with levels of endogenous CD44v3-containing proteins in Tam-R and Fas-R cells (Figure 6.4) which must be taken into consideration upon further analysis.

These results were further validated by immunofluorescence analysis using CD44 specific antibodies and visualisation of the EGFP-tagged constructs. The results also showed predominant cytoplasmic staining for CD44v3, CD44v3 Δ cyt and CD44v6 Δ cyt proteins, and predominant membrane staining for CD44v6 proteins, in MCF-7 cells compared to their untransfected lipid-treated control cells (Figures 6.5 and 6.6).

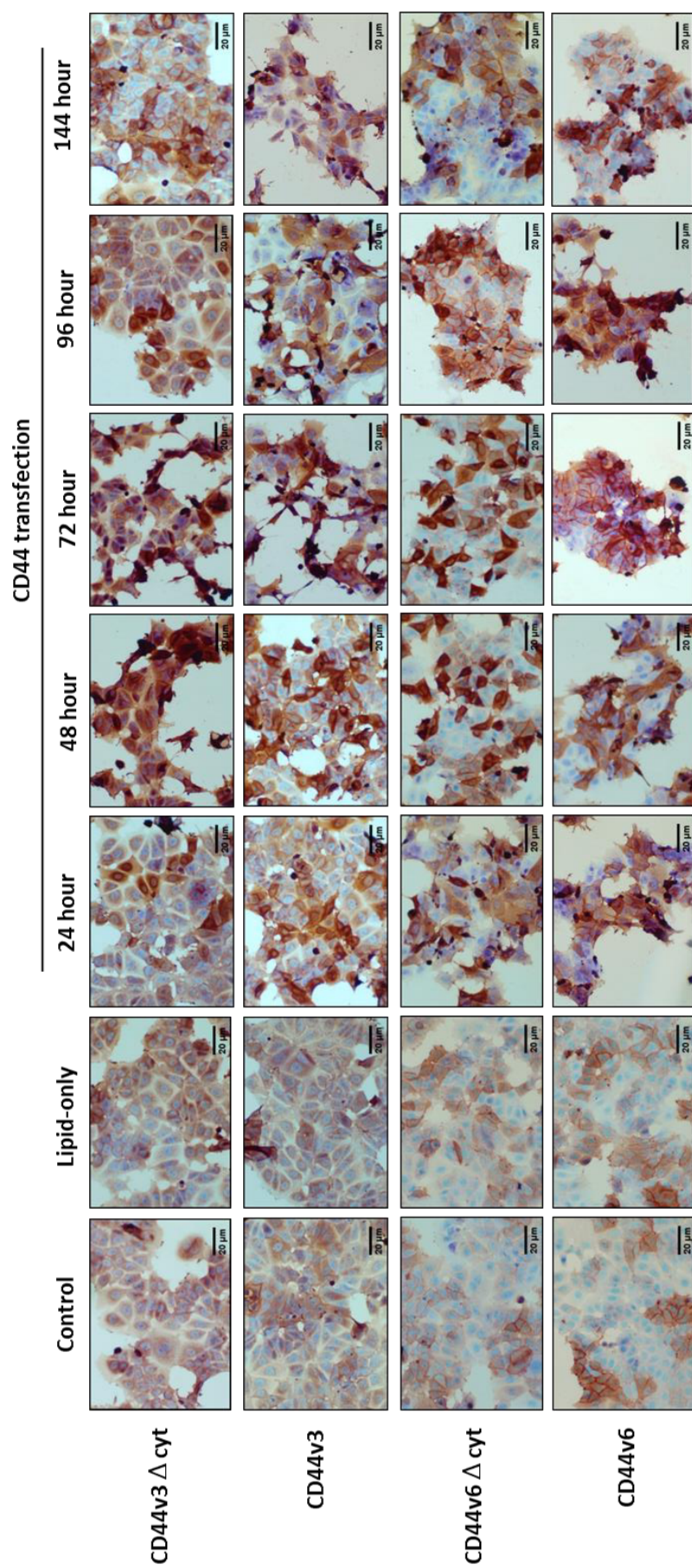


Figure 6.3. Representative images from 3 independent experiments showing CD44v3 Δ cyt, CD44v3, CD44v6 Δ cyt and CD44v6 expression from immunocytochemistry analysis (x20 magnification) in MCF-7 cells 24 hours – 144 hours post-transfection in comparison to the untreated and lipid-only treated cells.

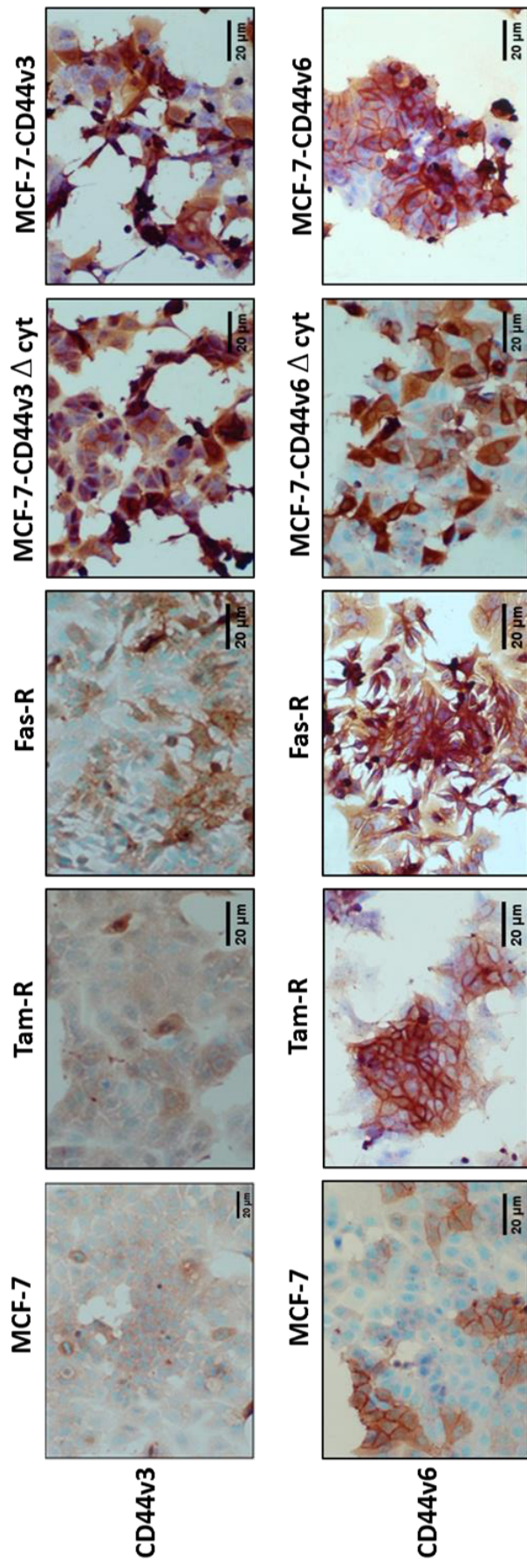


Figure 6.4. Representative images from 3 independent experiments showing CD44v3 and CD44v6 expression from immunocytochemistry analysis (x20 magnification) in endogenous MCF-7, Tam-R and Fas-R cells and MCF-7 cells after 72 hours transfection.

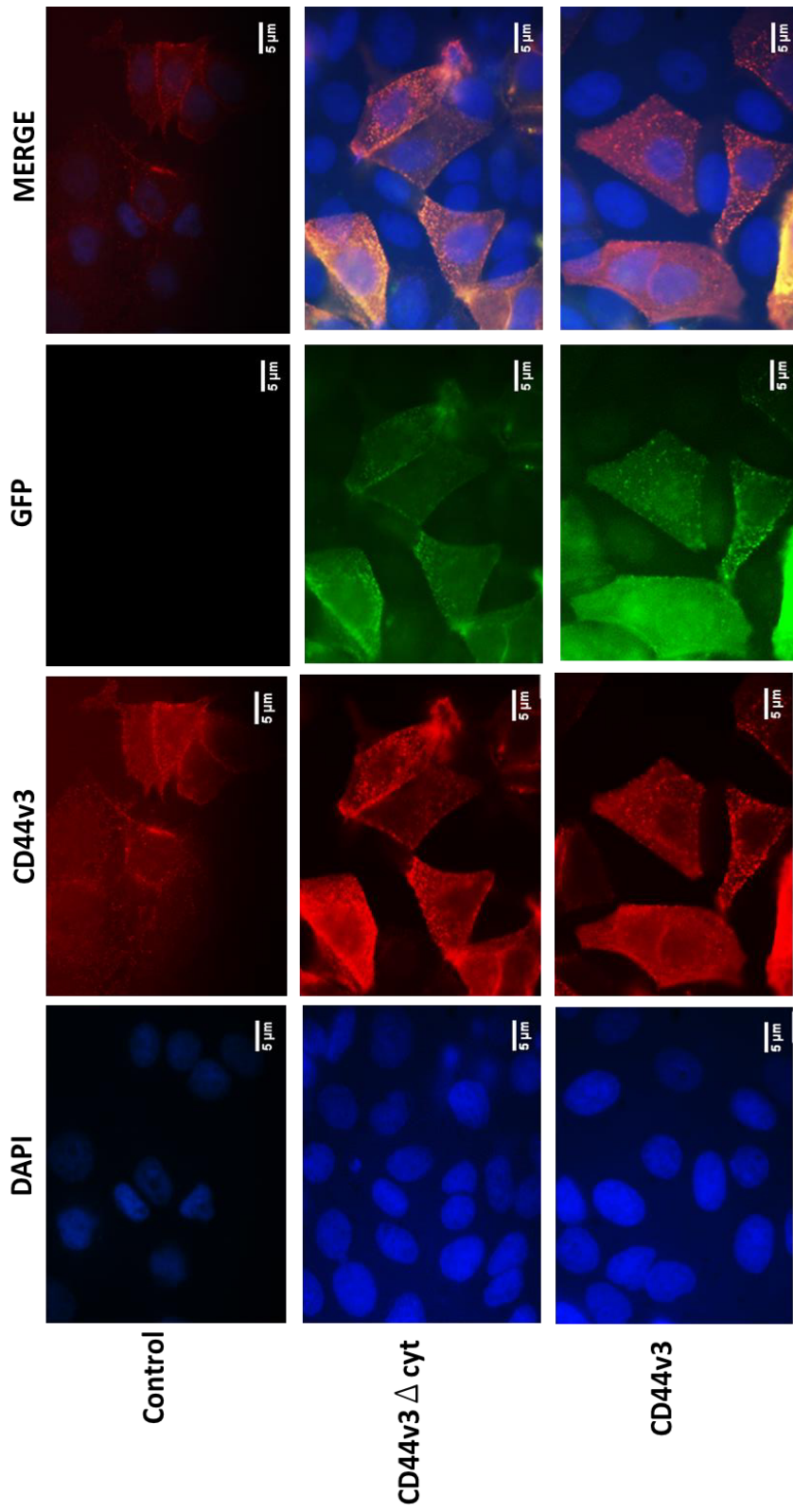


Figure 6.5. Representative images from 3 independent experiments showing CD44v3 Δ cyt and CD44v3 expression from immunofluorescence analysis (x63 magnification) in MCF-7 cells 72 hours post-transfection in comparison to the untransfected lipid-treated control cells.

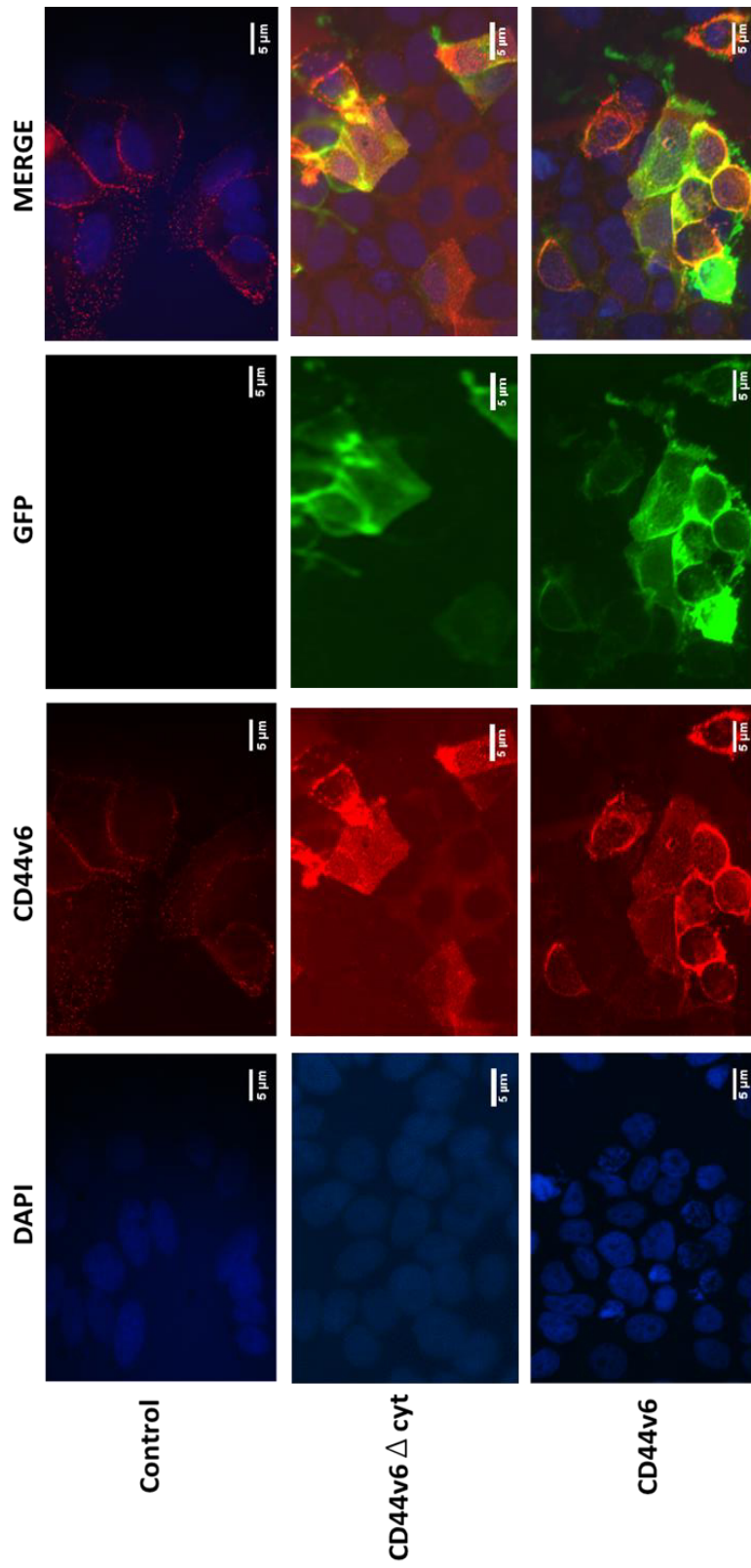


Figure 6.6. Representative images from 3 independent experiments showing CD44v6 Δ cyt and CD44v6 expression from immunofluorescence analysis (x63 magnification) in MCF-7 cells 72 hours post-transfection in comparison to the untransfected lipid-treated control cells.

6.2.2 CD44v6, but not CD44v3, overexpression enhanced the invasive capacity of MCF-7 cells and attenuated their sensitivity to fulvestrant

As previous data revealed that loss of global CD44 protein expression impaired the migratory, invasive and proliferative phenotype of both endocrine resistant models, the hypothesis that overexpression of CD44v3 and CD44v6 in endocrine sensitive MCF-7 cells may replicate these behaviours to some extent was explored. Previous data also revealed that the highly CD44-expressing endocrine resistant cell models were sensitised to HA, an observation not observed in the low CD44-expressing endocrine sensitive MCF-7 cells. Therefore it was also investigated whether overexpression of individual CD44 isoforms in MCF-7 cells augmented their sensitivity to HA leading to an enhanced aggressive phenotype. The same concentration of HA (100 µg/ml), previously shown to stimulate functional responses in the highly CD44-expressing Tam-R and Fas-R cells, was used for these assays.

Boyden chamber assays revealed that CD44v3 overexpression in MCF-7 cells reduced their endogenous and HA-stimulated migratory capacity across fibronectin-coated membranes, however enhanced HA-induced invasion through Matrigel compared to the CD44v3 Δ cyt transfection control cells (Figure 6.7). In contrast, CD44v6-overexpression in MCF-7 cells enhanced their endogenous invasive phenotype through Matrigel compared to the CD44v6 Δ cyt control (Figure 6.8).

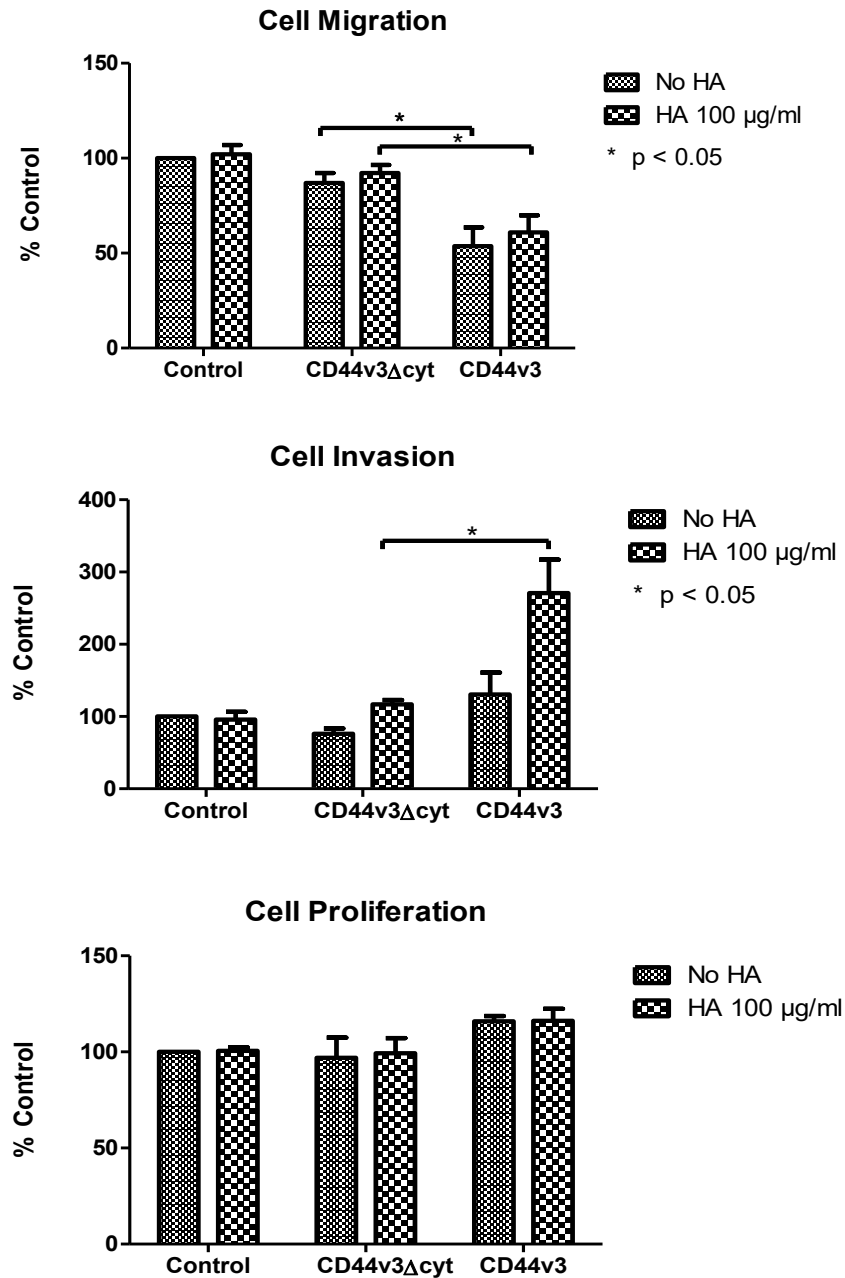


Figure 6.7. Measurement of endogenous and HA-stimulated cell behaviour responses of MCF-7 cells overexpressing CD44v3. MCF-7 cells were transfected with CD44v3 or CD44v3 Δ cyt plasmid DNA for 48 hours prior to the assessment of migration and invasion (Boyden Chamber assays) and proliferation (Coulter counter assays) in the presence (100 µg/ml) or absence of HA. Control cells represent lipid-treated MCF-7 cells. Error bars represent the average normalised data \pm SEM from 3 independent experiments and the data is presented as the percentage of the untreated control. Statistical analysis was performed using an unpaired t-test and significance set at $p < 0.05$.

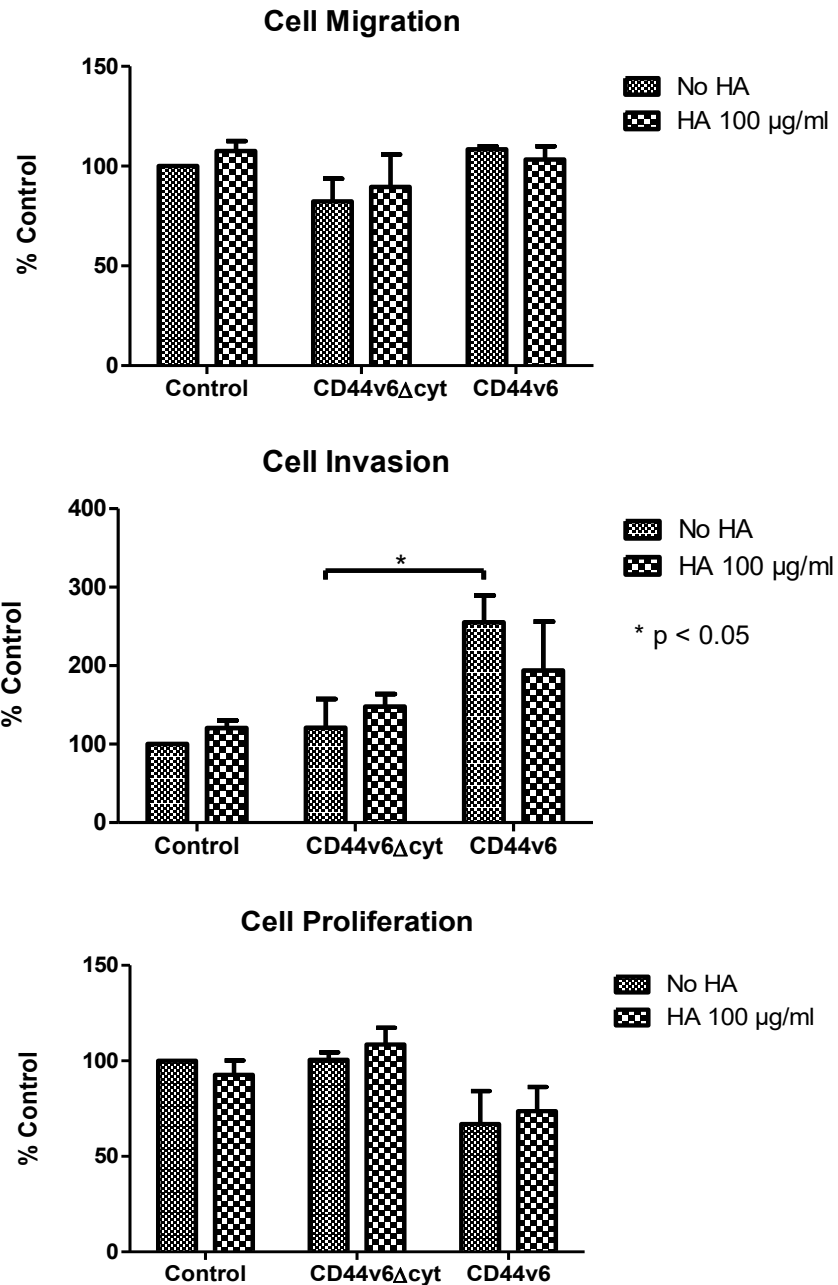


Figure 6.8. Measurement of endogenous and HA-stimulated cell behaviour responses of MCF-7 cells overexpressing CD44v6. MCF-7 cells were transfected with CD44v6 or CD44v6 Δ cyt plasmid DNA for 48 hours prior to the assessment of migration and invasion (Boyden Chamber assays) and proliferation (Coulter counter assays) in the presence (100 µg/ml) or absence of HA. Control cells represent lipid-treated MCF-7 cells. Error bars represent the average normalised data \pm SEM from 3 independent experiments and the data is presented as the percentage of the untreated control. Statistical analysis was performed using an unpaired t-test and significance set at $p < 0.05$.

Previous published studies from the Hiscox group (2012) suggested that CD44 expression may also limit endocrine response in breast cancer cells. To investigate this, the growth of CD44-transfected MCF-7 cells in the presence of tamoxifen or fulvestrant for 5 days was assessed. Coulter counter proliferation assays revealed that tamoxifen treatment significantly inhibited the growth of lipid-treated MCF-7 control cells and MCF-7 cells overexpressing CD44v3, CD44v3 Δ cyt, CD44v6 or CD44v6 Δ cyt proteins (Figure 6.9). However, whilst treatment with fulvestrant significantly reduced the growth of untransfected MCF-7 control cells, no significant impairment in growth was observed in MCF-7 cells overexpressing any of the CD44 constructs (Figure 6.10). Surprisingly, the CD44v3 Δ cyt and CD44v6 Δ cyt transfection controls exhibited a similar growth response in the presence of fulvestrant compared to their full length CD44v3 and CD44v6 counterparts respectively (Figure 6.10). ANOVA testing to reveal significant changes between each group revealed an increase in growth between untransfected and CD44v6-overexpressing MCF-7 cells in the presence of fulvestrant (Figure 6.10). These results suggest that CD44v6 overexpression attenuates the ability of MCF-7 cells to respond to fulvestrant, resulting in an enhanced proliferative capacity of these cells compared to the untransfected control cells.

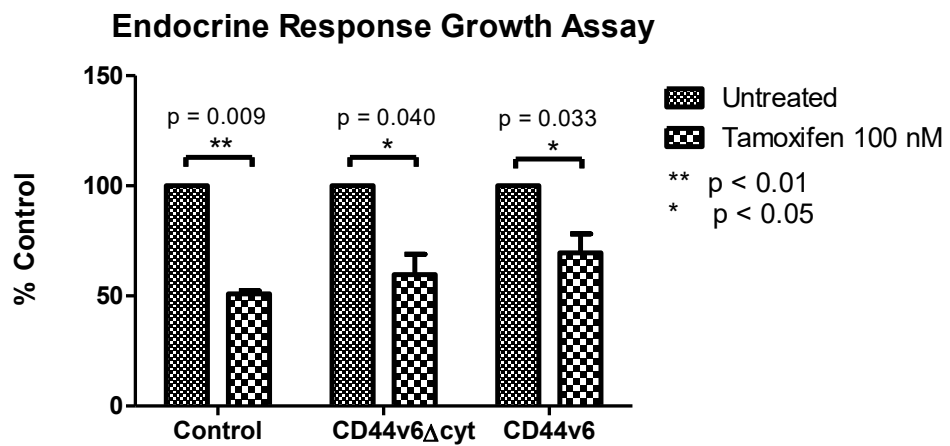
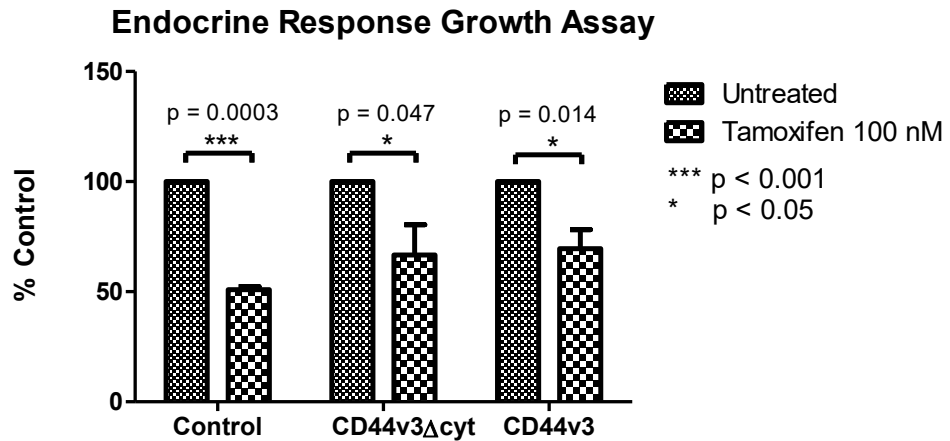


Figure 6.9. Measurement of growth response in MCF-7 cells overexpressing CD44 proteins in the presence of tamoxifen. MCF-7 cells were transfected with CD44v3, CD44v3 Δ cyt, CD44v6, or CD44v6 Δ cyt plasmid constructs for 48 hours prior to the assessment of growth (Coulter Counter assay) in the presence (100 nM) or absence of tamoxifen for 5 days. Control cells represent lipid-treated MCF-7 cells. Error bars represent the average normalised data \pm SEM from 3 independent experiments and the data is presented as the percentage of the untreated control for each group. Statistical analysis was performed using a paired t-test and one-way ANOVA with Tukey post-hoc testing and significance set at $p < 0.05$.

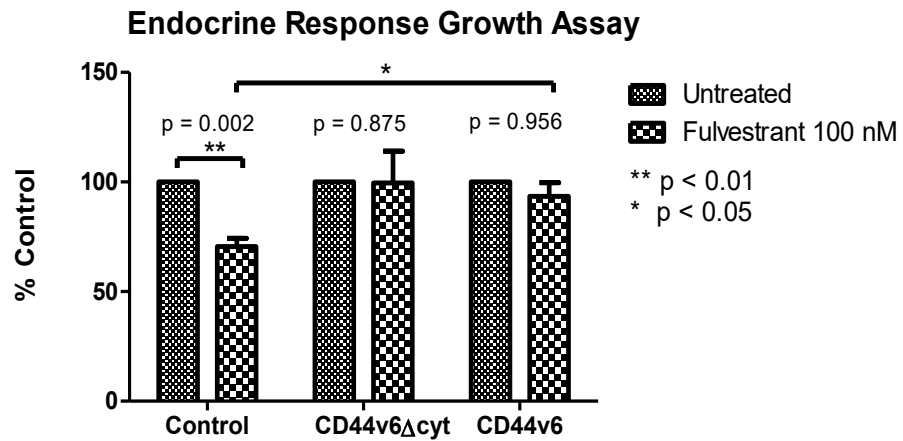
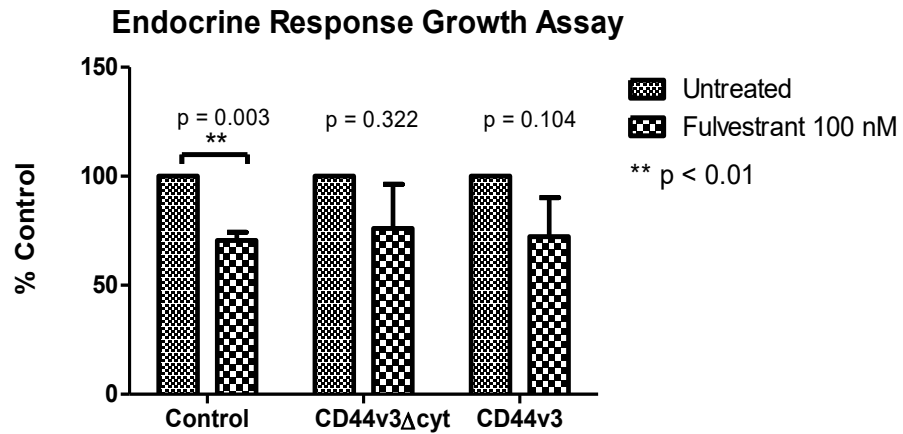


Figure 6.10. Measurement of growth response in MCF-7 cells overexpressing CD44 proteins in the presence of fulvestrant. MCF-7 cells were transfected with CD44v3, CD44v3 Δ cyt, CD44v6 or CD44v6 Δ cyt plasmid constructs for 48 hours prior to the assessment of growth (Coulter Counter assay) in the presence (100 nM) or absence of fulvestrant for 5 days. Control cells represent lipid-treated MCF-7 cells. Error bars represent the average normalised data \pm SEM from 3 independent experiments and the data is presented as the percentage of the untreated control for each group. Statistical analysis was performed using a paired t-test and one-way ANOVA with Tukey post-hoc testing and significance set at $p < 0.05$.

6.2.3 CD44v6 overexpression in MCF-7 cells enhanced EGFR pathway activity

Data generated from the global CD44 siRNA studies (Chapter 4) suggested a role for CD44 proteins in the activation of several signalling pathways potentially through co-receptor activation of receptor tyrosine kinases, EGFR, HER2 or c-Met. To explore the mechanisms through which CD44v3 and CD44v6 overexpression may alter the behavioural phenotype of MCF-7 cells, the activation of these signalling molecules were reassessed by Western blotting analysis in the presence (100 µg/ml) or absence of HA.

Surprisingly, the data revealed that the CD44v3Δcyt and CD44v6Δcyt transfection controls induced cellular signalling upon overexpression in MCF-7 cells, a previously unreported phenomenon (Figure 6.11 – 6.14). MCF-7 cells overexpressing either CD44v3 or CD44v3Δcyt proteins showed an enhanced endogenous activation of AKT, reduced HA-stimulated HER2 activation and reduced endogenous and HA-stimulated ERK1/2 compared to control cells (Figures 6.11 and 6.12). CD44v3 overexpression alone reduced endogenous and HA-stimulated EGFR and HA-stimulated Met activation compared to the control cells (Figures 6.11 and 6.12). Conversely, MCF-7 cells overexpressing either CD44v6 or CD44v6Δcyt proteins substantially enhanced endogenous and HA-induced activation of EGFR, AKT and ERK1/2 and reduced c-Met activation compared to the untransfected control cells (Figures 6.13 and 6.14). CD44v6 overexpression alone reduced HA-stimulated HER2 activation compared to the untransfected control cells (Figures 6.13 and 6.14). Surprisingly, overexpression of CD44 variants in MCF-7 cells did not appear to sensitise the cells to HA (Figures 6.11 – 6.14).

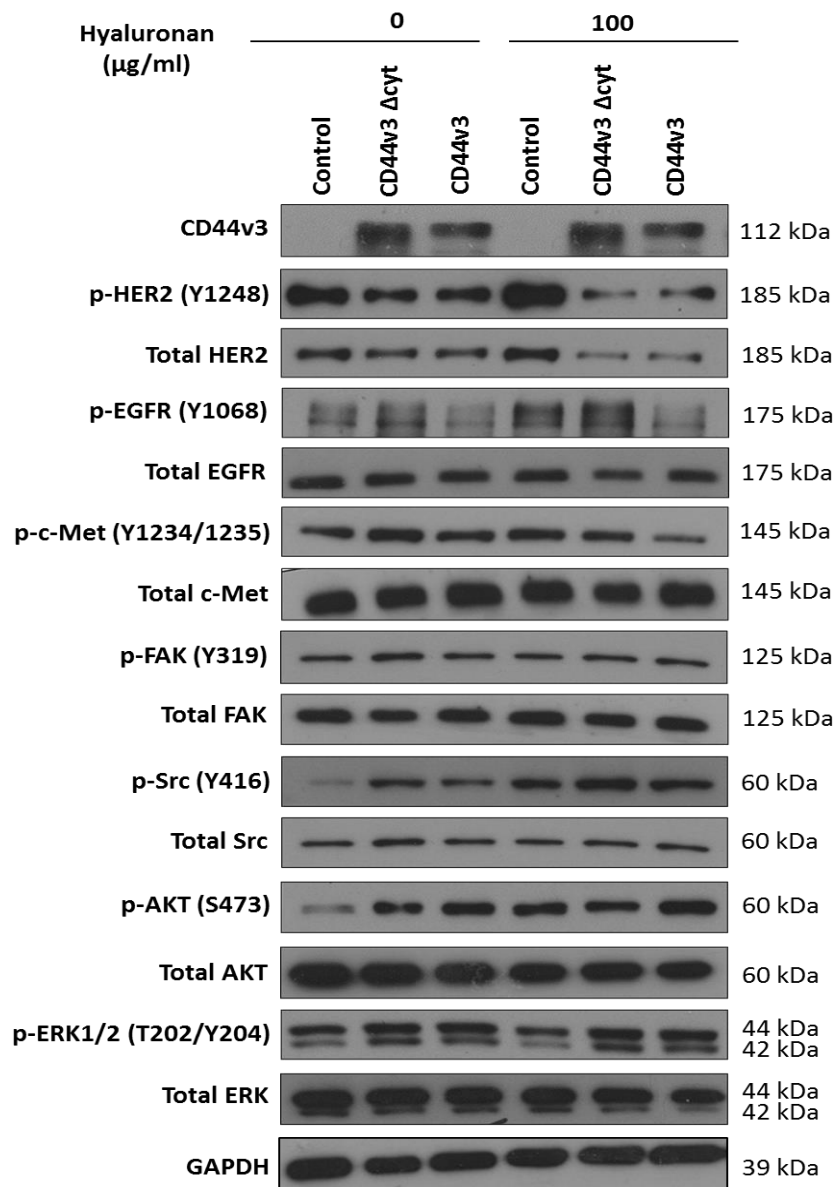


Figure 6.11. Representative Western blot images from 3 independent experiments showing HER2, EGFR, c-Met, FAK, Src, AKT and ERK1/2 activation in MCF-7 cells after 48 hour transfection with CD44v3 or CD44v3 Δcyt plasmid DNA in the presence (10 minute treatment, 100 $\mu\text{g/ml}$) or absence of HA. Control cells represent lipid-treated MCF-7 cells. Total protein levels were unchanged however total HER2 became reduced and GAPDH was used as a loading control.

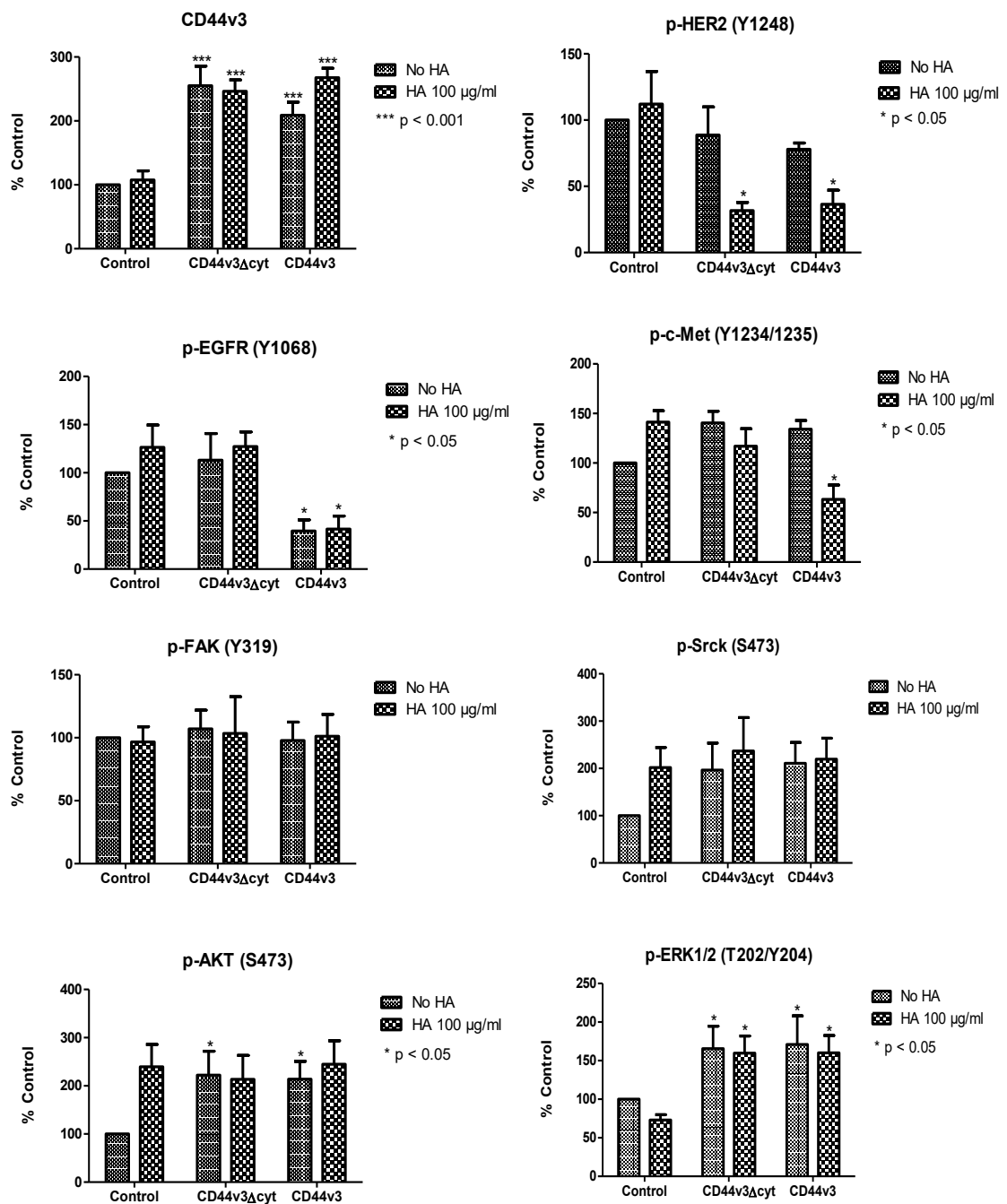


Figure 6.12. Densitometry graphs showing CD44v3 expression and HER2, EGFR, c-Met, FAK, AKT, Src and ERK1/2 activation in MCF-7 cells after 48 hour transfection with CD44v3 or CD44v3Δcyt plasmid DNA in the presence (10 minute treatment, 100 µg/ml) or absence of HA. The data shows the relative protein levels in the cell lines expressed as a ratio of the active protein:total protein normalised to GAPDH. Error bars represent the average normalised data \pm SEM from 3 independent experiments and the data is presented as the percentage of the untreated control. Statistical analysis was performed using an unpaired t-test and significance was set at $p < 0.05$.

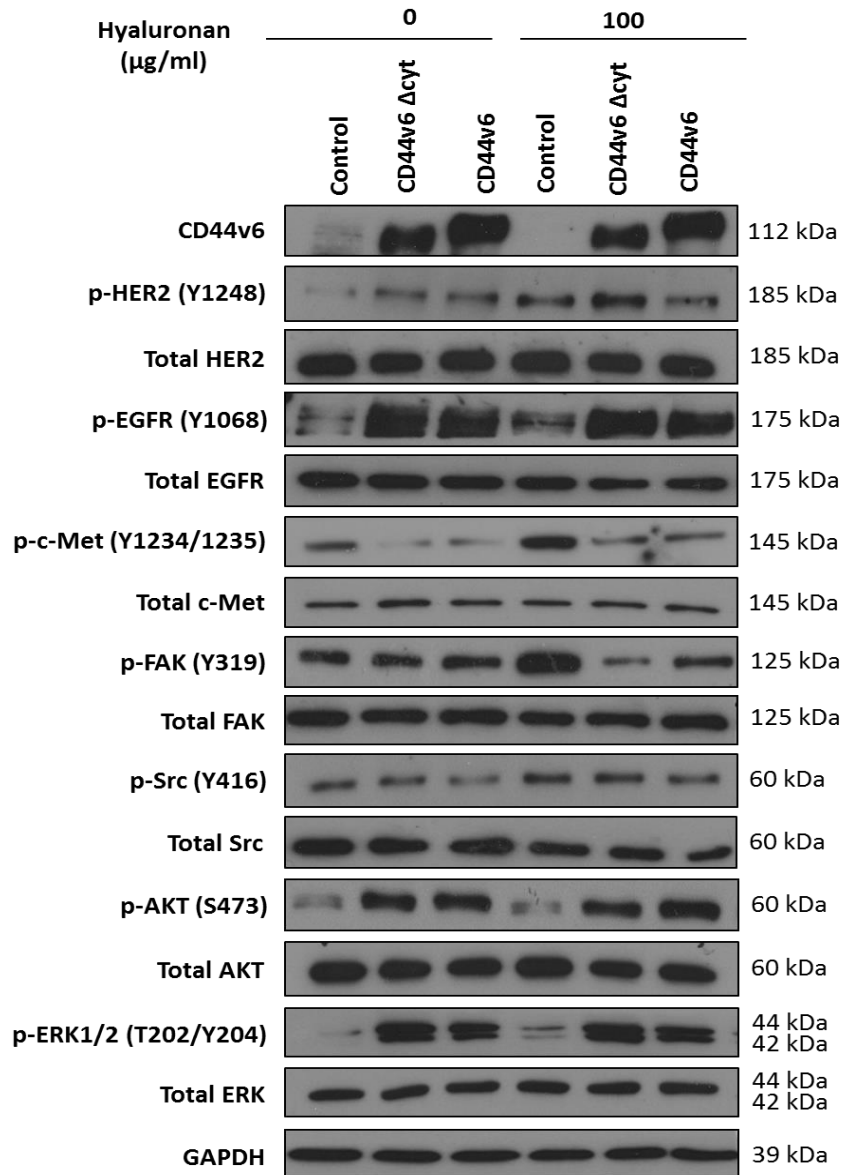


Figure 6.13. Representative Western blot images from 3 independent experiments showing HER2, EGFR, c-Met, FAK, Src, AKT and ERK1/2 activation in MCF-7 cells after 48 hour transfection with CD44v6 or CD44v6 Δcyt plasmid DNA in the presence (10 minute treatment, 100 $\mu\text{g/ml}$) or absence of HA. Control cells represent lipid-treated MCF-7 cells. Total protein levels were unchanged and GAPDH was used as a loading control.

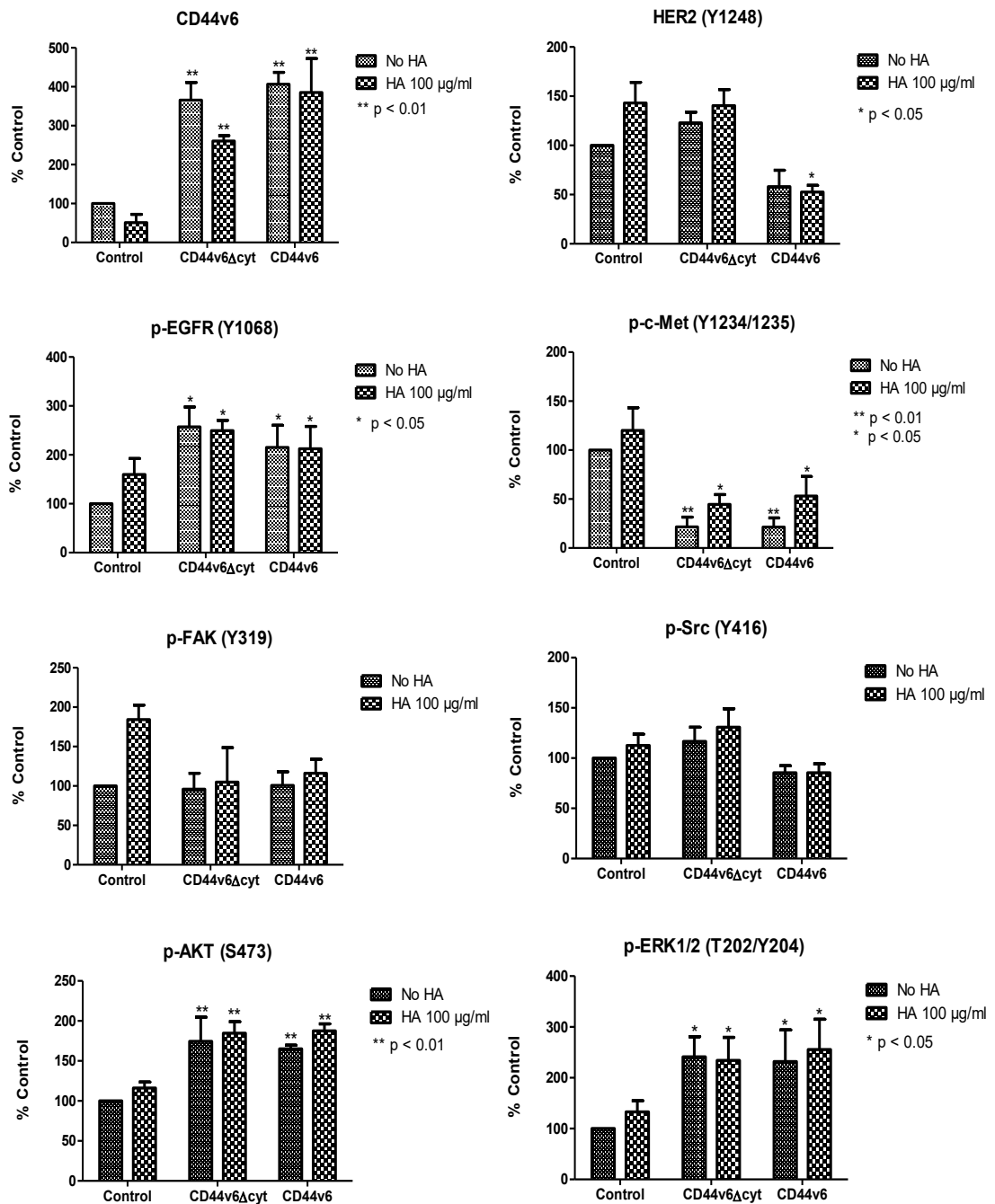


Figure 6.14. Densitometry graphs showing CD44v6 expression and HER2, EGFR, c-Met, FAK, AKT, Src and ERK1/2 activation in MCF-7 cells after 48 hour transfection with CD44v6 or CD44v6 Δ cyt plasmid DNA in the presence (10 minute treatment, 100 μ g/ml) or absence of HA. The data shows the relative protein levels in the cell lines expressed as a ratio of the active protein:total protein normalised to GAPDH. Error bars represent the average normalised data \pm SEM from 3 independent experiments and the data is presented as the percentage of the untreated control. Statistical analysis was performed using an unpaired t-test and significance was set at $p < 0.05$.

6.2.4 CD44v6 overexpression in MCF-7 cells enhanced cellular invasion via EGFR activation and subsequent downstream signalling responses

The data thus far suggested that CD44v6 overexpression in MCF-7 cells led to enhanced EGFR pathway activation and increased cellular invasion. To investigate the hypothesis that CD44v6 may promote the aggressive phenotype of MCF-7 cells through the activation of the EGFR pathway, inhibition of EGFR (by use of the inhibitor, gefitinib) and subsequent assessment of cellular invasion in MCF-7 cells was explored.

Boyden Chamber assays revealed a significant reduction in the ability of CD44v6-overexpressing MCF-7 cells to invade through Matrigel in the presence of gefitinib compared to the untreated CD44v6-overexpressing cells, and reduced their invasive capacity similar to the level of untransfected and CD44v6 Δ cyt-transfected MCF-7 control cells (Figure 6.15). Although CD44v6 Δ cyt overexpression in MCF-7 cells enhanced EGFR signalling, this did not lead to enhanced invasion and treatment with gefitinib did not alter the invasive capacity of these cells (Figure 6.15).

As previous data revealed that CD44v6 overexpression in MCF-7 cells enhanced the activation of the downstream effectors of the EGFR pathway, AKT and ERK1/2, the effect of gefitinib treatment upon the activity of these signalling molecules was investigated. Western blotting and densitometry analysis revealed that gefitinib treatment significantly attenuated the activity of EGFR, AKT and ERK1/2 in CD44v6- and CD44v6 Δ cyt-overexpressing MCF-7 cells compared to their untreated counterparts (Figure 6.16).

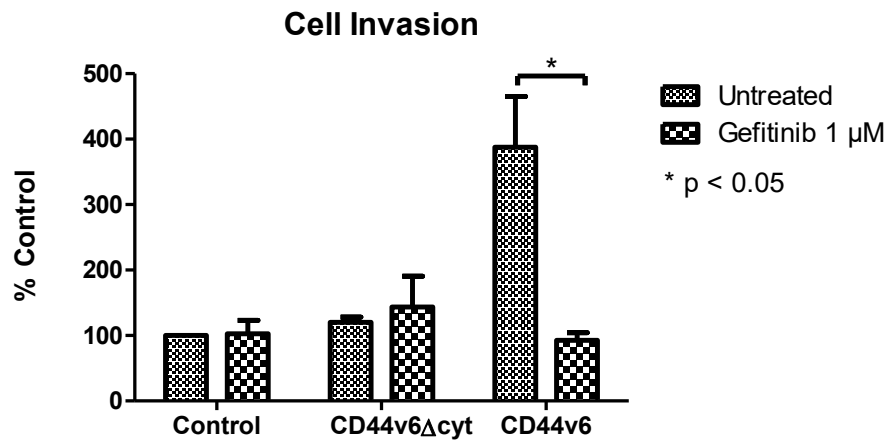


Figure 6.15. Measurement of cell invasion in MCF-7 cells overexpressing CD44v6 or CD44v6 Δ cyt proteins in the presence and absence of gefitinib. MCF-7 cells were transfected with CD44v6 or CD44v6 Δ cyt plasmid DNA for 48 hours prior to the assessment of invasion (Boyden Chamber assay) in the presence (1 μ M) or absence of the EGFR inhibitor, gefitinib. Control cells represent lipid-treated MCF-7 cells. Error bars represent the average normalised data \pm SEM from 3 independent experiments and the data is presented as the percentage of the untreated control. Statistical analysis was performed using a paired t-test and significance set at p < 0.05.

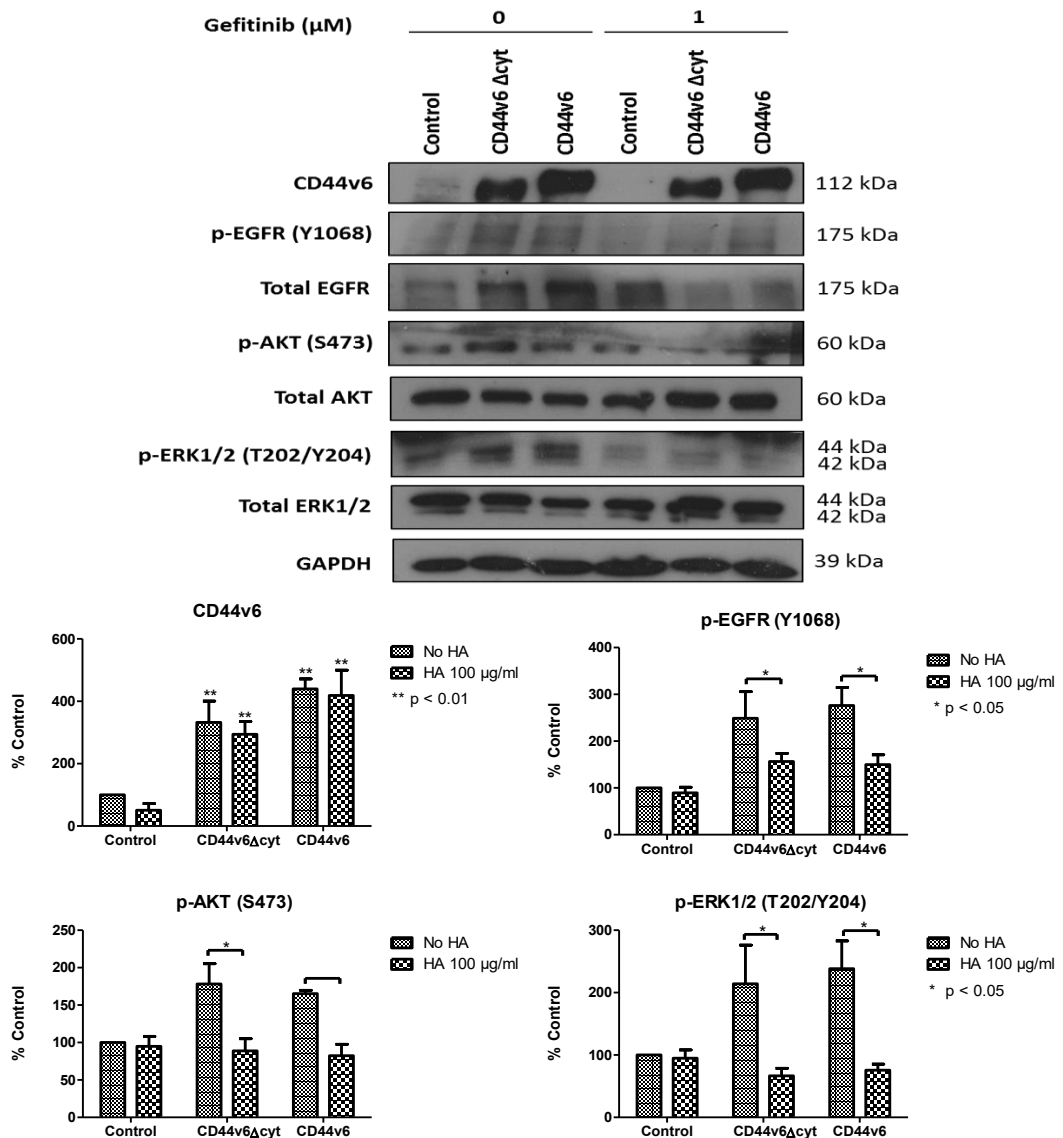


Figure 6.16. Representative Western blot images and densitometry graphs from 3 independent experiments showing EGFR, AKT and ERK1/2 activation in MCF-7 cells after 48 hour transfection with CD44v6 or CD44v6 Δcyt plasmid DNA in the presence (1 μM , 5 minutes) or absence of the EGFR inhibitor gefitinib. Control cells represent lipid-treated MCF-7 cells. Total protein levels were unchanged with the exception of total EGFR which was reduced in CD44v6 Δcyt and CD44v6 cells treated with gefitinib. GAPDH was used as a loading control. The data shows the relative protein levels in the cell lines expressed as a ratio of the active protein:total protein normalised to GAPDH. Error bars represent the average normalised data $\pm\text{SEM}$ from 3 independent experiments and the data is presented as the percentage of the untreated control. Statistical analysis was performed using an unpaired t-test and significance was set at $p < 0.05$.

6.2.5 CD44v6 suppression attenuated growth and invasion of Tam-R cells and enhanced their cellular migration

Based on the transfection data which suggested a role for both CD44v3 and CD44v6 as promoters of cellular invasion in MCF-7 cells, together with numerous reports revealing a correlation between overexpression of these isoforms and enhanced tumour metastasis and invasion in numerous carcinomas (Herrera-Gayol and Jothy 1999; Ni et al. 2002; Lui et al. 2005; Shi et al. 2013; Ni et al. 2014), the next step was to investigate whether these effects were also observed in the endocrine resistant cell models. For this purpose, CD44v6-specific siRNA was designed using BLOCK-iT™ RNAi Designer (Invitrogen Life Technologies, see Materials and Methods 2.12.1). However, due to the small size of CD44 variant 3 exon (126 bp), no unique sequence was available to specifically target this isoform, therefore investigation of CD44v3 function in endocrine resistant cell models using an siRNA based approach could not be undertaken.

Optimisation experiments revealed that treatment of Tam-R and Fas-R cells with CD44v6 siRNA resulted in a significant suppression of all CD44v6-containing isoforms compared to the NT-siRNA-treated cells between 24 - 144 hours post-transfection (Figure 6.17 and 6.18). Furthermore, these data confirmed that CD44v6 suppression did not substantially alter the expression of alternative CD44 isoforms in these cells (Figure 6.17 and Appendix Q). Whilst Western blotting analysis revealed that RHAMM expression become modestly suppressed in Tam-R cells between 48 – 72 hours post-transfection, densitometry analysis revealed that this was not significant (Appendix Q). Furthermore, a small reduction in CD44 Std isoform expression was

observed in these cells which is likely the result of the CD44 Std antibody recognising an epitope common to all CD44 isoforms (Figure 6.17). Densitometry analysis revealed that CD44 Std suppression was significant between 24 – 144 hours post-transfection in Tam-R cells, and at 144 hours post-transfection in Fas-R cells, compared to the NT- siRNA control cells (Appendix Q).

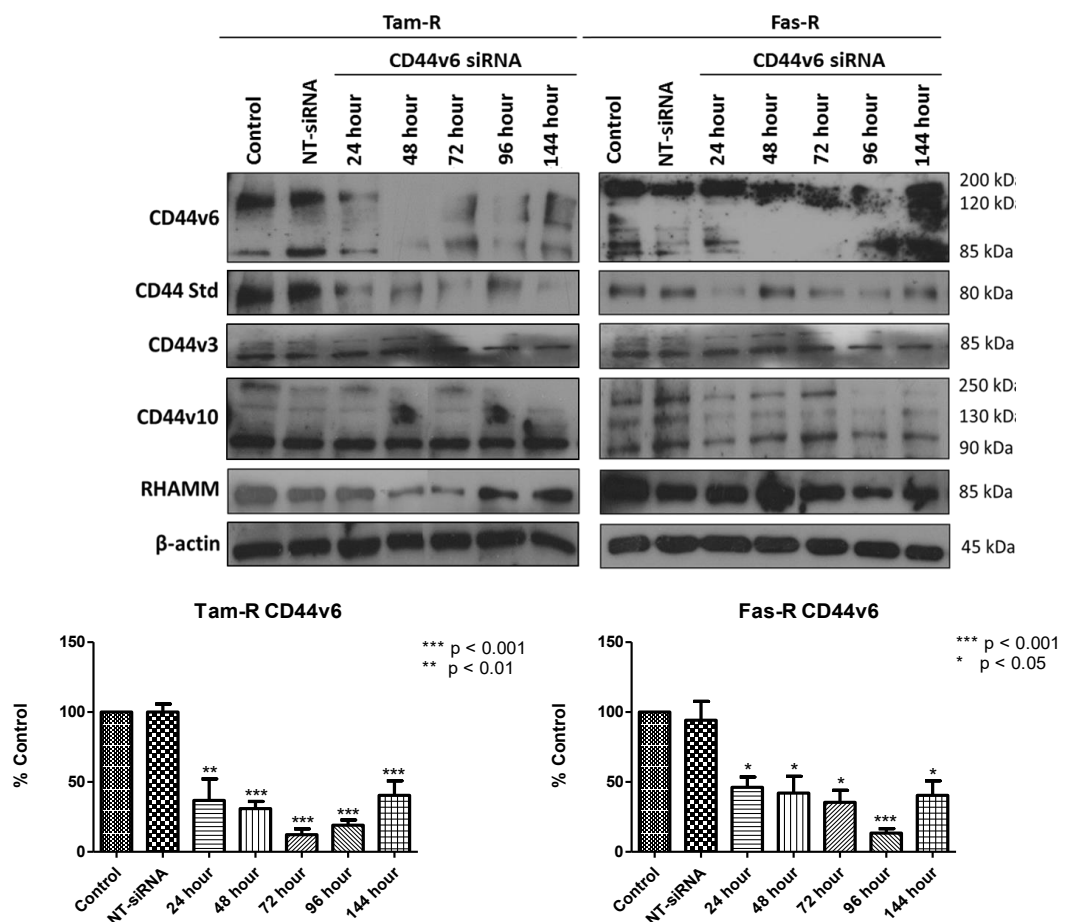


Figure 6.17. Representative Western blot images from 3 independent experiments showing CD44 isoform and RHAMM protein expression in Tam-R and Fas-R cells after treatment with CD44v6 siRNA for 24 – 144 hours in comparison to the untreated and NT-siRNA treated controls. GAPDH was used as a loading control. Densitometry graphs show CD44v6 expression in Tam-R and Fas-R cells between 24 – 144 hours post-transfection. Error bars represent the average normalised data \pm SEM from 3 independent experiments. Data is normalised to GAPDH and presented as the percentage of the untreated control. Statistical analysis was performed using an ANOVA test with tukey post-hoc analysis and values were compared to the NT-siRNA control sample.

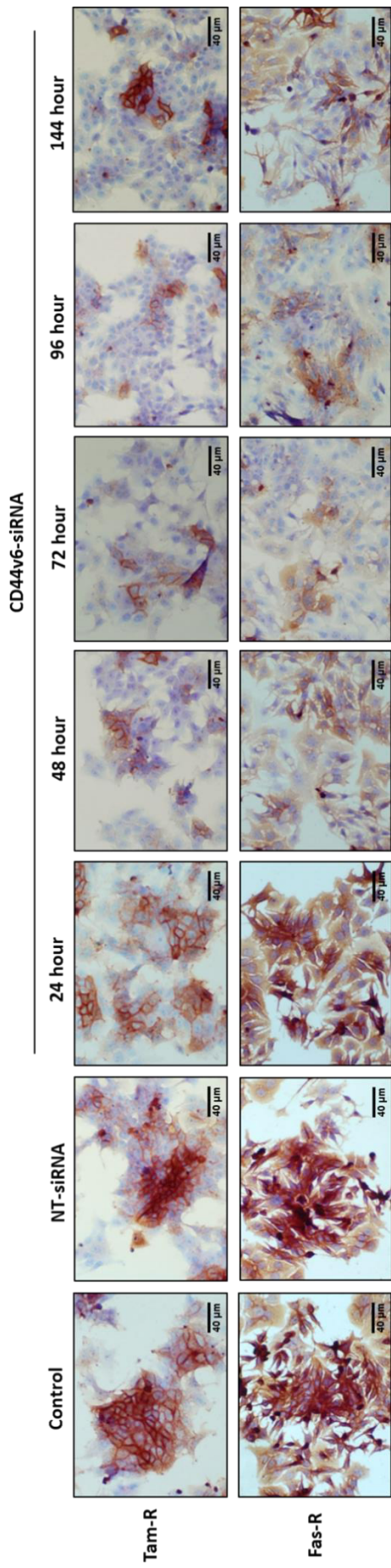


Figure 6.18. Representative images of CD44v6 protein expression from 3 independent experiments from immunocytochemistry analysis (x40 magnification) in Tam-R and Fas-R cells after treatment with CD44v6 siRNA for 24 – 144 hours post-transfection in comparison to the untreated and NT-siRNA treated control cells.

Analysis of the functional effects of CD44v6 suppression in the endocrine resistant cell lines revealed that Tam-R cells treated with CD44v6-siRNA led to a reduction in their invasive capacity through Matrigel and attenuated their endogenous and HA-induced proliferative capacity compared to the NT-siRNA control cells (Figure 6.19). In contrast, CD44v6 suppression enhanced the endogenous and HA-stimulated migratory capacity of Tam-R cells compared to the NT-siRNA control cells (Figure 6.19). Interestingly, CD44v6 suppression in Fas-R cells had no significant impact upon their migratory, invasive or proliferative behaviours compared to the NT-siRNA control cells (Figure 6.20).

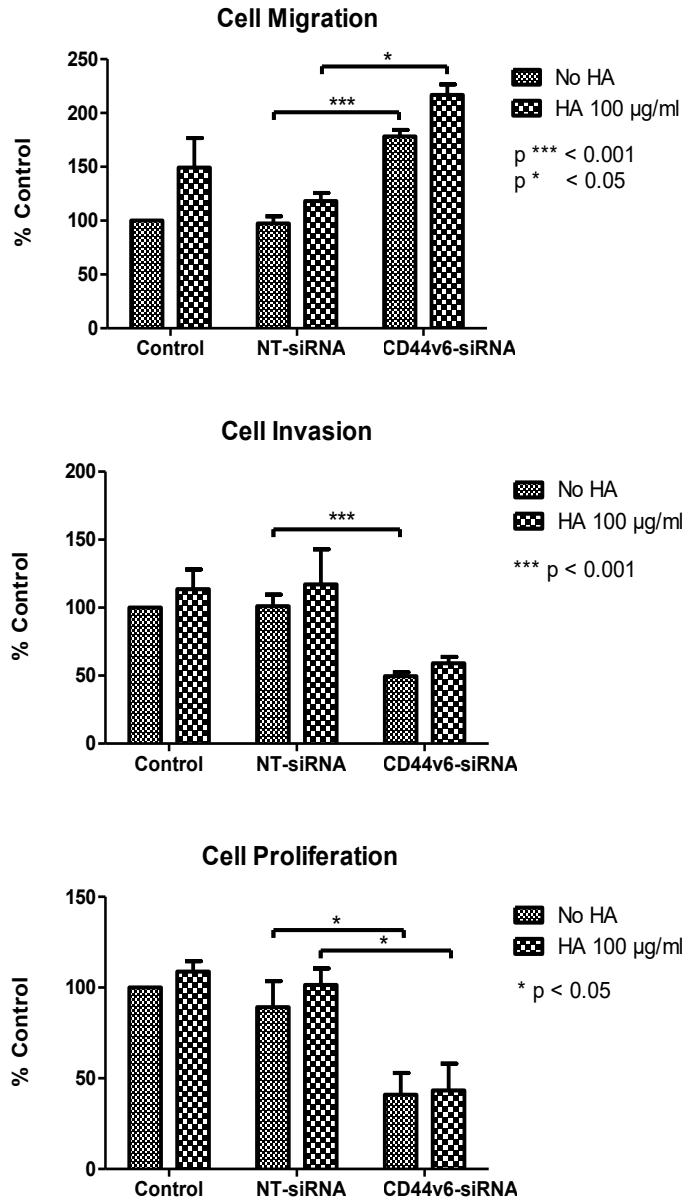


Figure 6.19. Measurement of endogenous and HA-stimulated cell behaviour responses of Tam-R cells upon CD44v6 suppression. Tam-R cells were transfected with NT- or CD44v6-siRNA for 48 hours prior to the assessment of migration and invasion (Boyden Chamber assays) and proliferation (Coulter counter assays) in the presence (100 µg/ml) and absence of HA. Error bars represent the average normalised data \pm SEM from 3 independent experiments and the data is presented as the percentage of the untreated control. Statistical analysis was performed using an unpaired t-test and significance set at $p < 0.05$.

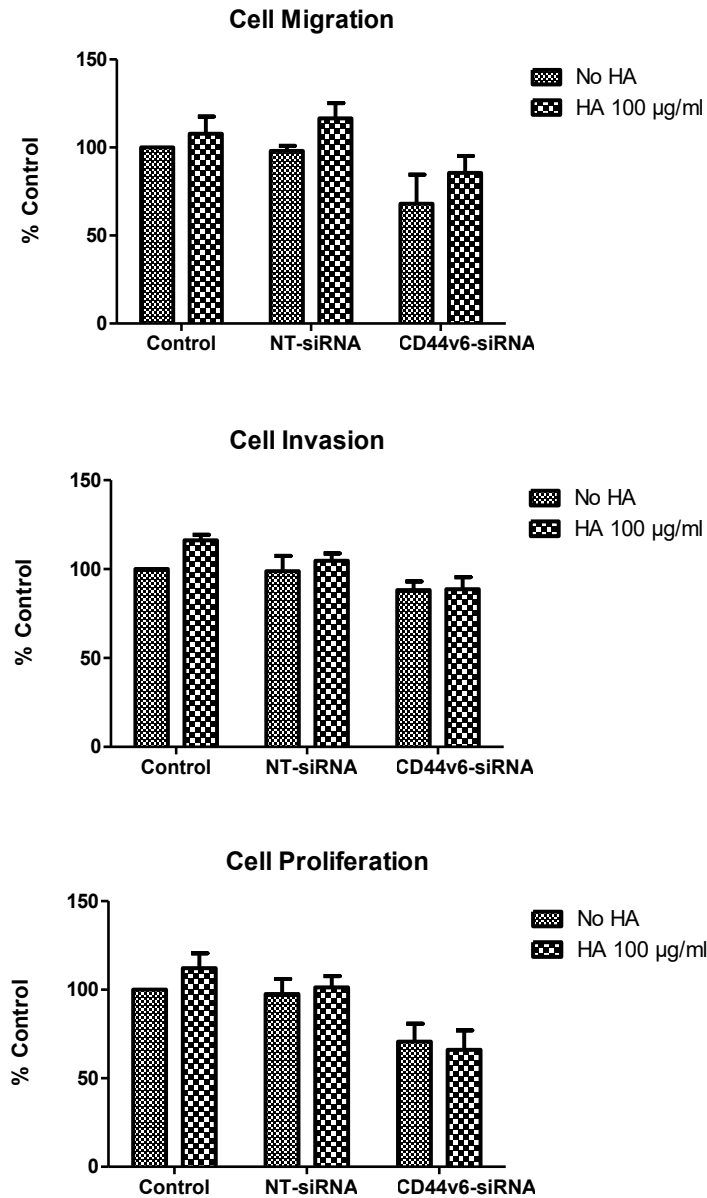


Figure 6.20. Measurement of endogenous and HA-stimulated cell behaviour responses of Fas-R cells upon CD44v6 suppression. Fas-R cells were transfected with NT- or CD44v6-siRNA for 48 hours prior to the assessment of migration and invasion (Boyden Chamber assays) and proliferation (Coulter counter assays) in the presence (100 µg/ml) and absence of HA. Error bars represent the average normalised data \pm SEM from 3 independent experiments and the data is presented as the percentage of the untreated control. Statistical analysis was performed using an unpaired t-test and significance set at $p < 0.05$.

Previous data revealed that CD44v6 overexpression in MCF-7 cells enhanced EGFR, AKT and ERK1/2 activation (Figure 6.12). To determine whether these proteins were modulated upon CD44v6 suppression in endocrine resistant cells, and to further explore the mechanisms through which CD44v6 suppression may alter the behavioural function of Tam-R cells, the activation of several signalling components were reassessed by Western blotting analysis in the presence or absence of HA. The effect of CD44v6 suppression upon cellular signalling was also investigated in Fas-R cells.

Western blotting and densitometry analysis revealed that CD44v6 suppression almost significantly reduced endogenous and HA-stimulated EGFR, AKT and ERK1/2 activation and HA-stimulated FAK in Tam-R cells compared to the NT-siRNA control cells (Figures 6.21 and 6.22). In Fas-R cells, CD44v6 suppression significantly reduced endogenous c-Met and AKT activation and HA-stimulated c-Met activation compared to the NT-siRNA control cells (Figure 6.23 and 6.24).

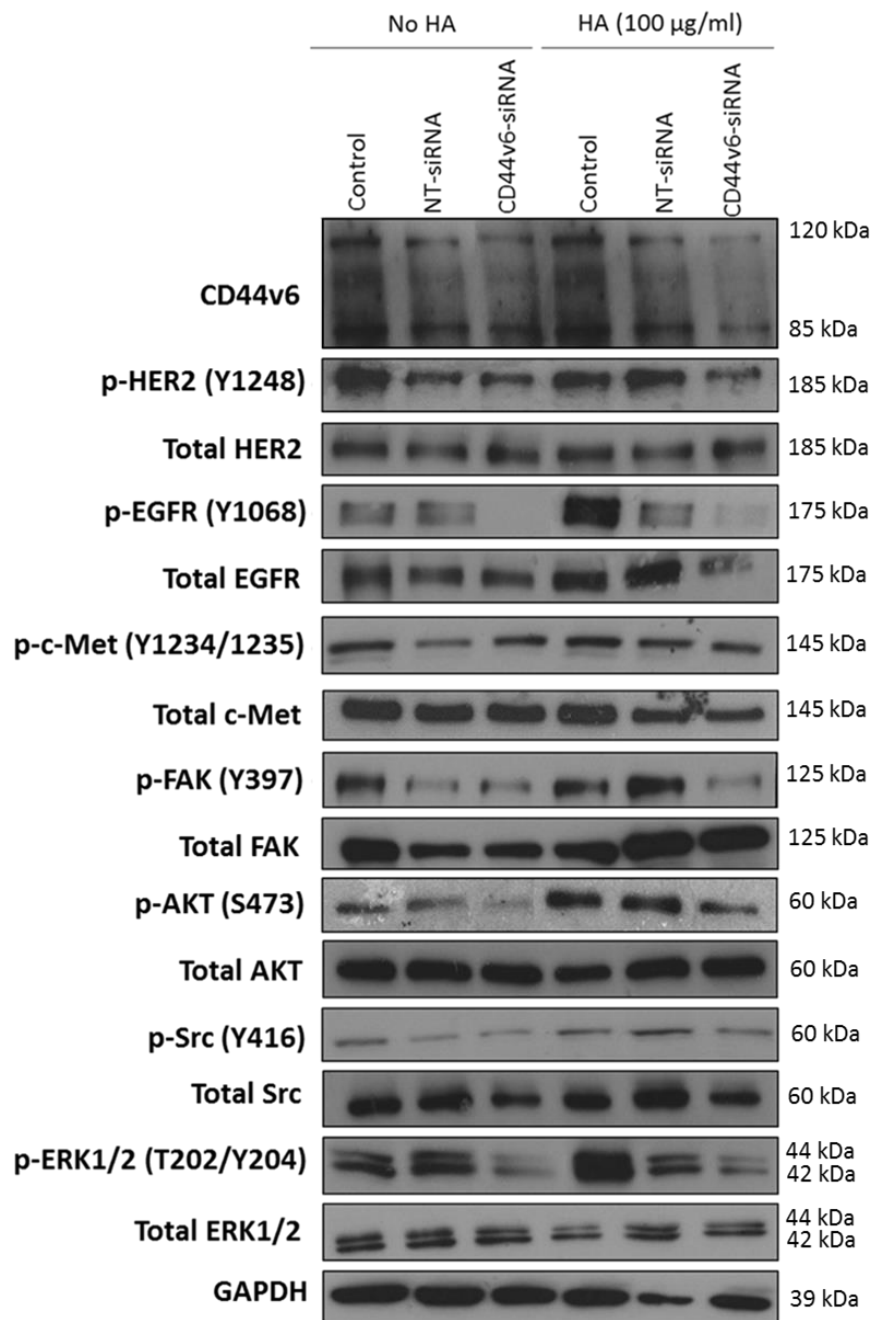


Figure 6.21. Representative Western blot images from 3 independent experiments showing HER2, EGFR, c-Met, FAK, AKT, Src and ERK1/2 activation in Tam-R cells after 48 hour transfection with NT- or CD44v6-siRNA in the presence (10 minute treatment, 100 µg/ml) or absence of HA. Total protein levels were unchanged and GAPDH was used as a loading control.

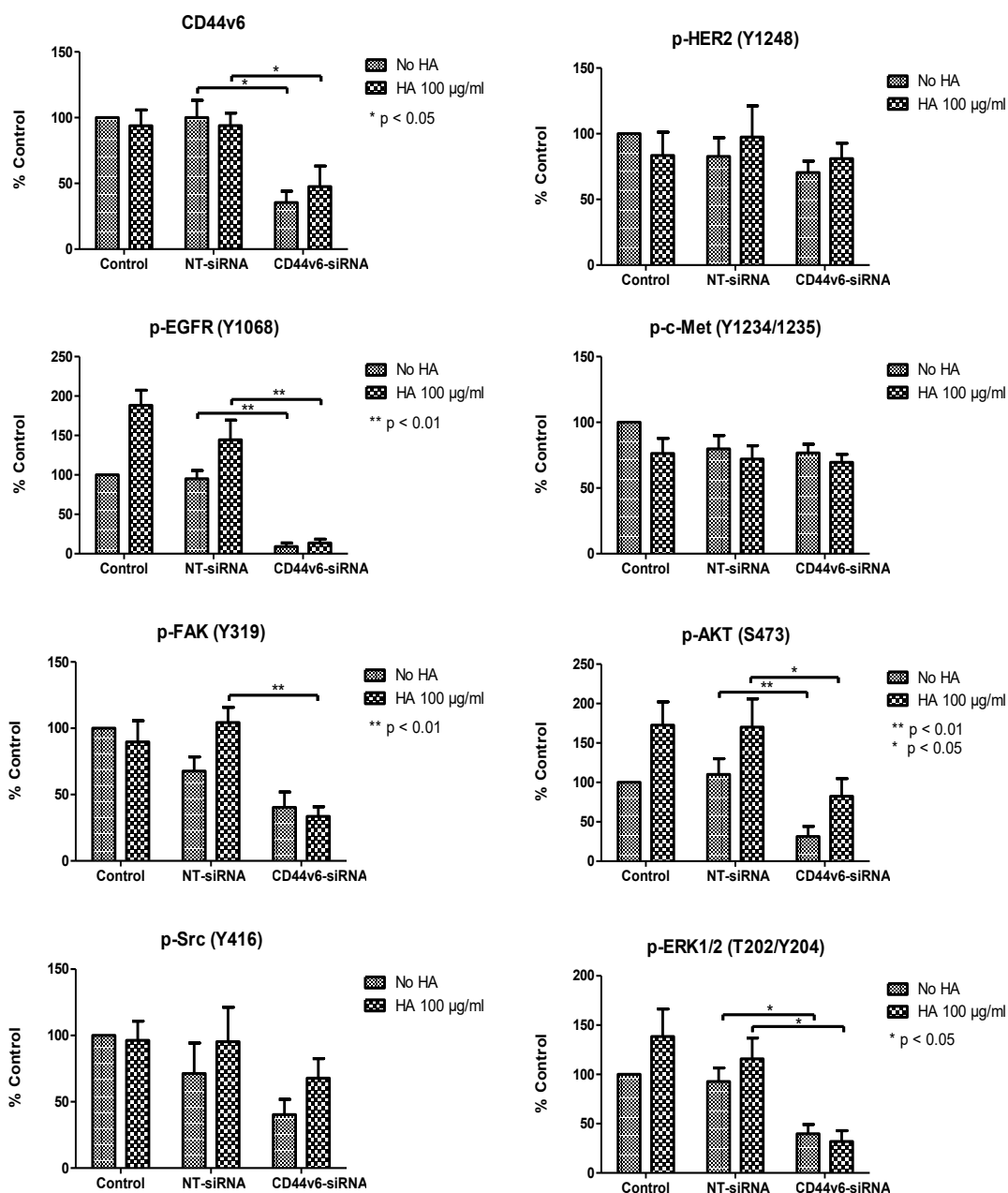


Figure 6.22. Densitometry graphs showing CD44v6 expression and HER2, EGFR, c-Met, FAK, AKT, Src and ERK1/2 activation in Tam-R cells after 48 hour treatment with CD44v6 siRNA in the presence (215 kDa, 100 µg/ml, 10 minutes) and absence of HA, before cell lysis and detection by Western blotting analysis. The data shows the relative protein levels in the cell lines expressed as a ratio of the active protein:total protein normalised to GAPDH. Error bars represent the average normalised data \pm SEM from 3 independent experiments and the data is presented as the percentage of the untreated control. Statistical analysis was performed using an unpaired t-test and significance was set at $p < 0.05$.

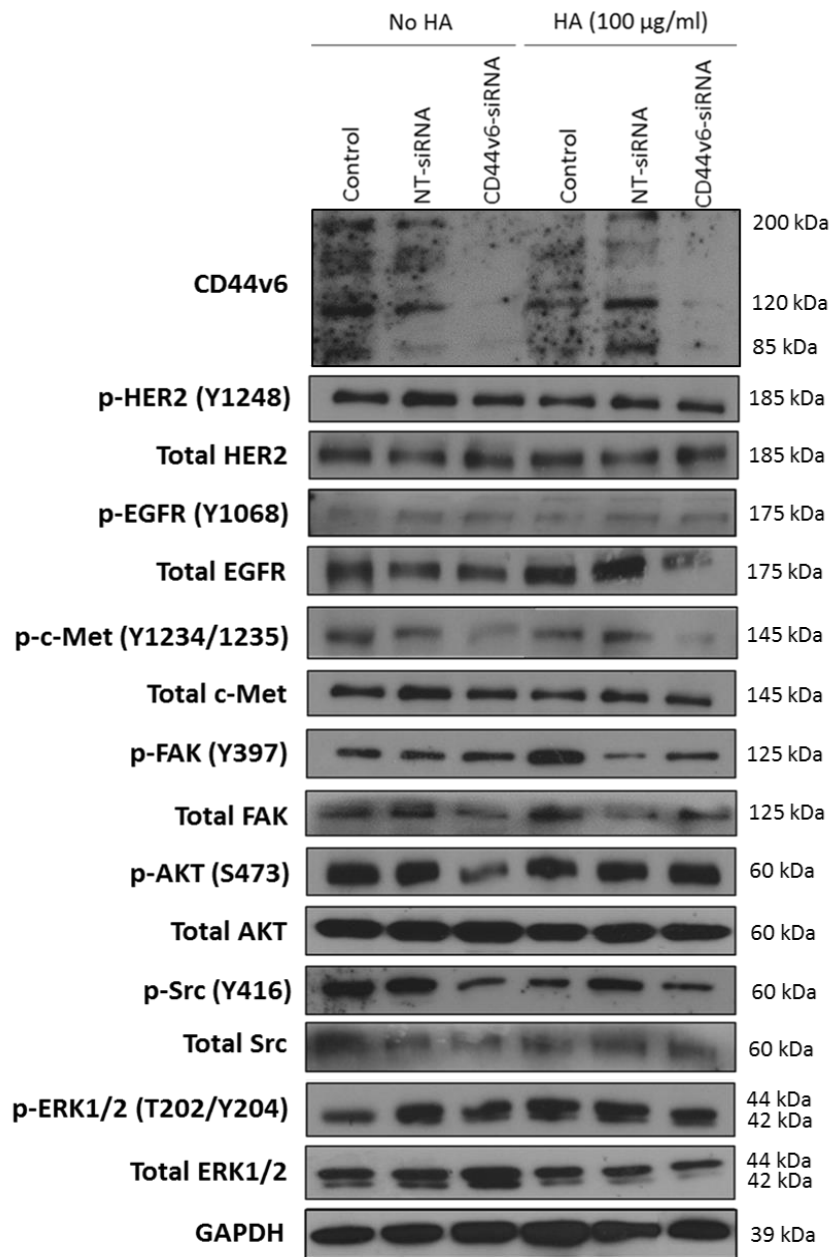


Figure 6.23. Representative Western blot images from 3 independent experiments showing HER2, EGFR, c-Met, FAK, AKT, Src and ERK1/2 activation in Fas-R cells after 48 hour transfection with NT- or CD44v6-siRNA in the presence (10 minute treatment, 100 µg/ml) or absence of HA. Total protein levels were unchanged and GAPDH was used as a loading control.

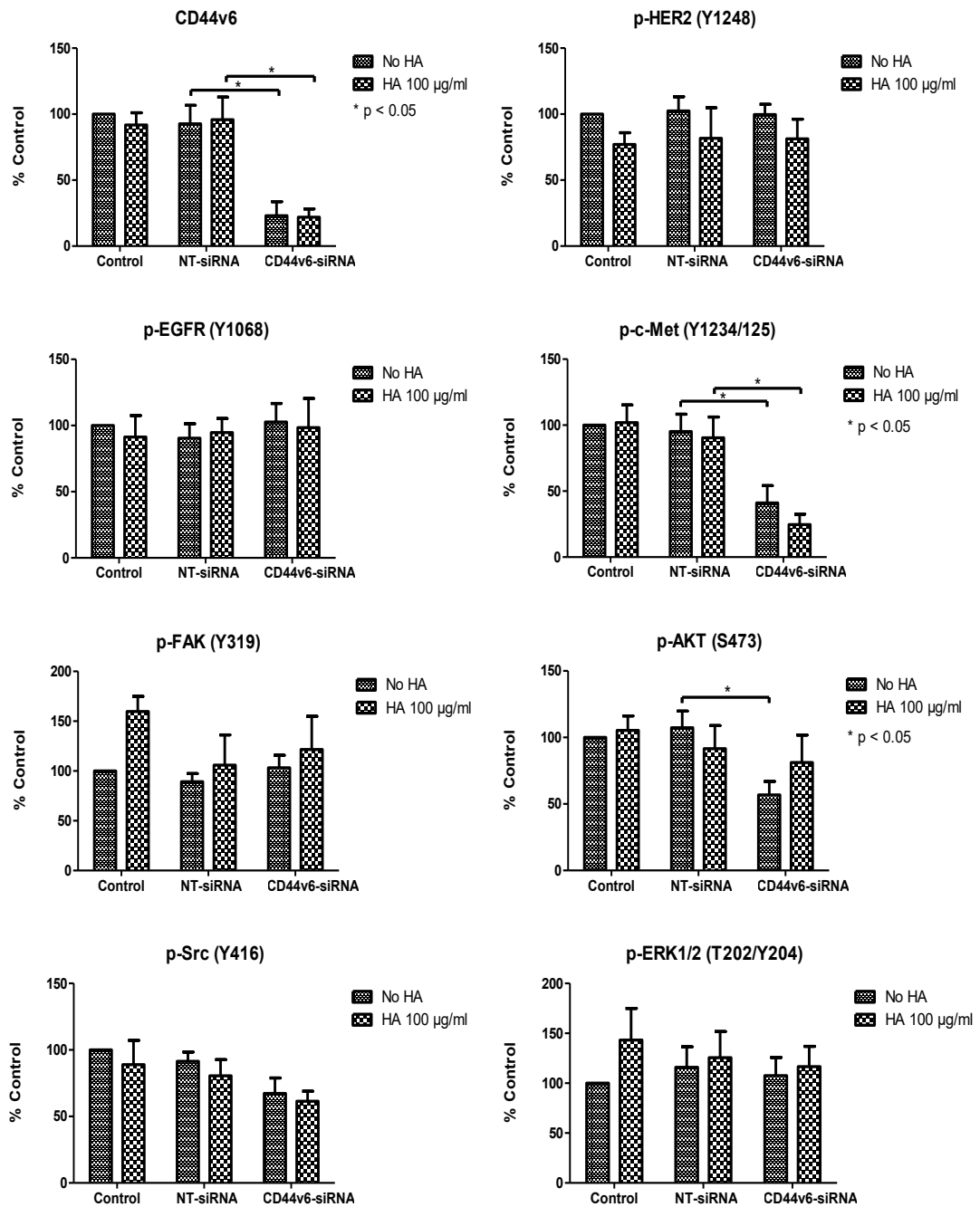


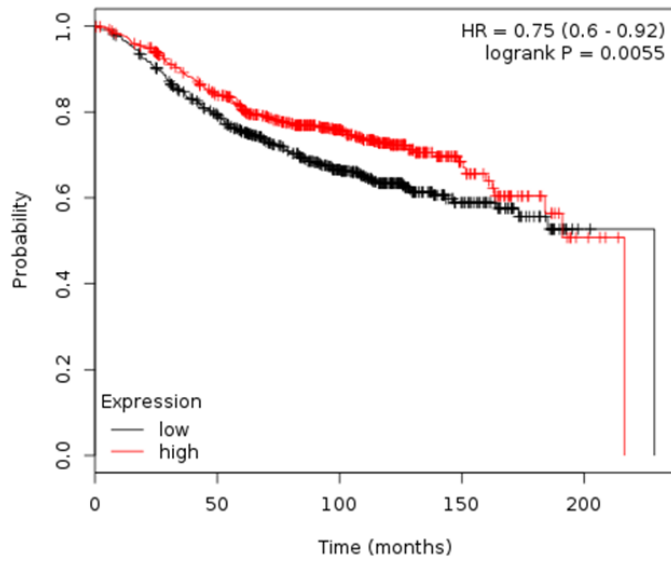
Figure 6.24. Densitometry graphs showing CD44v6 expression and HER2, EGFR, c-Met, FAK, AKT, Src and ERK1/2 activation in Tam-R cells after 48 hour treatment with CD44v6 siRNA in the presence (215 kDa, 100 µg/ml, 10 minutes) and absence of HA, before cell lysis and detection by Western blotting analysis. The data shows the relative protein levels in the cell lines expressed as a ratio of the active protein:total protein normalised to GAPDH. Error bars represent the average normalised data \pm SEM from 3 independent experiments and the data is presented as the percentage of the untreated control. Statistical analysis was performed using an unpaired t-test and significance was set at $p < 0.05$.

6.2.6 CD44 is associated with an increased duration of response to endocrine therapy in ER+ breast cancer

To begin to establish if there is an association between CD44 and clinical parameters, CD44 mRNA expression was analysed in clinical breast cancer using the publically available online KM Plotter tool (see Materials and Methods 2.4) to determine any clinical value following endocrine treatment. This tool is able to study publically available breast cancer gene microarray mRNA expression data collected from clinical samples prior to endocrine therapy and also contains associated survival-related information. KM plotter allows the generation of survival curves with Log Rank testing to determine any significant association between inherent expression levels for genes of interest and clinical outcome. As of yet, no fulvestrant-treated clinical microarray datasets are publically available for KM Plotter analyses.

To analyse the association between CD44 and duration of relapse free survival (RFS) in this project, the patient data was split into 2 groups using the optimal cut-off tool provided within KM Plotter using a Kaplan-Meier plot. RFS was used as the measure of clinical outcome and patients selected were ER+ and had subsequently received any form of endocrine therapy (excluding chemotherapy). Analysis revealed that high CD44 mRNA expression associated with significantly increased duration of response to endocrine therapy compared to patients with low CD44 mRNA expression ($p = 0.0055$) (Figure 6.25). However, when RFS was used as a measure of clinical outcome and patients selected were ER+ and subsequently received tamoxifen treatment only, although high levels of CD44 were again associated with increased duration of response, this did not reach significance ($p = 0.28$) (Figure 6.25).

CD44 mRNA expression, RFS, ER+, any endocrine treatment



CD44 mRNA expression, RFS, ER+, tamoxifen treatment only

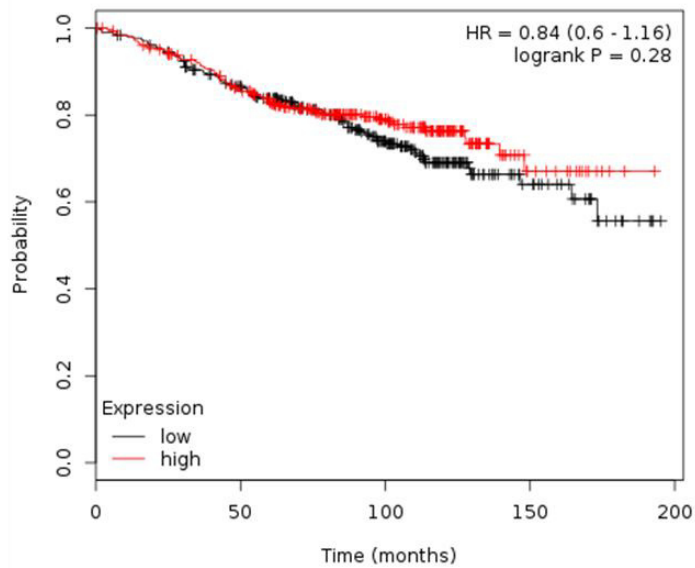


Figure 6.25. Kaplan Meier survival curves generated by KM Plotter to display the association between CD44 mRNA expression and relapse free survival (RFS) in ER+ treated with any endocrine therapy (n = 1190) or confined to tamoxifen treatment (n = 615). The survival curves were generated using the Jetset affymetrix gene probe for CD44 (212063_at) and patients were grouped by optimal fit (as calculated by KM Plotter). The Hazard Ratio (HR) (with 95% confidence intervals) and logrank p values are shown.

6.2.6.1 CD44v6 and EGFR co-expression is associated with a worsened outcome in a small exploratory patient series of tamoxifen-treated ER+ breast cancer patients

Whilst KM Plotter analyses revealed an association between high CD44 mRNA expression levels and prolonged RFS in endocrine-treated ER+ breast cancer patients, this analysis does not take into consideration the expression of specific CD44 isoforms and accounts only for total CD44 mRNA expression in these patients. Given that the experimental data suggested evidence for different roles for CD44 isoforms in breast cancer behaviours, notably implicating a role for CD44v6-mediated EGFR activation as a contributor towards cellular invasion in tamoxifen resistance, the clinical relevance of these findings using in-house immunohistochemistry data was explored.

A series of formalin-fixed paraffin-embedded tissue microarray (TMA) sections (provided by Dr Andrew Green, Nottingham University) including 140 patients with primary breast cancers from ER+ adjuvant tamoxifen patients with 20 year follow up was assessed by the group for CD44v6 using H-score analysis (see Appendix R). Derived H-scores were subsequently analysed in this project versus relevant clinicopathological parameters including: EGFR immunostaining (10 % cutpoint), disease-free interval (DFI) and overall survival (OS) available for all these in tamoxifen-treated patients. This allowed to further evaluate if any interplay existed between CD44v6 expression and EGFR in relation to tamoxifen resistance. The web-based algorithm X-tile was used to define optimal CD44v6 membrane cut point (47) versus patient outcome and statistical testing was performed using Log Rank. Of the 140 TMA's studied in this series, 20 were negative for CD44v6 membrane expression.

After the cutpoint was applied, 71/140 TMAs were >47. Figures 6.26 reveals representative images of TMA cores from this series with high and low CD44v6 immunostaining.

Using the respective cut points, 4 CD44v6/EGFR status phenotypes were discriminated in the 140 ER+ breast cancers examined in this series as shown in Table 6.1; the most abundant phenotypes were EGFR- thus reflecting this is an ER+ series. The survival curve data initially revealed that higher CD44v6 expression correlated with significantly better outcome in ER+ disease in tamoxifen-treated patients with a longer DFI ($p = 0.013$) and OS ($p = 0.001$) compared to patients whose tumours did not express CD44v6 (Figures 6.27 and 6.28). However these analyses suggested promising separation between CD44v6+ patients when subdivided with EGFR status. Whilst CD44v6+/EGFR- patients experienced the longest DFI (141.952 months), this was greatly reduced for patients whose tumours co-expressed CD44v6 and EGFR (CD44v6+/EGFR+) (105.662 months) ($p = 0.023$) (Figure 6.29). Interestingly, CD44v6+/EGFR+ patients displayed a similar DFI to patients whose tumours did not express either receptor (104.330 months) (Figure 6.29).

These analyses also suggested promising separation between CD44v6+ patients with high and low EGFR expression and OS. Whilst CD44v6+/EGFR- patients also displayed the longest OS on tamoxifen treatment (161.793 months), this was reduced for the sub-cohort of patients co-expressing CD44v6 and EGFR (138.130 months) ($p = 0.005$) (Figure 6.30). However, patients whose tumours phenotype were CD44v6-/EGFR+ or CD44v6-/EGFR- tumours also showed a comparatively poorer OS (134.465 and 132.465 months respectively) (Figure 6.30).

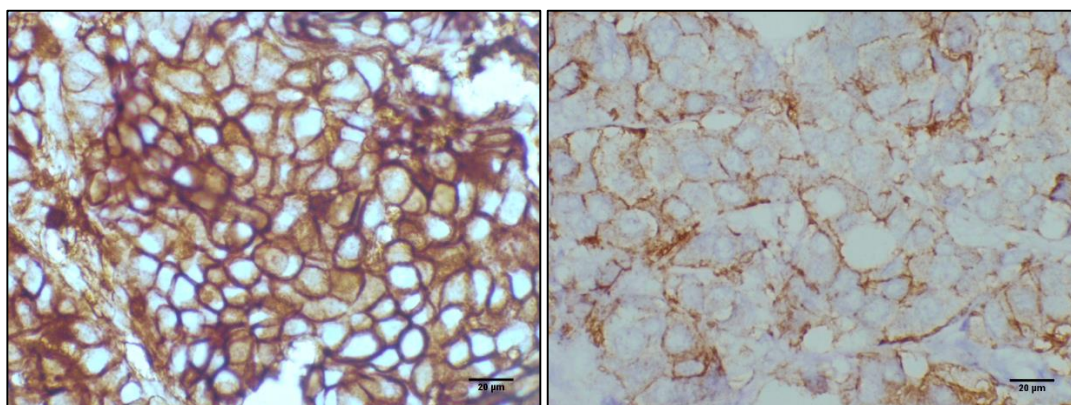
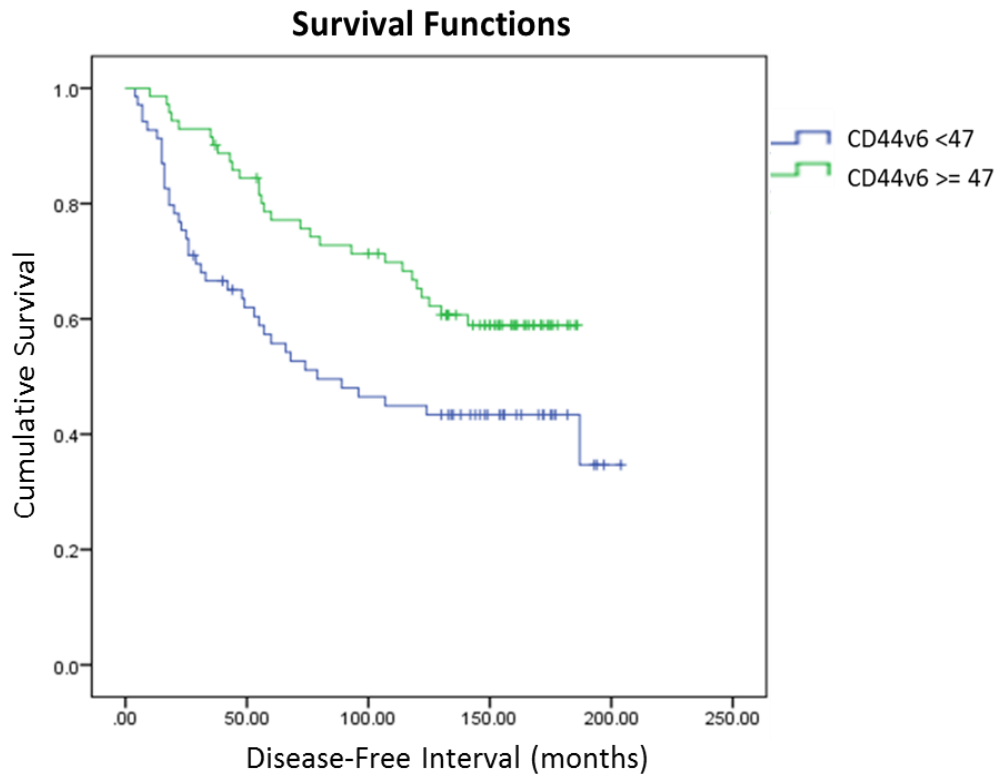


Figure 6.26. Representative images from TMA cores with high (left) and low (right) CD44v6 immunostaining from the Nottingham Immunohistochemical clinical series (x40 magnification).

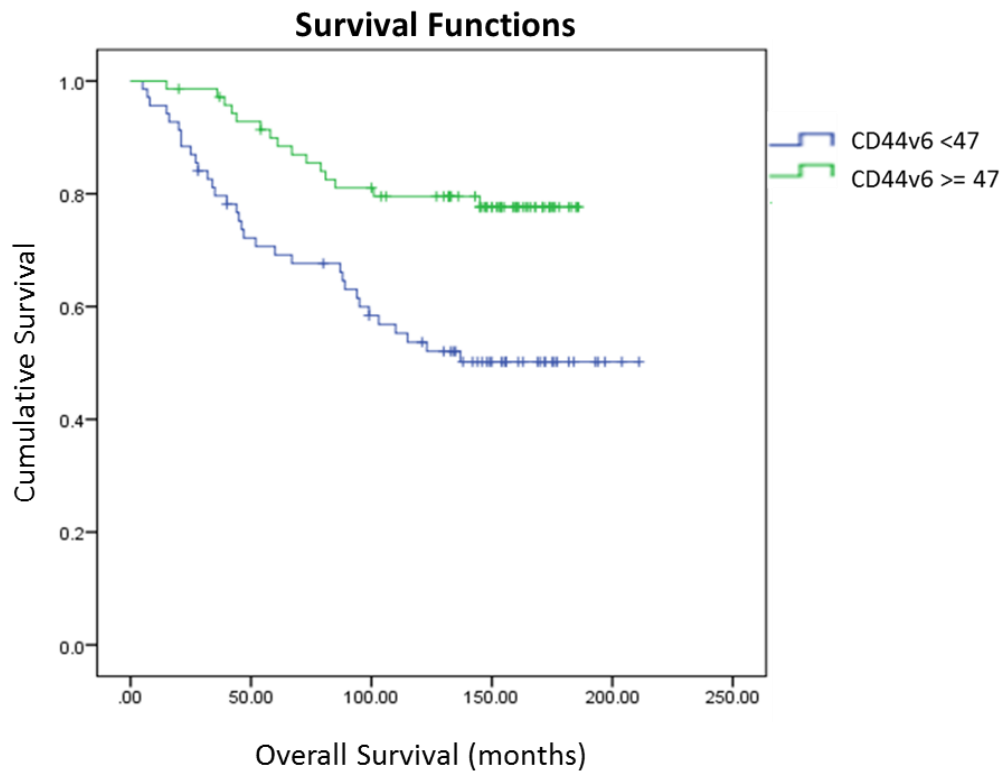
Tumour Phenotype	Patient Number	Patient Frequency (%)
CD44v6+/EGFR+	9	6.4
CD44v6+/EGFR-	62	44.3
CD44v6-/EGFR+	13	9.3
CD44v6-/EGFR-	56	40
Total	140	100

Table 6.1. The number of patients and associated percentage frequency for the 4 CD44v6 and EGFR tumour phenotypes in 140 ER+ tamoxifen-treated primary breast cancer patients from the TMA series.



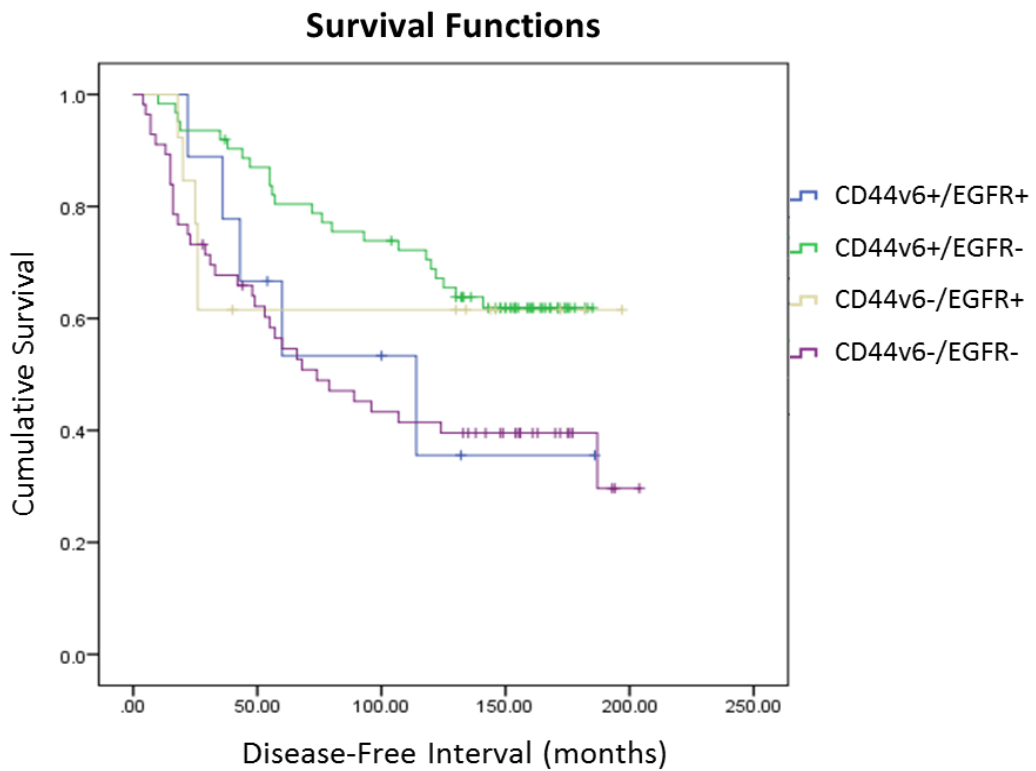
	Means for Disease-Free Interval (DFI) on tamoxifen			
	Estimate	Std. Error	95% Confidence Interval	
			Lower Bound	Upper Bound
CD44v6 <47	109.480	10.219	89.452	129.509
CD44v6 >=47	138.241	7.512	123.500	152.981
Overall	128.548	6.901	115.022	142.024

Figure 6.27. Investigation of high versus low CD44v6 membrane staining upon the impact of disease-free interval (DFI) in a small exploratory series of ER+ breast cancer patients treated with tamoxifen (n = 140). The Kaplan–Meier plot shows tumours grouped according to high versus low CD44v6 membrane expression (cut point 47) and analysed in relation to DFI ($p = 0.013$) in months. The table shows the corresponding mean survival estimates, standard error and lower and upper bound 95 % confidence intervals for each phenotype.



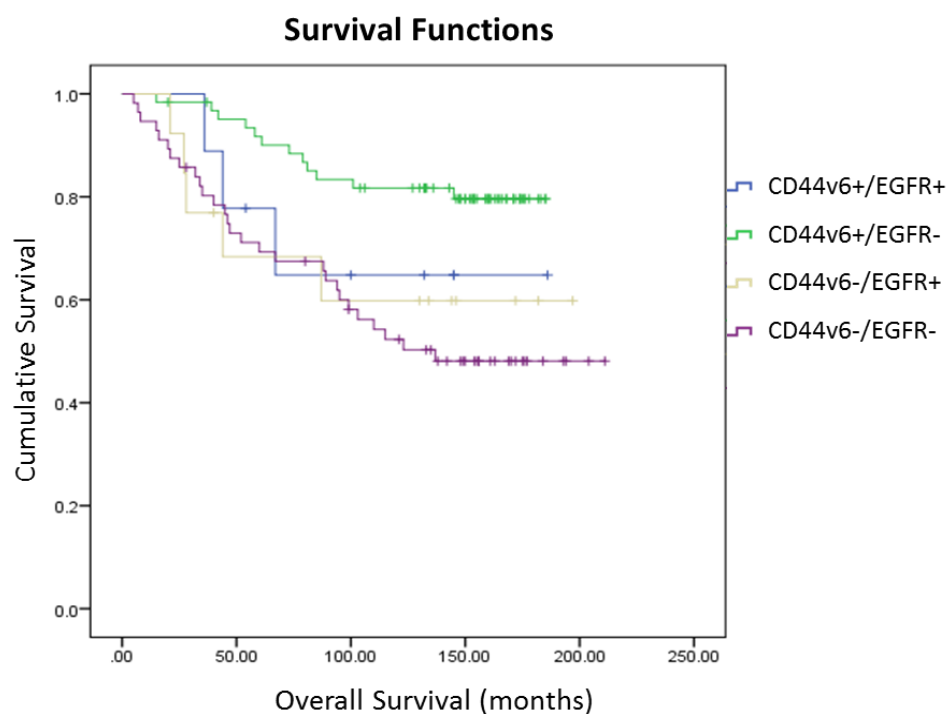
	Means for Overall Survival (OS) on tamoxifen			
	Estimate	Std. Error	95% Confidence Interval	
			Lower Bound	Upper Bound
CD44v6 <47	134.420	9.963	114.892	153.948
CD44v6 >=47	159.443	6.254	147.181	171.701
Overall	156.933	6.489	144.216	169.651

Figure 6.28. Investigation of high versus low CD44v6 membrane staining upon the impact of overall survival (OS) in a small exploratory series of ER+ breast cancer patients treated with tamoxifen (n = 140). The Kaplan–Meier plot shows tumours grouped according to high versus low CD44v6 membrane expression (cut point 47) and analysed in relation to OS ($p = 0.001$) in months. The table shows the corresponding mean survival estimates, standard error and lower and upper bound 95 % confidence intervals for each phenotype.



	Means for Disease-Free Interval (DFI) on tamoxifen			
	Estimate	Std. Error	95% Confidence Interval	
			Lower Bound	Upper Bound
CD44v6+/EGFR+	105.622	23.402	59.754	151.491
CD44v6+/EGFR-	141.952	7.713	126.834	157.070
CD44v6-/EGFR+	130.077	23.485	84.046	176.108
CD44v6-/EGFR-	104.330	11.069	82.634	126.026
Overall	128.548	6.901	115.022	142.074

Figure 6.29. Investigation of CD44v6 and EGFR co-expression upon the impact of disease-free interval (DFI) in a small exploratory series of ER+ breast cancer patients treated with tamoxifen (n = 140). The Kaplan-Meier plot shows tumours grouped according to the 4 phenotypes of CD44v6 and EGFR and analysed in relation to DFI in months (Log Rank p value = 0.023). The table shows the corresponding mean survival estimates, standard error and lower and upper bound 95 % confidence intervals for each phenotype.



	Means for Overall Survival (OS) on tamoxifen			
	Estimate	Std. Error	95% Confidence Interval	
			Lower Bound	Upper Bound
CD44v6+/EGFR+	138.130	22.459	94.111	182.149
CD44v6+/EGFR-	161.793	6.230	149.583	174.003
CD44v6-/EGFR+	134.906	21.920	91.943	177.869
CD44v6-/EGFR-	132.465	10.948	110.007	153.922
Overall	156.933	6.489	144.216	169.651

Figure 6.30. Investigation of CD44v6 and EGFR co-expression upon the impact of overall survival (OS) in a small exploratory series of ER+ breast cancer patients treated with tamoxifen (n = 140). The Kaplan-Meier plot shows tumours grouped according to the 4 phenotypes of CD44v6 and EGFR and analysed in relation to OS in months (Log rank p value = 0.005). The table shows the corresponding mean survival estimates, standard error and lower and upper bound 95 % confidence intervals for each phenotype.

6.3 Discussion

In this chapter, the contribution of specific CD44 variant isoforms to endocrine resistance was explored. Given that data previously identified that loss of global CD44 expression impaired cellular migration, invasion and proliferation in both endocrine resistant cell models and enhanced their sensitisation to HA (Chapter 4), it was next explored whether specific isoforms may act as dominant promoters of these processes. Initial characterisation data revealed enhanced expression of CD44v3 and CD44v6 proteins in endocrine resistant cells (Chapter 3), which have also been shown to become upregulated in primary breast carcinomas and correlate with numerous clinical parameters including metastasis, lymph node status and survival (Kuniyasa et al. 2002; Wang et al. 2007; Saito et al. 2013; Shi et al. 2013; Marzese et al. 2014), therefore these variant isoforms were decided to be the focus of this project.

Initially, optimisation data revealed that CD44v6 transfection into MCF-7 cells led to a similar endogenous expression and localisation pattern of CD44v6-containing proteins found in endocrine resistant Tam-R and Fas-R cells, thus allowing comparisons to be made between these cell models. However CD44v3 transfection into MCF-7 cells led to enhanced expression compared to the endogenous levels of CD44v3-containing proteins in endocrine resistant cells, although localisation patterns were similar; this must be taken into consideration upon interpretation of results. Functional analysis revealed that individual CD44 isoforms may mediate specific roles across the cell models. Indeed, the MCF-7 transfection data revealed that CD44v3 may act as a suppressor of cellular migration, whilst CD44v6 appeared to play an important role in the attenuation of endocrine response to fulvestrant.

Although both CD44 isoforms were implicated in invasion processes, CD44v6 overexpression in MCF-7 cells enhanced their endogenous invasion, whilst CD44v3 appeared to promote invasion upon HA binding.

The experimental data in this study which suggested CD44v3 may act to suppress cellular migration in MCF-7 cells appears to be in discordance with some other studies which suggest a role for CD44v3 proteins as promoters of a migratory phenotype in breast cancer (Bourguignon et al. 1998; Bourguignon et al. 1999), however it must be noted that these reports implicate the CD44v3,8-10 variant isoform in these processes. Thus, it may be suggested that CD44v3 isoforms require the additional presence of variant exons 8 - 10 to mediate cytoskeletal binding and promote a subsequently induced migratory response in these cells. Furthermore, discrepancies between the data and findings from others may be due to differences in the bioavailability of specific ligands and/or co-receptors. Indeed, CD44v3 contains the attachment site for HPS which has been shown to facilitate malignant behaviours in numerous carcinomas through the presentation of several growth factor receptors (Bennet et al. 1995; Van de Voort et al. 1999). Therefore variability in the expression of HPS and co-receptors, such as TGF β R1, MMP-9 and c-Met, between cancer cell lines may account for differences in the reported function of CD44v3 in the literature.

Conversely, the data here revealed a role for CD44v3 in enhanced invasion in MCF-7 cells upon HA stimulation, however the mechanism remains elusive (although unlike CD44v6-mediated invasion, a role for EGFR was not implicated) but may involve downstream activation of AKT, Src and ERK1/2. These results are supported by previous clinical findings by other groups which showed that CD44v3 was

upregulated in highly invasive breast tumours (Auvinen et al. 2005) where it has been shown to correlate with lymph node metastases (Kalish et al. 1999; Rys et al. 2003). Thus, given that HA is found in abundance in breast tumour stroma, this may suggest an important role for CD44v3 proteins in the enhancement of tumour progression behaviours in HA-rich environments. Taken together, the experimental data potentially implicate roles for CD44v3 proteins in both the suppression of cellular migration and enhancement of HA-stimulated invasion, however, validation of these results in endocrine resistant cell models could not be undertaken due to unavailability of siRNA to specifically target CD44v3 and lack of clinical data.

It must also be taken into consideration that sequencing analysis revealed a base pair mutation at position 17 in the CD44 variant 3 exon of the plasmid DNA leading to an amino acid substitution (N239D) from an arginine (uncharged, polar) to an aspartic acid (acidic) in the protein sequence (Appendix I). Whilst use of this CD44v3 plasmid has been published in several articles (including Meilgo et al. 2006 and 2007) the effect of the amino acid mutation remains unknown and may affect the results of this data. However the immunostaining data revealed similar localisation of transfected CD44v3 proteins in MCF-7 cells compared to their endogenous localisation in Tam-R and Fas-R cells suggesting that this amino acid substitution does not alter the localisation of CD44v3 proteins in these cells. To investigate whether this amino acid substitution may alter the function of the CD44v3 protein, several publically available online programmes were used to predict the effect of amino acid substitutions on protein function. Three separate online programmes were utilised for this purpose (referenced in Ng and Heinikoff 2006) and each predicted that the amino acid

substitution in CD44v3 was neutral, tolerated and unlikely to cause deleterious effects or change protein function (results shown in Appendix M). Furthermore, the attachment site for HPS found in variant exon 3 and critical for its reported functions is located between amino acid positions 32 – 39 in the DNA sequence and not near the site of the amino acid substitution (position 17) (Greenfield et al. 1999) thus suggesting low probability that the amino acid substitution may alter HPS binding. Finally, to assess whether any conserved sequences were found in the CD44 variant 3 exon which may be altered upon amino acid substitution, the publically available online conserved domain and protein classification database tool (<http://www.ncbi.nlm.nih.gov/Structure/cdd/wrpsb.cgi>) was utilised and revealed no known conserved sites in this exon (Appendix N). Taken together, these analyses suggest that the amino acid substitution in this exon is unlikely to change its protein function.

The experimental data further suggested a role for CD44v6-mediated activation of the EGFR pathway as a promoter of cellular invasion in tamoxifen resistance (depicted in Figure 6.31). Indeed the results revealed that overexpression of CD44v6 in MCF-7 cells enhanced cellular invasion in an EGFR-dependent manner, whilst loss of CD44v6 protein expression in Tam-R cells reduced invasion and proliferation and attenuated EGFR pathway signalling. Enhanced EGFR signalling has been heavily implicated in the acquisition of tamoxifen-resistance, therefore it could be hypothesised that CD44v6-mediated EGFR activation in MCF-7 cells may reduce their response to tamoxifen leading to the acquisition of resistance. Although this thesis did not reveal a role for CD44v6 in the attenuation of tamoxifen response in MCF-7

cells, these experiments were conducted over a short 5 day period due to the nature of the transient transfections. Thus, to further explore whether CD44v6 overexpression may reduce tamoxifen response by enhancing cellular invasion/proliferation through EGFR activation, future studies which involve culturing stable CD44v6-transfected MCF-7 cells in the presence of tamoxifen could be conducted. Surprisingly, loss of CD44v6 did not alter the behavioural functions of Fas-R cells, (although appeared to attenuate fulvestrant response in MCF-7 cells through an unidentified mechanism) however this endocrine resistant cell model expresses low levels of endogenous EGFR, which unlike Tam-R cells is not heavily implicated in the acquisition of fulvestrant-resistance, thus the inference would be that CD44v6 may play a more important role in cells where EGFR is co-expressed.

This was supported by data from a small exploratory clinical series which revealed that whilst high levels of CD44v6 correlated with a significantly better outcome in ER+ primary breast cancers treated with tamoxifen (potentially due to the enhancement of cellular migration observed in the experimental data), a promising separation was shown between CD44v6+ patients when subdivided with EGFR status. This data revealed that patients whose tumours co-expressed CD44v6 and EGFR (CD44v6+/EGFR+) displayed a worse outcome compared to CD44v6+/EGFR- patients. Interestingly, the cohort that associated with the worst overall outcome were patients whose tumours did not express either receptor (CD44v6-/EGFR-) and data suggested a clear clustering of CD44v6+/EGFR+ with the CD44v6- patients away from the CD44v6+/EGFR- cohort in both DFI and OS survival curves, thus suggesting that patients expressing low/negative CD44v6 levels perform badly irrespective of EGFR

status. These data suggest that other signalling pathways may drive misbehaviour of the CD44v6- cohorts (which may or may not involve interplay with EGFR) leading to worsened outcome.

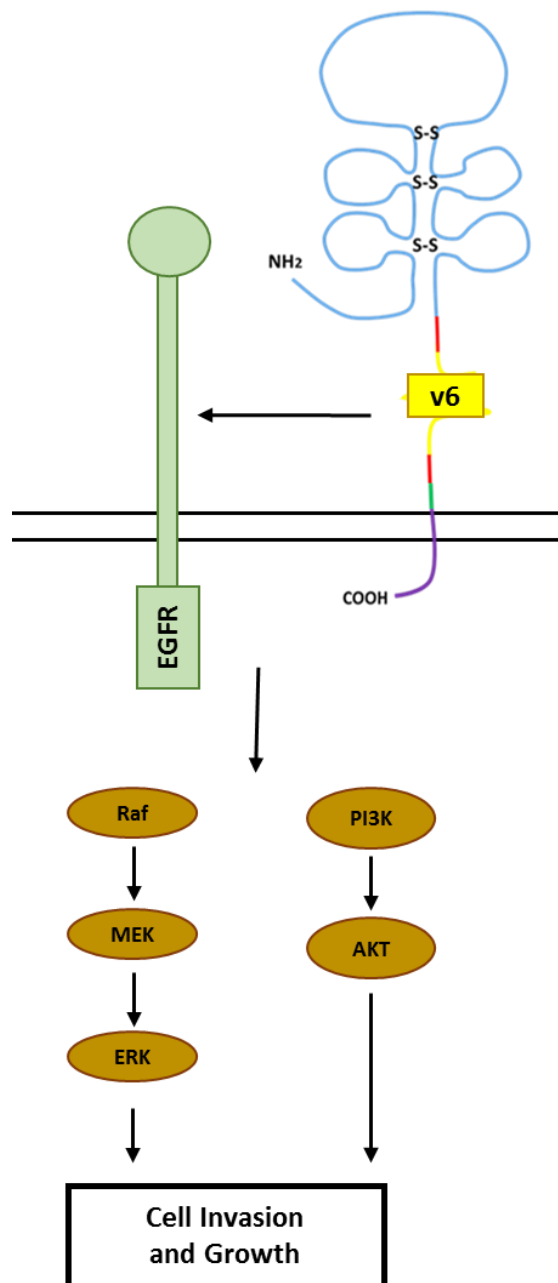


Figure 6.31. A proposed mechanism for CD44v6-mediated EGFR activation leading to enhanced cellular invasion and growth. This thesis identified that CD44v6 mediated EGFR activation led to enhanced AKT and ERK1/2 signalling and enhanced invasion and growth in Tam-R cells. Additional experimental analysis is required to determine whether a direct interaction between CD44v6 and EGFR occurs in these cells and to further elucidate the signalling mechanisms through which cellular invasion and growth is activated.

Overall, these data infer that high levels of CD44v6 expression are protective in ER+ patients treated with tamoxifen, however patients whose tumours co-express CD44v6 and EGFR could predict earlier relapse and a poorer overall outcome on tamoxifen (as seen in the experimental work with CD44v6 and EGFR interplay leading to enhanced invasion). Whilst this study remains exploratory due to low patient numbers (particularly for EGFR+ subsets, given this is a ER+ sample series) these results are in accordance with previous data from the BCMPG (Gee et al. 2012; IACR Manchester Group Abstract, personal communication) which has previously shown that CD44v6 expression strongly correlates to a better outcome in ER+ disease. Although significance was shown in both survival curves in this thesis, study numbers were too low to compare individual subgroups, therefore further studies are needed with larger TMA sections (including a greater sample number of EGFR+ patients) to validate these preliminary findings.

Whilst suppression of CD44v6 appeared to reduce endogenous invasion and HA-stimulated proliferation in Tam-R cells, a concomitant significant enhancement of cellular migration was also observed; an effect not shown upon CD44v6 overexpression in MCF-7 cells. Although the mechanism(s) through which this may occur remains undetermined and require future exploration, one hypothesis may be that different CD44v6-containing isoforms are involved in different cellular processes. Whilst only the CD44v6 isoform was overexpressed in MCF-7 cells, CD44v6 siRNA suppressed the expression of all isoforms containing the CD44v6 exon. Given that the characterisation data revealed the presence of several CD44v6-containing isoforms in Tam-R cells (Chapter 3), it may be postulated that certain isoforms e.g.

containing the variant 6 exon only, may possess greater affinity for co-receptors, e.g. EGFR, thus promoting cellular invasion, whilst others e.g. containing a combination of variant exons including variant 6, may have a prominent role in the suppression of cellular migration. These data may infer that specific CD44v6 isoforms mediate distinct behaviours in cells and may in part explain the contradictory results found between studies which have correlated enhanced CD44v6 expression with both favourable (Shah et al. 2010), unfavourable (Lian et al. 2006) or no association with clinical parameters (Morris et al. 2001; Diaz et al. 2003 Ma et al. 2005) in breast cancer.

Previous data from this study showed that CD44 global suppression in Tam-R and Fas-R cells reduced their migratory, invasive and proliferative phenotype. Given that overexpression of CD44v3/CD44v6 proteins in MCF-7 cells, and CD44v6 suppression in Tam-R cells, impaired cellular migration across these cell models, this may imply that alternative CD44 isoforms are involved in the promotion of aggressive cellular behaviours in Tam-R and Fas-R cells. Furthermore, CD44 global suppression attenuated the response of both endocrine resistant cell models to HA, thus potentially suggesting a role for CD44 proteins in HA-sensitisation. Therefore, it was hypothesised that overexpression of CD44 variants in endocrine sensitive MCF-7 cells would sensitise these cells to HA leading to enhanced cellular responses. However this was not observed in MCF-7 cells, and CD44 variant overexpression did not significantly impact HA-mediated signalling/responses. These data may potentially be explained by the lower reliance of MCF-7 cells for HA and may suggest that these cells require numerous changes in protein composition and phenotype, and not just

CD44 variant overexpression alone, to become sensitised to HA. Additionally, experimental environment may also account for the lack of response observed by MCF-7 transfected cells. Whilst both endocrine resistant cell models are maintained in experimental media (WRPMI media with charcoal-stripped serum), it was not possible to transfect MCF-7 cells in stripped serum therefore these cells were maintained in their maintenance media which contained foetal calf serum. An unquantified level of HA and additional growth factors may be present in this serum thus potentially masking the effect of additional HA stimulation in MCF-7 cells. Future experiments to determine the HA concentration required to stimulate these cells to observe behavioural outputs/stable CD44-overexpressing MCF-7 transfectants are required to assess the effect that CD44 overexpression causes upon HA sensitivity.

An additional interesting observation from this study revealed that whilst overexpression of CD44 Δ cyt proteins in MCF-7 cells led to the activation of several cell surface receptors and/or downstream signalling components (a previously unreported phenomenon), unlike their full length CD44 isoform counterparts, no significant modification of cellular behavioural processes was observed in these cells compared to the untransfected controls. One explanation for this phenomenon may be that whilst CD44 Δ cyt proteins are capable of being transported to the plasma membrane (as observed by immunoanalysis data) whereupon they activate numerous signalling components, these events may be transient due to the instability of these proteins and thus not sufficient to stimulate prolonged cellular signalling leading to functional outputs. This is supported by observations from numerous studies exploring the role of CD44 cytoplasmic tail truncated mutants

(Isacke 1994; Perschl et al. 1995; Jiang et al. 2002). Indeed, Neame and Isacke et al. 1993 showed that removal of the CD44 cytoplasmic tail in fibroblast cells does not prevent presentation of this protein at the plasma membrane however alters its localisation to the apical, rather than the baso-lateral, cell surface. In support of this, Sheik and Isacke 1996 identified a dihydrophobic leucine331/valine332 motif in the CD44 cytoplasmic tail required for the delivery of CD44 to the lateral plasma membrane of polarised epithelial MDCK cells. Furthermore, this study revealed a population of CD44 cytoplasmic tail mutants in intracellular vesicles suggesting that loss of cytoplasmic tail region may reduce protein stability leading to enhanced endocytosis and subsequent degradation by lysosomes and Wollner et al. 1992 reported that tailless CD44 mutants exhibit a 2 – 4 reduced stability compared to full length isoforms. It has also been suggested that removal of the CD44 cytoplasmic tail allows easier entry into the coated pit thus leading to enhanced internalisation and degradation of this molecule (Pelchen-Matthews et al. 1991; Neame and Isacke 1993).

Additionally, the cytoplasmic tail domain of CD44 is crucial to its cellular functions. This domain contains numerous motifs for cytoskeletal binding proteins, sites for post-translational modifications required for cellular motility events (Bretscher et al. 1997; Bourguignon et al. 1991; Legg et al. 2002; Thankamony et al. 2006; Babina et al. 2014), binding sites for intracellular signalling components (Bourguignon et al. 2003; Jia-Lin et al. 2008) and cleavage sites for translocation of the intracellular domain to the nucleus for the regulation of several genes (Okamoto et al. 2001; Murakami et al. 2003). Therefore, loss of the cytoplasmic domain may attenuate

numerous cellular processes particularly involving cellular motility and adhesion through loss of cross-linking ability with the cytoskeleton and binding to cytoskeletal/downstream effector molecules. Taken together, these observations may account for the increased intracellular localisation of CD44v3 Δ cyt and CD44v6 Δ cyt proteins observed in MCF-7 cells upon transfection and support an explanation as to why these isoforms were able to enhance cellular signalling but did not modify cellular behaviours in these cells. However future studies to further elucidate the mechanisms through which these cytoplasmic tail truncations may mediate cellular signalling, but not functional outputs, are required.

Given that the CD44 Δ cyt plasmid DNA constructs were provided by Dr Ursula Gunthert (Basel University, Switzerland) to use as transfection controls, however led to enhanced cellular signalling, experiments were undertaken at the end of this project to create an empty vector plasmid DNA backbone construct (without the inserted CD44 gene sequence) to use as an alternative transfection control. Given that the CD44 constructs contain a GFP-tag fused to their carboxy-terminus end, it was also investigated whether the presence of this tag altered cellular behaviours through transfection of MCF-7 cells with a pEGFP-N1 plasmid vector containing the GFP-tag construct only. These preliminary results (shown in Appendix S) suggest that the plasmid vector and GFP-tag do not substantially alter the behaviour of MCF-7 cells thus supporting that the effects observed by CD44v3/CD44v6 transfection arise from the activities of these proteins alone.

Summary 6.3.1

In this chapter, an important role was shown for CD44v6 proteins in EGFR-mediated cellular invasion in Tam-R cells which was supported by exploratory clinical analysis showing a trend for worsened outcome in ER+ breast cancer patients co-expressing high levels of CD44v6 and EGFR treated with tamoxifen. These preliminary findings require further exploration however suggest that co-expression of CD44v6 and EGFR may predict earlier relapse in a sub-cohort of ER+ breast cancer patients and could present as candidates for therapeutic targetting to delay resistance onset. Interestingly, CD44v6 suppression in Fas-R cells did not significantly alter cellular behaviours, and exploratory clinical analysis revealed that high levels of CD44v6 expression alone associated with a trend for better patient outcome in ER+ breast cancer patients treated with tamoxifen. These findings may infer that the contribution of CD44v6 to resistance is likely to depend upon other contextual and microenvironmental factors, e.g. the presence of co-receptor proteins, which may be specific to each resistant state.

7. General Discussion

Endocrine resistance is a major hurdle for the successful treatment of breast cancer therefore gaining knowledge of the molecular mechanisms that underlie this process may offer the opportunity for the identification of novel therapeutic targets through which resistance might be delayed or circumvented. Moreover, given that the literature supports that resistance is accompanied by an aggressive cell phenotype, targetting resistance mechanisms may also have the potential to suppress such cell behaviours. In light of a previous study by the BCMPG (Hiscox et al. 2012) which reported upregulation of total CD44 expression in a model of ER+ breast cancer-derived tamoxifen resistance where it associated with an enhanced migratory phenotype, part of the aims of this thesis were to extend these investigations into a further model of resistance, to the endocrine agent fulvestrant, in order to determine whether CD44 upregulation represented a generic feature of acquired resistance.

Furthermore, one aspect of CD44 which makes it difficult to study and undoubtedly contributes to variability between published studies is the extensive alternative splicing attributed to this molecule. Whilst CD44 is often found to become overexpressed in invasive breast cancer, CD44 isoforms have been shown to mediate both pro- and anti-tumoural signalling pathways in vitro (Cheng et al. 2006; Afify et al. 2008; Bourguignon et al. 2010; Babina et al. 2014) and have been correlated with both favourable and unfavourable patient outcome in clinical breast cancer (Morris et al. 2001; Rys et al. 2003; Ma et al. 2005; Lian et al. 2006; Afify et al. 2009). Therefore the main aims of this thesis were to explore CD44 isoform contribution to

tamoxifen- and fulvestrant- resistance and to investigate the hypothesis that specific CD44 isoforms promote an aggressive phenotype in these cells.

The findings from this thesis confirmed results from Hiscox et al. 2012 and showed that total CD44 expression was upregulated in Tam-R cells compared to their parental endocrine sensitive MCF-7 cells. Importantly, this thesis reported the novel finding that CD44 expression also becomes upregulated in the model of fulvestrant-resistance and further identified that a different expression profile of CD44 isoforms exists between resistant cell models thus suggesting that there is not a generic cohort of CD44 isoforms that become upregulated in resistance. Indeed, upregulation of CD44v3-containing proteins was specific to tamoxifen-resistance whilst CD44v10-containing proteins were upregulated only in Fas-R cells. Although CD44v6 proteins were upregulated in both models of resistance, Western blotting analysis revealed a differential expression profile of CD44v6 splice isoforms between these cell models; however the composition of these isoforms was not determined.

These findings may suggest that upregulation of particular CD44 isoforms may be specific to each resistant state. In support of this, Olsson et al. 2011 reported that individual CD44 isoform expression is associated with specific breast cancer characteristics and molecular subtypes and contributes to distinct oncogenic signalling pathways. For example, this study examined 187 primary breast tumours and 13 breast cancer cell lines and revealed that CD44v2-v10 and CD44v3-v10 isoforms correlated with luminal A breast cancer, CD44v8-v10 isoforms were predominantly expressed in basal-like breast cancers, and CD44 Std was associated with HER2+ breast cancer. Furthermore, this group showed a correlation between

CD44 isoform expression and different clinical biomarkers in tumours. The CD44v2/v3-v10 isoforms correlated with positive steroid hormone receptor status, CD44v8-v10 was strongly correlated with EGFR positive/HER2 low/negative status and CD44 Std associated with HER2 expression. This study concluded that CD44 isoforms may be part of a programme that drives development of distinct molecular subtypes in breast cancers or may be a consequence of this process.

Given that only two models of acquired endocrine resistance were examined in this thesis, it is difficult to draw firm conclusions between the expression of individual CD44 isoforms and specific resistant states, however future studies using alternative models of acquired resistance may confirm these observations. Interestingly, the findings from Olsson et al. 2011 suggested that CD44 expression may be linked to the ER, with the greatest total level of CD44 isoform expression found in luminal A (ER+) breast cancers. Conversely, other groups have reported that CD44 expression is inversely proportional to ER expression and associated with the most aggressive triple negative subtype of breast cancer (Klingbeil et al. 2010; Montgomery et al. 2012). In this thesis, the greatest level of total CD44 expression was shown in the ER-Fas-R cells, however CD44 was also elevated in ER+ Tam-R cells suggesting that an absolute relationship between CD44 and ER expression may not necessarily exist.

To determine whether a relationship exists between CD44 and the ER in the resistant cell models, the effects of short term endocrine treatment upon CD44 expression was investigated (Appendix T). The data revealed that MCF-7 cells treated with the ER downregulator, fulvestrant, abrogated CD44 expression, whilst tamoxifen and oestradiol treatment (partial agonist and agonist of the ER respectively) enhanced

CD44 expression between 3 – 52 day treatments, compared to the untreated control cells. This data suggested a potential role for the ER within the regulation of CD44 expression and further investigation by the Jason Carroll research group (Cancer Research UK, Cambridge Institute, personal communication) revealed that whilst the presence of an oestrogen receptor element (ERE) could not be found within the first 500 bp of the CD44 gene promoter, sites for p300 and CPB binding proteins (known to bind and regulate ER activity) were located in this region. Therefore these data may infer a potential role for the indirect regulation of CD44 expression by the ER, which may provide an explanation for the modulation of CD44 expression shown within MCF-7 cells treated with endocrine agents that differentially alter ER expression. However, whilst the loss of ER expression that occurs upon fulvestrant treatment in MCF-7 cells abrogated CD44 expression in early endocrine treatment, CD44 becomes upregulated upon acquisition of fulvestrant-resistance, thus suggesting that alternative signalling pathways may be activated which upregulate CD44 isoform expression at a later stage of fulvestrant treatment in these cells.

The data in this thesis showed that CD44 variant expression is upregulated in endocrine resistance, however the mechanisms which regulate CD44 alternative splicing are not yet fully understood. CD44 alternative splicing has been shown to occur in response to specific stimuli, such as oxidative stress (Takeo et al. 2009) and epigenetic changes on histones (Batsche et al. 2006; Ameyar-Zazou et al. 2012; Cappellari et al. 2013), however most often results from signalling transduction pathways, particularly MAPK activation (Matter et al. 2002; Cheng and Sharp 2006) and post-translational modifications that influence components of the alternative

splicing machinery, such as splicing factors (Weg-Remers et al. 2001; Cheng et al. 2006). Ras/MAPK signalling has been shown to phosphorylate and subsequently activate the splicing factors, Sam68 and SRm160, which regulate the inclusion of CD44 variant exons into mRNA transcripts (Weg-Remers et al. 2001; Matter et al. 2002; Cheng and Sharp 2006), however the signalling pathways between Ras/MAPK activation and stimulation of alternative splicing are not well defined. Cheng et al. 2006 revealed a positive feedback loop in HeLa cells which coupled Ras/MAPK signalling and CD44 alternative splicing. This group revealed that RTK signalling stimulated CD44 splicing (by induction of Ras/MAPK signalling) and in turn, the specific upregulation of the CD44v6 isoform promoted further sustained Ras/MAPK activation leading to cell cycle progression. The inclusion of variant exons into the CD44 mRNA transcript has additionally been shown to be mediated by the epithelial cell type specific splicing regulator proteins (ESPR1 and ESRP2), which also connects growth factor signalling and CD44 splicing (Warzecha et al. 2009; Brown et al. 2011). Therefore it may be hypothesised that upregulation of specific growth factor receptor signalling pathways that activate these splicing factors and lead to the subsequent production of CD44 variant isoforms, may be an important factor in the acquisition of endocrine resistance. Whilst changes in the gene expression of splicing factors across the cell models was not investigated in this thesis, enhanced RTK signalling occurs in response to oestrogen withdrawal (endocrine treatment) (Normanno et al. 2005) and has been shown to be involved within the acquisition of endocrine resistance in breast cancer causing cells to change from an oestrogen-dependent phenotype (endocrine responsive) to a non-responding phenotype and

eventually to oestrogen independence (Knowlden et al. 2003; Britton et al. 2006; Hiscox et al. 2006). Elevated ErbB receptor signalling has been shown to induce downstream signalling responses, including Ras/MAPK activation, which may lead to enhanced CD44 splicing in these cells (Kurokawa et al. 2000; Weigelt et al. 2010). Given that this thesis identified a role for CD44-mediated ErbB activation towards an aggressive phenotype, it may be postulated that this mechanism could lead to the enhanced aggressive phenotype in cells which accompanies endocrine resistance.

Indeed, it has been reported that tumours expressing CD44 variant isoforms are more aggressive than tumours expressing the CD44 standard isoform only, and numerous reports document upregulation of CD44 splice variants in aggressive carcinoma tissues compared to their normal tissues (Lui et al. 2005; Lian et al. 2006; Wang et al. 2007; Ni et al. 2014). Yae et al. 2012 showed that inoculation of the CD44 variant (v8-v10) isoform-expressing subpopulation of mouse T41 breast cancer cells into severely immunocompromised mice conferred metastatic potential and led to the formation of lung metastases which was accompanied by an expansion of stem-like cancer cells, an observation that was not seen in the CD44 variant-negative (CD44 Std) subpopulation. Further, Banky et al. 2012 reported that CD44 proteins containing variant exons 3 and 6 showed dominant expression compared to other CD44 variants across colorectal cancer cell lines and suggested that in a minority of tumour subclones these variants may act as 'metastasis genes' and drivers of the metastatic phenotype in these cells. In accordance with these findings, data from this thesis showed that the upregulation of CD44 variant isoforms in resistant cell models associated with an increase in their endogenous aggressive cellular behaviours. For

example, endocrine resistant cells showed a significantly enhanced invasive (Tam-R and Fas-R cells) and migratory and proliferative (Fas-R cells) capacity compared to their endocrine sensitive MCF-7 counterpart. However, whilst CD44 expression was greatest in Fas-R cells, this study suggested an importance for CD44 proteins in both models of endocrine resistance as global knockdown of CD44 significantly reduced the migratory, invasive and proliferative capacity of Tam-R and Fas-R cells.

As well as contributing to the endogenous aggressive phenotype of the resistant cell models, CD44 upregulation also led to the sensitisation of these cells to their principle ligand, hyaluronan (HA). The data revealed increased cellular migration (Tam-R and Fas-R cells), invasion and proliferation (Fas-R cells) in response to HA stimulation which was attenuated upon CD44 suppression. Interestingly, this thesis revealed that the mechanisms through which HA stimulation enhances the aggressive behaviour of Tam-R and Fas-R cells occurs through different pathways and thus may be dependent upon the composition of proteins in cells. For example, HA stimulation appeared to enhance cellular migration and invasion in Tam-R cells in an ErbB receptor dependent manner which corroborates from previous data from the BCMPG (Hiscox et al. 2012) and with other studies which have shown a role for CD44 activation of ErbB receptors towards the induction of the metastatic cascade (Bourguignon et al. 1997; Kim et al. 2008; Palyi-Krekk et al. 2008; Bao et al. 2011). However, the mechanisms through which HA stimulated the CD44-mediated functions in Fas-R cells remains elusive but this thesis does not heavily implicate the RTKs EGFR, HER2 or c-Met in this process. These data suggest an importance for the bioavailability of co-receptor proteins in the determination of CD44-mediated

functions in cells and suggests that the presence of HA is likely to promote adverse behaviours in breast tumours which highly express CD44 proteins. These findings may have important implications with regards to the augmentation of breast tumour sensitivity to HA which is often found to be abundantly expressed in the microenvironment of breast carcinomas (Auvinen et al. 2000; Auvinen et al. 2014). Indeed, both HA and CD44 have been shown to be highly expressed within the peritumour stroma and tumour mass, respectively, in breast cancer where they are associated with tumour metastasis, increased relapse and poor patient prognosis (Udabage et al. 2005a; Auvinen et al. 2013).

These data along with numerous other studies suggest that breast cancer cells which co-express high levels of HA and CD44 exhibit an enhanced susceptibility for metastasis and may predict tumour recurrence and therapeutic resistance. Whilst at present no current therapy is available which targets CD44 proteins in breast cancer, in recent years a large amount of interest has surrounded the exploitation of the HA-binding properties of CD44 a mechanism for targetting drugs to tumour cells to reduce off-target effects of chemotherapeutic agents (Hyun-Jong et al. 2011; Lui et al. 2011; Young-II et al. 2012). Yang et al. 2013 revealed that treatment of the highly CD44-expressing breast cancer cell lines, BT549 and MDA-MB-231, with oligosaccharide HA nanoparticles conjugated with the chemotherapeutic drug, paclitaxel, diminished their endogenous protective HA coating, enhanced their sensitivity to paclitaxel and demonstrated growth inhibition in a breast cancer xenograft mouse model. Furthermore, Ganesh et al. 2013 revealed the use of HA as a vehicle for the delivery of RNA interference therapies into highly CD44-expressing

tumours. This group synthesised and evaluated a series of HA-based nanosystems to stably encapsulate and deliver siRNAs to a range of highly CD44-expressing human cancer cell lines, including the breast cancer cell line, MDA-MB-486. The results showed that several of the engineered HA-based nanosystems were effective in entering the cell lines leading to gene silencing activity, and also showed inhibition in models of in vivo lung cancer with and without resistance to chemotherapeutic drugs. Whilst these approaches may represent therapeutic value, a large amount of work is required before they can become a viable clinical treatment option.

The overall aims of this thesis were to explore whether specific CD44 isoforms promote adverse cellular behaviours in endocrine resistance and the main findings of this study may go some way to explain the contradictory results found in CD44 research. This thesis identified that CD44v3 overexpression in MCF-7 cells enhanced HA-induced invasion and suppressed cellular migration, however these results could not be validated in endocrine resistant models due to unavailability of CD44v3 siRNA and lack of clinical data. Whilst this thesis identified that CD44v6 was upregulated in both endocrine resistant cell models, no consistent relationship was observed between CD44v6 expression and increased aggressive cell behaviour. Indeed, despite Fas-R cells exhibiting the highest level of CD44v6 expression compared to Tam-R cells, CD44v6 siRNA knockdown modulated the activity of Tam-R cells but did not significantly alter Fas-R cell behaviour. These data suggest that it is likely that the contribution of CD44v6 to resistance occurs amongst other contextual factors and microenvironmental cues which may be specific to each resistant state. For example, CD44v6 enhanced invasion in Tam-R cells in an EGFR-dependent manner, however

did not significantly alter the behaviour of Fas-R cells which exhibit endogenously low levels of EGFR. This may infer a reliance on specific CD44 isoforms for the expression of alternative co-receptors, e.g. EGFR, to mediate an aggressive phenotype in these cells. Indeed, this is further observed in the exploratory immunohistochemical study shown in this thesis, where high CD44v6 expression associated with a trend for better outcome in ER+ breast cancer patients treated with tamoxifen which may relate to its role in the suppression of cellular migration as observed in the experimental data. However, this clinical series showed a trend for worsened outcome in patients whose tumours co-express high levels of CD44v6 and EGFR compared to the CD44v6+/EGFR- sub-cohort of tumours. These preliminary findings require further exploration however may implicate CD44v6 as a marker for better outcome in ER+ patients on tamoxifen treatment, whilst co-expression of CD44v6 and EGFR may represent a sub-cohort of patients which may respond worse to this treatment.

Whilst this thesis is the first to investigate CD44 isoform expression in ER+ breast cancer endocrine resistance, other studies have revealed a role for CD44v6 and EGFR, along with a panel of several other proteins including c-Met, as markers of highly invasive breast carcinomas where their expression has been shown to predict poor clinical outcome and may identify patient cohorts that require more aggressive treatment strategies (Charpin et al. 2009a; Charpin et al. 2009b). Furthermore, Vermeulen et al. 2012 screened tissue microarrays containing 483 cases of highly invasive breast carcinomas to identify the minimal number of targetted antibody probes required for the highest possible detection rate. This group revealed that whilst no single membrane marker is likely to detect all breast cancers, 80 % of

samples expressed at least one of a panel of 5 markers including CD44v6, EGFR, HER2, IGFR1 and GLUT1; thus concluding that at least 5 probes may be required for a high detection rate of breast cancers in vivo by molecular imaging. These studies along with others have revealed that CD44v6 and EGFR (along with several other receptors) are established markers of highly invasive/basal breast carcinomas that may be used to enhance detection rates and better predict disease outcome in patients. Additional studies have also identified these receptors as prognostic markers in alternative carcinomas, particularly colorectal cancer (Elliot et al. 2014; Zhao et al. 2015). For example, Garouniatis et al. 2013 revealed that CD44v6, EGFR, c-Met and FAK were expressed in 183 cases of colorectal carcinoma and all correlated with cancer invasiveness and progression. Specifically, CD44v6 and FAK were demonstrated to be independent predictors of poor survival. This group further showed that aberrant co-expression of all receptor combinations remained significant thus also suggesting the occurrence of receptor cross-talk action. Collectively, these data revealed a predictive role for these receptors in colorectal carcinoma and highlighted their use as biomarkers for determining cohorts of patients which may respond worse to treatment and require more aggressive strategies.

7.1 Future Work

Given that global CD44 siRNA knockdown studies in this thesis reduced the migratory, invasive and proliferative capacity of Tam-R and Fas-R cells, these data may implicate additional CD44 isoforms within specific roles in endocrine resistance. Therefore, future work to explore alternative isoforms e.g. CD44 Std and CD44v10

proteins, and validate the role of CD44v3 in endocrine resistance, could be considered in these MCF-7 derived acquired resistant cell models.

Whilst this study revealed that CD44 variant isoform expression becomes upregulated in acquired endocrine resistant cell models which associated with an increase in their aggressive phenotype, this thesis focused upon early resistance (1.5 – 2 years) in MCF-7 derived tamoxifen- and fulvestrant- resistant cell models. To further explore the contribution of CD44 proteins to endocrine resistance, evaluation in the long term setting is required. During this thesis, the BCMPG developed MCF-7 cell-derived models of late (3 years) tamoxifen- and fulvestrant- resistance. Whilst time did not allow for the study of CD44 isoform expression and function in these cell models in this thesis, unpublished and ongoing work by the BCMPG has shown that although CD44 isoform expression (including CD44 Std, CD44v3 and CD44v6) is elevated in the models of late tamoxifen- and fulvestrant- resistant cells compared to their endocrine sensitive counterpart, this level of expression is lower than that found in early resistance. These studies further revealed that despite a reduction in CD44 expression, these models of late resistance still show a high level of basal migration (no other function was tested), particularly revealing an increase in migration in late tamoxifen resistance. Therefore future work is required to further investigate the roles of CD44 isoforms in late endocrine resistance in MCF-7 cells including the analysis of additional functional roles (invasion, proliferation) and interactions with RTKs and HA in these cells MCF-7 derived cell models to determine their roles in early versus late endocrine resistance.

In this thesis the MCF-7 cell line was used as the only model of acquired endocrine resistance in ER+ (HER2-) breast cancer as, at the beginning of the project, this was the only available cell model for which to study acquired endocrine resistance and MCF-7 cells are used as a 'standard' for ER+ breast cancer research ubiquitously around the world. Since the start of this project, the BCMPG have subsequently developed several other models of acquired tamoxifen- and fulvestrant- resistance in the ER+/HER2- breast cancer cell line, T47D, and in the ER+/HER2+ cell lines, BT474 and MDA-MB-361. The duration of this thesis did not allow time to study these additional cell models, therefore future work to investigate CD44 isoform expression, in particular the exploration of CD44v6 and EGFR and their contribution to the aggressive phenotype, in these models may validate the findings of this thesis.

Given that RTK signalling is heavily implicated in the acquisition of endocrine resistance, and is known to activate Ras/MAPK signalling which may influence alternative splicing of CD44 isoforms. Future work to investigate the mechanisms which regulate the splicing of CD44 variant isoforms leading to their upregulated expression in endocrine resistance may offer therapeutic value.

7.2 Conclusions

This thesis revealed upregulated CD44 expression in models of endocrine resistance which associated with an increase in their aggressive phenotype and suggested that CD44 variant isoforms may associate with specific resistant states. The main aims of this thesis were to explore the hypothesis that specific CD44 variant isoforms promote an aggressive phenotype in endocrine resistance. The experimental and

clinical data in this thesis points to the importance of cellular context for CD44 function. Whilst CD44v6 expression correlates with a better clinical outcome in ER+ breast cancer patients treated with tamoxifen, co-expression of CD44v6 and EGFR may provide a context where CD44v6 functions to enhance cellular invasion/growth leading to a worsened patient outcome. Whilst this finding requires validation from future work in a larger clinical series, CD44v6 and EGFR may have potential therapeutic value to predict a cohort of patients in ER+ breast cancer which relapse earlier on tamoxifen and may thus require more aggressive treatment strategies. Taken together, this thesis highlights that a clear understanding of the composition of CD44 splice variants and bioavailability of specific co-receptor proteins/ligands is of crucial importance towards understanding the role of CD44 in endocrine resistance and correlating this with clinical outcome. Whilst a predictive role for CD44 proteins may be given to specific CD44 isoforms alone or in combinations with other proteins, the complex dual nature of these proteins as shown in this thesis may go some way to explain the contradictory results surrounding CD44 research and provide an explanation as to why at present there are no definitive correlations between CD44 expression and clinical parameters in breast cancer.

8. References

- Aaltomaa, S. et al. 2001. Expression and prognostic value of CD44 Std and variant v3 and v6 isoforms in prostate cancer. *European Urology*. 39 (2) pp. 138 – 144.
- Abd El-Rehim, D. M. et al. 2005. High-throughput protein expression analysis using tissue microarray technology of a large well-characterised series identifies biologically distinct classes of breast carcinomas confirming recent cDNA expression analyses. *International Journal of Cancer*. 116 pp. 340 – 350.
- Abdulkareem, I and Zurmi, I. 2012. Review of hormonal treatment of breast cancer. *Nigerian Journal of Clinical Practice*. 15 (1) pp. 9 – 14. 180 pp. 53 – 66.
- Abraham, I. M. et al. 2004. Critical in vivo roles for classical estrogen receptors in rapid estrogen actions on intracellular signalling in mouse brain. *Endocrinology*. 145 (7) pp. 3055 – 3061.
- Adamia et al. 2005. Potential impact of a single nucleotide polymorphism in the hyaluronan synthase 1 gene in Waldenstrom's macroglobulinemia. *Clinical Lymphoma*. 5 (4) pp. 253 – 256.
- Adams, B. D. 2007. The micro-ribonucleic acid (miRNA) miR-20b targets the human estrogen receptor α (ER α) and represses ER α messenger RNA and protein expression in breast cancer cell lines. *Molecular Endocrinology*. 21 (5) pp. 1132 – 1147.
- Afify, A. et al. 2009. Role of CD44s and CD44v6 in human breast cell adhesion, migration and invasion. *Experimental and Molecular Pathobiology*. 86 pp. 95 – 100.
- Al-Hajj, M. et al. 2003. Prospective identification of tumourigenic breast cancer cells. *PNAS*. 100 (7) pp. 3983 – 3988.
- Alexaki, V. I. et al. 2004. Estrogen exerts neuroprotective effects via membrane estrogen receptors and rapid AKT/NOS action. *FASEB Journal*. 18 pp. 1594 – 1596.
- Alexander, F. E. and Roberts, M. M. 1987. The menopause and breast cancer. *Journal of Epidemiology, Communications and Health*. 41 pp. 94 – 100.
- Al-Magharbi, J. et al. 2012. Decreased immunoeexpression of standard form of CD44 is an independent favourable predictor of nodal metastasis in colorectal cancer. *Anticancer Research*. 32 (8) pp. 3455 – 3461.
- Ameyar-Zazou, M. et al. 2012. Argonaute proteins couple chromatin splicing to alternative splicing. *Nature Structural and Molecular Biology*. 19 (10) pp. 998 – 1004.
- Anderson, W. F. et al. 2002. Estrogen receptor breast cancer phenotypes in the surveillance, epidemiology and end results database. *Breast Cancer Research Treatment*. 76 pp. 27 – 36.
- Anttila, M. A. et al. 2000. High levels of stromal HA predict poor clinical outcome in epithelial ovarian cancer. *Cancer Research*. 60 (1) pp. 150 – 155.

- Arch, R. et al. 1992. Participation in normal immune responses of a metastasis inducing splice variant of CD44. *Science*. 257 pp. 682 – 685.
- Aruffo, A. et al. 1990. CD44 is the principle cell surface receptor for hyaluronate. *Cell*. 61 (7) pp. 1303 – 1313.
- Arpino, G. et al. 2008. Crosstalk between the estrogen receptor and the HER tyrosine kinase receptor family: molecular mechanisms and clinical implications for endocrine therapy resistance. *Endocrinology Reviews*. 29 (2) pp. 217 – 233.
- Assmann, V. et al. 1998. The human hyaluronan receptor RHAMM is expressed as an intracellular protein in breast cancer cells. *Journal of Cell Science*. 111 pp. 1685 – 1694.
- Assmann, V. et al. 1999. The intracellular hyaluronan receptor RHAMM/IHABP interacts with microtubules and actin filaments. *Journal of Cell Science*. 112 (22) pp. 3943 – 3954.
- Auvinen, P. et al. 2000. Hylauronan in peritumoral stroma and malignant cells associates with breast cancer spreading and predicts survival. 156 (2) pp. 529 – 536.
- Auvinen, P. et al. 2005. Expression of CD44s, CD44v3 and CD44v6 in benign and malignant breast lesions: correlation and colocalisation with hyaluronan. *Histopathology*. 47 pp. 420 - 428.
- Auvinen, P. et al. 2013. Increased HA content and stromal cell CD44 associated with HER2 positivity and poor prognosis in human breast cancer. *International Journal of Cancer*. 132 (3) pp. 531 – 539.
- Auvinen, P. et al. 2014. HA synthases (HAS1 – 3) in stromal and malignant cells correlate with breast cancer grade and predict patient survival. *Breast cancer research treatment*. 143 pp. 277 – 286.
- Babina, I.S. et al. 2014. A novel mechanism for regulating breast cancer cell migration via palmitoylation-dependent alternations in the lipid raft affiliation of CD44. *Breast Cancer Research*. 16 (1) pp. 3614.
- Baek, J. et al. 2011. Serum CD44 levels and overall survival in patients with HER2-positive breast cancer. *Breast Cancer Research Treatment*. 130 pp. 1029 – 1036.
- Balkwill, F.R. et al 2012. The tumour microenvironment at a glance. *Journal of Cell Science*. 125 pp. 5591 – 5596.
- Banjeri, S. et al. 1998. Characterisation of the functional hyaluronan binding domain from the human CD44 molecule expressed in Escherichia Coli. *Protein Expression Purification*. 14 pp. 371 – 381.
- Banjeri, S. et al. 1999. LYVE-1, A new homologue of the CD44 glycoprotein is a lymph-specific receptor for hyaluronan. *Journal of Cell Biology*. 144 (4) pp. 789 – 801.
- Banky, B. et al. 2012. Characteristics of CD44 alternative splicing pattern in the course of colorectal adenocarcinoma progression. *Molecular Cancer*. 11 (83) pp. 1 – 15.

- Bao, W. et al. 2011. HER2 interacts with CD44 to upregulate CXCR4 via epigenetic silencing of microRNA-130 in gastric cancer cells. *Gastroenterology*. 141 (6) pp. 2076 – 2088.
- Bao, P. P. et al. 2012. Fruit, vegetable and animal food intake and breast cancer risk by hormone receptor status. *Nutrition and Cancer*. 64 (6) pp. 806 – 819.
- Bartolazzi, A. 1994. Interaction between CD44 and hyaluronan is directly implicated in the regulation of tumour development. *Journal Experimental Medicine*. 180 (1) pp. 53 – 66.
- Batsche, E. et al. 2006. The human SWI/SNF subunit Brm is a regulator of alternative splicing. *Nature*. 13 (1) pp. 22 – 29.
- Baum, M. et al. 2003. Anastrozole alone or in combination with tamoxifen versus tamoxifen alone for adjuvant treatment of postmenopausal women with early stage breast cancer: results of the ATAC (Arimidex, Tamoxifen Alone or in Combination) trial efficiency and safety update analyses. *Cancer*. 98 (9) pp. 1802 – 1810.
- Beech, D. J. et al. 2002. Expression of PH-20 in normal and neoplastic breast tissue. *Journal of Surgical Research*. 103 (2) pp. 203 – 207.
- Bennet, K. L. et al. 1995. CD44 isoforms containing exon V3 are responsible for the presentation of heparin-binding growth factor. *Journal of Cell Biology*. 128 (4) pp. 687 – 698.
- Berg, J. et al. 1989. DNA binding specificity of steroid receptors. *Cell*. 57 pp. 1065 – 1068.
- Bergman, L. et al. 2000. Risk and prognosis of endometrial cancer after tamoxifen for breast cancer. Comprehensive Cancer Centres' ALERT group. Assessment of liver and endometrial cancer risk following tamoxifen. *Lancet*. 356 pp. 881 – 7.
- Berner, H. S. et al. 2003. Clinicopathological associations of CD44 mRNA and protein expression in primary breast carcinomas. *Histopathology*. 42. pp. 546 – 54.
- Bernstein, L. et al. 2003. Ethnicity-related variation in breast cancer risk factors. *Cancer*. 97 pp. 222 – 229.
- Bertrand, P. et al. 1997. Increased hyaluronidase levels in breast tumour metastasis. *International Journal of Cancer*. 73 (3) pp. 327 – 331.
- Berry, J. 2005. Are all aromatase inhibitors the same? A review of controlled clinical trials in breast cancer. *Clinical Therapeutics*. 27 (11) pp. 1671 – 1683.
- Bono, P. et al. 2001. Layalin, a novel integral membrane protein, is a hyaluronate receptor. *Molecular Biology of the Cell*. 12 pp. 891 – 900.
- Bono, P. et al. 2004. High LYVE-1-positive lymphatic vessel numbers are associated with poor outcome in breast cancer. *Clinical Cancer Research*. 10 (7144).
- Bono, P. et al. 2005. Layalin, a cell surface hyaluronan receptors interacts with merlin and radixin. *Experimental Cell Research*. 308 pp. 177 – 187.

- Bosworth, B. et al. 1991. Sequence of the bovine CD44 cDNA: comparison with human and mouse sequences. *Molecular Immunology*. 28 pp. 1131 – 1135.
- Bourguignon, L. Y. et al. 1986. A lymphoma plasma-membrane-associated protein with ankyrin-like properties. *Journal of Cell Biology*. 102 pp. 2115 – 2124.
- Bourguignon, L. Y. et al. 1991. Acylation of the lymphoma transmembrane glycoprotein, GP85, may be required for GP85-ankyrin interaction. *Journal of Cell Biology*. 266 pp. 11761 – 11765.
- Bourguignon, L. Y. et al. 1992. A CD44-like endothelial cell transmembrane glycoprotein (GP116) interacts with extracellular matrix and ankyrin. *Molecular and Cellular Biology*. 12 (10) pp. 4464 – 4471.
- Bourguignon, L. Y. et al. 1993. Hyaluronic acid-induced lymphocyte signal transduction and HA receptor (GP85/CD44)-cytoskeleton interaction. *Journal of Immunology*. 151 (12) pp. 6634 – 6644.
- Bourguignon, L. Y. et al. 1997. CD44 and the oncogene product p185HER2 promotes human ovarian tumour cell activation. *Journal of Biological Chemistry*. 272 (44) pp. 27913 – 27918.
- Bourguignon, L. Y. et al. 1998. CD44v(3, 8-10) is involved in cytoskeleton-mediated tumour cell migration and matrix metalloproteinase (MMP-9) association in metastatic breast cancer cells. *Journal of Cell Physiology*. 176 pp. 206 – 215.
- Bourguignon, L. Y. et al. 1999. Rho-kinase (ROK) promotes CD44v(3,8-10) ankyrin interaction and tumour cell migration in metastatic breast cancer cells. *Cell motility and the cytoskeleton*. 43 (4) pp. 269 – 287.
- Bourguignon, L. Y. et al. 2001. CD44 interaction with c-src kinase promotes cortactin-mediated cytoskeletal function and hyaluronan acid dependent ovarian tumour cell migration. *Journal of Cell Biology*. 276 (10) pp. 7327 – 7336.
- Bourguignon, L. Y. et al. 2002. Hyaluronan promotes signalling interaction between CD44 and the transforming growth factor β receptor I in metastatic breast tumor Cells. *The Journal of Biological Chemistry*. 277 (42) pp. 39703 – 39712.
- Bourguignon, L. Y. et al. 2003. HA-mediated CD44 interaction with RhoGEF and Rho kinase promotes Grb2-associated Binder-1-phosphorylation and phosphoinositide-3-K signalling leading to cytokine (macrophage-colony-stimulating factor). *The Journal of Biological Chemistry*. 278 pp. 29420 – 29434.
- Bourguignon, L. Y. et al. 2004. CD44 interaction with Na⁺H⁺ exchanger NHE1 creates acidic microenvironments leading to hyaluronidase-2 and cathepsin B activation and breast tumour cell invasion. *Journal of Biological Chemistry*. 279 (26) pp. 26991 – 27007.
- Bourguignon, L. Y. et al. 2006. Hyaluronan-CD44 interaction with leukemia-associated RhoGEF and epidermal growth factor receptor promotes Rho/Ras co-activation. Phospholipase C ϵ -Ca²⁺ signalling, and cytoskeleton modification in head

and neck squamous cell carcinoma cells. *Journal of Biological Chemistry*. 281 (20) pp. 14026 – 14040.

Bourguignon, L. Y. et al. 2008. Hyaluronan-CD44 interaction activates stem cell marker Nanog, Stat-3-mediated MDR1 gene expression, and ankyrin-regulated multidrug efflux in breast and ovarian tumour cells. *Journal of Biological Chemistry*. 283 (25) pp. 17635 – 17651.

Bourguignon, L. Y. et al. 2009. Hyaluronan-CD44 interaction with protein kinase C α promotes oncogenic signaling by the stem cell marker nanog and the production of microRNA-21, Leading to Anti-apoptosis and Chemotherapy Resistance in Breast Tumour Cells. *Journal of Biological Chemistry*. 284 (39) pp. 26533 – 26537.

Bourguignon, L. Y. et al. 2012. Hyaluronan-CD44v3 interaction with oct4-sox2-nanog promotes miR-302 expression leading to self-renewal, clonal formation and cisplatin resistance in cancer stem cells from head and neck squamous cell carcinoma. *Journal of Biological Chemistry*. 287 (39) pp. 32800 – 32824.

Bretscher, A. et al. 2002. ERM proteins and merlin: integrators at the cell cortex. *National Review of Molecular and Cellular Biology*. 3 pp. 586 – 599.

Britton, D. 2006. Bidirectional cross talk between ER α and EGFR signalling pathways regulates tamoxifen-resistant growth. *Breast Cancer Research and Treatment*. 96 pp. 131-146

Britton, D. et al. 2008. A novel serine phosphorylation site detected in the N-terminal domain of estrogen receptor isolated from human breast cancer cells. *Journal of the American Society for Mass Spectrometry*. 19 pp. 729 - 740.

Bjorkland, C. C. et al. 2013. Evidence for a role for CD44 and cell adhesion in mediating resistance to lenalidomide in multiple myeloma: therapeutic implications. *Leukaemia*. 28 (2) pp. 373 – 383.

Brodie, A. et al. 1981. Inactivation of aromatase in vitro by 4-hydroxy-4-androstene-3,17-dione and 4-acetoxy-4-androstene-3,12-dione and sustained effects in vivo. *Steroids*. 38 (6) pp. 693 – 702.

Brodie, A. et al. 2003. Aromatase inhibitor development and hormone therapy: A perspective. *Seminars in Oncology*. 30 pp. 12 – 22.

Brown, R. L. et al. 2011. CD44 splice isoform switching in human and mouse epithelium is essential for epithelial-mesenchymal-transition and breast cancer progression. *Journal of Clinical Investigation*. 121 (3) pp. 1064 – 1074.

Bruch, H. et al. 1992. Androstenedione metabolism in cultured human osteoblast-like cells. *Journal of Endocrinology and Metabolism*. 75 pp. 101 – 105.

Brufsky, A. et al. 2005. Hormone receptor status does not affect the clinical benefit of trastuzumab therapy for patients with metastatic breast cancer. *Clinical Breast Cancer*. 6 pp. 247 – 252.

Brzozwski, A. et al. 1997. Molecular basis of agonism and antagonism in the estrogen receptor. *Nature*. 389 pp. 753 – 758.

Bundred, N. et al. 2002. Fulvestrant, an estrogen receptor downregulator, reduces cell turnover index more effectively than tamoxifen. *Anticancer Research*. 22 pp. 2317 – 2319.

Burgess, A. et al. 2010. Loss of human Greatwall results in G2 arrest and multiple mitotic defects due to deregulation of the cyclin B-Cdc2/PP2A balance. *PNAS USA*. 107 pp. 12564 – 12569.

Butt, A. J. et al. 2005. Downstream targets of growth factor and oestrogen signalling and endocrine resistance: the potential roles of c-myc, cyclin D1 and cyclin E. *Endocrine Related Cancer*. 12 S47 – S59.

Buzdar, A. 2001. Endocrine therapy in the treatment of metastatic breast cancer. *Seminars in Oncology*. 28 pp. 291 – 304.

Buzdar, A. et al. 2001. Phase II, multicentre, double-blind randomised study letrozole, an aromatase inhibitor, for advanced breast cancer versus megestrol acetate. *Journal of Oncology*. 19 (14) pp. 3357 – 3366.

Byrne, C. et al. 1995. Mammographic features and breast cancer risk: effects with time, age, and menopause status. *Journal of the National Cancer Institute*. 87 (21) pp. 1622 – 1629.

Cain, J. W. et al. 2011. Identification of CD44 as a surface biomarker for drug resistance by surface proteome signature technology. *Molecular Cancer Research*. 9 (5) pp. 637 – 647.

Calderon-Margali, R. and Paltiel, O. 2004. Prevention of breast cancer in women who carry brca1 or brca2 mutations: a critical review of the literature. *International Journal of Cancer*. 112 (3) pp. 357 – 264.

Callaby, G. et al. 2002. Molecular classification of breast carcinomas using tissue microarrays. *Diagnostic Molecular Pathology*. 12 pp. 27 – 34.

Camp, R. et al. 1999. Met expression is associated with poor outcome in patients with axillary lymph node negative breast carcinoma. *Cancer*. 86 (11) pp. 2259 – 2265.

Camp, R. et al. 2003. Quantative analysis of breast cancer tissue microarrays shows that both high and normal levels of HER2 expression are associated with poor outcome. *Cancer Research*. 63 pp. 1145.

Campbell, R. A. et al. 2001. Phosphoinositol-I-3-K/AKT-mediated activation of estrogen receptor alpha: a new model for anti-estrogen resistance. *Journal of Biological Chemistry*. 276 pp. 9817 – 9824.

Cancer Genome Atlas Network. 2012. Comprehensive molecular portraits of human breast tumours. *Nature*. 490 pp. 61-70

- Cantley, L. et al. 2002. The phosphoinositide 3-kinase pathway. *Science*. 296 pp. 1655 – 1657.
- Cappellari, M. et al. 2014. The transcriptional co-activator SND1 is a novel regulator of alternative splicing in prostate cancer cells. *Oncogene*. 33 (29) pp. 3794 – 3802.
- Carlsson, J. et al. 2004. HER2 expression in breast cancer primary tumours and corresponding metastases. Original data and literature review. *British Journal of Cancer*. 90 pp. 2344 – 2348.
- Carter, W. G and Wayner, A. 1988. Characterisation of the class III collagen-receptor: a phosphorylated transmembrane glycoprotein expressed in nucleated human cells. *Journal of Biological Chemistry*. 263 pp. 4193 – 4201.
- Castro-Rivera E. et al. 2001. Estrogen regulation of cyclin D1 gene expression in ZR-75 breast cancer cells involves multiple enhancer elements. *Journal of Biological Chemistry*. 276 (33) pp. 30853 – 30861.
- Chakraborty, A. K. et al. 2010. Co-targeting the Insulin-like growth factor 1 receptor enhances growth inhibitory and pro-apoptotic effects of anti-oestrogens in human breast cancer cell lines. *Breast Cancer Research Treatment*. 120 p. 327 – 335.
- Charpin, C. et al. 2009a. A signature predictive of disease outcome in breast carcinomas identified by quantitative immunocytochemistry assays. *International Journal of Cancer*. 124 pp. 2124 – 2134.
- Charpin, C. et al. 2009b. Quantitative immunocytochemistry profile to predict early outcome of disease in triple negative breast carcinomas. *Journal of Oncology*. 34 (4) pp. 983 – 993.
- Chen, H. et al. 1996. Tamoxifen induces TGF-beta1 activity and apoptosis of human MCF-7 breast cancer cells in vitro. *Journal of Cell Biology*. 61 (1) pp. 9 – 17.
- Chen et al. 1988. Functions of hyaluronan in wound repair. *Wound Repair and Regeneration*. 7 (2) pp. 79 – 89.
- Chen, W. and Abatangelo, G. 1999. Functions of hyaluronan in wound repair
- Cheng, C. et al. 2006. A positive feedback loop couples ras activation and CD44 alternative splicing. *Genes and Development*. 20 (13) pp. 1715 – 1720.
- Cheng, C. and Sharp, A. 2006. Regulation of CD44 alternative splicing by SRm160 and its potential role in tumour cell invasion. *Molecular Cell Biology*. 26 (1) pp. 362 – 370.
- Cheung, W. et al. 1999. Receptor for hyaluronan-mediated motility (RHAMM) a hyaladherin that regulates cell responses to growth factors. *Biochemistry Society*. 27 pp. 135 – 142.
- Chlebowski, R. et al. 2005. Ethnicity and breast cancer: factors influencing differences in incidence and outcome. *Journal of the National Cancer Institute*. 97 (6) pp. 439 – 448.

- Chi, A. et al. 2012. Molecular characterisation of kidney cancer. Association of HA family with histological subtypes and metastasis. *Cancer*. 18 pp. 2394 – 2302.
- Chivasa, S. et al. 2006. Proteomic analysis of differentially expressing proteins in fungal elicitor-treated *Arabidopsis* cell cultures. *Journal of Experimental Botany*. 57 pp. 1553 – 1562.
- Cho, S. H. et al. 2012. CD44 enhances epithelial-mesenchymal-transition in association with colon cancer. *International Journal of Oncology*. 41 (1) pp. 211 – 218.
- Choi, Y. et al. 2012. Predicting the functional effect of amino acid substitutions and indels. *PLoS ONE*. 7 (10) e46688.
- Choueiri, T. 2004. Role of aromatase inhibitors in the treatment of breast cancer. *Clinical Therapies*. 26 (8) pp. 1199 – 1214.
- Chu, I. M. et al. 2008. The cdk inhibitor p27 in human cancer: prognostic potential and relevance to anticancer therapy. *Nature Reviews in Cancer*. 8 pp. 253 – 267.
- Chumsri, S. et al. 2011. Aromatase, aromatase inhibitors and breast cancer. *Journal of Steroid Biochemistry & Molecular Biology*. 125 pp. 13 – 22.
- Cichy, J. and Pure, E. 2000. Oncostatin, and transforming growth factor-beta 1 induce post-translation modification and hyaluronan binding to CD44 in lung-deprived epithelial tumour cells. *Journal of Biological Chemistry*. 275 (24) pp. 18061 – 18069.
- Claus, B. et al. 1994. Autosomal dominant inheritance of early-onset breast cancer. Implications for risk prediction. *Cancer*. 73 (3) pp. 643 – 651.
- Clemons, M. and Goss, P. et al. 2001. Estrogen and the risk of breast cancer. *The National England Journal of Medicine*. 344 (4) pp. 276 – 285.
- Clevenger, C. et al. 2003. The role of prolactin in mammary carcinoma. *Endocrinology Review*. 24 pp. 1 – 27.
- Collins, A. T. et al. 2008. Prospective identification of tumourigenic prostate cancer stem cells. *Cancer Research*. 65 (23) pp. 10946 – 10951.
- Colone, M. et al. 2008. The multidrug transporter P-glycoprotein: a mediator of melanoma invasion? *Journal of Investigative Dermatology*. 128 pp. 957 – 971.
- Corte, M. D. et al. 2010. Analysis of the expression of hyaluronan in intraductal and invasive carcinomas of the breast. *Journal of Cancer Research Clinical Oncology*. 136 (5) pp. 745 – 750.
- Couse, J. F. et al. 1997. Tissue distribution and quantitative analysis of estrogen receptor-alpha (ERalpha) and estrogen receptor-beta (ERbeta) messenger ribonucleic acid in the wild type and ERalpha-knockout mouse. *Endocrinology*. 138 (11) pp. 4613 – 4621.
- Cowley, S. M. et al. 1997. Estrogen receptors α and β form heterodimers on DNA. *Journal of Biological Chemistry*. 272 (32) pp. 19856 – 19862.

- Crainie, M. et al. 1999. Overexpression of receptor for HA mediated motility (RHAMM) characterises the malignant clone in multiple myeloma: identification of 3 distinct RHAMM variants. *Blood*. 93 (5) pp. 1684 -1696.
- Creighton, C. et al. 2012. Comprehensive molecular portraits of human breast tumours. *Nature*. 490 pp. 61 – 70.
- Crown, J. et al. 2012. Emerging targeted therapies in triple-negative breast cancer. *Annals of Oncology*. 23 (6) pp. 56 – 65.
- Cui, X. et al. 2005. Biology of progesterone receptor loss in breast cancer and its implications for endocrine therapy. *Journal of Clinical Oncology*. 23 pp. 7721 – 7735.
- Cui, J. et al. 2013. Estrogen synthesis and signalling pathways during aging: from periphery to brain. *Trends in Molecular Medicine*. 19 (3) pp. 197 – 209.
- Culty, M. et al. 1990. The hyaluronate receptor is a member of the CD44 (H-CAMM) family of cell surface glycoproteins. *Journal of Cell Biology*. 111 pp. 2765 – 2774.
- Cuzick, J. 2003. Aromatase inhibitors in prevention – data from the ATAC (Arimidex, Tamoxifen Alone or in Combination) trial and design of IBIS-II (the second International Breast Cancer Intervention Study). *Recent Results in Cancer Research*. 163 pp. 96 – 103.
- Davies, C. et al. 2013. Adjuvant Tamoxifen: Longer Against Shorter (ATLAS) Collaborative Group. Long-term effects of continuing adjuvant tamoxifen to 10 years versus stopping at 5 years after diagnosis of oestrogen receptor-positive breast cancer: ATLAS, a randomised trial. *Lancet*. 381 pp. 805-816.
- Dauvois, S. et al. 1992. Antiestrogen ICI 164.384 reduces cellular estrogen receptor content by increasing its turnover. *PNAS USA*. 89 pp. 4037 – 4041.
- Dauvois, S. et al. 1993. The antiestrogen ICI 182780 disrupts estrogen receptor nucleocytoplasmic shuttling. *Journal of Cell Science*. 106 pp. 1377 – 1388.
- Dawood, S. et al. 2010. Prognosis of women with metastatic breast cancer by HER2 status and trastuzumab treatment: an institutional-based review. *Journal of Clinical Oncology*. 28 (1) pp. 92 – 98.
- Day, A. and Sheehan, J. 2001. Hyaluornan: polysaccharide chaos to protein organisation. *Current Opinion in Structural Biology*. 11 pp. 617 – 622.
- Defriend, D. et al. 1994. Effects of 4-hydroxy-tamoxifen and a novel pure anti-oestrogen (ICI 182870) on the clonogenic growth of human breast cancer cells in vitro. *Br Journal of Cancer*. 70 pp. 204 – 211.
- DeSantis, C. et al. 2011. Breast cancer statistics 2011. *A Cancer Journal for Clinicians*. 61 (6) pp. 409 – 418.
- Dianzani, U. and Malavasi, F. 1995. Lymphocyte adhesion to endothelium. *Critical Reviews in Immunology*. 10 pp. 167 – 200.

- Diaz, L. K. et al. 2005. CD44 expression is associated with increased survival in node-negative invasive breast carcinoma. *Clinical Cancer Research*. 11 (9) pp. 3309 – 3314.
- Diessner, J. et al. 2014. Targeting of pre-existing and induced breast cancer stem cells with trastuzumab and trastuzumal-emtansine (T-DM1). *Cell Death and Disease*. 5. p. 11549.
- Donatello, S. et al. 2012. Lipid raft association restricts CD44-ezrin interaction and promotion of breast cancer cell migration. *American Journal of Pathology*. 181 (6) pp. 2172 – 2182.
- Dontu, G. et al. 2004. Breast Cancer, Stem/Progenitor Cells and the Estrogen Receptor. *TRENDS in Endocrinology and Metabolism*. 15 (5) pp. 194 – 197.
- Dougherty et al. 1991. Molecular cloning of CD44R1 and CD44R2 two novel isoforms of the human CD44 lymphocyte 'homing' receptor expressed by hemopoietic cells. *Journal of Experimental Medicine*. 174 (1) pp 1 – 5.
- Droll et al. 1995. Adhesive interactions between alternative spliced CD44 isoforms. *Journal of Biological Chemistry*. 270 pp. 1156 – 1173.
- Du, L. et al. 2008. CD44 is of functionally importance for colorectal cancer stem cells. *Clinical Cancer Research*. 14 (21) pp. 6751 – 6760.
- Du, W. W. et al. 2013. The role of versican in modulating breast cancer cell self-renewal. *Molecular Cancer Research*. 11 pp. 443 – 455.
- Dumitrescu, R. and Cotarla, I. 2005. Understanding breast cancer risk: where do we stand in 2005? *Cell Molecular Medicine*. 9 pp. 208 – 210.
- Dupont, W. et al. 1993. Breast cancer risk associated with proliferative breast disease and atypical hyperplasia. *Cancer*. 71 (4) pp. 1258 – 1265.
- Durham, C. R. et al. 1985. Regulation of aromatase activity of rat granulosa cells: induction of synthesis of NADPH-cytochrome P-450 reductase by FSH and dibutyryl cyclic AMP. *Molecular Cell Endocrinology*. 40 (2 – 3) pp. 211 – 219.
- Duru, N. et al. 2012. HER2-associated radioresistance of breast cancer stem cells isolated from HER2-negative breast cancer cells. *Clinical Cancer Research*. 18 (24) pp. 6634 – 6647.
- Easton, D. et al. 1997. Cancer risks in two large breast cancer families linked to BRCA2 on chromosome 13q12-13. *American Journal of Human Genetics*. 61 pp. 120 - 128.
- Early Breast Cancer Trialists' Collaborative Group (EBCTCG). 1988. Tamoxifen for early breast cancer: an overview of the randomised trials. *Lancet*. 351 (9114) pp. 1451 – 1467.
- Early Breast Cancer Trialists' Collaborative Group (EBCTCG). 2011. Relevance of breast cancer hormone receptors and other factors to the efficacy of adjuvant tamoxifen: patient-level meta-analysis of randomised trials. *Lancet*. 378 pp. 771-784

- Eisen, A. et al. 2008. Aromatase Inhibitors in Adjuvant Therapy for Hormone Receptor Positive Breast Cancer: A Systematic Review. *Cancer Treatment Reviews*. 34 pp. 157 – 174.
- Elliot, V. A. et al. 2014. Activation of c-met and upregulation of CD44 expression are associated with the metastatic phenotype in the colorectal cancer liver metastasis model. *PLOS One*. 9 (5) pp. 97432
- Elsberger, B. et al. 2012. Shorter disease-specific survival of ER-positive breast cancer patients with higher cytoplasmic Src kinase expression after tamoxifen treatment. *Journal of Cancer Research and Clinical Oncology*. 138 (2) pp. 327 – 332.
- Engbring, J. A. and Kleinman. H. K. 2002. The basement membrane matrix in malignancy. *Journal of Pathology*. 200 pp. 465 – 470.
- English, N. M. 1998. Site-specific De-N-glycosylation of CD44 can activate hyaluronan binding and CD44 activation states show distinct threshold densities for hyaluronan binding. *Cancer Research*. 58 pp. 3736 – 3742.
- Enmark, E. and Gustafsson, J. et al. 1999. Oestrogen receptors – an overview. *Journal of Internal Medicine*. 246 pp. 133 – 138.
- Entwistle, J. et al. 1995. Characterisation of the murine gene encoding the HA receptor RHAMM. *Gene*. 163 pp. 233 – 328.
- Ermack, G. et al. 1996. Novel CD44 messenger RNA isoforms in human thyroid and breast tissues feature unusual sequence rearrangements. *Clinical Cancer Research*. 2 pp 1251 – 1254.
- Evanko, S. et al. 2007. HA-dependent pericellular matrix. *Advanced Drug Delivery Reviews*. 59 pp. 1351 – 1365.
- Evans, R. M. 1988. The steroid and thyroid hormone receptor superfamily. *Science*. 240 pp. 889 – 895.
- Ewertz, M. et al. 1990. Age at first birth, parity and risk of breast cancer: a meta-analysis of 8 studies from the Nordic countries. *International Journal of Cancer*. 46 pp. 597 – 603.
- Ewertz, M. and Duffy, S. W. 1988. Risk of breast cancer in relation to reproductive factors. *British Journal of Cancer*. 58 pp. 99 – 104.
- Fackenthal, D. and Godley, L. A. 2008. Aberrant RNA splicing and its functional consequences in cancer cells. *Disease models and mechanisms*. 1 (1) pp. 37 – 42.
- Fahe, J et al. 2014. Rosiglitazone amplifies the sensitivity of docetaxel and reduces the expression of CD44v6. *Oncology Letters*. 7 (4) pp. 1284 – 1288.
- Favrot et al. 1993. CD44 – a new prognostic marker for neuroblastoma. *New England Journal of Medicine*. 329 pp. 1965.

Fawell, S. E et al. 1990. Inhibition of estrogen receptor-DNA binding by the 'pure' antiestrogen ICI 164,384 appears to be mediated by impaired receptor dimerization. *PNAS USA*. 87 pp. 6883 – 6887.

Fisher, B. et al. 1994. Endometrial cancer in tamoxifen-treated breast cancer patients: findings from the National Survey Adjuvant Breast and Bowel Project (NSABP) B-14. *Journal of the National Institute of Cancer*. 86 (7) pp 527 – 537.

Fisher, B. et al. 1998. Tamoxifen for the prevention of breast cancer: Report of the National Surgical Adjuvant Breast and Bowel Project P-1 Study. *Journal of the National Cancer Institute*. 90 pp. 1371 – 1388.

Fisher, B. et al. 2001. Five versus more than five years of tamoxifen for lymph node-negative breast cancer updated findings from the National Surgical Adjuvant Breast and Bowel Project B-14 randomized trial. *Journal of the National Cancer Institute*. 93 pp. 684 – 690.

Franzmann, E. J. et al. 2003. Expression of tumour markers hyaluronan and hyaluronidase (HYAL1) in head and neck tumours. *International Journal of Cancer*. 106 (3) pp. 438 – 445.

Fraser, G. T. and Shavlik, D. 1997. Risk factors, lifetime risks and age at onset of breast cancer. *Annals of Epidemiology*. 7 (6) pp. 375 – 382.

Foekens, J. A. et al. 1999. Prognostic value of CD44 variant expression in primary breast cancer. *International Journal of Cancer*. 84 (3) pp. 209 – 215.

Ford, D. et al. 1998. Genetic heterogeneity and penetrance analysis of the BRCA1 and BRCA2 genes in breast cancer families. *American Journal of Human Genetics*. 62 pp. 676 – 689.

Fox, S. et al. 1994. Normal human tissues, in addition to some tumours, express multiple different CD44 isoforms. *Cancer Research*. 54 pp. 4539 – 4546.

Fujimoto, T. et al. 2001. CD44 binds a chondroitin sulphate proteoglycan, aggrecan. *Immunological Letters*. 13 (3) pp. 359 – 366.

Fujita, Y. et al. 2002. CD44 signalling through focal adhesion kinase signalling and its anti-apoptotic effect. *FEBS Letters*. 528 (1 – 3) pp. 101 – 108.

Gal, I. et al. 2003. Role of the extracellular and cytoplasmic domains of CD44 in the rolling interaction of lymphoid cells with hyaluronan under physiological flow. *Journal of Biological Chemistry*. 278 pp. 11150 – 11158.

Ganesh, S. et al. 2013. Hyaluronic acid based self-assembling nanosystems for CD44 target mediated siRNA delivery to solid tumours. *Biomaterials*. 34 (13) pp. 3489 – 3502.

Gansauge, F. et al. 1995. Differential expression of CD44 splice variants in human pancreatic adenocarcinoma and in normal pancreas. *Cancer Research*. 55 pp. 5499 – 5503.

- Gao, F. et al. 2006. Expression and quantification of LYVE-1 in colorectal cancer. *Clinical Experimental Medicine*. 6 (2) pp. 65 – 71.
- Garouniatis, A. et al. 2013. . FAK, CD44v6, c-met and EGFR in colorectal cancer parameters: tumour progression, metastasis, patient survival and receptor crosstalk. *International Journal of Colorectal Disease*. 1 pp. 9 – 18.
- Gaub, M. P. et al. 1990. Activation of the ovalbumin gene by the estrogen receptor involves the Fos-Jun complex. *Cell*. 63 (6) pp. 1267 – 1276.
- Gautrau, A. et al. 2002. ERM proteins and NF2 tumour suppressor: the Yin and Yang of cortical actin organisation and cell growth signalling. *Current Opinion in Cell Biology*. 14 pp. 104 – 109.
- Gavet, O. and Pines, J. 2010. Progressive activation of cyclinB1-Cdk1 coordinates entry to mitosis. *Developmental Cell*. 18 pp. 533 – 543.
- Gaviraghi, M. et al. 2001. Pancreatic cancer spheres are more than just aggregates of stem marker-positive cells. *Biosciences Reports*. 31 (1) pp. 45 – 55.
- Geisler, J. 1996. Influence of anastrozole (Arimidex), a selective, non-steroidal aromatase inhibitor, on in vivo aromatisation and plasma oestrogen levels in postmenopausal women with breast cancer. *British Journal of Cancer*. 74 pp. 1286-1291
- Gee, J. et al. 2005. Epidermal growth factor receptor/Her2/Insulin-like growth factor receptor signalling and oestrogen receptor activity in clinical breast cancer. *Endocrine-Related Cancer*. 12 pp. 99 – 111.
- Ghayad, S. et al. 2010. Endocrine resistance associated with activated ErbB system in breast cancer cells is reversed by inhibitors MAPK or PI3/AKT signalling pathways. *International Journal of Cancer*. 126 pp. 545 – 562.
- Ghousab, R. et al. 1998. Expression of c-met is a strong prognostic factor in breast carcinoma. 82 (8) pp. 1513 – 1520.
- Giancinti, L et al. 2006. Epigenetic information and estrogen receptor alpha expression in breast cancer. *Oncologist*. 23 (11) pp. 2469 – 2476.
- Giordano, S. 2005. Adjuvant systemic therapy for male breast carcinoma. *Cancer*. 104 pp. 2359 - 2364.
- Ginestier, C. et al. 2002. Distinct and complementary information provided by use of tissue and DNA microarray in the study of breast tumour markers. *American Journal of Pathology*. 161 pp. 1223 – 1233.
- Ginestier, C. et al. 2009. Retinoid signalling regulates breast cancer stem cell differentiation. *Cell Cycle*. 8 (20) pp. 3297 – 3302.

- Goldstein, L. et al. 1989. A human lymphocyte homing receptor, the Hermes antigen, is related to cartilage proteoglycan core and link proteins. *Cell*. 56 pp. 1063 – 1072.
- Goldstein, L. A. and Butcher E.C. 1990. Identification of mRNA that encodes an alternative form of H-CAM (CD-44) in lymphoid and non-lymphoid tissues. *Immunogenesis*. 32 pp. 389 – 397.
- Goodfellow, P. N. et al. 1982. The gene MIC4 which controls expression of the antigen defined by monoclonal antibody F10.44.2 is on human chromosome 11. *European Journal of Immunology*. 12 pp. 659 – 663.
- Goodison, S. et al. 1999. CD44 cell adhesion molecules. *Journal of Clinical Pathology*. 52 pp. 189 – 196.
- Gong, Y. 2005. Expression of cell adhesion molecules, CD44s and E-cadherin and microvessel density in invasive micropapillary carcinoma of the breast. *Histopathology*. 46 pp 24 – 30.
- Gotoda, T. et al. 1998. Expression of CD44 variants and its associations with survival in pancreatic cancer. 9 (10) pp. 1033 – 1040.
- Gottlicher, M. et al. 1998. Transcriptional cross-talk, the second mode of steroid hormone receptor action. *Journal of Molecular Medicine*. 76 (7) pp. 480 – 489.
- Graveel, K. R. et al. 2009. Met induces diverse mammary carcinomas in mice and is associated with human basal breast cancer. *PNAS USA*. 106 (31) pp. 12909 – 12914.
- Green, S. and Chambon, P. 1991. The estrogen receptor: from perspective to mechanism. *Nuclear Hormone Receptors*. pp 15 – 38.
- Greenfield, B. et al. 1999. Characterisation of the heparan sulphate and chondroitin sulphate assembly sites in CD44. *Journal of Biological Chemistry*. 274 (4) pp. 2511 – 2517.
- Greaves, P. et al. 1993. Two year carcinogenicity study of tamoxifen in Alderley Park Wistar-derived rats. *Cancer Research*. 53 pp. 3919 – 3924.
- Groen, A. C. et al. 2004. XRHAMM functions in ran-dependent microtubule nucleation and pole formation during anastral spindle assembly. *Current Biology*. 14 pp. 1801 – 8111.
- Guerra, B. et al. 2003. Plasma membrane estrogen receptor mediates neuroprotection against β -amyloid toxicity through activation of Raf-1/MEK/ERK cascade in septal-derived cholinergic SN56 cells. *Journal of Neurochemistry*. 91 pp. 99 – 109.
- Guha et al. 1997. Proliferation of human malignant astrocytomas is dependent on Ras activation. *Oncogene*. 12 pp. 2755 – 2765.
- Gunthert, U. et al. 1991. A new variant of glycoprotein CD44 confers metastatic potential to rat carcinoma cells. *Cell*. 65 (1) pp. 13 – 24.

Guo, P. et al. 2014. ICAM-1 as a molecular target for triple negative breast cancer. *PNAS*. 10 (1075) pp. 14710 – 14715.

Gupta, A. et al. 2013. Promising non-invasive cellular phenotype of prostate cancer cells knockdown of matrix metalloproteinase 9. *The Scientific World Journal Volume*. pp. 1 – 13.

Gururaj, A. E. et al. 2006. Novel mechanism of resistance to endocrine therapy: genomic and non-genomic considerations. *Clinical Cancer Research*. 12 (3 Pt 2) 1001s – 1007s.

Gutierrez, C. M. et al. 2005. Molecular changes in tamoxifen-resistance breast cancer: relationship between estrogen receptor, HER2 and p38 mitogen activated protein kinase. *American Journal of Clinical Oncology*. 23 (11) pp. 2469 – 2476.

Gyorffy, B. et al. 2010. An online survival analysis tool to rapidly assess the effect of 22277 genes on breast cancer progression using microarray data of 1809 patients. *Breast Cancer Research and Treatment*. 123 pp. 725 – 731.

Habashy, H. O. 2009. Transferrin receptor (CD71) is a marker of poor prognosis in breast cancer and can predict response to tamoxifen. *Breast Cancer Research and Treatment*. 119 (2) pp. 283 – 293.

Haggarty, J. G. et al. 1992. Identification and characterisation of a cytoskeletal proteoglycan on keratinocytes. *Journal of Investigative Dermatology*. 99 pp. 374 – 380.

Hahn, E. F. et al. 1985. 19-Hydroxylation of androgens in the rat brain. *PNAS*. 82 (9) PP. 2728 – 2730.

Hall, C. et al. 1994. Hyaluronan and the hyaluronan receptor RHAMM promote focal adhesion turnover and transient tyrosine kinase activity. *Journal of Cell Biology*. 126 (2) pp. 575 – 588.

Hall, C. L. et al. 1995. Overexpression of the hyaluronan receptor RHAMM is transforming and is also required for H-ras transformation. *Cell*. 82 (1) pp. 19 – 26.

Hall, C. L. et al. 1996. pp-60 (c-src) is required for cell locomotion regulated by the HA receptor RHAMM. *Oncogene*. 13 (10) pp. 2213 – 2224.

Hall, J. M. and McDonnell, D. P. 1999. The estrogen receptor b-isoform (ERb) of the human estrogen receptor modulates Era transcriptional activity and is a key regulator of the cellular response to estrogens and antiestrogens. *Endocrinology*. 140 pp. 5566 – 5578.

Hall, C. L. and Turley, E. 1995. Hyaluronan: RHAMM mediated cell locomotion and signaling in tumorigenesis. *Journal of Neuro-Oncology*. 26 (3) pp. 221 – 229.

Hao, J. et al. 2012. In vitro and in vivo prostate cancer metastasis and chemoresistance can be modulated by expression of either CD44 or CD147. *Plos One*. 7 (8) e40716.

Hardwick, C. et al. 1992. Molecular cloning of a novel hyaluronan receptor that mediates tumour cell motility. *Journal of Cellular Biology*. 117 pp. 1343 – 1350.

Hardwick et al. 1993. *Journal of Cell Biology*. 117 pp. 1343- 1350.

Harris, E. and Weigel, P. 2008. The ligand-binding profile of HARE: hyaluronan and chondroitin sulfates A, C and D bind to overlapping sites distinct from the sites for heparin, acetylated low-density lipoprotein, dermatan sulfate and CS-E. *Glycobiology*. 18 (8) pp. 638 – 648.

Harris et al. 2007. Expression, processing and glycosaminoglycan binding of the recombinant human 315 kDa hyaluronic acid for endocytosis (HARE). *Journal of Cell Biology*. 282 (2) pp. 2785 – 2797.

Harrison, G. M et al. 2006. The influence of CD44v3-v10 on adhesion, invasion and MMP-14 expression in prostate cancer cells. *Oncology Reports*. 15 (1) pp. 199 – 206.

Harrison, H. et al. 2010. Regulation of breast cancer stem cell activity by signalling through the Notch 4 receptor. *Cancer Research*. 70 (2) pp. 709 – 718.

Harvey, E. B. et al. 1987. Alcohol consumption and breast cancer. *Journal of National Cancer Institute*. 78 pp. 657 – 661.

Harvey, J. M. et al. 1999. Estrogen receptor status by immunohistochemistry is superior to ligand-binding assay for predicting response to adjuvant endocrine therapy in breast cancer. *Journal of Clinical Oncology*. 17 pp. 1474 – 1481.

Hasenauer, S. et al. 2013. Internalisation of Met requires the co-receptor CD44v6 and its link to ERM proteins. *PLOS one*. 8 (9). e62357.

Hatano, H. et al. 2011. RHAMM/ERK interaction induces proliferative activities of cementifying fibroblasts cells through a mechanism based on the CD44-EGFR. *Laboratory Investigation*. 91 (3) pp. 379 – 391.

Hamilton, S. et al. 2007. The hyaluronan receptors CD44 and RHAMM (CD168) form complexes with ERK1,2 which sustain high basal motility in breast cancer cells. *Journal of Biological Chemistry*. 282 (2) pp. 16667 – 16680.

Hankinson, S. et al. 2004. Towards an integrated model for breast cancer etiology: the lifelong interplay of genes, lifestyle and hormones. *Breast Cancer Research*. 6 pp. 213 – 218.

Heldin, P. et al. 1996. Differential synthesis and binding of hyaluronan by human breast cancer cell lines. *Oncology Reports*. 3 (6) pp. 1011 – 1016.

Heldin, P. et al. 2013. Deregulation of hyaluronan synthesis, degradation and binding promotes breast cancer. *Journal of Biochemistry*. 154 (5) pp. 395 – 408.

Henderson, B. et al. 1982. Endogenous hormones as a major factor in human cancer. *Cancer Research*. 42 pp. 3232- 3239.

Henderson, B. E. et al. 1985. Do regular ovulatory cycles include breast cancer risk? *Cancer*. 56 pp. 1206 – 1208.

Henderson, B. et al. 1996. Cancer epidemiology and prevention. *New York Saunders Company*. pp 1022 – 1039.

Herrera-Gayol, A and Jothy, S. 1999a. CD44 modulates Hs578t human breast cancer cell adhesion, migration and invasiveness. Expression and molecular pathology.

Herrera-Gayol, A. and Jothy, S. 1999b. Adhesion proteins in the biology of breast cancer: contributor of CD44. *Experimental and Molecular Pathology*. 66 pp. 149 – 156.

Herishanu, Y. et al. 2011. CD44 signalling via PI3K/AKT and MAPK/ERK pathways protects CLL cells for spontaneous and drug-induced apoptosis through MCL-1. *Leukemia Lymphoma*. 52 (9) pp. 1758 – 1769.

Herynk, M. H. and Fuqua, S. A. 2004. Estrogen receptor mutations in human disease. *Endocrine Reviews*. 25 pp. 869 – 898.

Hibino, S. et al. 2004. Identification of an active site on the laminin alpha5 chain globular domain that binds to CD44 and inhibits malignancy. 64 (14) pp. 4810 – 4816.

Hill, P. et al. 1976. Prolactin levels in populations at risk of breast cancer. *Cancer Research*. 36 pp. 4102 – 4106.

Hiller, M. et al. 2005. Creation and disruption of protein features by alternative splicing. *Genome Biology*. 6 R58.

Hirano, H. et al. 1994. CD44 isoform expression mediated by alternative splicing: tissue-specific regulation in mice. *International Immunology*. 6 (1) pp. 49 – 59.

Hirose, Y. et al. 2012. Inhibition of Stabilin-2 elevates circulating hyaluronan levels and prevents tumour metastasis. *PNAS USA*. 109 (11) pp. 4263 – 4268.

Hiscox, S. et al. 2004. Tamoxifen resistance in breast cancer cells is accompanied by an enhanced motile and invasive phenotype: inhibition by gefitinib ('Iressa' ZD1839). *Clinical Expression and Metastasis*. 21 pp. 201 – 212.

Hiscox, S. et al. 2006. Chronic exposure to fulvestrant promotes overexpression of the c-met receptor in breast cancer cells: implications for tumour-stroma interactions. *Endocrine-related Cancer*. 13 pp. 1085 – 1099.

Hiscox, S. et al. 2011. Inhibition of focal adhesion kinase suppresses adverse phenotype of endocrine resistant breast cancer cells and improves endocrine response in endocrine sensitive cells. *Breast Cancer Research and Treatment*. 125 (3) pp. 659 – 669.

Hiscox, S. et al. 2012. Overexpression of CD44 accompanies acquired tamoxifen resistance in MCF-7 cells and augments their sensitivity to the stromal factors, heregulin and hyaluronan. *BMJ Cancer*. 12. 458. pp. 1 – 14.

Hiscox, S. and Jiang, W. G. 1999. Ezrin regulates cell-cell and cell-matrix adhesion, a possible role with E-cadherin/beta-catenin. *Journal of Cell Science*. 112 pp. 3081 – 3090.

Hoffmann, M. et al. 1991. CD44 splice variants confer metastatic behaviour in rats: homologous sequences are expressed in human tumour cell lines. *Cancer Research*. 51 pp. 5292 – 5297.

Hoffmann, M. et al. 1993. A link between Ras and metastatic behaviour of tumour cells. Ras induces CD44 promoter activity and leads to low level expression of metastatic spindle variants of CD44 in CREF cells. *Cancer Research*. 53 pp. 1516 – 1521.

Honeth et al. 2008. CD44+/CD24- phenotype found to correlate with the more aggressive basal-like subtype of breast cancer.

Howell, A. 2001. Preliminary experience with pure antiestrogens. *Clinical Cancer Research*. 7 pp. 4367 – 4375.

Howell, A. et al. 2002. Fulvestrant, formerly ICI 182,780, is as effective as anastrozole in postmenopausal women with advanced breast cancer progressing after prior endocrine treatment. *Journal of Clinical Oncology*. 20 pp. 3396-3403

Howell, A. 2006. Fulvestrant ('Faslodex'): Current and future role in breast cancer management. *Critical Reviews in Oncology/Hematology*. 57 pp. 265 – 273.

Ho-Yen, C. M. et al. 2014. C-met in invasive breast cancer: is there a relationship with the basal-like subtype? *Cancer*. 120 (2) pp. 163 – 171.

Hsieh, C. C. et al. 1990. Age at menarche, age at menopause, weight and obesity factors for breast cancer: associations and interactions in an international case control study. *International Journal of Cancer*. 46 pp. 796 – 800.

Hu, X. et al. 1993. Circumvention of tamoxifen resistance by the pure antiestrogen ICI 182, 780. *International Journal of Cancer*. 55 pp. 873 – 876.

Huang, Z. et al. 1997. Dual effects of weight and weight gain on breast cancer risk. *JAMA*. 278 pp. 1407 – 1411.

Huang, Y. et al. 2014. Cationic conjugated polymer/fluoresceinamine-hyaluronic acid complex for sensitive fluorescence detection of CD44 and targeted cell imaging. *ACS Applied Material Interfaces*. 6 (21) pp. 19144 – 19153.

Hudson, D. et al. 1995. CD44 is the major peanut lectin-binding glycoprotein of human epidermal keratinocytes and plays a role in intercellular adhesion. *Journal of Cell Science*. 108 pp. 1959 – 1970.

Huebener, P. et al. 2008. CD44 is critically involved in infract healing by regulating the inflammatory and fibrotic response. *Journal of Immunology*. 180 (4) pp. 2625 – 2633.

Huet, S. et al. 1989. CD44 contributes to T-cell activation. *Journal of Immunology*. 143 (3) pp. 798 - 801.

Huh, J. W. et al. 2009. Expression of standard CD44 in human colorectal carcinoma: association with prognosis. *Pathology International*. 59 (4) pp. 241 – 246.

Hunt, K. et al. 1990. Mortality in a cohort of long-term users of hormonal replacement therapy: an updated analysis. *Breast Journal of Obstetrics and Gynaecology*. 97 pp. 1080 – 1086.

Hunter, D. et al. 1993. Diet, body size and breast cancer. *Epidemiology Review*. 15 pp. 110 – 132.

Hurt, E. M. et al. 2008. CD44⁺/CD24⁻ prostate cells are early cancer progenitor/stem cells that provide a model for patients with poor prognosis. *Breast Journal Cancer*. 98 (4) pp. 756 – 765.

Hutcheson, I. et al. 2001. The novel ER downregulator, Faslodex, modulates EGFR/MAPK activity in tamoxifen-resistant MCF-7 breast cancer cells. *Clinical Cancer Research*. 61 pp. 6739 – 6746.

Hutcheson, I. et al. 2003. Estrogen receptor mediated modulation of the EGFR/MAPK pathway in tamoxifen-resistant MCF-7 cells. *Breast Cancer Research and Treatment*. 81 pp. 81 – 83.

Hyun-Jong, C. et al. 2011. Self-assembled nanoparticles based on hyaluronic-acid (HA-CE) and pluronic for tumour targeted delivery of docetaxal. *Biomaterials*. 33 (29) pp. 7181 – 7190.

Idowu, M. O. et al. 2012. CD44⁺/CD24^{low} cancer stem/progenitor cells are more abundant in triple negative breast cancer phenotype and are associated with poor outcome. *Human Pathology*. 43 (3) pp. 364 – 373.

Iida, N. and Bouguignon, L. Y. 1997. Coexpression of CD44 variant (v10/ex14) and CD44S in human mammary epithelial cells promotes tumorigenesis. *Journal of Cell Physiology*. 171 pp. 152 – 160.

Ingle, J. N. et al. 2004. Evaluation of fulvestrant in women with advanced breast cancer and progression on prior aromatase inhibitor therapy: a phase II trial of the North Central Cancer Treatment Group. *Breast Cancer Research and Treatment*. 88(Suppl 1): S38, (abstract 409).

Isacke, C. M. 1994. The role of the cytoplasmic domain in regulating CD44 function. *Journal of Cell Science*. 107. pp. 2353 – 2359.

Ishii, S. et al. 2004. CD44 participates in the adhesion of human colorectal carcinoma cells to laminin and type IV collagen. *Surgical Oncology*. 2 (4) pp. 255 – 264.

Ishikawa, T. et al. 2001. Inhibition of osteoclast differentiation and bone resorption by cathepsin K antisense oligonucleotides. *Molecular Carcinogenesis*. 32 pp. 84 – 91.

Jackson, D. et al. 1992. Multiple variants of the human lymphocyte homing receptor CD44 generated by insertion at a single site in the extracellular domain. *Journal of Biological Chemistry*. 267 pp. 4732 – 4739.

Jackson, D. et al. 1995. Proteoglycan forms of the lymphocyte homing receptor CD44 are alternatively spliced variants containing the V3 exon. *Journal of Cell Biology*. 128 (4) pp. 673 – 685.

- Jackson et al. 2009. Immunological functions of hyaluronan and its receptors in the lymphatics. *Immunology Review*. 230 (1) pp. 216 – 231.
- Jaggupilli, A. and Elkord, E. 2012. Significance of CD44 and CD24 as Cancer Stem Cell Markers: An Enduring Ambiguity. *Clinical and Developmental Immunology*.
- Jakacka, M. et al. 2002. An estrogen receptor (ER) alpha deoxyribonuclease acid-binding knock in mutation provides evidence for non-classical ER pathway signalling in vivo. *Molecular Endocrinology*. 16 (10) pp. 188 – 201.
- Jalkonen, S. and Jalkonen, M. 1992. Lymphocyte CD44 binds to the COOH-terminal heparin binding domain of fibronectin. *Journal of Cell Biology*. 116 pp. 817 – 825.
- Jansen, R. H. L. et al. 1996. CD44v6 is not a prognostic factor in primary breast cancer. *Annals of Oncology*. 9 (1) pp. 109 – 111.
- Jensen, E. and Jordan, C. 2003. The estrogen receptor: a model for molecular medicine. *Clinical Cancer Research*. 9 pp 1980.
- Jiang, H. et al. 2001. Antisense inhibition of alternatively spliced CD44 variant in human articular chondrocytes promotes hyaluronan internalisation. *Arthritis Rheumatism*. 44. pp. 2599 – 2610.
- Jiang, H. et al. 2002. A requirement for the CD44 cytoplasmic domain for hyaluronan binding, pericellular matrix assembly and receptor-mediated endocytosis in cos-7 cells. *Journal of Biological Chemistry*. 277 pp. 10531 – 10538.
- Jiang, J. et al. 2013. The cytoskeleton protein RHAMM and ERK1/2 activity maintain the pluripotency of murine embryonic stem cells. *PloS One*. 8 (9) e73548.
- Joensuu, H. et al. 2005. Aromatase inhibitors in the treatment of early and advanced breast cancer. *Acta Oncology*. 44 pp. 23 – 31.
- Jones, M et al. 2000. Heparan sulphate proteoglycan isoforms of the CD44 hyaluronan receptor induced human inflammatory macrophages cell function as paracrine regulators of fibroblast growth factor action. *Journal of Biological Chemistry*. 275 (11) pp. 7964 – 7974.
- Jordan, V. C. 1995. Tamoxifen: toxicities and drug resistance during the treatment and prevention of breast cancer. *Annual Review of Pharmacology and Toxicology*. 35 pp. 195 – 211.
- Jordan, V. 2004. Selective estrogen receptor modulation: concept and consequences in cancer. *Cancer Cell*. 5 pp. 207 – 213.
- Jordan, V. and Ford, C. 2011. Paradoxical clinical effect of estrogen on breast cancer risk: a 'new' biology of estrogen-induced apoptosis. *Cancer Prevention Research*. 4 (5) pp. 633 – 637.
- Joukov, V. et al. 2006. The BRCA1/BARD1 heterodimer modulates ran-dependent mitotic spindle assembly. *Cell*. 127 pp. 539 – 552.

Kalish, E. D. et al. 1999. A new CD44v3-containing isoform is involved in tumour cell growth and migration during human breast carcinoma progression. *Front Biosciences*. 4 pp. 1 – 8.

Kalomiris, E. L. and Bourguignon, L. Y. 1988. Mouse T-lymphoma cells contain a transmembrane glycoprotein (GP85) that binds ankyrin. *Journal of Cell Biology*. 106 (2) pp. 319 – 327.

Kalmyrzaev, B. et al. 2008. Hyaluronan-mediated motility receptor gene single nucleotide polymorphisms and risk of breast cancer. *Cancer Epidemiology, Biomarkers and Prevention*. 17 (21) pp. 3618 – 3620.

Karaer, O. et al. 2004. Aromatase inhibitors: possible future applications. 83 (8) pp. 699 – 706.

Karimi, Z. et al. 2014. Dietary patterns and breast cancer risk among women. *Public Nutrition and Health*. 17 (5) pp. 1098 – 1106.

Katzenellenbogen, B. 1996. Estrogen Receptors: Bioactivities and Interactions with Cell Signaling Pathways. *Biology of Reproduction*. (54) pp. 287 – 293.

Katzenellenbogen, B. et al. 2000. Molecular mechanisms of estrogen action: selective ligands and receptor pharmacology. *Journal of Steroid Biochemistry & Molecular Biology*. 74 pp. 279 – 285.

Kaufmann et al. 1995. CD44 variant exon epitopes in primary breast cancer and length of survival. *Lancet*. 345 pp. 615 – 619.

Kawashima, H. et al. 2000. Binding of a large chondroitin sulphate/dermate sulphate proteoglycan, versican, to L-selectin, P-selectin and CD44. *Journal of Biological Chemistry*. 275 (45) pp. 35448 – 35456.

Kaya, G. et al. 1997. Selective suppression of CD44 in keratinocytes of mice bearing an antisense CD44 transgene driven by a tissue-specific promoter disrupts hyaluronate metabolism in the skin and impairs keratinocyte proliferation. *Genes and Development*. 11. pp. 996 – 1007.

Kaya, G. et al. 1999. Cutaneous delayed-type hypersensitivity response is inhibited in transgenic mice with keratinocyte-specific CD44 expression defect. *Journal of Investigative Dermatology*. 133 pp. 137 – 138.

Kaya, G. et al. 2000. Decrease in epidermal CD44 expression as a potential mechanism for abnormal hyaluronate accumulation in superficial dermis in Lichen Sclerosus et Atrophis. *Journal of Investigative Dermatology*. 115. pp. 1054 – 1058.

Kennel, S. et al. 1993. CD44 expression on murine tissues. *Journal of Cell Science*. 104 pp. 373 – 382.

Kelly, M. J. and Levin, E. R. 2001. Rapid actions of plasma membrane estrogen receptors. *Trends in Endocrinology and Metabolism*. 12 (4) pp. 152 – 156.

- Kelsey, J. L. et al. 1993. Breast cancer epidemiology: summary and future directions. *Epidemiology Review*. 15 pp. 256 – 263.
- Kelsey, J. and Bernstein, L. 1996. Epidemiology and prevention of breast cancer. *Annual Review of Public Health*. 17 pp. 47 – 67.
- King, M. C. et al. 2003. Breast and ovarian cancer risks due to inherited mutations in BRCA1 and BRCA2. *Science*. 302 (5645) pp. 643 – 646.
- Kim, Y. et al. 2008. CD44-Epidermal growth factor receptor (EGFR) interaction mediates hyaluronan-promoted cell motility by activating protein kinase C signalling involving Akt, Rac1, p38, reactive oxygen species, focal adhesion kinase and MMP-2. *Journal of Biological Chemistry*. 283 (33) pp. 22513 – 22528.
- Kimata, K. et al. 1983. Increased synthesis of hyaluronan by mouse mammary carcinoma cell variants with high metastatic potential. *Cancer Research*. 43 (3) pp. 1347 – 1354.
- Kinashi, T. and Springer. T. 1994. Adhesion molecules in hematopoietic cells. *Blood Cells*. 2- pp. 25 – 44.
- Kischel, P. et al. 2004. Versican overexpression in human breast cancer lesions: known and new isoforms for stromal tumour targeting. *International Journal of Cancer*. 126 (3) pp. 640- 650.
- Kito, H. et al. 2001. Hypermethylation of the CD44 gene is associated with prognosis and metastasis of human prostate cancer. *The Prostate*. 49 (2) pp. 110 – 115.
- Klingbeil, P. et al. 2009. CD44 variant isoforms promote metastasis formation by a tumour cell matrix cross-talk that supports adhesion and apoptosis resistance. *Molecular Cancer Research*. 7 pp. 168 – 179.
- Klingbeil, P. et al. 2010. CD44 is overexpressed in basal like breast cancer but is not a driver of 11p13 amplification. *Breast Cancer Research Treatment*. 120 pp. 95 – 109.
- Klinge, C. M. et al. 2004. Estrogen receptor element-dependent regulation of transcription activation of estrogen receptors alpha and beta by coactivators and corepressors. *Journal of Molecular Endocrinology*. 33 (2) pp. 387 – 410.
- Knowlden, J. et al. 2003. Elevated levels of epidermal growth factor receptor/c-erbB2 heterodimers mediate an autocrine growth regulatory pathway in tamoxifen-resistant MCF-7 cells. *Endocrinology*. 144 (3) pp. 1032 – 1044.
- Knudson, W. et al. 1989. The role and regulation of tumour-associated hyaluronan. *Ciba Foundation Symposium*. 143 pp. 150 – 159.
- Knudson, W. et al. 2002. CD44 mediated uptake and degradation of hyaluronan. *Matrix Biology*. 21 (1) pp. 15 – 23.
- Knutson, J.R 1996. CD44/chondroitin sulphate proteoglycan and $\alpha 2/\beta 1$ integrin mediate human melanoma cell migration on type IV collagen and invasion of basement membranes. *Molecular Biology of the Cell*. 7 pp. 383 – 396.

- Kohda, D. et al. 1996. Solution structure of the link module: a hyaluronan-binding domain involved in extracellular matrix stability and cell migration. *Cell*. 86 pp. 767 – 775.
- Konig, H. et al. 1996. Trans-acting factors regulate the expression of CD44 splice variants. *EMBO Journal*. 15 pp. 4030 – 4039.
- Koopman, G. et al. 1993. Activated human lymphocytes and aggressive non-Hodgkins lymphomas express a homologue of the rat metastasis-associated variant of CD44. *Journal of Experimental Medicine*. 177 pp. 897 – 904.
- Koppe, M. et al. 2004. Safety pharmacokinetics, immunogenicity and biodistribution of ¹⁸⁶re-labelled humanised monoclonal antibody BIWA (Bivatuzumab) in patients with early stage breast cancer. *Cancer Biotherapy and Radiopharmaceuticals*. 19 (6) pp. 720 – 729.
- Kousteni, S. et al. 2001. Non-genotrophic, sex-non-specific signalling through the estrogen and androgen receptors dissociation from transcriptional activity. *Cell*. 104 pp. 719 – 790.
- Kow, L. M. and Pfaff, D. W. 2004. The membrane actions of estrogens can potentiate their lordosis behaviour-facilitating genomic actions. *PNAS USA*. 101 pp. 12354 – 12357.
- Kramer, M. et al. 2011. Association of HA family members (HAS1, HAS2, HYAL1) with bladder cancer diagnosis and prognosis. *Cancer*. 117 pp. 1197 – 1209.
- Kuiper, G. G. et al. 1996. Cloning of a novel estrogen receptor expression in rat prostate and ovary. *PNAS USA*. 93 (12) pp. 5925 – 5930.
- Kuiper, G. G. et al. 1997. Comparison of the ligand binding specificity and transcript tissue distribution of estrogen receptors alpha and beta. *Endocrinology*. 138 (3) pp. 863 – 870.
- Kultti, A. 2009. 4-methylumbelliferone inhibits HA synthesis by depletion of cellular UDP-glucuronic acid and downregulation of HAS2 and HAS3. *Experimental Cell Research*. 315 pp. 1914 – 1928.
- Kumar, V. and Chambon, P. 1988. The estrogen receptor binds tightly to its responsive element as a ligand-induced homodimer. *Cell*. 55 pp. 145 – 156.
- Kuman, R. et al. 1996. Overexpression of HER2 modulates bcl-2, bcl-xl and tamoxifen-induced apoptosis in human MCF-7 breast cancer cells. *Clinical Cancer Research*. 2 (7) pp. 1215 – 1219.
- Kumar, V. et al. 2011. The dynamic structure of the ER. *The Journal of Amino acids*. 812540.
- Kumar, P. et al. 2009. Predicting the effects of coding non-synonymous variants on protein function using the SIFT algorithm. *Nature Protocols*. 4 (7) pp. 1073 – 1081.

Kurokawa, H. et al. 2000. Inhibition of mitogen-activated protein kinases enhances tamoxifen action against Her2-overexpressing, tamoxifen-resistant breast cancer cells. *Cancer Research*. 60 (20) pp. 5887 – 5994.

Kuncova, J. et al. 2005. Expression of CD44v6 correlates with cell proliferation and cellular atypia in urothelial carcinoma cell lines 5637 and HTII97. *Folia Biologica*. 51 (1) pp. 3 – 11.

Kung, C. I. et al. 2012. Enhanced membrane-type 1 matrix metalloproteinase expression by hyaluronan oligosaccharides in breast cancer cells facilitates CD44 cleavage and tumour cell migration. *Oncology Reports*. 28 (5) pp. 1808 – 1814.

Kuniyasu, H. et al. 2001. Heparan sulfate enhances invasion by human colon carcinoma cell lines through expression of CD44 variant exon 3. *Clinical Cancer Research*. 7 pp. 4067 – 4072.

Kuniyasa, H. et al. 2002. Coexpression of CD44v3 and heparanase is correlated with metastasis in human colon cancer. *International journal of molecular medicine*. 10 (3) pp. 333 – 337.

Kunugasa, Y. et al. 2014. CD44 expression on cancer-associated fibroblasts is a functional molecule supporting the stemness and drug resistance of malignant cancer cells in the tumour microenvironment. *Stem Cells*. 32 (1) pp. 145 – 156.

Lammich, S. et al. 2002. Presenilin-dependent intramembrane proteolysis of CD44 leads to the liberation of its intracellular domain and the secretion of an Abeta-like peptide. *Journal of Biological Chemistry*. 277 pp. 44754 – 44759.

Lauritzen, C. and Meier, F. 1984. Risks of endometrial and mammary cancer, morbidity and mortality in long-term oestrogen treatment. *The Climacteric: an update*. pp. 207 – 216.

Lavinsky, R. et al. 1998. Diverse signaling pathways modulate nuclear receptor recruitment of N-CoR and SMRT complexes. *PNAS USA*. 95 pp. 2920 – 2925.

LaVecchia, C. et al. 1985. Menstrual cycle patterns and the risk of breast disease. *European Journal of Cancer*. 21 pp. 417 – 422.

Leach, J. and Schmidt, C. 2004. Hyaluronan. *Encyclopedia of Biomaterials and Biomedical Engineering*. Marcel Dekker, New York pp. 779 – 789.

Lee, J. and Spicer, A. 2000. Hyaluronan: a multifunctional, megaDalton, stealth molecule. *Current Opinion in Cell Biology*. 12 pp. 581 – 586.

Legg et al. 2002. A novel PKC-regulated mechanism controls CD44-ezrin association and directional cell motility. *National Cell Biology*. 4 pp. 399 – 407.

Legg, J. and Isacke, C. 1998. Identification and functional analysis of the ezrin-binding site in the hyaluronan receptor, CD44. *Current Opinion in Cell Biology*. 8 pp. 705 – 708.

- Lengyel, E. et al. 2005. C-met overexpression in node-positive breast cancer identifies patients with poor clinical outcome independent of Her2/neu. *International Journal of Cancer*. 113 (4) pp. 678 – 682.
- Lesley, J. et al. 1992. Requirements for hyaluronan binding by CD44: a role for the cytoplasmic domain and activation by antibody. *Journal of Experimental Medicine*. 175 pp. 257 – 266.
- Lesley, J. et al. 1995. Variant cell lines selected for alterations in the function of hyaluronan receptor CD44 show differences in glycosylation. *Journal of Experimental Medicine*. 182 pp. 431 – 437.
- Lesley, J. et al. 2000. HA binding by cell surface CD44. *The Journal of Biological Chemistry*. 275 (35) pp. 26967 – 26975.
- Lewinsohn, D. et al. 1990. Hematopoietic progenitor cell expression of the H-CAM (CD44) homing-associated adhesion molecule. *Blood*. 75 (3) pp. 589 – 595.
- Lewis, J and Jordan, C. 2005. Selective estrogen receptor modulators (serms): mechanisms of anticarcinogenesis and drug resistance. *Mutation Research*. pp. 247 – 263.
- Li, N. et al. 2000. Analysis of CD44 isoform v10 expression and its prognostic value in renal cell carcinoma. *BJU International*. 85 pp. 514 – 518.
- Li, C. et al. 2007a. Identification of pancreatic cancer stem cells. *Cancer Research*. 67 (3) pp. 1030 – 1037.
- Li, Y. et al. 2007b. Silencing of HAS2 suppresses the malignant phenotype of invasive breast cancer cells. *International Journal of Cancer*. 120 (12) pp. 2557 – 2567.
- Li, C. Z. et al. 2008a. Inhibition of CD44 expression by small interfering RNA to suppress the growth and metastases of ovarian cancer cells in vitro and in vivo. *Folia Biologica*. 54 (6) pp. 180 – 186.
- Li, X. et al. 2008b. Intrinsic resistance of tumourigenic breast cancer cells to chemotherapy. *Journal of the National Cancer Institute*. 100 (9) pp. 672 – 679.
- Li, Z. et al. 2009. Expression of lymphatic vessel endothelial hyaluronan receptor 1 in human colorectal cancer and its clinical significance. *Chinese Journal of Gastrointestinal Surgery*. 12 (5) pp. 511 – 514.
- Li, Q et al. 2011. Jetset: selecting the optimal probe set to represent a gene. *BMC Bioinformatics*. 12 (474).
- Lian Z.Q. et al. 2006. Expression and clinical significance of adhesive molecule CD44v6 in breast invasive ductal carcinoma. *Ai Zheng*. 25 (10) pp. 1291 – 1295.
- Lida, J et al. 2014. DNA aptamers against exonv10 of cd44 inhibit breast cancer cell migration. *PLOS ONE*. 9 (2) pp. 8712.

- Lin, Y-H et al. 2000. Coupling of osteopontin and its cell surface receptor CD44 to the cell survival response elicited by interleukin-3 or granulocyte-macrophage colony stimulation factor. *Molecular Cell Biology*. 20 (8) pp. 2734 – 2742.
- Link, L. B. et al. 2013. Dietary patterns and breast cancer risk in the California teachers study cohort. *American Journal of Clinical Nutrition*. 98 (6) pp. 1524 – 1532.
- Liehr, J. 2000. Is estradiol a genotoxic mutagenic carcinogen? *Endocrine Reviews*. 21 (1) pp. 40 – 54.
- Llangumaran, S. et al. 1998. CD44 selectively association with active src family protein tyrosine kinases lck and fyn in glycosphingolipid-rich plasma-membrane domains of human peripheral blood lymphocytes. *Blood*. 91 (10) pp. 3901 – 3908.
- Lokeshwar, B. L. et al. 1995. Expression of CD44 in prostate cancer cells: association with cell proliferation and invasive potential. *Anticancer Research*. 15 (4) pp. 1191 – 1198.
- Lokeshwar, V. B. et al. 2000. Urinary hyaluronan and hyaluronidase: markers for bladder cancer detection and evaluation for grade. *Journal of Urology*. 163 (1) pp/ 348 – 356.
- Lokeshwar, V. B. et al. 2001. Stromal and epithelial expression of tumour markers hyaluronan and HYAL1 in prostate cancer. *Journal of Biological Chemistry*. 276 pp. 11922 – 11932.
- Lokeshwar, V. B. and Bourguignon, L. Y. 1992. The lymphoma transmembrane glycoprotein GP85 (CD44) is a novel guanine nucleotide-binding protein which regulates GP85 (CD44)-ankyrin interaction. *Journal of Biological Chemistry*. 267 pp. 22073 – 22078.
- Lonard, D. M. et al. 2004. Selective estrogen receptor modulators 4-hydroxytamoxifen and raloxifene impact the stability and function of SRC-1 and SRC-3 coactivator proteins. *Molecular Cellular Biology*. 24 (1) pp. 14 – 24.
- Long, B. et al. 1992. Changes in epidermal receptor growth factor expression and response to ligand associated with acquired tamoxifen resistance or oestrogen independence in the ZR-75-1 human breast cancer cell line. *British Journal of Cancer*. 65 pp. 865 – 869.
- Lonning, P. et al. 2003. Pharmacokinetics of third generation aromatase inhibitors. *Seminars in Oncology*. 30 pp. 23 – 32.
- Looi, L. M et al. 2006. CD44 expression and axillary lymph node metastasis infiltrating ductal carcinoma of the breast. *The Malaysian journal of pathology*. 28 (2) pp. 83 – 86.
- Lopez, J. I. et al 2005. CD44 attenuates metastatic invasion during breast cancer progression. *Cancer Research*. 65 (1) pp 6755 – 6763.

Louderbough, J. M. V. et al. 2011. CD44 promotes epithelial mammary gland development and exhibits altered localisation during cancer progression. *Genes and Cancer*. 2 (8) pp. 771 – 781.

Lowry, O. H. et al. 1951. Protein measurement with the Folin phenol reagent. *Journal of Biological Chemistry*. 193 (1) pp. 265 – 275.

Lui, S. et al. 2005. Expression and significance of CD44s, CD44v6 and nm23 mRNA in human cancer. *World Journal of Gastroenterology*. 11 (42) pp. 66011 – 6606.

Lui, C. et al. 2011. Identification of miR-34a as a potent inhibitor of prostate cancer progression and metastasis by directly repressing CD44. *National Medicine*. 17 (2) pp. 211 – 215.

Lui, Y. et al. 2011. Dual-targeting folate-conjugated hyaluronic-acid polymeric micelles for paclitaxel delivery. *Investigative Journal of Pharmaceuticals*. 421 (1) pp. 160 – 169.

Ma et al. 2005. The prognostic value of adhesion molecule CD44v6 in women with primary breast carcinomas: a clinicopathologic study. *Clinical Oncology (Royal College of Radiology (GB))*. 17 (4) pp. 258 – 263.

MacGregor-Schafer, J. et al. 2000. Rapid development of tamoxifen stimulated mutant p53 breast tumours (T47D) in athymic mice. *Clinical Cancer Research*. 6 pp. 4373 – 4380.

Mackay et al. 1994. Expression and modulation of CD44 variant isoforms in humans. *Journal of Cell Biology*. 124 pp. 71 – 82.

MacKallip, R. J. et al. 2002. Role of CD44 in activation-induced cell death: CD44-deficient mice exhibit enhanced T cell response to conventional and superantigens. *International Immunology*. 14 (9) pp. 1015 – 1020.

Manzanares, D. et al. 2007. Apical oxidative HA-degradation stimulates airway ciliary beating via RHAMM and RON. *American Journal of Respiratory Cell Molecular Biology*. 37 (2) pp 160 – 168.

Marcherl-Bauer, A. et al. 2015. CDD: NCBI's conserved domains database. *Nucleic Acids Research*. 43 (D) 222 – 226.

Marhaba et al. 2005. CD44v6 promotes proliferation by persisting activation of MAP Kinases. *Cell Signalling*. 17 pp. 961 – 973.

Marshall, L. et al. 1997. Risk of breast cancer associated with atypical hyperplasia of lobular and ductal types. *Cancer Epidemiology Biomarkers and Prevention*. 6 (5) pp. 297 – 301.

Martegani, M. P et al. 1999. Structural variability of CD44v molecules and reliability of immunodetection of CD44 isoforms using mAbs specific for CD44 variant exon products. *American Journal of Pathology*. 154 (1) pp. 291 – 300.

- Martin et al. 2003. The role of the CD44/Ezrin complex in cancer metastasis. *Critical Review of Oncology and Hematology*. 46 pp. 165 – 168.
- Marzese, D. M. et al. 2014. Brain metastasis is predetermined in early-stages of cutaneous melanoma by CD44v6 expression through epigenetic regulation of the spliceosome. *Pigment and Melanoma research*. 28 (1) pp. 82 – 93.
- Massarweh et al. 2006. Mechanisms of tumour regression and resistance to estrogen deprivation and fulvestrant in a model of estrogen receptor – positive, HER-2/neu-positive breast cancer. *Cancer Research*. 66 (16) pp. 8266 – 8273.
- Massarweh, S. et al. 2008. Tamoxifen resistance in breast cancer is driven by estrogen receptor genomic function receptor signalling with repression of classic estrogen receptor genomic function. *Cancer Research*. 68 pp. 826 – 833.
- Matter et al. 2002. Signal-dependent regulation of splicing via phosphorylation of sam68. *Nature*. 420 (6916) pp. 615 – 186.
- Matthews, J. and Gustafsson, J. A. Estrogen signalling: a subtle balance between Estrogen receptor alpha and ER alpha and ER beta. *Molecular Interventions*. 3 (5) pp. 281 – 292.
- Matze, A. et al. 2007. Haploinsufficiency of c-met in CD44 $-/-$ mice identifies a collaboration of CD44 and c-met in vivo. *Molecular and Cellular Biology*. 27 (24) pp. 8797 – 8806.
- Maxwell, C. et al. 2003. RHAMM is a centrosomal protein that interacts with dynein and maintains spindle pole stability. *Molecular Biology of the Cell*. 14 pp. 2262 – 2276.
- Maxwell, C. A. et al. 2004. RHAMM expression and isoform balance predict aggressive disease and poor survival in multiple myeloma. *Blood*. 104 (4) pp. 1151 – 1158.
- Maxwell, C. A. et al. 2008. Cell-surface and mitotic-spindle RHAMM: moonlighting or dual oncogenic functions? 121 (7) pp. 925 – 932.
- Maxwell, C. A. et al. 2011. Interplay between BRCA1 and RHAMM regulates epithelial apicobasal polarisation and may influence risk of breast cancer. *PLOS-Biology*. 9 (11). e1001199.
- McClelland, R. et al. 1996. Effects of short-term antiestrogen treatment of primary breast cancer on estrogen receptor mRNA and protein expression and on estrogen-regulated genes. *Breast Cancer Research Treatment*. 41 pp. 31 – 41.
- McClelland, R. et al. 2001. Enhanced epidermal growth factor receptor signalling in MCF-7 breast cancer cells after long-term culture in the presence of the pure antiestrogen ICI 182 780 (Faslodex). *Endocrinology*. 142 pp. 2776 – 2788.
- McDonnel, D. P. et al. 1995. Analysis of ER function in vitro reveals three distinct classes of anti-oestrogens. *Molecular Endocrinology*. 9 pp. 659 – 669.

- McDonnel, D. P. 1999. The molecular pharmacology of SERMs. *Trends in Endocrinology and Metabolism*. 10 (8) pp. 301 – 311.
- McGowan, P. M. et al. 2011. Notch1 inhibitor alters the CD44^{hi}/CD44^{lo} population and reduces the formation of brain metastases from breast cancer. *Molecular Cancer Research*. 9 (7) pp. 834 – 844.
- McGuire et al. 1992. Size dependent hyaluronate degradation by cultured cells. *Journal of Cellular Physiology*. 133. pp. 267 – 276.
- McKenna, N. Y. et al. 1999. Nuclear receptor coregulators: cellular and molecular biology. *Endocrinology Reviews*. 20 pp. 321 – 344.
- McKenna, N. Y. and O'Malley, B. W. 2001. Nuclear receptors, coregulators, ligands and selective estrogen receptor modulators: making sense of the patchwork quilt. *Annals of the New York Academy of Sciences*. 949 pp. 3 – 5.
- Menard, S. et al. 2001. HER2 overexpression in various tumour types focussing on its relationship to the development of invasive breast cancer. *Annals of Oncology*. 12 (1) pp. 15 – 19.
- Metivier, R. et al. 2003. Estrogen receptor-alpha directs ordered, cyclical and combinatorial recruitment of cofactors on a natural target promoter. *Cell*. 115 (6) pp. 751 – 763.
- Metzger, D. et al. 1995. Conditional site-specific recombination in mammalian cells using a ligand-dependent chimeric cre recombinase. *PNAS USA*. 92 (15) pp. 6991 – 6995.
- Mi, H. et al. 2013a. PANTHER classification system. Large-scale gene functional analysis with the PANTHER classification system. *Nature Protocols*. 8 pp. 1511 – 1566.
- Mi, H. et al. 2013b. PANTHER in 2013: Modelling the evolution of gene function and other gene attributes in the context of phylogenetic trees. *Nucleic Acids Research*. D377 – 86.
- Michaud, L. B et al. 2001. Combination endocrine therapy in the management of breast cancer. *Oncologist*. 6 pp. 538 - 546.
- Mielgo, A. et al. 2006. A novel anti-apoptotic mechanism based on interference of Fas signalling by CD44 variant isoforms. *Cell Death and Differentiation*. 13 pp. 465 – 477.
- Mielgo, A. et al. 2007. The CD44 standard/ezrin complex regulates Fas-mediated apoptosis in Jurkat cells. *Apoptosis*. 12 pp. 2051 – 2066.
- Mio, K. and Stern, S. 2002. Inhibitors of the hyaluronidases. *Matrix Biology*. 21 (1) pp. 31 – 37.
- Miletti-Gonzalez, K. E. et al. 2005. The CD44 receptor interacts with P-glycoprotein to promote cell migration and invasion in cancer. *Cancer Research*. 65 pp. 6660 – 6667.

- Miller, W. R. 2003. Aromatase inhibitors: mechanism of action and role in the treatment of breast cancer. *Seminars in Oncology*. 30 pp. 3 – 11.
- Misra, S. et al. 2011. Hyaluronan-CD44 interaction as potential targets for cancer therapy. 278 (9) pp. 1429 – 1143.
- Montgomery, N. et al. 2012. CD44 enhances invasion of basal-like breast cancer cells by upregulating serine proteases and collagen-degrading enzymatic expression and activity. 14 (3). R84.
- Moras, D. and Gronemeyer, H. 1998. The nuclear receptor ligand-binding domain: structure and function. *Current Opinion in Cell Biology*. 10 pp. 384 – 391.
- Morgan, L. et al. 2009. Elevated Src kinase activity attenuates tamoxifen response in vitro and is associated with poor prognosis clinically. *Cancer Biology and Therapy*. 8 (16) pp. 1550 – 1558.
- Morimoto, L. M. et al. 2002. Obesity, body size and risk of postmenopausal breast cancer: the women's health initiative (U.S). *Cancer Causes and Control*. 13 (8) pp. 741 – 751.
- Morris, S. F. et al. 2001. The prognostic significance of CD44s and CD44v6 in stage 2 breast carcinomas: an immunohistochemistry study. *European Journal of Surgical Oncology*. 27 (6) pp. 527 – 531.
- Morrison, H. et al. 2001. The NF2 tumour suppressor gene product, merlin, mediates contact inhibition through interactions with CD44. *Genes and Development*. 15 pp. 968 – 980.
- Mosselman, S. et al. 1996. ER beta: identification and characterisation of a novel human estrogen receptor. *FEBS Letters*. 392 (1) pp. 49 – 53.
- Muchmore, D. B. 2000. Raloxifene: A selective estrogen receptor modulator (SERM) with multiple target system effects. *Oncologist*. 5 (5) pp. 388 – 392.
- Muller et al. 1997. Expression and prognosis value of the CD44 splicing variants v5 and v6 in gastric cancer. *Journal of Pathology*. 185 pp. 222 – 227.
- Murakami, D. et al. 2003. Presenilin-dependent gamma secretase activity mediates the intramembraneous cleavage of CD44. *Oncogene*. 22 pp. 1511- 1516.
- Murai, T. et al. 2004. CD44-chondroitin sulphate interactions mediate leukocyte rolling under physiological conditions. *Immunology Letters*. 93 (2 – 3) pp. 163 – 170.
- Musgrove, E. A. and Sunderland, R. L. 2009. Biology determinants of endocrine resistance in breast cancer. *National Reviews in Cancer*. 9 pp. 631 – 643.
- Mylona, E. et al. 2006. CD44 regulates myoblast migration and differentiation. *Journal of Cellular Physiology*. 209 (2) pp. 314 – 231.
- Nagano, O. et al. 2004. Cell matrix interaction via CD44 is independently regulated by different metalloproteinases activated in response to Extracellular Ca²⁺ influx and PKC activation. *Journal of Cell Biology*. 165 (6) pp. 893 – 902.

- Nagasaki, K. and Miki, Y. 2006. Gene expression profiling of breast cancer. *Breast Cancer*. 13 (1) pp. 2 – 7.
- Naor, D. et al. 1997. CD44: structure, function and association with the malignant process. *Advanced Cancer Research*. 71 pp. 241 – 319.
- Naor, D. et al. 2002. CD44 in cancer. *Critical Review of Clinical Laboratory Science*. 39 pp. 527 – 579.
- Neame, S. et al. 1995. CD44 exhibits a cell type dependent interaction with triton C-100 insoluble, lipid rich, plasma membrane domains. *Journal of Cell Science*. 108 pp. 3127 – 3125.
- Neame, S. and Isake, C. 1993. The cytoplasmic tail of CD44 is required for basolateral localisation in epithelial MDCK cells but does not mediate association with the detergent insoluble cytoskeleton of fibroblasts. *Journal of Cell Biology*. 121 pp. 1299 – 1310.
- Nedvetski, S. et al. 2004. RHAMM, a receptor for HA-mediated motility, compensates for CD44 in inflamed CD44 knockout mice: a different interpretation of redundancy. *PNAS USA*. 101 (52) pp. 18081 – 18086.
- Negi, L. et al. 2012. Role of CD44 in tumour progression and strategies for targeting. *Journal of Drug Targeting*. 20 (7) pp. 561 – 573.
- Negri, E. et al. 1990. Age at first birth and second births and breast cancer risk in biparous women. *International Journal of Cancer*. 45 pp. 428 – 430.
- Ng, K. C. et al. 1992. The extracellular processing and catabolism of hyaluronan in cultured adult articular cartilage explants. *Arch Biochemistry and Biophysics*. 298. pp. 70 – 79.
- Ng, P. C. and Heinikoff, S. 2006. Predicting the effects of amino acid substitutions on protein function. *Annual Review of Genomics and Human Genetics*. 7 pp. 61 – 80.
- Ni, J. et al. 2014. CD44 variant 6 is associated with prostate cancer metastasis and chemo-/radioresistance. *The Prostate*. 74 (6) pp. 602 – 617.
- Nicholson, R. et al. 1993. Relationship between EGF-R and c-erbB-2 protein expression and Ki67 immunostaining in breast cancer and hormonal sensitivity. *European Journal of Cancer*. 29A pp. 1018 – 1023.
- Nicholson, R. et al. 1995. Responses to pure antiestrogens (ICI 164384, ICI 182780) in estrogen-sensitive and -resistant experimental and clinical breast cancer. *Annals of the New York Academy of Sciences*. 761 pp. 148 – 163.
- Nicholson, R. et al. 1999. Involvement of steroid hormone and growth factor cross-talk in endocrine response in breast cancer. *Endocrine Related Cancer*. 6 pp. 373 – 387.
- Nicholson, R. et al. 2001. EGFR and cancer prognosis. *European Journal of Cancer*. 4 pp. 9 – 15.

- Nicholson, R. et al. 2004. Growth factor-driven mechanisms associated with resistance to estrogen deprivation in breast cancer: new opportunities for therapy. *Endocrine-Related Cancer*. 11 pp. 623 – 641.
- Norfleet, A. M. et al. 1999. Estrogen receptor-alpha detected on the plasma membrane of aldehyde-fixed GH2/B6/F10 rat pituitary tumour cells by enzyme-linked immunocytochemistry. *Endocrinology*. 120 pp. 3805 – 3814.
- Normanno, N. et al. 2005. Mechanisms of endocrine resistance and novel therapeutic strategies in breast cancer. *Endocrine-Related Cancer*. 12 pp. 721 – 747.
- Nykopp, T. et al. 2010. HA synthases (HAS1 – 3) and hyaluronidases (HYAL1 – 2) in the accumulations of HA in endometrial carcinoma. *BMC Cancer*. 10 pp. 512.
- Okada, M. et al. 2009. AKT phosphorylation of Merlin enhances its binding to phosphatidylinositol and inhibits tumour suppressive activities of Merlin. *Cancer Research*. 69 (9) pp. 4043.
- Okamoto, I. et al. 1999. Regulated CD44 cleavage under the control of protein kinase C, calcium influx and the Rho family of small G proteins. *Journal of Biological Chemistry*. 274. Pp. 25525 – 25534.
- Okamoto, I. et al. 2001. Proteolytic release of CD44 intracellular domain and its role in the CD44 signalling pathway. *Journal of Cell Biology*. 155 (5) pp. 755 – 762.
- Okasha, M. et al. 2003. Exposures in childhood, adolescence and early adulthood and breast cancer risk: a systemic review of the literature. *Breast Cancer Research Treatment*. 78 pp. 223 – 276.
- Oksala, O. et al. 1995. Expression of proteoglycans and hyaluronic acid during wound healing. *Journal of Histochemistry and Cytochemistry*. 43 (2) pp. 125 – 135.
- Okuda, H. et al. 2012. HA synthase (HAS2) promotes tumour progression in bone stimulating the interaction of breast cancer stem-like cells with macrophages and stromal cells. *Cancer Research*. 72 pp. 537 – 547.
- O'loné, R. et al. 2004. Genomic targets of nuclear estrogen receptors. *Molecular Endocrinology*. 18 (8) pp. 1859 – 1875.
- Oliferenko, S. et al. 2000. Hyaluronic acid (HA) binding to CD44 activates Rac1 and induces lamellipodia outgrowth. *Journal of Cell Biology*. 148 (6) pp. 1159 – 1164.
- Olson Jr, J. A. et al. 2009. Improved surgical outcomes for breast cancer patients receiving neoadjuvant aromatase inhibitor therapy: results from a multicentre phase II trial. *Journal of the American College of Surgeons*. 208 pp. 906 – 914.
- Olsson, E. et al. 2011. CD44 isoforms are heterogeneously expressed in breast cancer and correlate with tumour subtypes and cancer stem cell markers. *BMC Cancer*. 11 pp. 1 – 13.
- Orian-Roussaeu, V. et al. 2002. CD44 is required for two consecutive steps in HGF/c-met signalling. *Genes and Development*. 16 (23) pp 3074 – 3086.

Osborne, C. K. et al. 1994. The importance of tamoxifen metabolism in tamoxifen-stimulated breast tumour growth. *Cancer Chemotherapy and Pharmacology*. 34 pp. 89 – 95.

Osborne, C. K. e al. 1995. Comparison of the effects of a pure steroidal antioestrogen with those of tamoxifen in a model of human breast cancer. *Journal of the National Cancer Institute*. 87 pp. 746 – 750.

Osborne, C. K et al. 2002. Double-blind, randomized trial comparing the efficacy and tolerability of fulvestrant versus anastrozole in postmenopausal women with advanced breast cancer progressing on prior endocrine therapy: results of a North American trial. *Journal of Clinical Oncology*. 20 pp. 3386-3395.

Osborne, E. and Schiff, R. 2003. Growth factor receptor cross-talk with estrogen receptor as a mechanism for tamoxifen resistance in breast cancer. *The Breast*. 12 pp. 362 – 367.

Osipo, C. et al. 2007. Role of Her2/neu and Her3 in fulvestrant-resistant breast cancer. *International Journal of Oncology*. 30 pp. 509 – 520.

Ouhtit, A. et al. 2013. TGF- β 2: A novel target of CD44-promoted breast cancer invasion. *Journal of Cancer*. 4 (7) pp. 566 – 572.

Paech, K. et al. 1997. Differential ligand activation of estrogen receptors ER α and ER β at AP1 sites. *Science*. 227 (5331) pp. 1508 – 1510.

Palyi-Krekk, Z. et al. 2008. EGFR and ErbB2 are functionally coupled to CD44 and regulate shedding, internalisation and motogenic effects of CD44. *Cancer Letters*. 263 pp. 231 – 242.

Park, K. et al. 2008. Role of hyaluronan in glioma invasion. *Cell Adhesion and Migration*. 2 (3) pp. 202 - 207.

Parker, M. G. 1993. Action of 'pure' antiestrogens in inhibiting estrogen receptor action. *Breast Cancer Research Treatment*. 26 pp. 131 – 137.

Parkin, M. and Fernandez, L. 2006. Use of statistics to assess the global burden of breast cancer. *The Breast Journal*. 12 (1) pp. 70 – 80.

Parise, C. et al. 2009. Breast cancer subtypes as defined by the estrogen receptor (ER), progesterone receptor (PR), and the human epidermal growth factor receptor 2 (HER2) among women with invasive breast cancer in california, 1999 – 2004. *The Breast Journal*. (6) 593 – 602.

Paruthiyil, S. et al. 2004. Estrogen receptor beta inhibits human breast cancer cell proliferation and tumour formation by causing a G2 cell cycle arrest. *Cancer Research*. 64 (1) pp. 423 – 428.

Pawlak, J. et al. 2005. Estrogen receptor-alpha is associated with the plasma membrane of astrocytes and coupled to MAP/Src kinase pathway. *Glia*. 50 (3) pp. 270 – 275.

- Pearce, S. and Jordan, V. et al. 2004. The biological role of estrogen receptors alpha and beta in cancer. *Critical Review of Oncology and Hematology*. 50 pp. 3 – 22.
- Pearson, M. et al. 2000. Structure of the ERM protein moesin reveals the FERM domain fold masked by an extended actin binding tail domain. *Cell*. 101 pp. 259 – 270.
- Pelchen-Matthews, A. et al. 1991. Differential endocytosis of CD44 in lymphocytic and non-lymphocytic cells. *Journal of Experimental Medicine*. 173 pp. 575 – 587.
- Perey, L. 2004. Fulvestrant (Faslodex) as hormonal treatment in postmenopausal patients with advanced breast cancer (ABC) progressing after treatment with tamoxifen and aromatase inhibitors: update of a phase II SAKK trial. *Breast Cancer Research and Treatment*. 88(Suppl 1): S236, (abstract 6048).
- Perez-Tenorio, G. et al. 2006. Cytoplasmic p21 WAF1/CIP1 correlates with AKT activation and poor response to tamoxifen in breast cancer. *International Journal of Oncology*. 28 pp. 1031 – 1042.
- Perou, C. M. et al. 2000. Molecular portraits of human breast tumours. *Nature*. 406 pp. 742 – 752.
- Perschl et al. 1995. Role of CD44 cytoplasmic domain in hyaluronan binding. *European Journal of Immunology*. 25. pp. 495 – 501.
- Peterson, G. L. 1977. A simplification of the protein assay method of Lowry et al. which is more generally applicable. *Analytical Biochemistry*. 83 (2) pp. 346 – 356.
- Peyssonnaud, C. and Eychenne, A. 2001. The Raf/MEK/ERK pathway: new concepts of activation. *Biology of the Cell*. 93 pp. 53 – 62.
- Pham, P. V. et al. 2011. Differentiation of breast cancer stem cells by knockdown of CD44: promising differentiation therapy. *Journal of Translational Medicine*. 7 (9) pp. 209.
- Phillips, T. M. et al. 2006. The response of CD24^{-/low}/CD44⁺ breast cancer initiating cells to radiation. *Journal of National Cancer Institute*. 98 (24) pp. 1777 – 1785.
- Pietras, A. et al. 2014. Osteopontin-CD44 signalling in the glioma perivascular niche enhances cancer stem cell phenotype and promotes aggressive tumour growth. *Cell Stem Cell*. 14 (3) pp. 357 – 369.
- Pike, M. C. et al. 1993a. Estrogens, progesterones, normal breast cancer proliferation and breast cancer risk. *Epidemiologic Reviews*. 15 (1) pp. 17 – 35.
- Pike, A. et al. 1993b. Structural insights into the mode of action of a pure antiestrogen. *Structure*. 9 pp. 145 – 153.
- Pink, J. and Jordan, V. 1996. Models of estrogen receptor regulation by estrogens and antiestrogens in breast cancer cell lines. *Cancer Research*. 56 pp. 2321 – 2330.

- Pirinen, R. et al. 2001. Prognostic value of hyaluronan expression in non-small-cell lung cancer: increased stromal expression indicates unfavourable outcome in patients with adenocarcinoma. *International Journal of Cancer*. 95 (1) pp. 2 – 7.
- Ponta et al. 2003. CD44: from adhesion molecules to signalling regulators. *Nature Review of Molecular Cell Biology*. 4 pp. 33 – 45.
- Ponti, D. et al. 2006. Breast cancer stem cells: an overview. *European Journal of Cancer*. 42. Pp. 1219 – 1224.
- Posey, T. J. et al. 2003. Evaluation of the prognostic potential of HA and hyaluronidase (HYAL-1) for prostate cancer. *Cancer Research*. 63 pp. 2638 – 2644.
- Potischman, N. and Troisi, R. 1999. In-utero and early life exposures in relation to risk of breast cancer. *Cancer Causes and Control*. 10 (6) pp. 561 – 573.
- Potapova, T. A. et al. 2011. Mitotic progression becomes irreversible in prometaphase and collapses when Wee1 and Cdc25 are inhibited. *Molecular Biology of the Cell*. 22 pp. 1191 – 1206.
- Powell, E. and Xu, W. 2008. Intermolecular interactions identify ligand selective activity of estrogen receptors α/β dimers. *PNAS USA*. 105 (48) PP. 19012 – 19017.
- Preston-Martin, S. et al 1990. Increased cell division as a cause of human cancer. *Cancer Research*. 50 pp. 7415 – 7421.
- Protin, U. et al. 1999. CD44-deficient mice develop normally with changes in subpopulations and recirculation of lymphocyte subsets. *Journal of Immunology*. 163 (9) pp. 4917 – 4923.
- Pure, E. and Cuff, A. 2001. A crucial role for CD44 in inflammation. *Trends in Molecular Medicine*. 7 pp. 213 – 221.
- Qhattal, H. S and Lui, S.X. 2011. Characterisation of CD44 mediated cancer cell uptake and intracellular distribution of hyaluronan-grafted liposomes. *Molecular Pharmacology*. 8 (4) pp. 1233 – 1246.
- Qian, C. et al. 2013. Suppression of pancreatic tumour growth by targeted arsenic delivery with anti-CD44v6 single chain antibody-conjugated nanoparticles. *Biomaterials*. 34 (26) pp. 6175 – 6184.
- Qui, J. et al. 2003. Rapid signalling of estrogen in hypothalamic neurons involves a novel G-protein-couple estrogen receptor that activates protein kinase C. *Journal of Neuroscience*. 23 (29) pp. 9529 – 9540.
- Raghav, K. P. et al. 2012. c-MET and phospho-cMET protein levels in breast cancers and survival outcomes. *Clinical Cancer Research*. 18 (8) pp. 2269 – 2277.
- Reed, K. C. and Ohno, S. 1976. Kinetic properties of human placental aromatase. Application of an assay measuring $3\text{H}_2\text{O}$ release from 1beta,2beta- 3H -androgens. *Journal of Biological Chemistry*. 251 (6) pp. 1625 – 1631.

- Reis-Filho, J. S. et al. 2006. EGFR amplification and lack of activating mutations in metaplastic breast carcinomas. *Journal of Pathology*. 209 pp. 445 – 453.
- Renehan, A. et al. 2004. Insulin-like growth factor (IGF)-1, IGF binding protein-3 and cancer risk: systematic review and meta-regression analysis. *Lancet*. 363 pp. 1346 – 1353.
- Ricciardelli, C. et al. 2002. Regulation of stromal versican expressed by breast cancer cells and importance to relapse-free survival in patients with node-negative primary breast cancer. *Clinical Cancer Research*. 8 (4) pp. 1054 – 1060.
- Rimm, D. L. et al. 2001. Amplification of tissue by construction of microarrays. *Experimetal Molecular Pathology*. 70 pp. 225 – 264.
- Roa, B. et al. 1996. Ashkenazi Jewish population frequencies for common mutations in BRCA1 and BRCA2. *National Genetics*. 14 pp/ 185 – 187.
- Rooney, P. et al. 1995. The role of hyaluronan in tumour neovascularization (Review). *International Journal of Cancer*. 60 (5) pp. 632 – 636.
- Robertson, J. et al. 2001. Comparison of the short-term biological effects of 7alpha-(9-(4,4,5,5,5-pentafluoropentylsulfinyl)-nonyl)-estra-1,3,5, (10)-triene-3, 17beta-diol (Faslodex) versus tamoxifen in postmenopausal women with primary breast cancer. *Cancer Research*. 61 pp. 6738 – 6746.
- Robertson, J. 2003. Fulvestrant versus anastrozole for the treatment of advanced breast carcinoma in postmenopausal women: a prospective combined analysis of two multicenter trials. *Cancer*. 98 pp. 229-238
- Robertson, J. 2005. Endocrine treatment options for advanced breast cancer – the role of fulvestrant. *European Journal of Cancer*. (41) pp. 346 – 356.
- Robertson, J. 2009. Activity of fulvestrant 500 mg versus anastrozole 1 mg as first-line treatment for advanced breast cancer: results from the FIRST study. *Journal of Clinical Oncology*. 27 pp. 4530-4535.
- Rohan, T. E. et al. 2013. Body fat and breast cancer risk in postmenopausal women: a longitudinal study. *Journal of Cancer Epidemiology*. 754815.
- Rosette, C. et al. 2005. Role of ICAM-1 in invasion of human breast cancer cells. *Carcinogenesis*. 26 (5) pp. 943 – 950.
- Rossbach, H. C. et al. 1996. An antibody to CD44 enhances hematopoiesis in long-term narrow cultures. *Experimental Hematology*. 24 (2) pp. 221 – 227.
- Rudzki, Z. and Jothy, S. 1997. CD44 and the adhesion of neoplastic cells. *Molecular Pathology*. 50 pp. 57 – 71.
- Ryffel, G. et al. 1998. The estrogen responsive DNA element: structure and interaction with the estrogen receptor. *Journal of Steroid Biochemistry*. 35 pp. 219 – 222.

- Rys, J. et al. 2003. The role of CD44v3 expression in female breast carcinomas. *Pathology*. 54 pp. 243 – 247.
- Sahlberg, S. H. et al. 2014. Evaluation of cancer stem cell markers CD133, CD44, CD24: association with AKT isoforms and radiation resistance in colon cancer cells. *PLOS one*. 9 (4) e94621.
- Saito, S. et al. 2013. CD44v6 expression is related to mesenchymal phenotype and poor prognosis in patients with colorectal cancer. *Oncology Reports*. 29 (4) pp. 1570 – 1578.
- Savani, R. C. et al. 2001. Differential involvement of hyaluronan (HA) receptors CD44 and receptor for HA-mediated motility in endothelial cell function and angiogenesis. *Journal of Biological Chemistry*. 276 (39) pp. 36770 – 36778.
- Savkur, R. and Burris, T. 2004. The coactivator LXXLL nuclear receptor recognition motif. *The Journal of Peptide Research*. 63 (3) pp. 207 – 212.
- Schiff, R. et al. 2003. Breast cancer endocrine resistance: how growth factor signalling and estrogen receptor coregulators modulate response. *Clinical Cancer Research*. 9 pp. 447 – 454
- Schmits, R. et al. 1997. CD44 regulates hematopoietic progenitor distribution, granuloma formation and tumorigenicity. *Blood*. 90 (6) pp. 2217 – 2233.
- Schrag, D. et al. 2000. Life expectancy gains from cancer prevention strategies for women with breast cancer and BRCA1 or BRCA2 mutations. *JAMA*. 283 (5) pp. 617 – 624.
- Schwabe, J. et al. 1993. The crystal structure of the estrogen receptor DNA-binding domain bound to DNA: how receptors discriminate between their response elements. *Cell*. 75 pp. 567 – 578.
- Screaton, G. et al. 1992. Genomic structure of DNA encoding the lymphocyte homing receptor CD44 reveals at least 12 alternatively spliced exons. *PNAS USA*. 89 PP. 12160 – 12164.
- Screaton, G. et al. 1993. The identification of a new alternative exon with highly restricted tissue expression in transcripts encoding the mouse Pgp-1 (CD44) homing receptor: comparison of all 10 variable exons between mouse, human and rat. 286 pp. 12235 – 12238.
- Seiter, S. et al. 1993. Prevention of tumour metastasis formation by anti-variant CD44. *Journal of Experimental Medicine*. 177 pp. 443 – 455.
- Shah, N. G. et al. 2010. CD44v6 expression in primary breast carcinoma in western India: a pilot clinicopathologic study. *Tumorigenesis*. 96 (6) pp. 971 – 977.
- Shang, Y. and Brown, M. 2002. Molecular determinants for the tissue specificity of SERMs. *Science*. 295 pp 5564.

- Sheridan, C. et al. 2006. CD44⁺/CD24⁻ breast cancer cells exhibit enhanced invasive properties: an early step necessary for metastasis. *Breast Cancer Research*. 8 (5).
- Sherman, L. et al. 1994. Hyaluronate receptors: key players in growth, differentiation, migration and tumour progression. *Current Opinions in Cellular Biology*. 6 pp. 726 – 733.
- Sherman, L. et al. 1996. The CD44 proteins in embryonic development and in cancer. *CMTI*. 213 pp. 249 – 269.
- Sherman, L. et al. 1998. A splice variant of CD44 expressed in the apical ectodermal ridge presents fibroblast growth factors to limb mesenchyme and is required for limb outgrowth. *Genes and Development*. 12 pp. 1058 – 1071.
- Shi, L. et al. 2009. Expression of ER α 36, a novel variant estrogen receptor α and resistance to tamoxifen treatment in breast cancer. *Journal of Clinical Oncology*. 27 (21) pp. 3423 – 3429.
- Shi, C. et al. 2010. CD44⁺ CD133⁺ population exhibits cancer stem cell-like characteristics in human gallbladder carcinoma. *Cancer Biology Therapeutics*. 10 (11) pp. 1182 – 1190.
- Shi, J. et al. 2013. Correlation of CD44v6 expression with ovarian cancer progression and recurrence. *BMC cancer*. 13 (182) pp. 1 – 10.
- Shtivelman, E. and Bishop, J. M. 1991. Expression of CD44 is repressed in neuroblastoma cells. *Molecular Cell Biology*. 11 (11) S446 – S453.
- Shou, J. et al. 2004. Mechanisms of tamoxifen resistance: increased estrogen receptor-her2/neu cross-talk in ER/Her2-positive breast cancer. *Journal of the National Cancer Institute*. 96 (12) pp. 926 – 935.
- Simpson, E. R. et al. 1992. Aromatase cytochrome P-450, the enzyme responsible for estrogen biosynthesis. *Endocrinology Review*. 15 (3) pp. 342 – 355.
- Simpson, E. et al. 1997. Aromatase expression in health and disease. *Recent Progress in Hormone Research*. 52 pp. 185 – 213.
- Simpson, M. A. et al. 2002. Inhibition of prostate tumour cell hyaluronan synthesis impairs subcutaneous growth and vascularisation in immunocompromised mice. *American Journal of Pathology*. 161 (3) pp. 849 – 857.
- Simpson, M. A and Lokeshwar, V.B, 2008. Hyaluronan and hyaluronidase in gastrourinary tumours. *Frontiers in Bioscience*. 13 pp. 5664 – 5680.
- Singh, R. and Kumar, R. 2005. Steroid hormone receptor signalling in tumorigenesis. *Journal of Biological Chemistry*. 96 pp. 490 – 505.
- Singleton, P. and Bourguignon, L. 2002. CD44v10 interaction with Rho-Kinase (ROK) activates Inositol 1, 4, 5 Triphosphate (IP3) receptor-mediated Ca²⁺ signalling during hyaluronan (HA)-induced endothelial cell migration. *Cell Motility and the Cytoskeleton*. 53 (4) pp. 6634 – 6644.

- Singleton, P. and Bourguignon, L. 2004. CD44 interaction with ankyrin and IP3 receptor in lipid rafts promotes HA-mediated Ca²⁺ signalling leading to nitric oxide production and endothelial cell adhesion and proliferation. *Experimental Cell Research*. 295 (1) pp. 102 – 118.
- Skelton, T. et al. 1998. Glycosylation provides both stimulatory and inhibitory effects on cell surface and soluble CD44 binding to hyaluronan. *Journal of Cell Biology*. 140 pp. 431 – 446.
- Slattery, M. L. and Kerber, R. A. 1993. A comprehensive evaluation of family history and breast cancer risk. *JAMA*. 270 pp. 1563 – 1568.
- Sleeman, J. et al. 1996. Regulated clustering of variant CD44 proteins increases their hyaluronate binding capacity. *Journal of Cell Biology*. 135 pp. 1139 – 1150.
- Sleeman, J. et al. 1997. Variant exons v6 and v7 together expand the repertoire of glycosaminoglycans bound by CD44. *The Journal of Biology Chemistry*. 272 (50) pp. 313837 – 31844.
- Sliomany, M. et al. 2009. Inhibition of functional hyaluronan-CD44 interactions in CD122-positive primary human ovarian carcinoma cells by small hyaluronan oligosaccharides. *Clinical Cancer Research*. 15 pp. 7593 – 7601.
- Snyder, E. L. 2009. Identification of CD44v6+/CD24- breast carcinoma cells in primary tumours by quantum dot-conjugated antibodies. *Laboratory Investigations*. 89 pp. 857 – 866.
- Solis, M. et al. 2011. Hyaluronan regulates cell behaviour: a potential niche matrix for stem cells. *Biochemistry Research International*. 346972.
- Sonobo et al. 2005. Prognostic value of CD44 isoform expression in thymic epithelial neoplasms. *Cancer*. 103. Pp. 2015 – 2020.
- Sorlie, T. et al. 2001. Gene expression patterns of breast carcinomas distinguish tumor subclasses with clinical implications. *PNAS*. 98 (19) pp. 10869 – 10874.
- Soitrou, C. et al. 2003. Breast cancer classification and prognosis based on gene expression profiles from a population-based study. *PNAS*. 100 pp. 10393 – 10398.
- Smith-Warner, S. et al. 1998. Alcohol and breast cancer in women: a pooled analysis of cohort studies. *JAMA*. 279 (7) pp. 535 – 540.
- Soner, B. C. et al. 2014. Induced growth inhibition, cell cycle arrest and apoptosis in CD133+/CD44+ prostate cancer stem cells by flavopipidol. *International Journal of Molecular Medicine*. 34 (5) pp. 1249 – 1256.
- Spector, N. L. and Blackwell, K. L. 2009. Understanding the mechanism behind the trastuzumab therapy for Human Epidermal Receptor 2 breast cancer. *Journal of Clinical Oncology*. 27 (34) pp. 5838 – 5847.
- Stamenkovic, L. et al. 1989. A lymphocyte molecule implicated in lymph node homing is a member of the cartilage link protein family. *Cell*. 56 pp. 1057 – 1062.

- Stamenkovic, L. et al. 1991. The hematopoietic and epithelial forms of CD44 are distinct polypeptides with different adhesion potentials for hyaluronate-bearing cells. *EMBO Journal*. 10 pp. 343 – 348.
- Steger, G. G. et al. 2005. Fulvestrant ('faslodex') in pre-treated patients with advanced breast cancer: a single centre experience. *European Journal of Cancer*. 41 pp. 2655 – 2661.
- Streuwing, J. et al. 1997. The risk of cancer associated with specific mutations in BRCA1 and BRCA2 in Ashkenazi Jews. *New England Journal of Medicine*. 336 pp. 1401 – 1408.
- Strom, A. et al. 2004. Estrogen receptor β inhibits 17- β -estradiol-stimulated proliferation of the breast cancer cell line T47D. *PNAS USA*. 101 (6) pp. 1566 – 1571.
- Subramaniam, V. et al. 2007. CD44 regulates cell migration in human colon cancer cells via lyn kinase and AKT phosphorylation. *Journal of Physiology*. 83 (2) pp. 207 – 215.
- Suzuki, R. W. et al. 2009. Body weight and incidence of breast cancer defined by estrogen and progesterone receptor status: a meta analysis. *International Journal of Cancer*. 124 (3) pp. 698 – 712.
- Sy et al. 1991. Distinct effects of two CD44 isoforms on tumour growth in vivo. *Journal of Experimental Medicine*. 174 pp. 859 – 866.
- Takeo, K. et al. 2009. Oxidative stress-induces alternative splicing of transformer 2beta(SFRS10) and CD44 pre-mRNA's in gastric epithelial cells. *American Journal of Physiology. Cell Physiology*. 297 (2) pp. C330 – 338.
- Taher, T. E. et al. 1996. Signalling through CD44 is mediated by tyrosine kinases. Association with p56lck in T-lymphocytes. *Journal of Cell Biology*. 271 pp. 2863 – 2867.
- Takada, M. et al. 1994. The significance of CD44 in human pancreatic cancer: II. The role of CD44 in human pancreatic adenocarcinoma invasion. *The Pancreas*. 9 (6) pp. 753 – 757.
- Takahara, Y. et al. 2012. CD44 expression in pancreatic cells is associated with a favourable prognosis and inhibits cancer cell migration by regulation of actin filaments. *European Journal of Surgical Oncology*. 38 (9) pp. 738.
- Tammi, R. H. et al. 1998. HA bound to CD44 on keratinocytes is displaced by HA disaccharides and not hexasaccharides. *Journal of Biological Chemistry*. 273 pp. 28878 – 28888.
- Tammi, R. H. et al. 2008. HA in human tumours: pathobiology and prognostic messages from cell-associated and stromal HA. *Seminars in Cancer Biology*. 18 pp. 288 – 295.
- Tammi, R. H. et al. 2011. Transcriptional and post-transcriptional regulation of HA synthesis. *FEBS Journal*. 278 pp. 1419 – 1428.

- Tan, J-X. et al. 2006. Effect of silencing hyaluronidase gene HYAL1 by RNA interference on proliferation of human breast cancer cells. *Ai Zheng*. 25 (7) pp. 844 – 848.
- Tan, J-X. et al. 2011. Upregulation of HYAL1 expression in breast cancer promoted tumour cell proliferation, migration, invasion and angiogenesis. *PLoS ONE*. 6 (7) pp. 22836.
- Teder, P. et al. 2002. Resolution of lung inflammation by CD44. *Science*. 296 (5565) pp. 155 - 158.
- Tei, H. et al. 2014. Expression profile of CD44s, CD44v6, CD44v10 in localised prostate cancer. Effect on prognosis outcomes following radical prostatectomy. *Urology Oncology*. 32 (5) pp. 697 – 700.
- Terpe et al. 1994. CD44 variant isoforms are preferentially expressed in basal epithelia of non-malignant human fetal and adult tissues. *Histochemistry*. 101 pp. 70 – 89.
- Terpe, H. J. et al. 1996. Expression of CD44 isoforms in renal cell tumours: positive correlation to tumour progression. *American Journal of Pathology*. 148 pp. 453 – 463.
- Thankamony, P. and Knudson, K. 2006. Acetylation of CD44 and its association with lipid rafts are required for receptors and endocytosis. *Journal of Biological Chemistry*. 281 (45) pp. 34601 – 34609.
- Thomas, L. et al. 1992. CD44H regulates tumour migration on hyaluronate-coated substrate. *Journal of Biological Chemistry*. 118 pp. 971 – 977.
- Thompson, E. A. and Siiten, P. K. 1974. Utilisation of oxygen and reduced nicotinamide adenine dinucleotide phosphate in human placental microsomes during aromatisation of androstenedione. *Journal of Biological Chemistry*. 249 (17) pp. 5364 – 5372.
- Thorlacius, S. et al. 1997. Population-based study of risk of breast cancer in carriers of BRCA2 mutation. *The Lancet*. 352 (9137) pp. 1337 – 1339.
- Tjink, B. M. et al. 2006. A phase I dose escalation study with anti-CD44v6 bivatuzumab mertansine in patients with incurable squamous cell carcinoma of the head and neck or esophagus. *Clinical Cancer Research*. 15 (12) pp. 6064 – 6074.
- Todaro, M. et al. 2014. CD44v6 is a marker of constitutive and reprogrammed cancer stem cells driving colon cancer metastasis. *Cell Stem Cell* 14 (3) pp. 342 – 356.
- Tokunaga, E. et al. 2006. The association between Akt activation and resistance to hormone therapy in metastatic breast cancer. *European Journal of Cancer*. 42 (5) pp. 629 – 635.
- Tolg, C. et al. 1993. Splicing choice from ten variant exons establishes CD44 variability. *Nucleic Acids Research*. 21 pp. 1225 – 1229.

- Tolg, C. et al. 2006. Rhamm -/- fibroblasts are defective in CD44-mediated ERK1,2 mitogenic signalling, leading to defective skin wound repair. *Journal of Cell Biology*. 175 (6) pp. 1017 – 1028.
- Tolg, C. et al. 2010. RHAMM promotes interphase microtubule instability and mitotic spindle integrity through MEK1/ERK1/2 activity. *Journal of Biological Chemistry*. 285 (34) pp. 26461 – 26474.
- Toole, B. P. and Hascall, V.C. 2002. Hyaluronan and tumour growth. *American Journal of Pathology*. 161 (3) pp. 745 – 747.
- Toole, B. and Slomiany, M. 2008. Hyaluronan: a constitutive regulator of chemoresistance and malignancy in cancer cells. *Seminars of Cancer Biology*. 18 (4) pp. 244 – 250.
- Toole, B. 2009. Hyaluronan-CD44 interactions in cancer: paradoxes and possibilities. *Clinical Cancer Research*. 15 (24) pp. 7462 – 7468.
- Tremmel, M. et al. 2009. A CD44v6 peptide reveals a role for CD44 in VEGFR-2 signalling and oncogenesis. *Blood*. 114 (25) pp. 5236 – 5244.
- Trichopoulos, D. 1990. Hypothesis: does breast cancer originate in utero? *The Lancet*. 335 (8652) pp. 939 – 940.
- Tsai, M. J. and O'Malley, B. W. 1994. Molecular mechanisms of action of steroid/thyroid receptor superfamily members. *Annual Review of Biochemistry*. 63 pp. 451 – 486.
- Tsukita et al. 1994. ERM family members as molecular linkers between the cell surface glycoprotein CD44 and actin-based cytoskeletons. *Journal of Cell Biology*. 126. pp. 391 – 401.
- Tsuneki, M and Madri, J. A. 2014. CD44 regulation of endothelial cell proliferation and apoptosis via modulation of CD31 and VE-cadherin expression. *Journal of Cell Biology*. 289 (9) pp. 5357 – 5370.
- Tuhkanen, A-L. 1997. CD44 substituted with heparan-sulphate and endo- β -galactitol-sensitive oligosaccharides: a major proteoglycan in adult human epidermis. *Journal of Investigative Dermatology*. 109 pp. 213 – 218.
- Turley, E. 2002. Signalling properties of hyaluronan receptors. *The Journal of Biological Chemistry*. 272 (7) pp. 4584 – 4592.
- Tzuckerman, M. T. et al. 1994. Human estrogen receptor transactivation capacity is determined by both cellular and promoter context and mediated by 2 functionally distinct intramolecular regions. *Molecular Endocrinology*. 8 (1) pp. 21 – 30.
- Udabage, L. et al. 2005a. The overexpression of HAS2, Hyal-2 and CD44 is implicated in the invasiveness of breast cancer. *Experimental Cell Research*. 310 pp. 205 – 217.

- Udabage, L. et al. 2005b. Anti-sense mediated suppression of hyaluronan synthase 2 inhibits the tumorigenesis and progression of breast cancer. *Cancer Research*. 65 pp. 6139 – 6150.
- Van Hal, N. L. et al. 1999. Characterisation of v6 isoforms in head and neck squamous cell carcinoma. *International journal of cancer*. 82 (6) pp. 837 – 845.
- Valledares, L. E and Payne, A. H. 1979. Induction of testicular aromatisation by luteinising hormone in mature rats. *Endocrinology*. 105 (2) pp. 431 - 436.
- Vasudevan, N. et al. 2004. Integration of steroid hormone initiated membrane action to genomic function in the brain. *Steroids*. 70 (5 – 7) pp. 388 – 396.
- Van den Brandt, P. et al. 2000. Pooled analysis of perspective cohort studies on height, weight and breast cancer risk. *American Journal of Epidemiology*. 152 pp. 514 – 527.
- Van der Voort, R. et al. 1999. Heparan sulphate-modified CD44 promotes hepatocyte growth factor/scatter factor-induced signal transduction through the receptor tyrosine kinase c-met. *Journal of Biological Chemistry*. 274 (10) pp. 6499 – 6506.
- Veisheh, M. et al. 2014. Cellular heterogeneity profiling HA probes reveals an invasive but slow-growing breast tumour subsets. *PNAS USA*. 11 (17) pp. 1731 – 1739.
- Verkaik, N. S. et al. 2000. Silencing of CD44 expression in prostate cancer by hypermethylation of the CD44 promoter region. *Laboratory Investigations; a journal of technical methods and pathology*. 80 (8) pp. 1291 – 1298.
- Vermeulen, J. F. et al. 2012. Immunophenotyping invasive breast cancer: pairing the road for molecular imaging. *BMC Cancer*. 12 pp. 240.
- Vermeulen, J. F. et al. 2013. Analysis of expression of membrane-bound tumour markers in ductal carcinoma in situ of the breast: paving the way for molecular imaging. *Cell Oncology*. 36 (4) pp. 333 – 340.
- Wainwright, D. et al. 1996. A splice variant of CD44 expression in the rat apical ectodermal ridge contributes to limb outgrowth. *Annals of the New York Academy of Sciences*. 785 pp. 345 – 349.
- Walter, P. et al. 1985. Cloning of the human estrogen receptor cDNA. *PNAS USA*. 82 (23) pp. 7889 – 7893.
- Wakeling, A.E. et al. 1991. A potent specific pure antiestrogen with clinical potential. *Cancer Research*. 51 pp. 3867 – 3873.
- Wakeling, A. E. et al. 1995. Use of pure anti-oestrogens to elucidate the mode of action of oestrogens. *Biochemistry and Pharmacology*. 49 pp. 1545 – 1549.
- Wakeling, A. E. 2000. Similarities and distinctions in the mode of action of different classes of antioestrogens. *Endocrine Related Cancer*. 7 pp. 17 - 28

- Wang, J. D. et al. 1993. Molecular basis of genetic variation in debrisoquin hydroxylation in Chinese subjects: polymorphism in RFLP and DNA sequence of CYP2D6. *Clinical Pharmacology*. 53 pp. 410 – 418.
- Wang, C. et al. 1998. The overexpression of RHAMM, a hyaluronan binding protein that regulates ras signalling, correlates with overexpression of mitogen activated protein kinase and is a significant parameter in breast cancer progression. *Clinical Cancer Research*. 4 pp. 567 – 576.
- Wang, S. J. et al. 2007. Association of CD44v3 containing isoforms in tumour cell growth, migration and metallo-proteinase expression and lymph node metastasis in head and neck cancer. *Head Neck*. 29 pp. 550 – 558.
- Wang, F. et al. 2008. HYAL1 and HYAL2 inhibits tumour growth in vivo but not in vitro. *PLoS ONE*. 3 (8) pp. 3031.
- Wang, S. J. 2009. CD44 variant isoforms in head and neck squamous cell carcinoma progression. *Laryngoscope*. 119 pp. 1518 – 1530.
- Wang, H. et al. 2013. Tspan8, v6 and alpha6beta4 are biomarkers of migrating pancreatic cancer-initiating cells. *International Journal of Cancer*. 133 (2) pp. 416 – 426.
- Wang, Z. et al. 2014. Interplay of mevalonate and Hippo pathways regulates RHAMM transcription via YAP to modulate breast cancer cell motility. *PNAS USA*. 111 (1) pp. 89 – 98.
- Wang, S. J. and Bourguignon L. Y. 2006. Hyaluronan and the interaction between CD44 and epidermal growth factor receptor in oncogenic signalling and chemotherapy resistance in head and neck cancer. *Archives of Otolaryngology – Head and Neck Surgery*. 132 (7) pp. 771 – 778.
- Warzecha, C. et al. 2009. The epithelial splicing factors ESRP1 and ESRP2 positively and negatively regulate diverse types of alternative splicing events. 6 (5) pp. 546 – 562.
- Wardley, A. M. 2002. Fulvestrant: a review of its development, pre-clinical and clinical data. *International Journal of Clinical Practice*. 56 pp. 305 – 309.
- Watanabe, O. et al. 2005. Expression of a CD44 variant and VEGF-C and the implications for lymphatic metastasis and long-term prognosis of human breast cancer. *Journal of Experimental Clinical Cancer Research*. 24 pp. 75 - 82.
- Watters, J. et al. 1997. Rapid membrane effects of steroids in neuroblastoma cells: effects of estrogen on mitogen activated protein kinase signalling cascade and c-fos immediate early gene transcription. *Endocrinology*. 138 (9) pp. 4030 – 4033.
- Watters, J. J. and Dorsa, D. M. 1998. Transcription effects of estrogen on neuronal neurotensin gene expression involve cAMP/PKA-dependent signalling mechanisms. *Journal of Neuroscience*. 18 pp. 6672 – 6680.

- Weber, G. et al. 1996. Receptor-ligand interaction between CD44 and osteopontin (Eta-1). *Science (New York)*. 271 (5248) pp. 509 – 512.
- Wegner, N. K. and Grady, D. 1999. Postmenopausal hormone therapy SERMs and coronary heart disease in women. *Journal of Endocrinological Investigations*. 22 (8) pp. 616 – 624.
- Weg-Remers et al. 2001. Regulation of alternative pre-mRNA splicing by ERK MAP-kinase pathway. *EMBO Journal*. 20 (15) pp. 4194 – 4203.
- Weigel, P. H. and DeAngelis, P. L. 2007. Hyaluronan synthases: A decade-plus of novel glycotransferases. *Journal of Biological Chemistry*. 282 pp. 36777 – 36781.
- Weinburg, O. et al. 2005. New approaches to reverse resistance to hormonal therapy in human breast cancer. 8 pp. 219 – 233.
- Wielenga, V. J. M. et al. 2000. Expression of c-met and heparan sulphate proteoglycan forms of CD44 in colorectal cancer. *American Journal of Pathology*. 157 (5) pp. 1564 – 1573.
- Williams, G. M. et al. 1993. The triphenylethylene drug tamoxifen is a strong liver carcinogen in the rat. *Carcinogenesis*. 14 pp. 315 – 317.
- Willet, W. et al. 2004. Epidemiology and non-genetic causes of breast cancer. *Diseases of the Breast*. pp. 223 – 276.
- Wittig, B. et al. 2000. Abrogation of experimental colitis correlates with increased apoptosis in mice deficient for CD44 variant exon 7 (CD44v7). *Journal of Experimental Medicine*. 191 pp. 2053 – 2064.
- Wollner, D. et al. 1992. Remodelling the cell surface distribution of membrane protein during the development of epithelial cell polarity. *Journal of Cell Biology*. 116 pp. 889 – 899.
- Wu, M. H. et al. 2006. Hormonal and body-size factors in relation to breast risk: a prospective study of 11, 880 women in a low incidence area. *Annual Epidemiology*. 16 pp. 223 – 229.
- Wurtz, J. et al. 1996. A canonical structure for the ligand binding domain of nuclear receptors. *Nature Structural Biology*. 3 pp. 87 – 94.
- Xing, Y. et al. 2003. Widespread production of novel soluble protein isoforms by alternative splicing removal of transmembrane anchoring domains. *FEBS Letters*. 555 (3) pp. 572 – 578.
- Yabushita, H. et al. 2004. HAS expression in ovarian cancer. *Oncology Reports*. 12 pp. 739 – 743.
- Yae, T et al. 2012. Alternative splicing of CD44 mRNA by ESRP1 enhances lung colonisation of metastatic cancer cell. *Nature Communications*. 3 (883) pp. 1 – 9.
- Yamada, Y. et al. 2004. Elevated transcript level of HAS1 gene correlates with poor prognosis of human colon cancer. *Clinical Experimental Metastasis*. 21 pp. 57 – 63.

- Yanamoto, S. et al. 2014. Expression of the cancer stem cell marker CD44v6 and ABCG2 in tongue cancer. Effect of neoadjuvant chemotherapy on local recurrence. *International Journal of Oncology*. 44 (4) pp. 1153 – 1162.
- Yang, C. et al. 2013. The use of HA oligosaccharide-loaded nanoparticles to breach the endogenous hyaluronic acid glycoalyx for breast cancer therapy. *Biomaterials*. 34 (28) pp. 6829 – 6838.
- Yang, H. et al. 2010. Reduced expression of toll-like receptor 4 inhibits human breast cancer cells proliferation and inflammation cytokines secretion. *Journal of Expression of Clinical Cancer Research*. 29 (92).
- Yang, H. et al. 2014. Toll-like receptor 4 prompts human breast cancer cells invasiveness via lipopolysaccharides stimulation and its overexpression in patients with lymph node metastasis. *Plos One*. 9 (10) e109980.
- Yang, X. et al. 2013. Toll-like receptor 4 genetic variants and progression of breast cancer. *Tissue Antigen*. 81 (4) pp. 221 – 226.
- Yang, X-Y. et al. 2012. Hyaluronic acid-coated nanostructured lipid carriers for targeting paclitaxel to cancer. *Cancer Letters*. 334 (2) pp. 338 – 345.
- Yang, Y. M. and Chang, J. W. 2008. Bladder cancer initiating cells are among EMA-CD44v6⁺ subset: novel methods for isolating undetermined cancer stem (initiating) cells. *Cancer Investigation*. 26 (7) pp. 725 – 733.
- Yared, E. et al. 2002. Genotoxic effects of oestrogen in breast cells detected by the micronucleus assay and the comet assay. *Mutagenesis*. 17 (4) pp. 345 – 352.
- Yin, H. et al. 2011. The phenotype radiation resistance of CD44⁺/CD24^{-/low} breast cancer stem cells is mediated through enhanced activation of ATM signalling. *PLOS one*. 6 (9) e2408.
- Yonemura et al. 1998. Ezrin/Radixin/Moesin (ERM) proteins bind to a positively charged amino acid cluster in the juxta-membrane cytoplasmic domain of CD44, CD43 and ICAM2. *Journal of Cell Biology*. 140 pp. 885 – 895.
- Yonemura, S. et al. 1999. Direct involvement of ezrin/radixin/moesin (ERM)-binding membrane proteins in the organisation of microvilli in collaboration with activated ERM proteins. *Journal of Cell Science*. 145 (7) pp. 1497 – 1509.
- Young-II, et al. 2011. Self-assembled nanoparticles of hyaluronic-acid/poly (DL-lactide-co-glycolide) block polymer. *Colloids and Surfaces 13: Biointerfaces*. 90 (1) pp. 28 – 35.
- Yu, W. et al. 2002. CD44 anchors the assembly of matrilysin/MMP-7 with heparin-binding epidermal growth factor precurose and ErbB4 and regulates female reproductive organ remodelling. *Genes and Development*. 16 pp. 307 – 323.
- Yu, P. et al. 2010. Clinical significance of pAKT and CD44v6 overexpression with breast cancer. *Journal of Cancer Research Clinical Oncology*. 136 pp. 1283 – 1292.

- Yu, Q and Stamenkovic, I. 1999. Localisation of matrix metalloproteinase 9 to the cytoskeleton provides a mechanism for CD44-mediated tumour invasion. *Genes and Development*. 13 (1) pp. 35 – 48.
- Zagouri, F. et al. 2013. High MET expression is an adverse prognostic factor in patients with triple negative breast cancer. *Breast Journal Cancer*. 108 (5) pp. 1110 – 1115.
- Zhang, S. et al. 1998. The hyaluronan receptor RHAMM regulates extracellular-regulated kinase. *The Journal of Biological Chemistry*. 273 pp. 11342 – 11348.
- Zhang, J. et al. 2011. Epidermal growth factor receptor gene mutations, amplification and clinicopathology correlation in patients with lung cancer. *Chinese Journal of Pathology*. 40 (10) pp. 675 – 678.
- Zhao, L. et al. 2015. CD44v6 expression in patients with stage II or stage III sporadic colorectal cancer is superior to CD44 expression for predicting progression. *International Journal of Clinical and Experimental Pathology*. 8 (1) pp. 692 – 701.
- Zhou, Y. et al. 2007. Enhanced NF kappa B and AP-1 transcriptional activity associated with antiestrogen resistant breast cancer. *BMC Cancer*. 7 pp. 59.
- Zohar, R. et al. 2000. Intracellular osteopontin is an integral component of the CD44-ERM complex involved in cell migration. 184 (1) pp. 118 – 130.
- Zoller, M. et al. 1994. CD44 and metastasis. *Onkologie*. 17. pp. 114 – 122.
- Zoller, M. et al. 1997. Transient absence of CD44 expression and delay in development by anti-CD44 treatment during ontogeny: a surrogate of an inducible knockout? *Cell Growth and Differentiation*. 8 (11) pp. 1211 – 1223.

9. Appendices

Appendix A. Charcoal-stripping procedure for 100 ml FCS

Charcoal-stripped FCS (SFCS) was added to the culture media in replacement of FCS to mimic oestrogen deprivation conditions through the removal of non-polar materials including steroid hormones. A charcoal solution (2 g activated charcoal, 0.01 g dextran T70 diluted in 18 ml distilled water) was stirred for one hour at room temperature. A solution of FCS used in routine culture media was adjusted to pH 4.2 with HCl (5M) and equilibrated at 4 °C for 30 minutes. To 100 ml of adjusted FCS solution was added 5 ml charcoal solution and stirred gently for 16 hours at 4 °C. The charcoal contained within this solution was then removed by centrifugation at room temperature for 40 minutes, 12, 000 rpm (Labofuge 400R centrifuge, Heraeus, Germany). The resultant supernatant was coarse-filtered through Whatman filter paper NO.4 to ensure complete charcoal removal. The remaining solution was then readjusted to pH 7 using NaOH (5 M) and filter sterilised with a 2 µM Super Vacucap membrane (Gellman Laboratory Pall, Ann Arbor, USA). The resultant charcoal-stripped FCS was aliquotted into sterile universal tubes and stored at - 20 °C. This procedure was performed by research technician staff in the Breast Cancer Molecular Pharmacology Group (BCMPG), Cardiff University.

Appendix B. Jetset gene probes

The affymetrix microarray platform contains multiple gene probe sets for each target gene which differ slightly in sequence. These differences in gene probe set sequences may lead to inconsistent or contradictory measurements dependent upon their

performance on the microarray platform which may ultimately result in difficulties determining the expression of the target gene. To assess the efficacy of each probe set sequence, Li et al. 2011 developed a method to score their performance based on 3 determinants which assessed overall specificity, coverage and degradation resistance (reviewed in Li et al. 2011). All probes sets achieve a score ranging from 0 – 1 and the probe with the highest performance score (closer to 1) is determined as the Jetset probe.

Appendix C. CD44 gene sequence and primer sequences

The human gene sequence encoding CD44 mRNA obtained from the NCBI database (<http://www.ncbi.nlm.nih.gov/>) (Figure 9.1) with each variant exon depicted and described in Table 9.1 below. This sequence was utilised to (i) design primers for RT-PCR analysis that bound to specific regions of DNA encoding the desired target exon corresponding to a specific CD44 isoform, (ii) design siRNA molecules which bound specifically to a sequence within the CD44v6 exon and (iii) confirm the specificity of the global CD44 siRNA molecules (purchased by Thermo Scientific, Dharmacon, UK) to the gene sequence. The primers that were designed and utilised for CD44 detection in this project are highlighted in the gene sequence below and described in Table 9.2. The DNA sequences to which each siRNA target molecule used within this project bound to the CD44 gene are highlighted in the sequence below and described in the Table 9.3.

gagaagaaagccagtgcggtctctgggagcaggggcccagtggggctcggaggcacaggcaccocgagc
actccaggttccccgaccacgctccctggcagccccgattatttacagcctcagcagagcacggggcg
ggggcagagggggcccgccgggagggctgctacttcttaaaacctctgcgggctgcttagtcacagcc
ccccttgcttgggtgtgtocttgcctcgcctccctccctcctgcttaggtcactgttttcaacctcga
taaaaactgcagccaacttccgaggcagcctcattgcccagcggaccccagcctctgcccaggttcggt
ccgccatcctcgtcccgctcctccgcccctgccccgcccaggatcctccagctcctttcggc
cgcgcctcctcgtcccgctcctccgacaccatgacaagttttgggtggcacgcagcctgggactctgcctc
gtgccgctgagcctggcgcagatcgatttgaatataacctgcccgtttgcaggtgtattccacgtgga
gaaaaatggtcgtacagcatctctcggacggaggccgctgacctctgcaaggctttcaatagcacct
tgcccacaatggcccagatggagaaagctctgagcatcggatttgagacctgcaggtatgggttcata
gaagggcacgtggtgattccccggatccaccccaactccatctgtgcagcaaacacacaggggtgta
catcctcacatccaacacctccagtatgacacatattgcttcaatgcttcaggtccacctgaagaag
attgtacatcagtcacagacctgcccattgcctttgatggaccaattaccataaactattgttaacctg
gatggcaccgctatgtccagaaaggagaatacagaacgaatcctgaagacatctaccccagcaacc
tactgatgatgacgtgagcagcggctcctccagtgaaaggagcagcacttcaggaggttacatctttt
acaccttttctactgtacccccatcccagacgaagacagtccttgatcaccgacagcacagacaga
atcctgctaccactttgatgagcactagtgctacagcaactgagacagcaaccaagaggcaagaaac
ctgggattgggttttcatgggttttctaccatcagagtcaaagaatcatcttcacacaacaacacaaa
tggctggtaagcttccaaataccatctcagcaggctgggagccaaatgaagaaaaatgaagatgaaaga
gacagacacctcagttttctggatcaggcattgatgatgataagaattttatctccagcaccaattc
aacacaccacgggcttttgaccacacaaaacagaaccaggactggaccagtggaaccaagccatt
caaatccggaagtgtacttcagacaaccacaaggatgactgatgtagacagaaaaatggcaccactgct
tatgaaggaaactggaaccagaagcacacctcccctcattcaccatgagcatcatgaggaagaaga
gacccacattctacaagcacaatccaggcaactcctagtagtacaacggaagaaacagctaccaga
aggaacagtggttttggcaacagatggcatgagggatctcgcaaacaccccaagaaagactcccattcg
acaacagggacagctgcagcctcagctcataccagccatccaatgcaagggaaggacaacaccaagccc
agaggacagttcctggactgatttttcaacccaatctcacaccccatgggacgaggtcatcaagcag
gaagaaggatggaatagactccagtcatagtataacgcttcagcctactgcaaatccaaacacaggt
ttgggtggaagatttggacaggacaggacctctttcaatgacaacgcagcagagtaattctcagagctt
ctctacatcacatgaaggcttggagaagataaaagaccatccaacaactctactctgacatcaagca
ataggaatgatgtccaggtggaagaagagacccaaatcattctgaaggctcaactactttactggaa
ggttatacctctcattaccacacacgaaggaaagcaggaccttcacccagtgacctcagctaaagc
tgggtcctttggagttactgcagttactgttggagattccaacttataatgtcaatcgttccttatcag
gagaccaagacacattccaccccagtggggggtcccataccactcatggatctgaatcagatggacac
tccatgggagtcagaagggtggagcaaacacaacctctggtcctataaggacaccccaatccaga
atggctgatcatcttggcatcctcttggccttggctttgattcttgcagtttgcattgcagtcaca
gtcgaagaaggtgtgggcagagaaaaagctagtgatcaacagtggaatggaactgtgtggaggacaga
aagccaagtggactcaacgggagaggccagcaagtctcaggaaatggtgcatttgggtgaacaaggagtc
gtcagaaaactccagaccagtttatgacagctgatgagacaaggaacctgcagaatgtggacatgaaga
ttgggggtgtaacacctacaccattatcttggaaagaaacaaccgttggaaacataaccattacagggg
gctgggacacttaacagatgcaatgtgctactgattgtttcattgcaaatcttttttagcataaaaatt
ttctactctttttgtttttgtgtttttgttcttttaaagtccaggtccaatttgtaaaaacagcattgct
ttctgaaattagggcccattaataatcagcaagaatttgatcgttccagttcccacttggaggcctt
tcatccctcgggtgtgctatggatggcttctaacaaaaactacacatagtattcctgatcgccaacc
tttccccaccagctaaaggacatttcccagggttaatagggcctggctcctgggaggaaatttgaatg
ggtccattttgccttccatagcctaatacctgggcattgctttccactgaggttgggggttgggggtg
tactagttacacatcttcaacagacccccctctagaaatttttcagatgcttctgggagacacccaaag
ggtgaagctatttatctgtagtaaaactatttatctgtgtttttgaaatattaaacctggatcagtc
tttgatcagttataatttttttaagttactttgtcagaggcacaacaaagggtttaaaactgattcataata
aatatctgtacttcttcgatcttcaccttttgtgctgtgattcttcagtttctaaaccagcactgtct

gggtcocctacaatgtatcaggaagagctgagaatggtaaggagactcttctaagtcttcatctcagag
 accctgagttcccactcagacccactcagccaaatctcatggaagaccaaggaggcagcactgtttt
 tgttttttgttttttgttttttttttgacactgtccaaaggtttccatcctgtcctggaatcagag
 ttggaagctgaggagcttcagcctcttttatggtttaatggccacctgttctcctgtgaaaggctt
 tgcaaagtacattaagtgttgcacacactgttatccctggggccctatttcatagaggctggccctat
 tagtgatttccaaaaacaatatggaagtgccttttgatgtcttacaataagagaagaagccaatggaa
 atgaaagagattggcaaaggggaaggatgatgccatgtagatcctgtttgacatttttatggctgat
 ttgtaaaccttaaacacaccagtgctgttcttgatgcagttgctatttaggatgagtttaagtgcctgg
 ggagtcctcctcaaaaggttaaagggattcccatcattggaatcttatcaccagataggcaagtttatga
 ccaacaagagagtagtggctttatcctctaacctcatalttttctcccacttggcaagtctttgtgg
 catttattcatcagtcaggggtgctcgattggctctagaacttccaaaggctgcttgtcatagaagcca
 ttgcatctataaaagcaacggctcctgtttaaattggatctcctttctgaggctcctactaaaagtcatt
 tgttacctaaacttatgtgcttaacaggcaatgcttctcagaccacaaagcagaaagaagaagaaaag
 ctctgactaaatcagggctgggcttagacagagttgatctgtagaataatctttaaaggagagatgtc
 aactttctgcaactattcccagcctctgctcctccctgtctaccctctcccctcctctctccctccac
 ttcccccaaatcttgaaaacttctttctcttctgtgaacatcattggccagatccattttcagtg
 gtctggatttcttttttattttcttttcaacttgaagaaactggacattaggccactatgtgttgta
 ctgccactagtgttcaagtgctcctgttttccagagatttccctgggtctgccagaggccagacag
 gctcactcaagctctttaaactgaaaagcaacaagccactccaggacaaggttcaaaatggttacaaca
 gcctctacctgtgccccagggagaaagggtagtgatacaagctcatagccagagatggttttcca
 ctcttcttagatattcccaaaaagaggctgagacaggaggttattttcaattttattttggaattaaa
 tacttttttccctttattactgtttagtccctcacttggatatacctctgtttttcacgatagaaata
 agggagggtctagagcttctattccttggccattgtcaacggagagctggccaagtcttcacaaaccct
 tgcaacattgcctgaagtttatggaataagatgtattctcactcccttgatctcaagggcgtaactct
 ggaagcacagcttgactacacgtcatttttaccaatgattttcaggtgacctgggctaagtcatttaa
 actgggtctttataaaaagtaaaaggccaacatttaatttttgcmaaagcaacctaaagagctaaagat
 gtaatttttcttgcaattgtaaatcttttgtgtctcctgaagacttcccttaaaattagctctgagtg
 aaaaatcaaaagagacaaaagacatcttccgaatccatatttcaagcctggtagaattggcttttctag
 cagaacctttccaaaagttttatattgagattcataacaacaccaagaattgattttgtagccaacat
 tcattcaatactgttatatcagaggagtaggagagaggaaacatttgacttatctggaaaagcaaaat
 gtaacttaagaataagaataacatgggtccattcacctttatgttatagatatgtctttgtgtaaatcat
 ttgttttgagttttcaagaatagcccattgttcattcttgtgctgtacaatgaccactgttattgtt

Figure 9.1. The human CD44 mRNA sequence obtained by NCBI. Base pairs shown in **dark yellow** depict the non-coding sequence and base pairs shown in black depict the coding sequence. Base pair letters highlighted in **bold and underlined** represent the first base pair of each exon. The sequence highlighted in **red** shows the start codon found in exon 1. The sequence highlighted in **green** shows the polyA site found in exon 20. CD44 variant exons are depicted by a different colour (described in Table 9.1) and the base pair sequences targetted by primers or siRNA molecules are highlighted (described in Table 9.2 and 9.3 respectively).

actttgacttttcagagcacacccttccctctggtttttgtatatttattgatggatcaataataatga
 ggaaagcatgatatgtatattgctgagttgaaagcacttattggaaaatattaaaaggctaacattaa
 aagactaaaggaaacag **AAAAAAAAAAAAAAAA**

Exon number	Standard/Variant number	Colour	Base pair size
1	Standard 1		501
2	Standard 2		166
3	Standard 3		134
4	Standard 4		69
5	Standard 5		231
6	Variant 1	Not translated to mRNA	-
7	Variant 2	Red	129
8	Variant 3	Purple	126
9	Variant 4	Green	114
10	Variant 5	Dark Blue	117
11	Variant 6	Orange	129
12	Variant 7	Dark Green	132
13	Variant 8	Dark red	102
14	Variant 9	Dark Yellow	90
15	Variant 10	Light Blue	204
16	Standard 6		63
17	Standard 7		73
18	Standard 8		79
19	Standard 9	Not translated to mRNA	-
20	Standard 10		3271

Table 9.1. A list of the exon number, corresponding standard/variant exon number and their depicted colour and base pair size (as shown in Figure 9.1) for each exon in the human CD44 mRNA sequence obtained from the NCBI. It is important to note that exon 6 (variant 1) is not translated into mRNA in the human genome due to the position of a stop codon in exon 6 (Screaton et al. 1992). Exon 19 (standard 9) is usually absent from most CD44 proteins as inclusion of this exon results in the formation of a short-tail CD44 isoform due to the presence of an alternative translation stop codon (Goldstein and Butcher 1990).

Gene	Forward Sequence	Reverse Sequence
CD44 Std	5'-GACACATATTGC TTCAATGCTTCAGC-3'	5'-GATGCCAAGATGAT CAGCCATTCTGGAAT-3'
CD44v3	5'-CGTCTTCAAAT ACCATCTCAGC-3'	5' TCATCATCAA TGCCTGATCC-3'
CD44v6	5'-CAACGGAAGA AACAGCTACCC-3'	5' CCTGTTGTCG AATGGGAGTC-3'
CD44v10	5'-GGAATGATGTCA CAGGTGGA-3'	5'-AAGGCCTGCT TTCCTTCGT-3'

Table 9.2. A list of the CD44 primers used in this project with their corresponding forward and reverse sequences and colour in which they are shown in the above human CD44 mRNA sequence (Figure 9.1).

Target siRNA	RNA sequence	DNA sequence
NT-siRNA (control)	UGGUUUACAUGUCGACUAA UGGUUUACAUGUUGUGUGA UGGUUUACAUGUUUUCUGA UGGUUUACAUGUUUCCUA	TGGTTTACATGTCGACTAA TGGTTTACATGTTGTGTGA TGGTTTACATGTTTTCTGA TGGTTTACATGTTTTCTTA
CD44 (total)	GAAUUAACCUGCCGCUU CAAGUGGACUCAACGGAGA CGAAGAAGGUGUGGGCAGA GAUCAACAGUGGCAAUGGA	GAATATAACCTGCCGCTT CAAGTGGACTCAACGGAGA CGAAGAAGGTGTGGGCAGA GATCAACAGTGGCAAUGGA
CD44v6	CAGAUGGCAUGAGGGAUUCGCCAA	CAGATGGCATGAGGGATATCG CCAA

Table 9.3. A list of the target siRNAs and their corresponding RNA and DNA sequences for each siRNA used in this project. The colour of each target siRNA DNA sequence identifies their location in the above human CD44 mRNA sequence (Figure 9.1).

Appendix D. HMMR gene sequence and primer sequences

The human gene sequence encoding HMMR (RHAMM) mRNA obtained from the NCBI database (<http://www.ncbi.nlm.nih.gov/>) (Figure 9.2) with each exon depicted and described in Table 9.4. This gene sequence was utilised to design primers for RT-PCR analysis that bound to DNA sequences common to all RHAMM isoforms (shown in Table 9.4)

```
attctttcttcgtgttctctgtgctgggattggtgtgccaggggtttggctttccaattggctaacgcc
gggggtgggtggggaatgtggggagatttgaatttgaaaccggtagggagtgataatccgcattcagtt
gtcggaggagtgccagtcaccttcagtttctggagctggccgtcaacatgctcctttcctaaggcgcct
tgaaacgattcaatgacccttctggttgtgcacatctccaggtgcttatgatgttaaaactttagaa
gtattgaaaggaccagtatcctttcagaaatcacaagatttaacaacaaaaagaaatcctaacaacaaa
tcttaatggttgacaaagatactaccttgccctgcttcagctagaaaaagttaagtcttcggaatcaaaga
aggaatctcaaaagaatgataaagatttgaagatattagagaaaagagaaatcgtgttctctacaggaa
cgtggtgcccaggacaggcggatccaggatctggaaactgagttggaaaagatggaagcaaggctaaa
tgctgcactaagggaaaaaacatctctctctgcaataatgctacactggaaaaacaacttattgaaat
tgaccaggactaatgaactactaaaatctaagtcttctgaaaatggtaaccagaagaatttgagaatt
ctaagcttgaggtgatgaaacttagaaacaaaagagaaacaaagatgaggggtatgatggctaagca
agaaggcatggagatgaagctgcaggtcaccacaaaggagtctcgaagagtctcaagggaaaaatagccc
aactggaggggaaaaacttggttcaatagagaaagaaaagattgatgaaaaatctgaaacagaaaaactc
ttggaatacatcgaagaaattagttgtgcttcagatcaagtggaaaaatacaagctagatattgcca
gttagaagaaaaatttgaaagagaagaatgatgaaattttaagccttaagcagtctcttgaggagaata
ttgttatattatctaaacaagtagaagatctaaatgtgaaatgtcagctgcttgaaaaagaaaaagaa
gaccatgtcaacaggaatagagaacacacgaaaatctaaatgcagagatgcaaaacttaaacagaa
gtttattcttgaacaacaggaacgtgaaaagcttcaacaaaaagaattacaaattgattcacttctgc
aacaagagaaaagaaattatcttcgagcttcatcagaagctctgttcttttcaagaggaaatgggttaa
gagaagaatctggttgaggaagaattaaagcaaacactggatgagcttgataaattacagcaaaaagga
ggaacaagctgaaaggctggtcaagcaattggaagaggaagcaaaatctagagctgaagaattaaac
tcttagaagaaaagctgaaagggaaggaggtgaaactggagaaaagtagtgctgctcatacccaggcc
accctgcttttgcaggaaaagtgatgacagatggtgcaaaccttgaaagatgttactgctcaatttga
aagctataaaagcgttaacagccagtgagatagaagatcttaagctggagaactcatcattacaggaaa
aagcggccaaggctgggaaaaatgcagaggatgttcagcatcagattttggcaactgagagctcaaat
caagaatgatgaaggatgcttctagatctgcagaccaagtcagcactaaaggaaaacagaaattaaaga
aatcacagtttcttttcttcaaaaaataactgatttgcagaaccaactcaagcaacaggaggaagact
ttagaaaacagctggaagatgaagaaggaagaaaagctgaaaaagaaaatacaacagcagaattaact
gaagaaattaacaagtggcgtctcctctatgaagaactatataataaaaacaaaccttttcagctaca
actagatgcttttgaagtagaaaaacaggcattggtgaaatgaaatggtgcagctcaggaacagctaa
ataaaaataagagattcatatgctaaattattgggtcatcagaatttgaaacaaaaaatcaagcatgtt
gtgaagttgaaagatgaaaatagccaactcaaatcgaagatcaaaaactccgctgtcagctttgctaa
aaaaaacaaagtggagacaaaacttcaagaggaattgaataaagttctaggtatcaaacactttgatc
cttcaaggcttttcatcatgaaagtaagaaaaatttgcccctgaagacccattaaaaagaaggcaat
acaaactgttaccgagctoctatggagtgcaagaatcatggaagtaaacatctgagaaacctgttgga
agattatttcttcgtcttggtttattgatgttgctgttattatatttgacatgggtattttataat
gttgattttaaactgccaatccttaaatatgtgaaaggaacatttttaccacaaagtgtctttt
gacattttatttttcttgcacaatacctcctccctaagctcacctttatcacctcattctgaacct
```

```

ttcgcgtggcgtttccagcgttagaatgcatctcatcaacttaaaagtcagtatcatattattatcctcct
gttctgaaaccttagtttcaagagtcctaaacccagattcttcagccttgatcctggaggctcttttcta
gtctgagccttcttagctaggctaaaacaccttggccttgattgcctctactttgattctgataatg
ctcacttggctcctacctattatccttctacttgtccagttcaaataagaaataaggacaagcctaact
tcatagaaacctctctatTTTTTaatcagttgTTTtaataatttacagggtcttaggctccatcctgttt
gtatgaaattataatctgtggattggcctTTaagcctgcattcttaacaaactcttcagttaattctt
agatacataaaaaatctgagaaactctacatgtaactatttcttcagagtttgtcataatactgcttgtc
atctgcatgtctactcagcatttgattaacatttgTgtaatatgaaataaaattacacagtaagtcac
ttaaccaatt

```

Figure 9.2. The human HMMR (RHAMM) mRNA sequence obtained by NCBI. Base pairs shown in **dark yellow** depict the non-coding sequence and base pairs shown in black depict the coding sequence. Base pair letters highlighted in **bold and underlined** represent the first base pair of each exon. The sequence highlighted in **red** shows the start codon found in exon 1. The sequence highlighted in **green** shows the polyA site found in exon 18. HMMR (RHAMM) base pair sizes and position of primer pairs (highlighted in grey) are described in Tables 9.4 and 9.5 respectively. The existence of several HMMR (RHAMM) isoforms have so far been characterised which contain N-terminal truncations of i) exon 4, ii) exon 5, iii) exon 13, iv) exons 1 – 5 and v) exons. 1 – 9.

Exon	Base pair size
1	228
2	99
3	80
4	48
5	189
6	87
7	101
8	75
9	179
10	149
11	215
12	117
13	147
14	153
15	100
16	177
17	163
18	836

Table 9.4. A list of the exon number and corresponding base pair size for each exon in the human HMMR (RHAMM) gene.

Gene	Forward Sequence	Reverse Sequence
HMMR	5'-TGCAGCTCAGGAACAGCTAA-3'	5'-GCTGACAGCGGAGTTTTGAT-3'

Table 9.5. The HMMR primer used in this project with its corresponding forward and reverse sequence and colour in which it is highlighted in the mRNA sequence (Figure 9.2).

Appendix E. Densitometry analysis using ImageJ software

Band intensities obtained from Western blotting detection were quantified using the ImageJ software programme (<http://imagej.nih.gov/ij/download.html>) for analysis of protein expression levels. Each image analysed was scanned and uploaded into the software programme and converted to grayscale by using the Image>Type>8-bit command. Using the rectangle icon on the ImageJ selection toolbar a tall narrow rectangle was drawn around the first band representing the expression level of a protein of interest. It was important to draw the box as close to the protein band as possible whilst containing all of the band in the box. Using the tool bar, the Analyse>Gels>Select First Lane command was then used to highlight the box and identify it as lane '1'. The box in lane 1 was then copied and pasted (to ensure all boxes were the same size for comparison) and moved to the protein band situated in lane 2. Using the tool bar, the Analyse>Gels>Select Next Lane command was then used to highlight the box and identify it as lane '2'. This was then repeated for each band in the image. Once all bands contained a rectangle around their perimeter including the number corresponding to their lane position, profile plots were then drawn for each band using the Analyse>Gel>Plot Lanes command. The resulting plots showed the relative density within each of the highlighted lanes. The width of the peaks represented the size/area of the bands and the peak height represented the shade/darkness of the bands. The straight line tool situated on the ImageJ selection toolbar was then used to draw a line across the base of each peak to enclose it so that the area could be measured with little/no background noise. This required subjective judgement as to where each peak ended and the background began. After

each peak was enclosed the wand tool from the ImageJ selection toolbar was used to measure and highlight each peak. Measurements for each peak appeared in a results pop-up window. When all peaks were highlighted using the wand tool, the peaks were then labelled using the Analyse>Gels>Label Peaks command on the toolbar. This labelled each peak with its size, expressed as a percentage of the total size of all the highlighted peaks. The values were then exported to an Excel spreadsheet to calculate the relative density of each peak. This process was repeated for bands representing housekeeping/loading control proteins. To determine the relative density of a protein normalised to the loading control the following formula was calculated. The relative densitometry value (RDV) for each loading standard band was calculated by dividing the percentage value for each lane by the percentage value in the control lane. The RDV for each sample band was then calculated by dividing the percentage value for each lane by the percentage value in the control lane. The total RDV for each protein was then calculated by dividing the RDV for each sample lane by the RDV of the loading control.

Appendix F. (3-Aminopropyl)triethoxysilane-coating of coverslips

Glass coverslips were cleaned with 100 % ethanol and allowed to air dry. Once fully dried, coverslips were incubated with 2 % (3-Aminopropyl)triethoxysilane (Tespas) in acetone for 5 seconds. The coverslips were then placed into 100 % acetone for 2 minutes before undergoing 2 x 1 minute washes in distilled water. Coated-coverslips were air-dried and sterilised before use. This procedure was performed by research technician staff in the BCMPG, Cardiff University.

Appendix G. Total cell fluorescence analysis using ImageJ software

The total level of cell fluorescence was quantified for each image taken by immunofluorescence analysis using the ImageJ software analysis programme (<http://imagej.nih.gov/ij/download.html>). Each image was uploaded into the programme and each channel was measured separately and converted to 8-bit by using the Image>Colour>Split Channels command on the toolbar. Using the Analyse>Set Measurements command on the toolbar the following parameters alone were selected: area, integrated density and grey value. Each cell in the image was then outlined using the freehand tool on the ImageJ selection toolbar which allowed the user to precisely draw around the perimeter of the cells. The images were then measured using the Analyse>Measure command on the toolbar and the values for each parameter appeared in a results pop-up window. To obtain a background reading, a region with no fluorescence was selected and measured using the Analyse>Set Measurements command. To gain an accurate reading of the background fluorescence, 3 measurements of no fluorescence were taken. The data in the pop-up window was then imported into an Excel spreadsheet and total cell fluorescence for each cell was calculated using the following formula: integrated density – (area of selected cell x mean of fluorescence of background readings). The mean total cell fluorescence for all cells in the image was then calculated and 3 independent experiments were repeated.

Appendix H. CD44 plasmid construct map

The plasmid construct map common to each CD44 plasmid used in this project. Plasmid DNA constructs containing sequences encoding CD44v3, CD44v6 and their cytoplasmic tail truncation mutants (denoted as CD44v3 Δ cyt and CD44v6 Δ cyt) fused with an EGFP-tag in a p-PGKT-T7/2 vector were a kind gift from Dr Ursula Gunthert (Basel University, Switzerland).

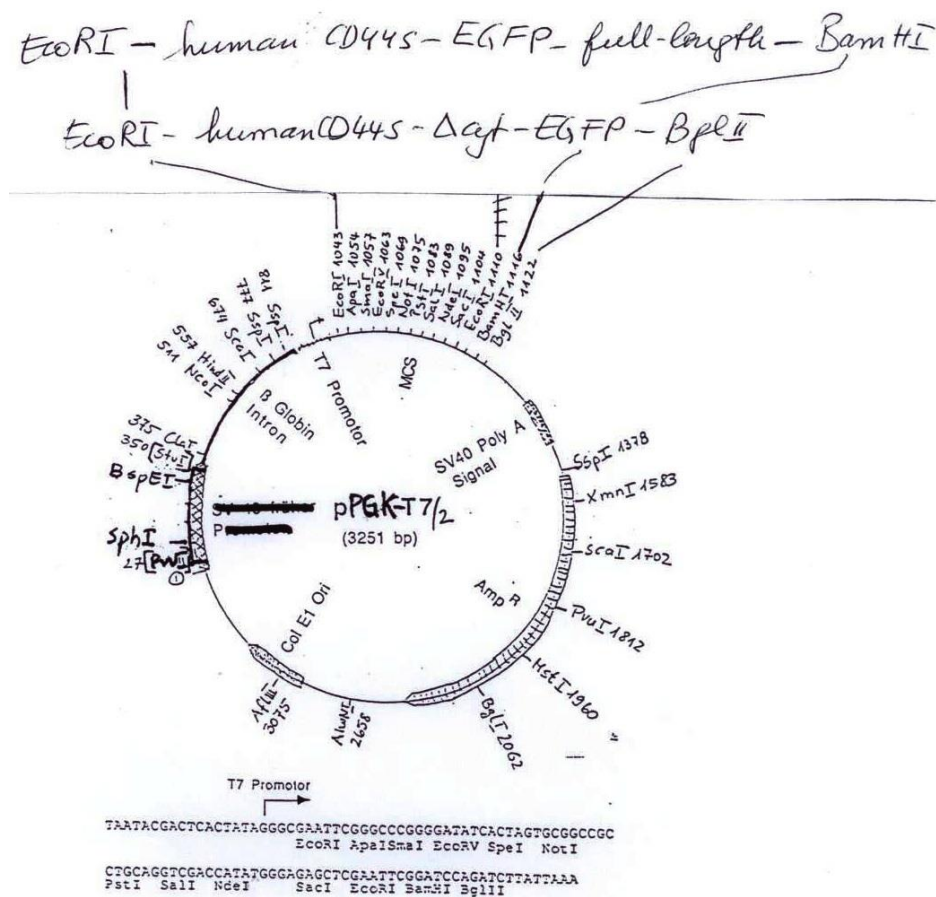


Figure 9.3. The plasmid construct map for the CD44v3, CD44v3 Δ cyt, CD44v6 and CD44v6 Δ cyt constructs obtained from Dr Ursula Gunthert, Basal University, Switzerland. This p-PGKT-T7/2 vector map shows the T7 promoter region, multiple cloning site (MCS) containing the CD44 gene insertion flanked by restriction enzymes EcoRI and BglII/BamHI and the Ampicillin resistance (Amp^R) conferred within this vector.

Appendix I. CD44 Sequencing Results

The sequencing results for each DNA plasmid construct used in this project, sequenced by the CBS and analysed using the Chromas Lite software programme (<http://technelysium.com.au/>). Each DNA sequence was translated into its protein sequence using the Expsy (<http://web.expasy.org/translate/>) online analysis software tool.

CD44v3 plasmid DNA sequence

Original sequence

Plasmid sequence

Promoter sequence

EGFP tag

gcggttaccgac

atggacaagttttggtggcacgcagcctggggactctgcctcgtgccgctgagcctggcgcagatcgatttgaat
atggacaagttttggtggcacgcagcctggggactctgcctcgtgccgctgagcctggcgcagatcgatttgaat

ataacctgccgctttgaggtgtattccacgtggagaaaaatggctcgtctacagcatctctcggacggaggccgct
ataacctgccgctttgaggtgtattccacgtggagaaaaatggctcgtctacagcatctctcggacggaggccgct

gacctctgcaaggctttcaatagcaccttgcccacaatggcccagatggagaaagctctgagcatcggatttgag
gacctctgcaaggctttcaatagcaccttgcccacaatggcccagatggagaaagctctgagcatcggatttgag

acctgcaggtatgggttcatagaaggcacgtggtgattccccggatccacccaactccatctgtgcagcaaac
acctgcaggtatgggttcatagaaggcacgtggtgattccccggatccacccaactccatctgtgcagcaaac

aacacaggggtgtacatcctcacatccaacacctcccagatgacacatattgcttcaatgcttcagctccacct
aacacaggggtgtacatcctcacatccaacacctcccagatgacacatattgcttcaatgcttcagctccacct

gaagaagattgtacatcagtcacagacctgccaatgcctttgatggaccaattaccataactattgttaaccgt
gaagaagattgtacatcagtcacagacctgccaatgcctttgatggaccaattaccataactattgttaaccgt

gatggcaccgctatgtccagaaaggagaatacagaacgaatcctgaagacatctaccccagcaaccctactgat
gatggcaccgctatgtccagaaaggagaatacagaacgaatcctgaagacatctaccccagcaaccctactgat

gatgacgtgagcagcgctcctccagtgaaggagcagcacttcaggaggttacatcttttacaccttttctact
gatgacgtgagcagcgctcctccagtgaaggagcagcacttcaggaggttacatcttttacaccttttctact

gtacaccccatcccagacgaagacagtcctcctggatcaccgacagcacagacagaatcctgctaccaggtacgtct
gtacaccccatcccagacgaagacagtcctcctggatcaccgacagcacagacagaatcctgctaccaggtacgtct

tcaaataccatctcagcaggctgggagccaaatgaagaaaatgaagatgaaagagacagacacctcagttttct
tcaaataccatctcagcaggctgggagccaaatgaagaaatgaagatgaaagagacagacacctcagttttct

ggatcaggcattgatgatgatgaagattttatctccagcaccagagaccaagacacattccaccccagtgggggg
ggatcaggcattgatgatgatgaagattttatctccagcaccagaccaagacacattccaccccagtgggggg

tcccataccactcatggatctgaatcagatggacactcacatgggagtcgaagaaggtggagcaaacacaacctct
tcccataccactcatggatctgaatcagatggacactcacatgggagtcgaagaaggtggagcaaacacaacctct

```

ggtcctataaggacaccccaaatccagaatggctgatcatcttggcatccctcttggccttggctttgattctt
ggtcctataaggacaccccaaatccagaatggctgatcatcttggcatccctcttggccttggctttgattctt

gcagtttgattgcagtcacagtcgaagaaggtgtgggcagaagaaaaagctagtgatcaacagtggaatgga
gcagtttgattgcagtcacagtcgaagaaggtgtgggcagaagaaaaagctagtgatcaacagtggaatgga

gctgtggaggacagaaagccaagtggactcaacggagagccagcaagtctcaggaaatggcatttggcgaac
gctgtggaggacagaaagccaagtggactcaacggagagccagcaagtctcaggaaatggcatttggcgaac

aaggagtcgtagcagaaactccagaccagtttatgacagctgatgagacaaggaacctgcagaatgtggacatgaag
aaggagtcgtagcagaaactccagaccagtttatgacagctgatgagacaaggaacctgcagaatgtggacatgaag

attggggtgtaa
attgggtagat

agatccccgggccgggtcgccaccatggtgagcaagggcgagagctgttcaccgggggtgtgcatcctgtcgac
tggacgcagcgtaaacgacacagttcagcgtgtccggcgaggccgaagccgaatgactaccgcaaggtgaacc
ctgaagtttcaaattcttgtgca

```

CD44v3 DNA to protein translation

Original sequence

Plasmid sequence

```

MDKFWHAAWGLCLVPLSLAQIDLNITCRFAGVFHVEKNGRYSISRTEAADLCKAFNSTL
MDKFWHAAWGLCLVPLSLAQIDLNITCRFAGVFHVEKNGRYSISRTEAADLCKAFNSTL

```

```

PTMAQMEKALSIGFETCRYGFIEGHVVIPIRIHPNSICAANNTGVYILTSNTSQYDITYCFN
PTMAQMEKALSIGFETCRYGFIEGHVVIPIRIHPNSICAANNTGVYILTSNTSQYDITYCFN

```

```

ASAPPEEDCTSVTDLPNAFDGPITITIVNRDGTRYVQKGEYRTNPEDIYPSNPTDDDVS
ASAPPEEDCTSVTDLPNAFDGPITITIVNRDGTRYVQKGEYRTNPEDIYPSNPTDDDVS

```

```

GSSSERSSTSGGYIFYTFSTVHPIPEDESPWITDSTDRIPATSTSSNTISAGWEPNEENE
GSSSERSSTSGGYIFYTFSTVHPIPEDESPWITDSTDRIPATSTSSNTISAGWEPNEEDE

```

```

DERDRHLSFSGSGIDDEDFFISRDQDTFHPSGGSHTTHGSESDGHSHGSEQEGGANTTSGP
DERDRHLSFSGSGIDDEDFFISRDQDTFHPSGGSHTTHGSESDGHSHGSEQEGGANTTSGP

```

```

IRTPQIPEWLIILASLLALALILAVCIAVNSRRRCGQKKKLVINSGNGAVEDRKPSGLNG
IRTPQIPEWLIILASLLALALILAVCIAVNSRRRCGQKKKLVINSGNGAVEDRKPSGLNG

```

EASKSQEMVHLVNKESSETPDQFMTADETRNLQNVDKIGV Stop

EASKSQEMVHLVNKESSETPDQFMTADETRNLQNVDKIGV Stop

Figure 9.4. The DNA sequencing results performed by the CBS and analysed using the software programmes Chromas Lite and Expsy for the CD44v3 plasmid construct. The variant 3 exon is highlighted in bold and underlined. The plasmid DNA sequence revealed a substitution mutation from guanine to alanine in the variant 3 exon (highlighted in yellow). Protein analysis using the online protein translation tool Expsy revealed this base pair substitution converted the amino acid from an asparagine (N) to an aspartic acid (D). No other differences between the original and plasmid CD44v3 sequence were found.

CD44v3Δcyt plasmid DNA and protein sequence

Original sequence

Plasmid sequence

Promoter sequence

EGFP tag

ccccttcccacccccgcc

atggacaagttttggtggcagcgagcctggggactctgctcgtgccgctgagcctggcgcagatcgatttgaat
atggacaagttttggtggcagcgagcctggggactctgctcgtgccgctgagcctggcgcagatcgatttgaat

ataacctgccgctttgaggtgtattccacgtggagaaaaatggtcgctacagcatctctcggacggaggccgct
ataacctgccgctttgaggtgtattccacgtggagaaaaatggtcgctacagcatctctcggacggaggccgct

gacctctgcaaggtttcaatagcaccttgcccacaatggcccagatggagaaagctctgagcatcgatttgaat
gacctctgcaaggtttcaatagcaccttgcccacaatggcccagatggagaaagctctgagcatcgatttgaat

acctgcaggtatgggttcatagaagggcacgtgggtgattccccggatccaccccactccatctgtgcagcaaac
acctgcaggtatgggttcatagaagggcacgtgggtgattccccggatccaccccactccatctgtgcagcaaac

aacacaggggtgtacatcctcacatccaacacctcccagatgacacatattgcttcaatgcttcagctccacct
aacacaggggtgtacatcctcacatccaacacctcccagatgacacatattgcttcaatgcttcagctccacct

gaagaagattgtacatcagtcacagacctgccaatgcctttgatggaccaattaccataactattgttaaccgt
gaagaagattgtacatcagtcacagacctgccaatgcctttgatggaccaattaccataactattgttaaccgt

gatggcacccgctatgtccagaaaggagaatacagaacgaatcctgaagacatctaccccagcaaccctactgat
gatggcacccgctatgtccagaaaggagaatacagaacgaatcctgaagacatctaccccagcaaccctactgat

gatgacgtgagcagcgctcctccagtgaaggagcagcacttcaggaggttacatcttttacaccttttctact
gatgacgtgagcagcgctcctccagtgaaggagcagcacttcaggaggttacatcttttacaccttttctact

gtacaccccattcccagacgaagacagtcctctggatcacccgacagcacagacagaatccctgctaccaggtacgtct
gtacaccccattcccagacgaagacagtcctctggatcacccgacagcacagacagaatccctgctaccaggtacgtct

tcaaataccatctcagcaggctgggagccaaatgaagaaatgaagatgaaagagacagacacctcagttttct
tcaaataccatctcagcaggctgggagccaaatgaagaaatgaagatgaaagagacagacacctcagttttct

ggatcaggcattgatgatgaagattttatctccagcaccagagaccaagacacattccaccccagtgggggg
ggatcaggcattgatgatgaagattttatctccagcaccagagaccaagacacattccaccccagtgggggg

tccataaccactcatggatctgaatcagatggacactcacatgggagtcagaaggtggagcaaacacaacctct
tccataaccactcatggatctgaatcagatggacactcacatgggagtcagaaggtggagcaaacacaacctct

ggtcctataaggacacccccaaattccagaatggctgatcatcttggcatccctcttggccttggtttgattctt
ggtcctataaggacacccccaaattccagaatggctgatcatcttggcatccctcttggccttggtttgattctt

gcagtttgattgcagtcacagtcgaagaaggtgtgggcagaagaaaaagctagtgatcaacagtggaatgga
gcagtttgattgcagtcacagtcgaagaaggtgtgggcagaagaaaaagctagtgatcaacagtggaatgga

gctgtggaggacagaaagccaagtggactcaacggagagccagcaagtctcaggaaatggtgcatttggtgaaac

aaggagtcgtcagaaactccagaccagtttatgacagctgatgagacaaggaacctgcagaatgtggacatgaag

attgggtgtaa

agatccccggcggctgccaccatggtgagcaagggcgaggagctgttaccgggggtggtgccatcctggtcga
gctggacggcgacgtaaacggccacaagttcagcgtgtccggcgagggcgagggcgatgccacctacggcaagct

gaccctgaagttcatctgcaccaccggcaagctgcccgctgccctggcccaccctcgtgaccaccctgacctacgg
cggcgcagtgctttcagccgctaccccgaccacatgaagcagcagcacttcttcagtcgccatgcccgatgcta
cgttcagagcgcaacaatctctcagacgacggcaacctacaagaccgcccaggtgaaggttcgaagggcgac
aac

DNA to protein translation

Original sequence

Plasmid sequence

MDKFWWHAAGLCLVPLSLAQIDLNITCRFAGVFHVEKNGRYSISRTEAADLCKAFNSTL
MDKFWWHAAGLCLVPLSLAQIDLNITCRFAGVFHVEKNGRYSISRTEAADLCKAFNSTL

PTMAQMEKALSIGFETCRYGFIEGHVVIPIRIHPNSICAAANTGVYILTSNTSQYDTYCFN
PTMAQMEKALSIGFETCRYGFIEGHVVIPIRIHPNSICAAANTGVYILTSNTSQYDTYCFN

ASAPPEEDCTSVTDLPNAFDGPITITIVNRDGRYVQKGEYRTNPEDIYPSNPTDDDVS
ASAPPEEDCTSVTDLPNAFDGPITITIVNRDGRYVQKGEYRTNPEDIYPSNPTDDDVS

GSSSERSSTSGGYIFYTFSTVHPIPEDSPWITDSTDRI **PATSTSSNTISAGWEPNEENE**
GSSSERSSTSGGYIFYTFSTVHPIPEDSPWITDSTDRI **PATSTSSNTISAGWEPNEED**

DERDRHLSFSGSGIDDED FISRDQTFHPSGGSHTTHGSESDGSHSGSQEGGANTTSGP
DERDRHLSFSGSGIDDED FISRDQTFHPSGGSHTTHGSESDGSHSGSQEGGANTTSGP

IRTPQIPEWLIILASLLALALILAVCIAVNSRRRCGQKKKLVINSNGNGAVEDRKPSGLNG
IRTPQIPEWLIILASLLALALILAVCIAVN

EASKSQEMVHLVNKESSETPDQFMTADETRNLQNVDKIGV Stop

Figure 9.5. The DNA sequencing results as performed by the CBS and analysed using the software programmes Chromas Lite and Expasy for the CD44v3Δcyt plasmid construct. The variant 3 exon is highlighted in bold and underlined. The DNA and protein sequence show the loss of the cytoplasmic tail starting at amino acid position 330. The plasmid DNA sequence revealed a substitution mutation from guanine to alanine in the variant 3 exon (highlighted in yellow). Protein analysis using the online protein translation tool Expasy revealed this base pair substitution converted the amino acid from an asparagine (N) to an aspartic acid (D). No other differences between the original and plasmid CD44v3Δcyt sequence were found.

CD44v6 plasmid DNA and protein sequence

Original sequence

Plasmid sequence

Promoter sequence

EGFP tag

acggatacacgctc

atggacaagttttggtggcagcgagcctggggactctgcctcgtgccgctgagcctggcgagatcgatttgaat
atggacaagttttggtggcagcgagcctggggactctgcctcgtgccgctgagcctggcgagatcgatttgaat

ataacctgccgctttgaggtgtattccacgtggagaaaaatggtcgctacagcatctctcgacggagggccgct
ataacctgccgctttgaggtgtattccacgtggagaaaaatggtcgctacagcatctctcgacggagggccgct

gacctctgcaaggctttcaatagcaccttgcccacaatggcccagatggagaaagctctgagcatcgatttgag
gacctctgcaaggctttcaatagcaccttgcccacaatggcccagatggagaaagctctgagcatcgatttgag

acctgcaggtatgggttcatagaaggcagctgggtgattccccggatccaccccaactccatctgtgcagcaaac
acctgcaggtatgggttcatagaaggcagctgggtgattccccggatccaccccaactccatctgtgcagcaaac

aacacaggggtgtacatcctcacatccaacacctcccagatgacacatattgcttcaatgcttcagctccacct
aacacaggggtgtacatcctcacatccaacacctcccagatgacacatattgcttcaatgcttcagctccacct

gaagaagattgtacatcagtcacagacctgccaatgcctttgatggaccaattaccataactattgttaaccgt
gaagaagattgtacatcagtcacagacctgccaatgcctttgatggaccaattaccataactattgttaaccgt

gatggcaccgctatgtccagaaaggagaatacagaacgaatcctgaagacatctaccccagcaaccctactgat
gatggcaccgctatgtccagaaaggagaatacagaacgaatcctgaagacatctaccccagcaaccctactgat

gatgacgtgagcagcgctcctccagtgaaggagcagcacttcaggaggttacatcttttacaccttttctact
gatgacgtgagcagcgctcctccagtgaaggagcagcacttcaggaggttacatcttttacaccttttctact

gtacaccccatcccagacgaagacagtcctctggatcaccgacagcacagacagaatcctctgctacca**ccaggca**
gtacaccccatcccagacgaagacagtcctctggatcaccgacagcacagacagaatcctctgctacca**ccaggca**

actcctagtagtacaacggaagaacagctaccagaaggaacagtggtttggcaacagatggcatgagggatat
actcctagtagtacaacggaagaacagctaccagaaggaacagtggtttggcaacagatggcatgagggatat

cgccaaacacccaaagaagactcccattcgacaacagggacagctggagaccaagacacattccaccccagtggg
cgccaaacacccaaagaagactcccattcgacaacagggacagctggagaccaagacacattccaccccagtggg

gggtccataccactcatggatctgaatcagatggacactcacatgggagtcagaaggtggagcaaacacaacc
gggtccataccactcatggatctgaatcagatggacactcacatgggagtcagaaggtggagcaaacacaacc

tctggtcctataaggacaccccaattccagaatggctgatcatcttggcatcctcttggccttggcctttgatt
tctggtcctataaggacaccccaattccagaatggctgatcatcttggcatcctcttggccttggcctttgatt

cttgacgtttgcattgcagtcacagtcgaagaaggtgtgggcagaagaaaagctagtgatcaacagtggaat
cttgacgtttgcattgcagtcacagtcgaagaaggtgtgggcagaagaaaagctagtgatcaacagtggaat

ggagctgtggaggacagaaagccaagtggactcaacggagagggcagcaagtctcaggaatggtgcatttggtg
ggagctgtggaggacagaaagccaagtggactcaacggagagggcagcaagtctcaggaatggtgcatttggtg

aaaagagctcgtcagaactccagaccagtttatgacagctgatgagacaaggaacctgcagaatgtggacatg
aaaagagctcgtcagaactccagaccagtttatgacagctgatgagacaaggaacctgcagaatgtggacatg

aagattgggggtgtaa

aagattggggtagat

agatccccgggcccgggtcgccaccatggtgagcaaggacgaggagctgttcaccgggggtggtgccatcctggtc
gagctgggacggcgacgttaaacgtcacagtttcagcgtgtccgccaagtcgaagtcgatgccaccgtaccggca
gcttgaacctgaaggttcat

DNA to protein translation

Original sequence

Plasmid sequence

MDKFWHAAWGLCLVPLSLAQIDLNITCRFAGVFHVEKNGRYSISRTEAADLCKAFNSTL
MDKFWHAAWGLCLVPLSLAQIDLNITCRFAGVFHVEKNGRYSISRTEAADLCKAFNSTL

PTMAQMEKALSIGFETCRYGFIEGHVVIPIRIHPNSICAAANTGVYILTSNTSQYDTCFN
PTMAQMEKALSIGFETCRYGFIEGHVVIPIRIHPNSICAAANTGVYILTSNTSQYDTCFN

ASAPPEEDCTSVTDLPNAFDGPITITIVNRDGTRYVQKGEYRTNPEDIYPSNPTDDDVS
ASAPPEEDCTSVTDLPNAFDGPITITIVNRDGTRYVQKGEYRTNPEDIYPSNPTDDDVS

GSSSERSSTSGGYIFYTFSTVHPIPEDDSPWITDSTDRIPAT**IQATPSSTEETATQKEQW**
GSSSERSSTSGGYIFYTFSTVHPIPEDDSPWITDSTDRIPAT**IQATPSSTEETATQKEQW**

FGNRWHEGYRQTPKEDSHSTTGTAGDQDTFHPSGGSTTHGSESDGHSHGSQEGGANTTSG
FGNRWHEGYRQTPKEDSHSTTGTAGDQDTFHPSGGSTTHGSESDGHSHGSQEGGANTTSG

PIRTPQIPEWLIILASLLALALILAVCIAVNSRRRCGQKKKLVINSGNGAVEDRKPSGLN
PIRTPQIPEWLIILASLLALALILAVCIAVNSRRRCGQKKKLVINSGNGAVEDRKPSGLN

GEASKSQEMVHLVNKESSETPDQFMTADETRNLQNVDKIGV Stop

GEASKSQEMVHLVNKESSETPDQFMTADETRNLQNVDKIGV Stop

Figure 9.6. The DNA sequencing results as performed by the CBS and analysed using the software programmes Chromas Lite and Expsy for the CD44v6 plasmid construct. The variant 6 exon is highlighted in bold and underlined. No differences between the original and plasmid CD44v6 DNA and protein sequence were found.

CD44v6Δcyt plasmid DNA and protein sequence

Original sequence

Plasmid sequence

Promoter sequence

EGFP tag

acacttcacgac

atggacaagttttggtggcagcagcctggggactctgcctcgtgccgctgagcctggcgcagatcgatttgaat
atggacaagttttggtggcagcagcctggggactctgcctcgtgccgctgagcctggcgcagatcgatttgaat

ataacctgccgctttgaggtgtattccacgtggagaaaaatggctcgtacagcatctctcggacggaggccgct
ataacctgccgctttgaggtgtattccacgtggagaaaaatggctcgtacagcatctctcggacggaggccgct

gacctctgcaaggctttcaatagcaccttgcccacaatggcccagatggagaaagctctgagcatcgatttgaat
gacctctgcaaggctttcaatagcaccttgcccacaatggcccagatggagaaagctctgagcatcgatttgaat

acctgcaggtatgggttcatagaaggacacgtggtgattccccggatccccccaactccatctgtgcagcaaac
acctgcaggtatgggttcatagaaggacacgtggtgattccccggatccccccaactccatctgtgcagcaaac

aacacaggggtgtacatcctcacatccaacacctcccagtatgacacatattgcttcaatgcttcagctccacct
aacacaggggtgtacatcctcacatccaacacctcccagtatgacacatattgcttcaatgcttcagctccacct

gaagaagattgtacatcagtcacagacctgccaatgcctttgatggaccaattaccataactattgttaaccgt
gaagaagattgtacatcagtcacagacctgccaatgcctttgatggaccaattaccataactattgttaaccgt

gatggaccccgctatgtccagaaaggagaatacagaacgaatcctgaagacatctaccccagcaaccctactgat
gatggaccccgctatgtccagaaaggagaatacagaacgaatcctgaagacatctaccccagcaaccctactgat

gatgacgtgagcagcgctcctccagtgaaggagcagcacttcaggaggttacatcttttacaccttttctact
gatgacgtgagcagcgctcctccagtgaaggagcagcacttcaggaggttacatcttttacaccttttctact

gtacaccccatcccagacgaagacagtcctctggatcacccagacagcagacagaatccttgcctacca**tcaggca**
gtacaccccatcccagacgaagacagtcctctggatcacccagacagcagacagaatccttgcctacca**tcaggca**

actcctagtagtacaacggaagaacagctaccagaaggaacagtgggttggcaacagatggcatgagggatat
actcctagtagtacaacggaagaacagctaccagaaggaacagtgggttggcaacagatggcatgagggatat

cgccaaacacccaagaagactcccattcgacaacagggacagctggagaccaagacacattccaccccagtggg
cgccaaacacccaagaagactcccattcgacaacagggacagctggagaccaagacacattccaccccagtggg

gggtccatataccactcatggatctgaatcagatggacactcacatgggagtcagaagggtggagcaaacacaacc
gggtccatataccactcatggatctgaatcagatggacactcacatgggagtcagaagggtggagcaaacacaacc

tctggtcctataaggacaccccaattccagaatggctgatcatcttggcatccctcttggccttggctttgatt
tctggtcctataaggacaccccaattccagaatggctgatcatcttggcatccctcttggccttggctttgatt

cttgacgtttgcattgcagtcacagtcgaagaaggtgtgggcagaagaaaaagctagtgatcaacagtgggcaat
cttgacgtttgcattgcagtcacagtcgaagaaggtgtgggcagaagaaaaagctagtgatcaacagtgggcaat

ggagctgtggaggacagaaagccaagtggactcaacggagagggccagcaagtctcaggaaatgggtgcatttgggtg

aacaaggagtcgtcagaaactccagaccagtttatgacagctgatgagacaaggaacctgcagaatgtggacatg

aagattgggggtgtaa

agatccccggcggctgccaccatggtgagcaaggcgaggagctgttcacgggggtggtgccatcctggctoga
gctggacggcgacgtaaacggccacaagttcagcgtgtccggcgagggcgagggcgatgccacctacggcaagct
gacctgaagttcatctgcaccaccggcaagctgcccgtgcctggcccacctcgtgaccacctgacctacgg
cgtgcagtgcttcagccgctaccccagcaatggagcagcagacttctcagtcgccatgccgatgcctacg
tcagagcgcacatctctcaagacgaccgcaacctacaagaccggcgcccggaggggtgaagtcg

DNA to protein translation

Original sequence

Plasmid sequence

MDKFWHAAWGLCLVPLSLAQIDLNITCRFAGVFHVEKNGRYSISRTEAADLCKAFNSTL
MDKFWHAAWGLCLVPLSLAQIDLNITCRFAGVFHVEKNGRYSISRTEAADLCKAFNSTL

PTMAQMEKALSIGFETCRYGFIEGHVVIPIRHPNSICAAANTGVYILTSNTSQYDTYCFN
PTMAQMEKALSIGFETCRYGFIEGHVVIPIRHPNSICAAANTGVYILTSNTSQYDTYCFN

ASAPPEEDCTSVTDLPNAFDGPITITIVNRDGTRYVQKGEYRTNPEDIYPSNPTDDDVS
ASAPPEEDCTSVTDLPNAFDGPITITIVNRDGTRYVQKGEYRTNPEDIYPSNPTDDDVS

GSSSERSSTSGGYIFYTFSTVHPIPEDSPWITDSTDRIPAT**IQATPSSTEETATQKEQW**
GSSSERSSTSGGYIFYTFSTVHPIPEDSPWITDSTDRIPAT**IQATPSSTEETATQKEQW**

FGNRWHEGYRQTPKEDSHSTTGTAGDQDTFHPSGGSTTHGSESDGHSHGSQEGGANTTSG
FGNRWHEGYRQTPKEDSHSTTGTAGDQDTFHPSGGSTTHGSESDGHSHGSQEGGANTTSG

PIRTPQIPEWLIILASLLALALI LAVCIAVNSRRRCGQKKKLVINSGNGAVEDRKPSGLN
PIRTPQIPEWLIILASLLALALI LAVCIAVN

GEASKSQEMVHLVNKESSETPDQFMTADETRNLQNVDMKIGV Stop

Figure 9.7. The DNA sequencing results as performed by the CBS and analysed using the software programmes Chromas Lite and Expasy for the CD44v6 Δ cyt plasmid construct. The variant 6 exon is highlighted in bold and underlined. The DNA and protein sequence show the loss of the cytoplasmic tail starting at amino acid position 330. No other differences between the original and plasmid CD44v6 Δ cyt sequence were found.

Appendix J. Optimisation of HA stimulation across MCF-7, Tam-R and Fas-R cells

The effect of high molecular weight HA upon the induction of growth factor signalling across the cell models. The cell lines were treated with high molecular weight HA (>500 kDa, R&D Systems, UK) for 10 minutes before cell lysis and investigation of protein activation by Western blotting. The results revealed that high molecular weight HA stimulated less of a signalling response to HER2, EGFR and ERK1/2 across the cell models compared to stimulation with medium molecular weight HA (215 kDa) (shown in Figure 4.3). Therefore medium molecular weight HA was used for subsequent exogenous HA stimulation in this project.

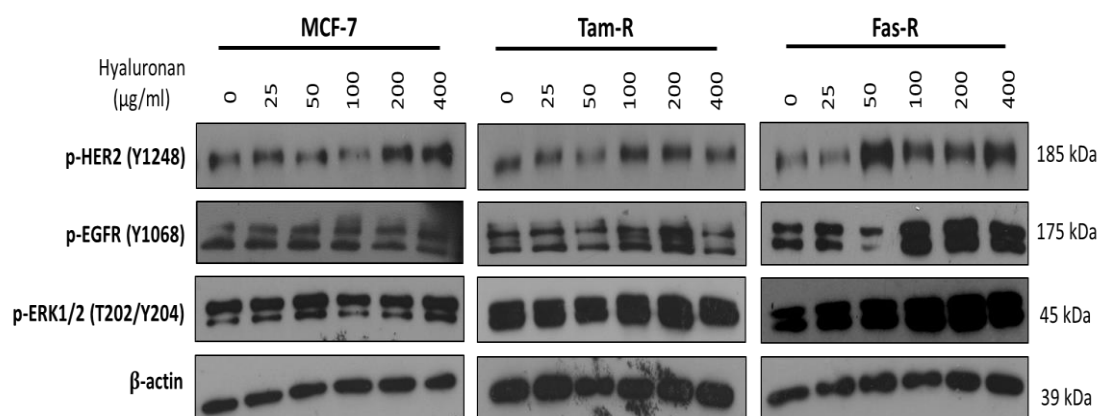


Figure 9.8. Representative Western blot images from 3 independent experiments showing HER2, EGFR and ERK1/2 activation in MCF-7, Tam-R and Fas-R cells in response to dose-dependent high molecular HA stimulation (>500 kDa, 0 – 400 μg/ml) for 10 minutes with β actin as a loading control.

Appendix K. Densitometry analysis for CD44 isoform and RHAMM expression in

Tam-R and Fas-R cells treated with global CD44 siRNA

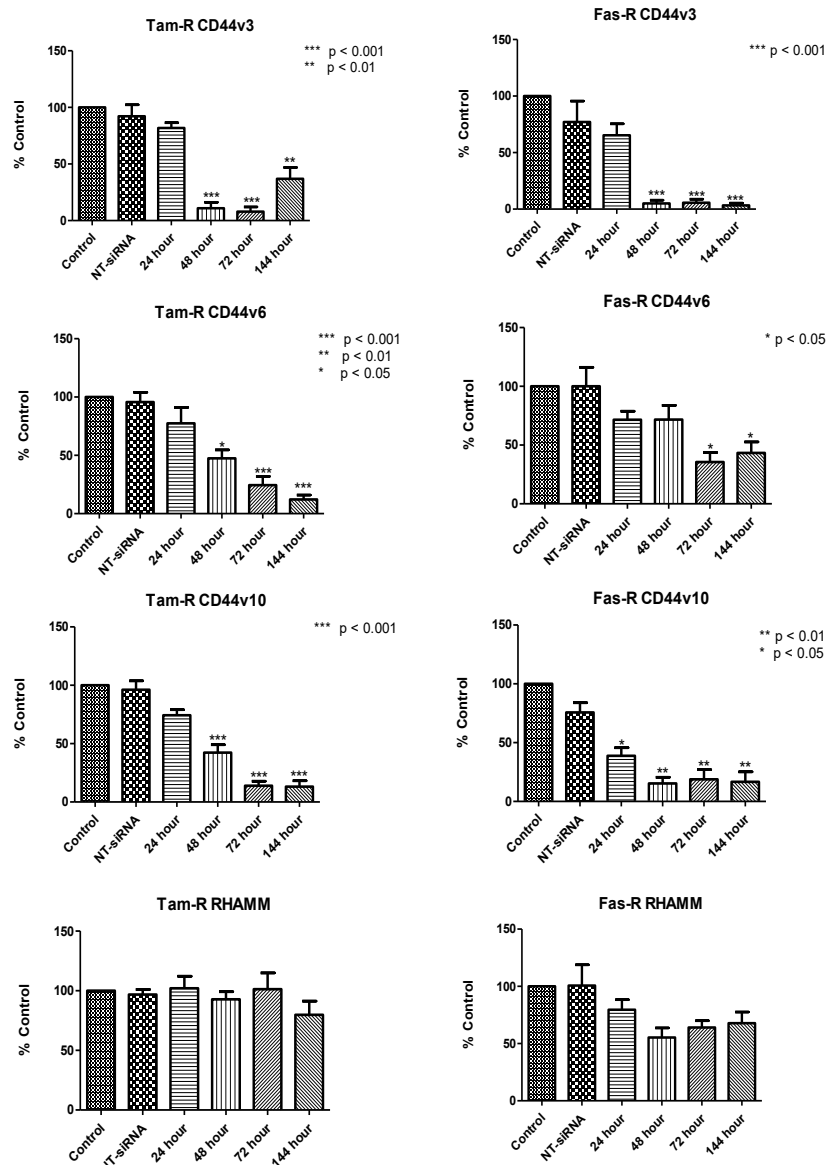


Figure 9.10. Densitometry graphs showing CD44v3, CD44v6, CD44v10 and RHAMM expression in Tam-R and Fas-R cells after 24 – 144 hour treatment with global CD44 siRNA before cell lysis and detection by Western blotting analysis. The data shows the total protein levels in the cell lines normalised to GAPDH. Error bars represent the average normalised data \pm SEM from 3 independent experiments and the data is presented as the percentage of the untreated control. Statistical analysis was performed using a one-way ANOVA with Tukey post-hoc testing and all values were compared to the NT-siRNA control to identify any significant changes across all 3 cell models. Significance was set at $p < 0.05$.

Appendix L. Densitometry analysis for CD44 isoform expression in Tam-R and Fas-R-

R cells treated with global RHAMM siRNA

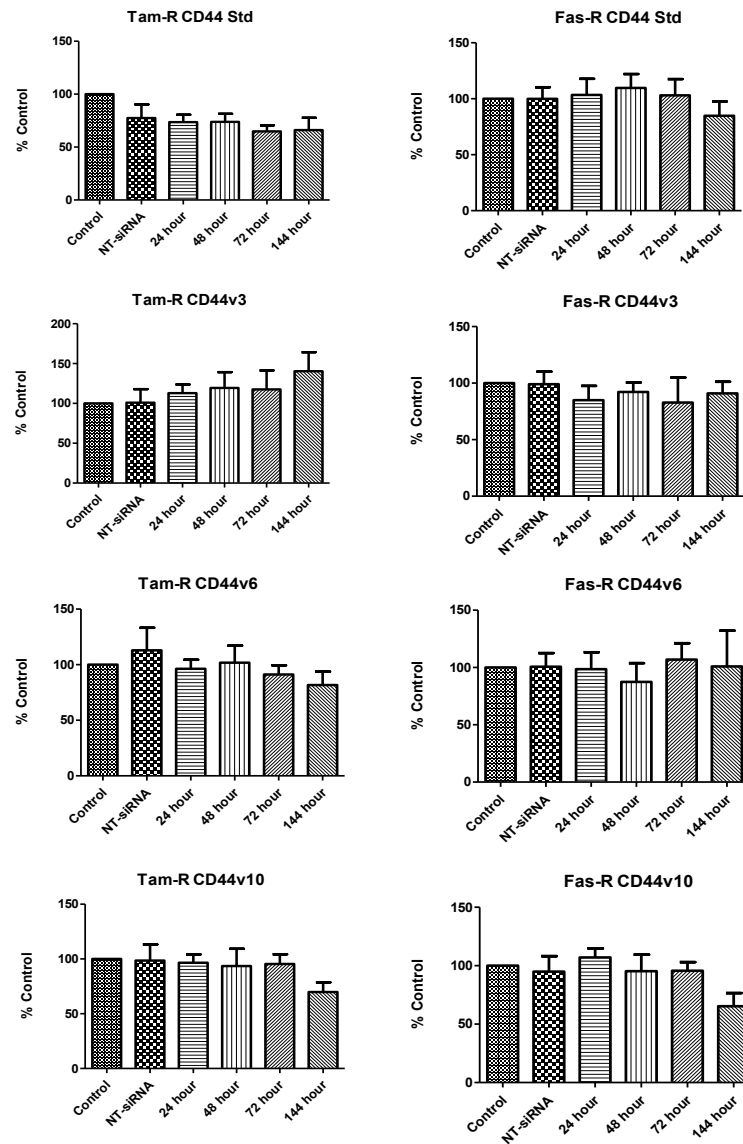


Figure 9.11. Densitometry graphs showing CD44 Std, CD44v3, CD44v6 and CD44v10 expression in Tam-R and Fas-R cells after 24 – 144 hour treatment with global RHAMM siRNA before cell lysis and detection by Western blotting analysis. The data shows the total protein levels in the cell lines normalised to GAPDH. Error bars represent the average normalised data \pm SEM from 3 independent experiments and the data is presented as the percentage of the untreated control. Statistical analysis was performed using a one-way ANOVA with Tukey post-hoc testing and all values were compared to the NT-siRNA control to identify any significant changes across all 3 cell models. Significance was set at $p < 0.05$.

Appendix M. Predicting the effect of amino acid substitutions on protein function

To predict whether the N239D amino acid substitution (arginine to aspartic acid) detected by sequencing analysis in the variant 3 exon of the CD44v3/CD44v3Δcyt plasmid constructs may alter its protein function, several online publically available software programmes were utilised.

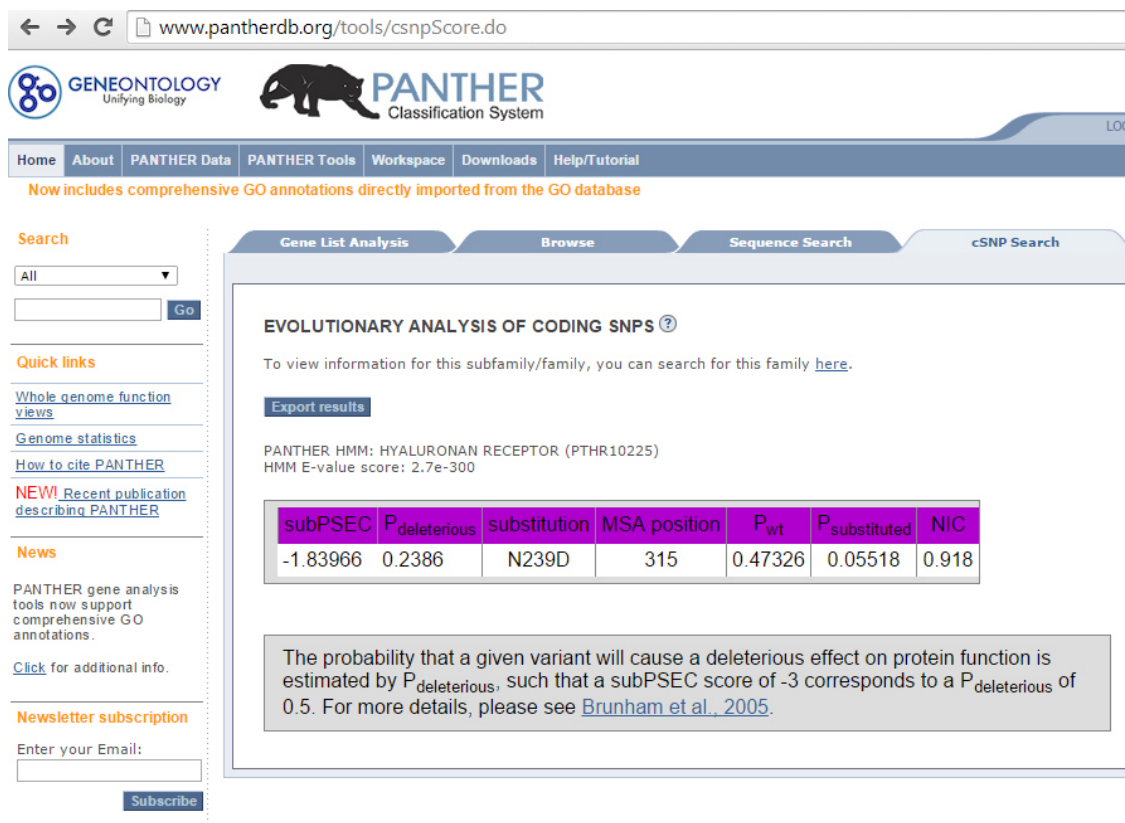
PROVEAN

The Protein Variation Effect Analyser (PROVEAN) online software tool (<http://provean.jcvi.org/index.php>) was utilised to predict whether the amino acid substitution (N239D) in the variant 3 exon may alter its protein function (Choi et al. 2012). The results revealed a PROVEAN score of -1.436 which scored above the -2.5 threshold thus suggesting that this substitution was 'neutral' and did not have a deleterious effect upon protein function.

PROVEAN Prediction - Job ID: 012466680014698		
Query sequence (fasta)		
Supporting sequence set used for prediction		
Number of sequences: 163 (fasta , E-values)		
Number of clusters: 30		
Score thresholds for prediction		
(1) Default threshold is -2.5, that is:		
-Variants with a score equal to or below -2.5 are considered "deleterious,"		
-Variants with a score above -2.5 are considered "neutral."		
(2) How to use a more stringent threshold.		
Variant	PROVEAN score	Prediction (cutoff= -2.5)
N239D	-1.436	Neutral

PANTHER

The online Protein Analysis Through Evolutionary Relationships (PANTHER) classification System tool (www.pantherdb.org/) (Mi et al. 2013a; Mi et al. 2013b) was used as an additional means to investigate the effect of the N239D amino acid substitution in the CD44v3 exon. The results confirmed those gathered from the PROVEAN tool and the subPSEC score was -1.83966 which was above the threshold of -3 suggesting that this substitution does not have a deleterious effect upon protein function.



The screenshot shows the PANTHER website interface. The browser address bar displays www.pantherdb.org/tools/csnpscore.do. The page features the PANTHER logo and navigation tabs for Home, About, PANTHER Data, PANTHER Tools, Workspace, Downloads, and Help/Tutorial. A search bar is present with a dropdown menu set to 'All' and a 'Go' button. Below the search bar are quick links for 'Whole genome function views', 'Genome statistics', 'How to cite PANTHER', and 'NEW! Recent publication describing PANTHER'. A 'News' section mentions that PANTHER tools now support comprehensive GO annotations. A 'Newsletter subscription' form is also visible.

The main content area is titled 'EVOLUTIONARY ANALYSIS OF CODING SNPS' and includes an 'Export results' button. The results for the N239D substitution in the PTHR10225 protein family are shown in the following table:

subPSEC	P _{deleterious}	substitution	MSA position	P _{wt}	P _{substituted}	NIC
-1.83966	0.2386	N239D	315	0.47326	0.05518	0.918

A text box below the table explains that the probability of a deleterious effect is estimated by P_{deleterious}, and that a subPSEC score of -3 corresponds to a P_{deleterious} of 0.5, citing Brunham et al., 2005.

SIFT

The Sorting Intolerant From Tolerant (SIFT) sequence online tool (http://sift.jcvi.org/www/SIFT_seq_submit2.html) provides predictions for a given

FASTA sequence whether an amino acid substitution may alter protein function (Ng and Henikoff 2006; Kumar et al. 2009). SIFT scores of <0.05 were predicted to be deleterious. The results of this analysis revealed a score of 0.74 with the amino acid substitution at this position predicted to be tolerated. The web page below shows the list of tolerated amino acids sequences in the CD44v3 exon. At position 239 the amino acid asparagine (N) is predicted to tolerate the substitution to an aspartic acid (D).

← → ↻ sift.bii.a-star.edu.sg/sift-bin/catfile.csh?/opt/www/sift/tmp/948025f438_sequences.siftresults

Predictions

Substitution at pos 239 from N to D is predicted to be TOLERATED with a score of 0.74.
 Median sequence conservation: 3.37
 Sequences represented at this position:7

← → ↻ sift.bii.a-star.edu.sg/sift-bin/catfile.csh?/opt/www/sift/tmp/4e748fc7df_sequences.aatable3 ☆

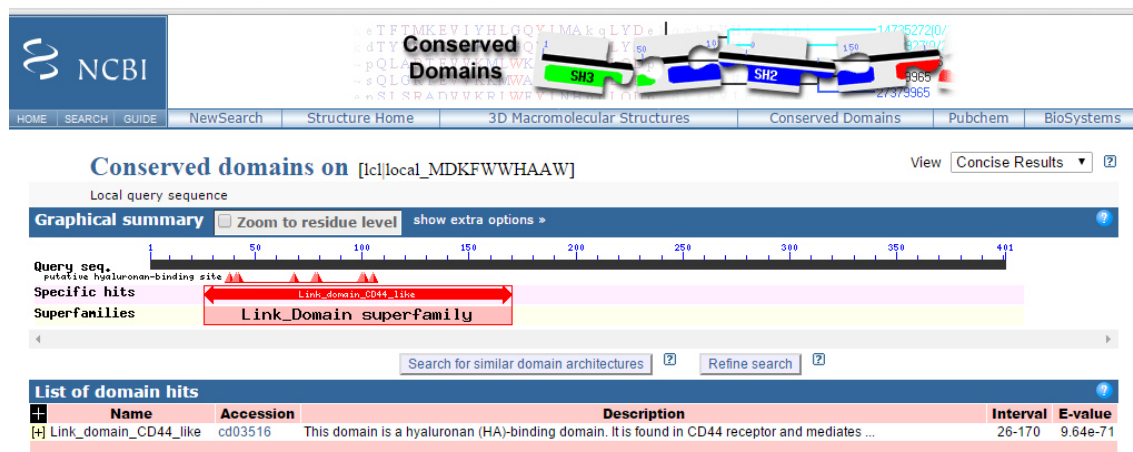
Predictions for positions 201 through 300

Threshold for intolerance is 0.05.
 Amino acid color code: nonpolar, uncharged polar, basic, acidic.
 Capital letters indicate amino acids appearing in the alignment, lower case letters result from prediction.
 'Seq Rep' is the fraction of sequences that contain one of the basic amino acids. A low fraction indicates the position is either severely gapped or unalignable and has little information. Expect poor prediction at these positions.

Predict Not Tolerated	Position Seq Rep	Predict Tolerated
w	239N 0.24	y c f Mh i P v l GNr t q d S Ak E

Appendix N. Conserved domains in the CD44v3 sequence

To determine whether any conserved domains in the CD44v3 sequence existed which may become altered upon amino acid substitution, the online Conserved Domains and Protein Classification tool was utilised (<http://www.ncbi.nlm.nih.gov/Structure/cdd/wrpsb.cgi>) (Marcherl-Bauer et al. 2015). This tool revealed that the only conserved sequence found in the CD44v3 protein sequence was the link module (HA binding domain) found in the extracellular domain of CD44 and not within the variant 3 exon.



Appendix O. Densitometry analysis for CD44 isoform expression and RHAMM in

MCF-7 cells treated with CD44v3 and CD44v3 Δ cyt plasmid DNA

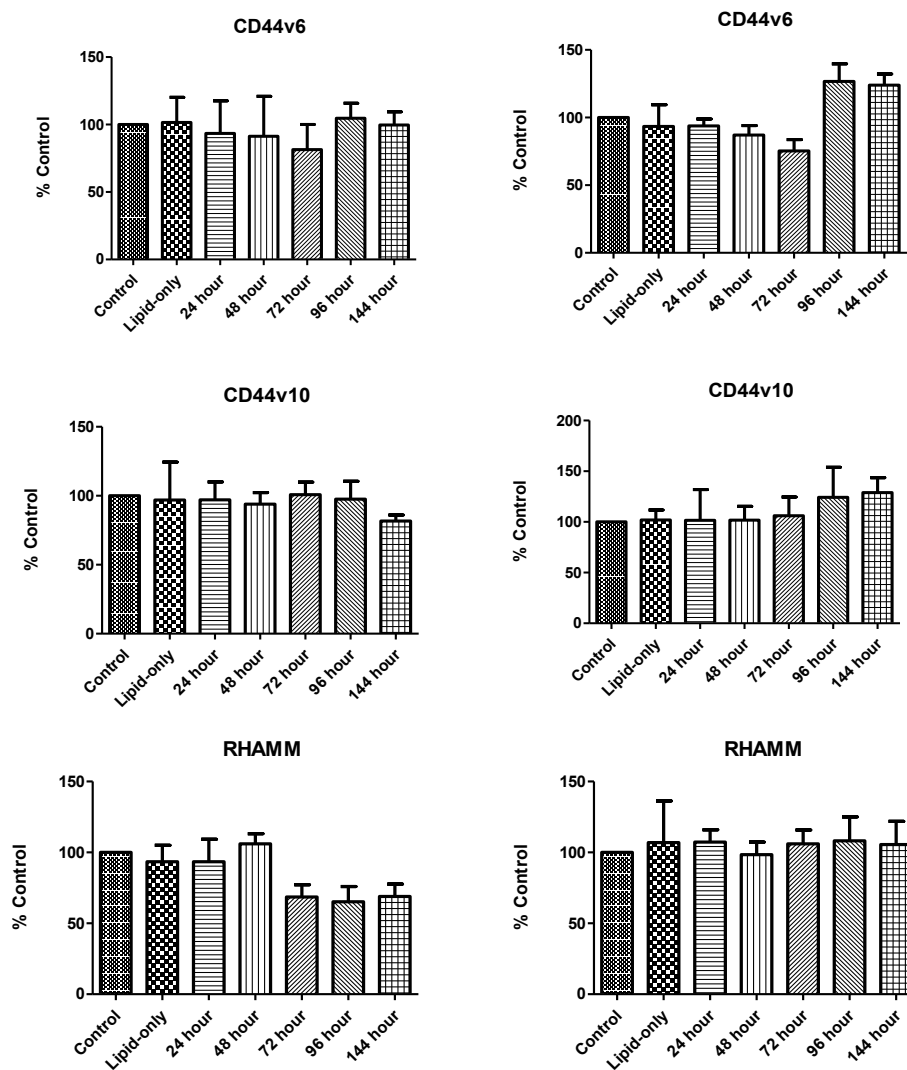


Figure 9.12. Densitometry graphs showing CD44v6, CD44v10 and RHAMM expression in MCF-7 cells after 24 – 144 hour treatment with CD44v3 (left) or CD44v3 Δ cyt (right) plasmid DNA, before cell lysis and detection by Western blotting analysis. The data shows the total protein levels in the cell lines normalised to GAPDH. Error bars represent the average normalised data \pm SEM from 3 independent experiments and the data is presented as the percentage of the untreated control. Statistical analysis was performed using a one-way ANOVA with Tukey post-hoc testing and all values were compared to the lipid-only control to identify any significant changes across all 3 cell models. Significance was set at $p < 0.05$.

Appendix P. Densitometry analysis for CD44 isoform expression and RHAMM in

MCF-7 cells treated with CD44v6 and CD44v6 Δ cyt plasmid DNA

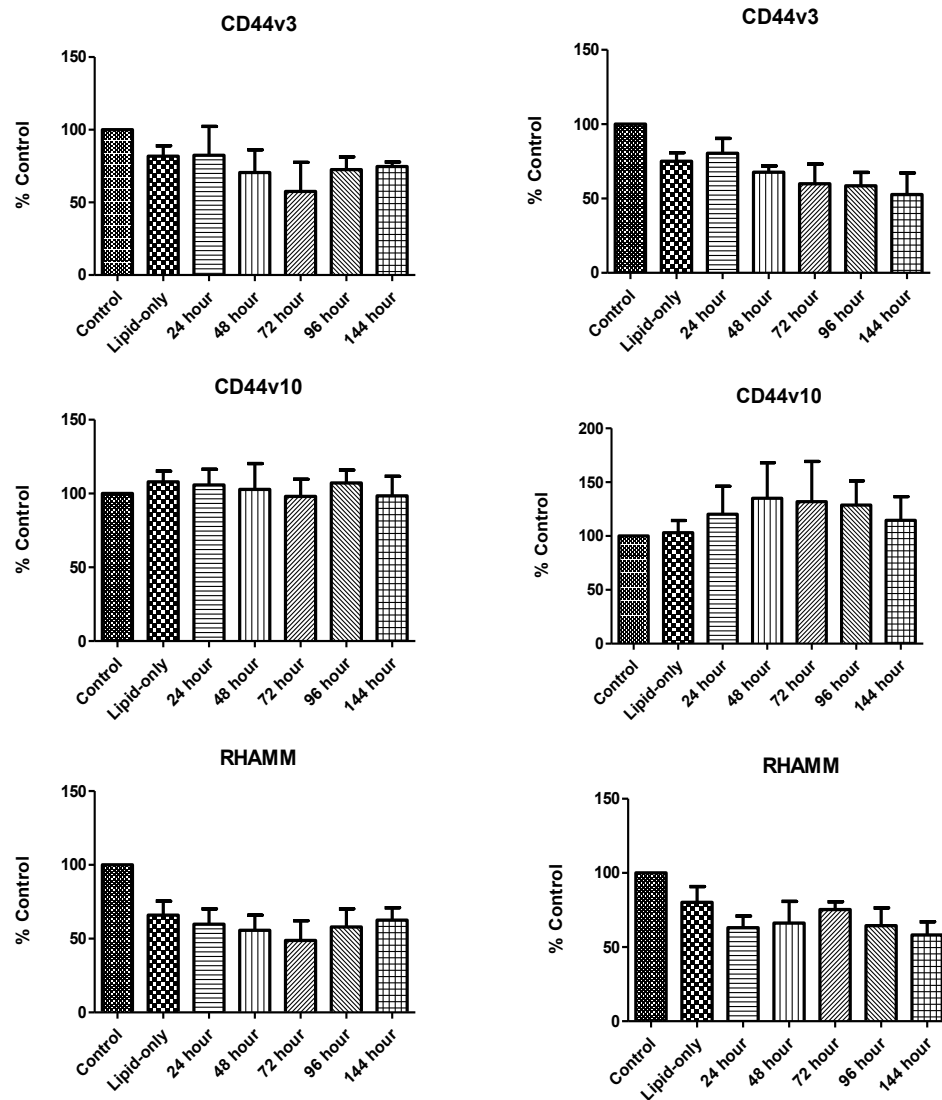


Figure 9.13. Densitometry graphs showing CD44v3, CD44v10 and RHAMM expression in MCF-7 cells after 24 – 144 hour treatment with CD44v6 (left) or CD44v6 Δ cyt (right) plasmid DNA, before cell lysis and detection by Western blotting analysis. The data shows the total protein levels in the cell lines normalised to GAPDH. Error bars represent the average normalised data \pm SEM from 3 independent experiments and the data is presented as the percentage of the untreated control. Statistical analysis was performed using a one-way ANOVA with Tukey post-hoc testing and all values were compared to the lipid-only control to identify any significant changes across all 3 cell models. Significance was set at $p < 0.05$.

Appendix Q. Densitometry analysis for CD44 isoform expression and RHAMM in

Tam-R and Fas-R cells treated with CD44v6 siRNA

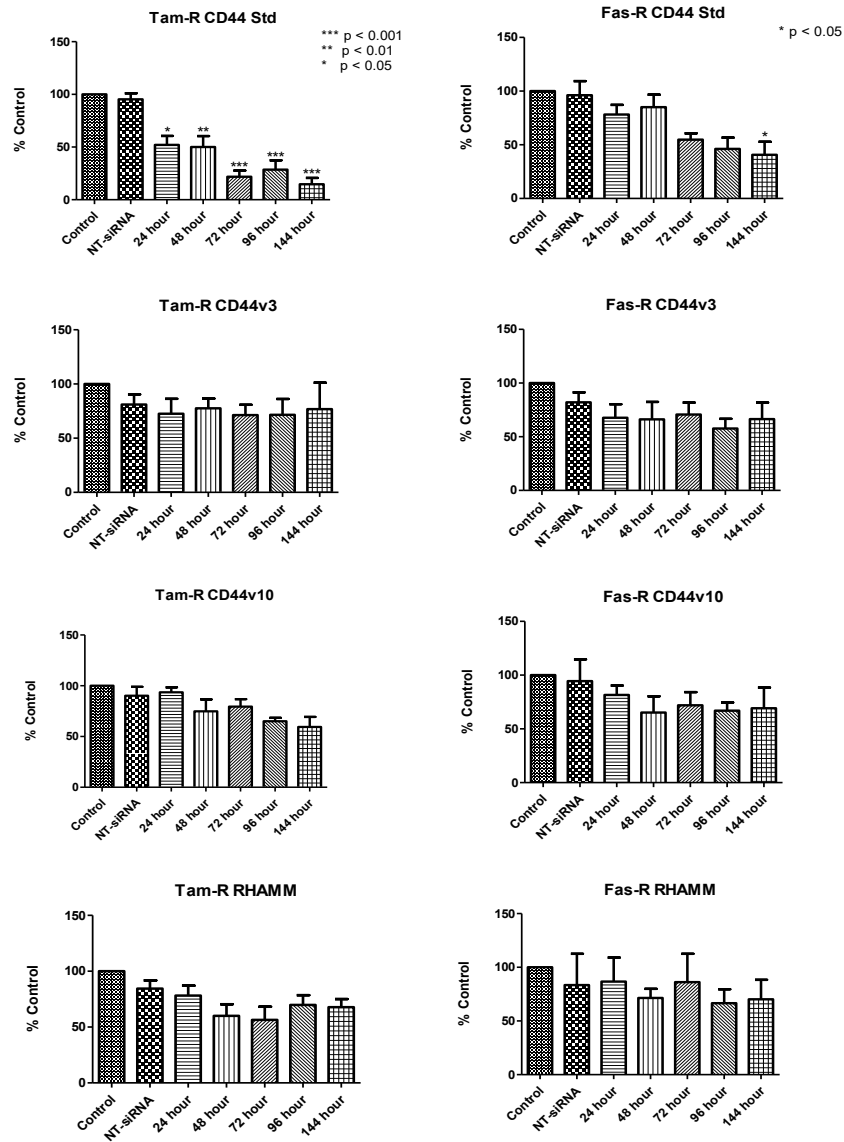


Figure 9.14. Densitometry graphs showing CD44v3, CD44v6, CD44v10 and RHAMM expression in Tam-R and Fas-R cells after 24 – 144 hour treatment with CD44v6 siRNA, before cell lysis and detection by Western blotting analysis. The data shows the total protein levels in the cell lines normalised to GAPDH. Error bars represent the average normalised data \pm SEM from 3 independent experiments and the data is presented as the percentage of the untreated control. Statistical analysis was performed using a one-way ANOVA with Tukey post-hoc testing and all values were compared to the NT-siRNA control to identify any significant changes across all 3 cell models. Significance was set at $p < 0.05$.

Appendix R. Immunohistochemical analysis of CD44v6 expression in clinical breast cancer

This technique and quantitation analysis was performed by the BCMPG research technician, Sue Kyme. Formalin-fixed paraffin-embedded tissue microarray sections (TMAs) (provided by Andrew Green, Nottingham University) were studied comprising 140 breast cancers from ER+ adjuvant tamoxifen patients with 20 year follow up. The study population was derived from the Nottingham Tenovus Primary Breast Cancer series of women aged 70 or less who presented with primary operable invasive breast carcinoma (with tumours less than 5 cm diameter on clinical/pre-operative measurement stage I and II) between 1986 – 1998 (Rec: C2020313) (Abd El-Rehim et al. 2005; Habashy et al. 2009). For immunohistochemical analysis, the TMA's were sectioned on a Microtome (3 – 5 microns) and dried at 37 °C overnight before being incubated at 60 °C for 20 minutes and allowed to cool. TMA's were dewaxed and rehydrated by the following incubation steps: xylene (2 x 7 minutes), 100 % ethanol (2 x 2 minutes), 90 % ethanol (2 x 2 minutes), 70 % ethanol (2 x 2 minutes) and distilled water (1 x 5 minutes). A 3 % aqueous solution of hydrogen peroxide was then applied to the sections for 5 minutes to eliminate endogenous peroxidases before being washed in distilled water for 5 minutes. For antigen retrieval, TMA's were microwaved in 1 L 0.01 M Sodium Citrate buffer pH 6 for 30 minutes at Power level 6 (560 W) and cooled in running tap water for 5 minutes. TMA's were then blocked in 10 % normal human serum diluted in PBS for 10 minutes. Excess blocking reagent was then removed before the addition of the primary antibody CD44v6 (1/40 dilution in PBS, R&D Systems, UK)) for 2 hours at room temperature. Following

incubation TMA's were washed for 3 minutes in PBS and 2 x 5 minutes in 0.02 % PBS/Tween. Dako EnVision secondary antibody (Dako Envision+ system-HRP labelled polymer anti-mouse) was then applied to the TMA's for 90 minutes at room temperature. Following incubation TMA's underwent a 2 x 1 minute wash in PBS and 2 x 5 minute washes in 0.02 % PBS/Tween. Dako 2,3-diaminobenzidine (DAB)/substrate chromogen system solution was then applied to the TMA's for 10 minutes at room temperature and after incubation underwent 2 x 5 minute washes in distilled water. Counterstaining was performed by the addition of 1 % methyl green (diluted in distilled water) to the TMA's for 15 minutes followed by 3 x 2 minute washes in distilled water. TMA's were air dried before being mounted with coverslips using di-butylphthalatexylene (DPX) mountant (a mixture of Distyrene, a plasticizer, and xylene). The tumour epithelial cells in sections were assessed for staining level and localisation simultaneously by 2 observers blinded to the clinical data using a dual-viewing light microscope (Olympus BH-2) at x40 magnification. Plasma membrane percentage positivity and intensity were then assessed to derive a CD44v6 membrane H-score value for each TMA core (described in Materials and Methods section 2.7.1). Along with pathological parameters, EGFR and disease-free interval (DFI) and breast cancer-specific survival (OS) were available for analysis versus CD44v6 membrane expression in this endocrine treated series. The web-based algorithm X-tile was used to define optimal CD44v3/CD44v6 membrane cut point versus patient outcome. Mantel-cox (Log Rank) statistical analysis was employed using SPSS96.0 and performed by BCMPG statistician Lynne Farrow.

Appendix S. Construction of alternative transfection controls

In order to create an alternative transfection control to confirm that the effects observed by CD44 transfection into MCF-7 cells were due to the presence of the CD44 variant isoforms and not the transfection method, experiments at the end of this project were undertaken in an attempt to create an empty vector plasmid DNA backbone construct (without the inserted CD44 gene sequence). However, the DNA sequence of the plasmid vector was not provided by Dr Gunthert therefore the plasmid map alone (Appendix H) was utilised for this investigation. The map revealed that the inserted full length CD44 sequences into the vector backbone are flanked by the restriction enzymes EcoRI and BamHI, however, these restriction enzymes were not compatible to create sticky ends for re-ligation after restriction digest. Using the vector map alone, no compatible restriction enzymes for vector re-ligation could be identified and the plasmid vector was not commercially available. Therefore, due to time limitations, a BamHI restriction enzyme was used to cut the CD44v6 plasmid vector at two sites: (i) at the end of the multiple cloning site and (ii) at the beginning of the CD44 sequence (Appendix H). This led to the creation of a plasmid vector which contained the backbone and the first 273 bp's of the CD44 sequence, referred to as 'empty vector' (EV). Given that the CD44 constructs contained a GFP-tag fused to their carboxy-terminus end, it was also investigated whether the presence of the GFP protein altered cellular behaviours through transfection of MCF-7 cells with a pEGFP-N1 plasmid vector containing the GFP-tag construct only (referred to as GFP). The below sections show the methodology and results from these experiments.

DNA restriction endonuclease digest and electrophoresis detection

To create an empty vector for use as an alternative control for the plasmid DNA constructs, the plasmid containing the CD44v6 DNA sequence was digested using a BamHI restriction enzyme to cut the plasmid vector at two sites: (i) at the end of the MCS and (ii) at the beginning of the CD44 sequence. For a 2 µl double DNA digest reaction, to a sterile eppendorf was added: 5 µl 10X NEBuffer 3, 4 µl plasmid DNA (diluted in RNase-free water), 2 µl BamHI restriction enzyme and 39 µl sterile RNase-free water. The reaction was gently mixed by pipetting and allowed to incubate at 37 °C for 1.5 hours. To visualise the results of the DNA double digest reaction, the samples were electrophoresed on a 0.7 % agar gel (0.7 g agar, 100 ml 1X TAE buffer (20 ml 50X TAE buffer (242g Tris, 57.1 ml glacial acetic acid, 100 ml 0.5 EDTA, 1 L distilled water, pH 8.3) diluted in 1 L distilled water), 2 mg/ml crystal violet solution (diluted in sterile water)). The set agar gels were placed into a Mini-Sub Cell GT electrophoretic tank (Bio-Rad Laboratories Ltd, Hertfordshire, UK) filled with 1 X TAE buffer (ensuring no contamination with ethidium bromide). 5 µl hyperladder I was used as a marker. To 9 µl DNA digest reaction was added 5 µl loading buffer (4 g sucrose, crystal violet, 10 ml distilled water) and pipetted into the wells of the agar gel. The electrophoresis reaction was allowed to run for 4 hours at 75 volts constant to ensure complete separation of differential sized digested DNA bands. The agar gel was then removed from the tank and transferred onto a light box where DNA bands intercalated with crystal violet could be viewed. The desired DNA fragment (containing the vector DNA backbone) was excised from the agarose gel using a sterile razor blade (ensuring as little agarose gel transfer as possible) and placed into

a sterile microfuge tube. The microfuge tube was weighed before and after the addition of the DNA/agarose fragment to determine its weight.

Gel extraction and purification

The excised DNA/agarose sample then underwent gel extraction and purification using a QIAquick Gel Extraction Kit (QIAGEN Ltd, Manchester, UK), all equipment and reagents used for this process were contained within the kit upon purchase. Table 3.12 lists all reagents used with their corresponding composition, storage temperature and function. Once the weight of the DNA/agarose fragment was determined, 3 volumes of Buffer QG was added to 1 volume of gel fragment (100 mg = 100 μ l) and incubated in a hot plate (Techne DRI-Block DB.2, Bibby Scientific Limited, Staffordshire, UK) at 50 °C for 10 minutes. During this incubation period, the sample was removed from the hot plate every 2 minutes and briefly vortexed to ensure the agarose gel was completely dissolved into the solution. After incubation, 1 gel volume of isopropanol was added to the sample (100 mg = 100 μ l) and mixed. A QIAquick spin column was then placed into a 2 ml collection tube and the sample was applied to the column and spun in a centrifuge (Labofuge 400R centrifuge, Heraeus, Germany) for 1 minute (room temperature, 13,000 rpm). The flow-through was then discarded and 0.5 ml Buffer QG was added to the column and centrifuged again for 1 minute (room temperature, 13,000 rpm). The column was then washed by addition of 0.75 ml Buffer PE and centrifuged for 1 minute (room temperature, 13,000 rpm). The flow-through was discarded and the centrifugation step was repeated (1 minute, room temperature, 13,000 rpm). For DNA elution, the column was then placed into a sterile 1.5 ml microcentrifuge tube and 30 μ l Buffer EB was

added to the centre of the column (directly applied to the membrane) and incubated at room temperature for 1 minute. The column was then centrifuged for 1 minute (room temperature, 13,000 rpm). DNA concentration was determined using a Nanodrop™ 2000/2000c spectrophotometer (Thermo Scientific, UK). The DNA programme was selected on the spectrophotometer and 2 µl TE buffer was measured twice as a blank. 2 µl of DNA sample was added to the spectrophotometer and measured in ng/µl, the spectrophotometer was then cleaned and the process was repeated for each sample. DNA samples were stored at - 20 °C.

Component	Composition	Storage °C	Function
Buffer QC	5 mM guanide thiocyanate (GuSCN) 20 mM Tris HCl pH 6.6	15 – 25	Solubilisation of agarose gel pH indicator
Buffer PE	10 mM Tris-HCl pH 7.5 80 % ethanol	15 – 25	Washing agent (removes excess salt from the membrane)
Buffer EB	10 mM Tris Cl, pH 8.5	15 – 25	Elution buffer
Isopropanol	100 %	15 – 25	DNA precipitation

Table 9.6. A list of the components purchased with the QIAquick Gel Extraction kit (QIAGEN, Manchester, UK) detailing their composition, storage temperature and function.

Vector DNA ligation

For a 20 µl DNA ligation reaction, a sterile microcentrifuge tube was placed on ice and to this was added: 2 µl 10X T4 DNA ligase buffer (thawed and resuspended at room temperature), 50 ng vector DNA, 1 µl T4 DNA ligase (added last to the reaction) and made up to a volume of 20 µl by addition of sterile RNase free water. The reaction was gently mixed by pipetting, briefly microfuged and incubated at room temperature for 10 minutes. The samples were then heat inactivated at 65 °C for 10 minutes in a hot plate (Techne DRI-Block DB.2, Bibby Scientific Limited, Staffordshire,

UK) before being chilled on ice and stored at -20 °C. To visualise the results and determine the success of the DNA ligation reaction, the samples were electrophoresed on a 1.2 % agar gel (1.2 g agar, 100 ml 1X TAE buffer, 1 µl ethidium bromide) as previously described. The samples were then stored at -20 °C.

Transformation of plasmid constructs and transfection into MCF-7 cells

The transformation of the plasmids were carried out following the protocol described in Materials and Methods 12.3.2. The EV was then sent to the CBS for sequencing using the T7 promoter (see Material and Methods 2.12.4) and analysed using the online Chromas Lite DNA sequencing software programme and ExPASy protein translation tool and the results are shown below. The transfection procedure was undertaken as described in Materials and Methods 2.12.5 using 100 ng of EV and GFP plasmid DNA.

Empty vector plasmid DNA gene sequence

Vector

CD44 plasmid sequence

CD44 original sequence

```
          atggacaagttttggtggcacgcagcctggggactctgcctcgtgccgctgagcctggcg
gggtgtcccccgccatggtcaagttttggtggcacgcagcctggggactctgcctcgtgccgctgagcctggcg
cagatcgatttgaatataaacctgccgctttgcaggtgtattccacgtggagaaaaatggtcgctacagcatctct
cagatcgatttgaatataaacctgccgctttgcaggtgtattccacgtggagaaaaatggtcgctacagcatctct
cggacggaggccgctgacctctgcaaggctttcaatagcaccttgcccacaatggcccagatggagaaagctctg
cggacggaggccgctgacctctgcaaggctttcaatagcaccttgcccacaatggcccagatggagaaagctctg
agcatcggatttgagacctgcaggtatgggttcatagaagggcacgtggtgattccccgatcttattaagcag
agcatcggatttgagacctgcaggtatgggttcatagaagggcacgtggtgattccccgatc
gaacttgtttattgcagcttataatggttacaataaagcaatagcatcacaatttccacaataaagcattttt
ttcactgcattctagttgtggtttgtccaaactcatcaatgtatcttatcatgtctggtcgagcaggtggcactt
ttcggggaaatgtgctgagcgaacccctatttgtttatttttctaaatacattcaaatatgtatccgctcatgagac
aataaccctgataaatgcttcaataatattgaaaaaggaagagtatgagtattcaacatttccgctgctgcacctta
ttcccttttttgcggcattttgccttctctgttttgtcaccagaaaacgctggtgaaagtaaaagatgctgaag
atcagttgggtgcacgagtggtttacatcgaactggatctcaacagcggtaagatccttgagagttttcgccccg
aagaacgttttccaatgatgagcacttttaagttctgctatgtggcgcggtattatcccgatttgacgccccggc
aagagcaactcggctgcccatacactattctcagaatgacttgggttgagtactcaccagtcacagaaaagcat
cttacggatgggcatgacagtaaggagattatgcagtgtgcccataaccatgatgatacactgctcaacctaa
ctttctgacacggatcgggaggaaccgaaaaag
```

DNA to protein translation

```
MDKFWWHAAWGLCLVPLSLAQIDLNITCRFAGVFHVEKNGRYSISRTEAADLCKAFNSTL
MDKFWWHAAWGLCLVPLSLAQIDLNITCRFAGVFHVEKNGRYSISRTEAADLCKAFNSTL
PTMAQMEKALSIGFETCRYGFIEGHVVI PRIHPNSICAAANTGVYILTSNTS QYD TYCFN
PTMAQMEKALSIGFETCRYGFIEGHVVI PRI
ASAPPEEDCTSVTDLPNAFDGPITITIVNRDGTTRYVQKGEYRTNPEDIYPSNPTDDDVS
GSSSERSSTSGGYIFYTFSTVHPIPEDSPWITDSTDRI PATIQATPSSTEETATQKEQW
FGNRWHEGYRQTPKEDSHSTTGTAGDQDTFHPSGGSTTHGSESDGHS HGSQEGGANTTSG
PIRTPQIPEWLIILASLLALALILAVCIAVNSRRRCGQKKKLVINSNGAVEDRKPSGLN
GEASKSQEMVHLVNKESSETPDQFMTADETRNLQNVD MKIGV Stop
```

Figure 9.15. The DNA sequencing results as performed by the CBS and analysed using the software programmes Chromas Lite and ExPASy for the Empty Vector plasmid construct. The CD44 DNA sequence (1 – 273 bp) and protein (1 – 91 amino acids) expressed in this vector are highlighted in red (plasmid DNA sequence) and black (original DNA sequence).

Plasmid map for the pEGFP-N1 vector

pEGFP-N1 Vector Information
GenBank Accession #U55762

PT3027-5
Catalog #6085-1

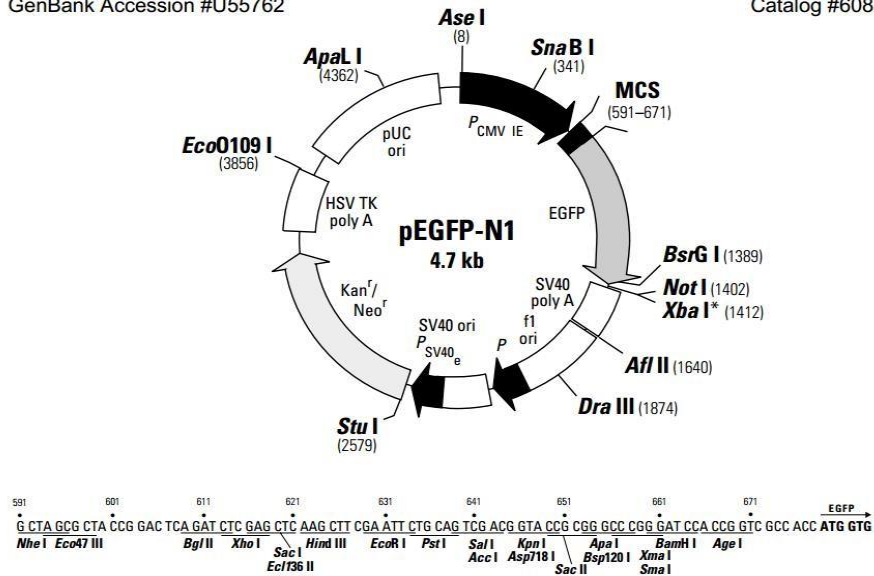


Figure 9.16. A map of the pEGFP-N1 vector used for transfection of MCF-7 cells in this project.

Transfection of MCF-7 cells with EV and GFP plasmid constructs

Western blotting analysis revealed that transfection of EV or GFP constructs into MCF-7 cells did not alter CD44 isoform or RHAMM expression between 24 – 72 hours post-transfection compared to lipid-treated control cells, however a modest reduction in CD44v10 expression was observed (Figure 9.11). Immunofluorescence analysis was further used to determine transfection efficiency and analyse CD44 expression and localisation in MCF-7 cells transfected with the EV or GFP constructs; with CD44v6 used as a positive transfection control. Results revealed that GFP constructs were transfected into MCF-7 cells at a similar efficiency to the CD44v6 constructs and did not alter total CD44 expression level or localisation in these cells

compared to the lipid-treated control (Figure 9.12). However transfection of the EV construct appeared to modestly enhance total CD44 expression at the cell surface compared to the untreated and lipid-treated control cells (Figure 9.12).

To investigate whether transfection of these constructs altered cellular signalling activities in MCF-7 cells, EGFR and ERK1/2 activity was assessed, as these signalling components were modulated upon transfection of these cells with the CD44v3 and CD44v6 plasmid constructs. The results revealed that transfection of the GFP plasmid into MCF-7 cells did not alter EGFR activity, however transfection of the EV plasmid reduced EGFR activity, compared to the lipid-treated cells (Figure 9.13) and CD44v6 enhanced EGFR expression as previously observed in Chapter 6. Transfection of both EV and GFP constructs led to a modest increase in ERK1/2 activity compared to the lipid-treated control cells, however this was less than compared to cells transfected with CD44v6 (Figure 9.13).

To analyse the effect of these constructs upon MCF-7 cell function, endogenous and HA-stimulated (100 µg/ml) cellular migration was assessed. The results revealed that transfection of MCF-7 cells with EV and GFP constructs led to a small reduction in endogenous and HA-stimulated migration compared to the lipid-only treated control cells, however this effect was not significant (Figure 9.14). Whilst these preliminary data require further validation, these experiments suggest that transfection of the vector backbone and GFP-tag into MCF-7 cells does not significantly alter cell function, thus supporting that the effects observed from CD44v3/CD44v6 transfection arise from the activities of these proteins alone. Future experimentation

is required to create a plasmid vector backbone without the CD44 sequence to confirm these observations.

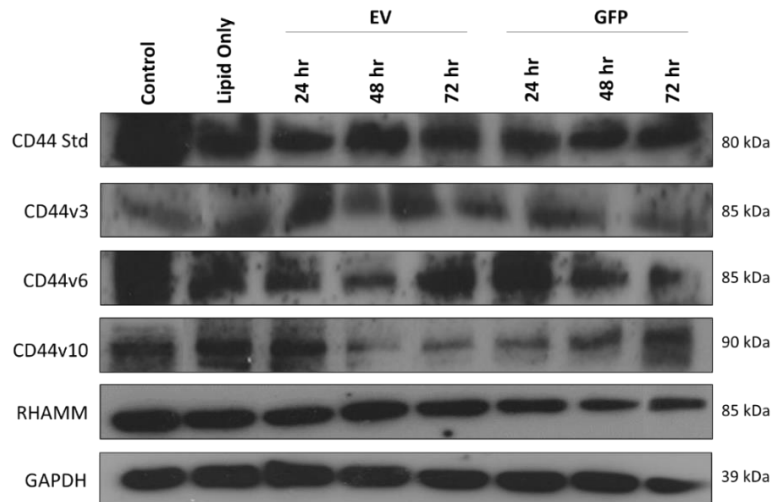


Figure 9.17. Western blot images showing CD44 isoform and RHAMM expression in MCF-7 cells after 24 - 72 hour transfection with the EV or GFP plasmid DNA compared to the untreated and lipid-only treated control (n=1). GAPDH was used as a loading control.

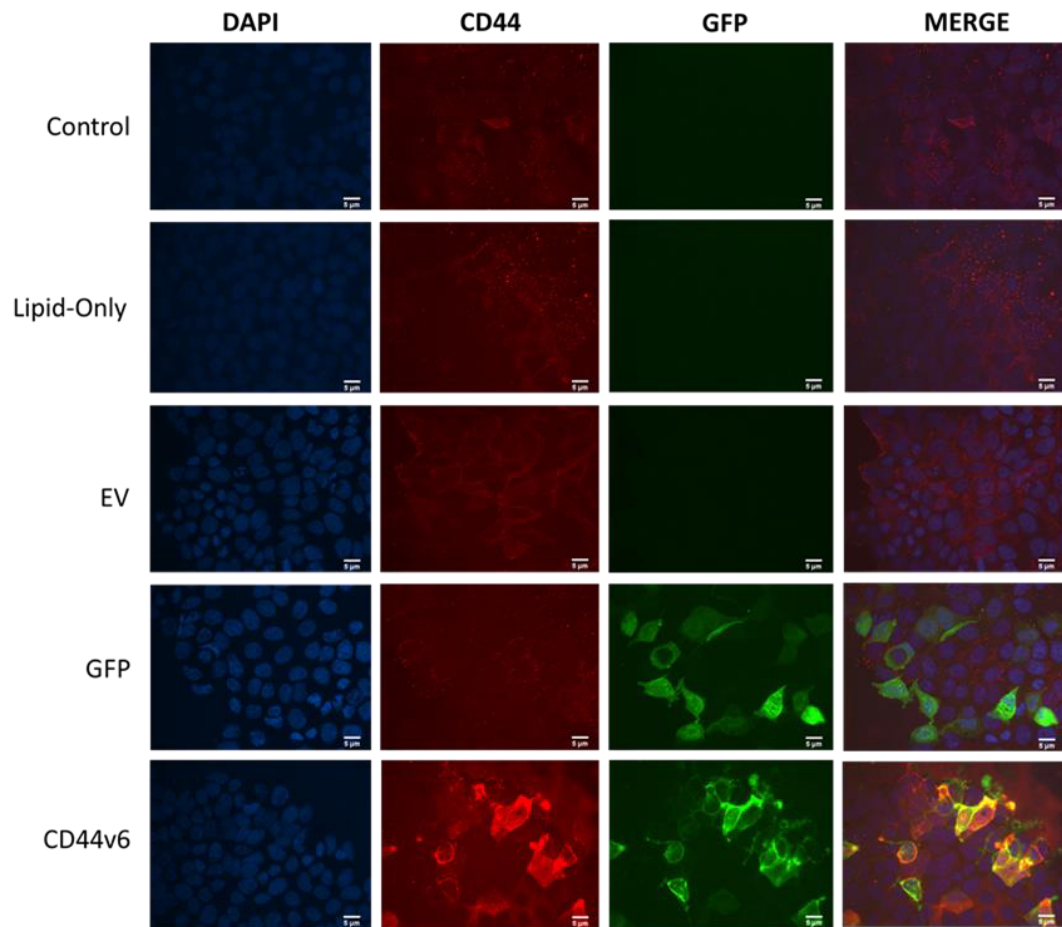


Figure 9.18. Immunofluorescence images showing CD44 Std expression in MCF-7 cells after 72 hour transfection with the EV, GFP or CD44v6 plasmid DNA compared to the untreated and lipid-only treated control (x63 magnification) (n=1).

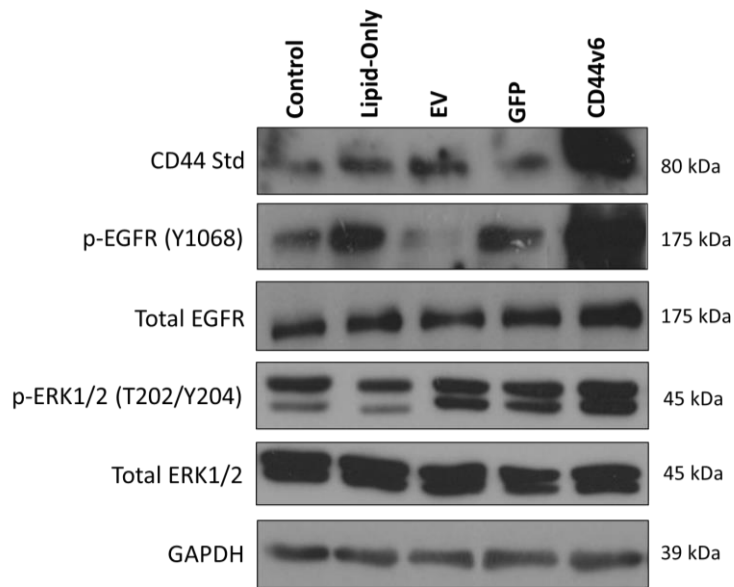


Figure 9.19. Western blotting images showing CD44 Std expression and EGFR and ERK1/2 activation in MCF-7 cells after 72 hour transfection with the EV, GFP or CD44v6 plasmid DNA compared to the untreated and lipid-only treated control. Total protein level was unaltered and GAPDH was used as a loading control (n=1).

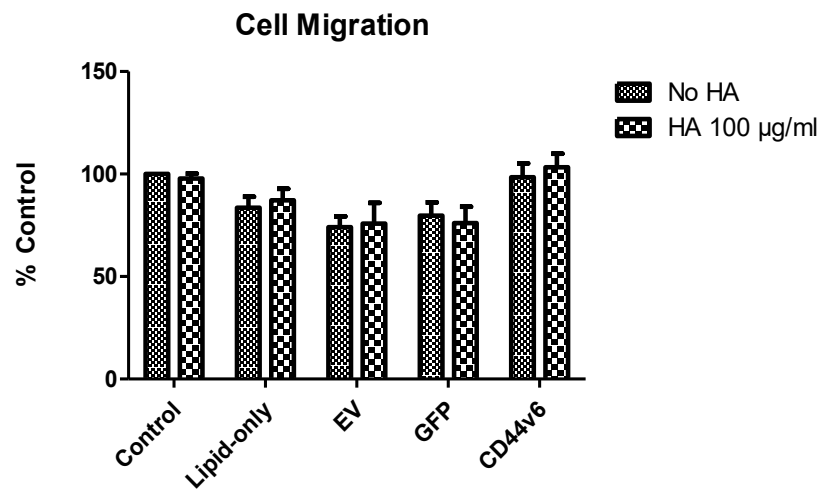


Figure 9.20. Measurement of endogenous and HA-stimulated cellular migration in MCF-7 cells transfected with EV, GFP or CD44v6 plasmid DNA. MCF-7 cells were transfected with the EV, GFP and CD44v6 plasmid DNA for 48 hours prior to the assessment of cellular migration (Boyden Chamber assay) in the presence (100 µg/ml) and absence of HA (n = 3). Error bars represent standard error of the means and statistical testing was performed using a one-way ANOVA and significance was set at p < 0.05.

Appendix T. The effect of endocrine treatment upon CD44 expression in MCF-7

cells

To investigate whether a relationship exists between CD44 and ER, MCF-7 cells were treated with endocrine agents and the effect upon CD44 expression was investigated. Heatmap analysis (generated by Affymetrix analysis, see Materials and methods 2.3) revealed that the majority of gene probes corresponding to CD44 showed enhanced gene expression in MCF-7 cells treated with oestradiol and tamoxifen for 10 days, however 10 day fulvestrant treatment reduced CD44 gene expression compared to the untreated control cells. Furthermore, Western blotting analysis revealed that CD44 Std expression became enhanced in MCF-7 cells upon 3 – 52 day tamoxifen and oestradiol treatment, whilst fulvestrant treatment abrogated CD44 expression during this exposure time, compared to the untreated control cells.

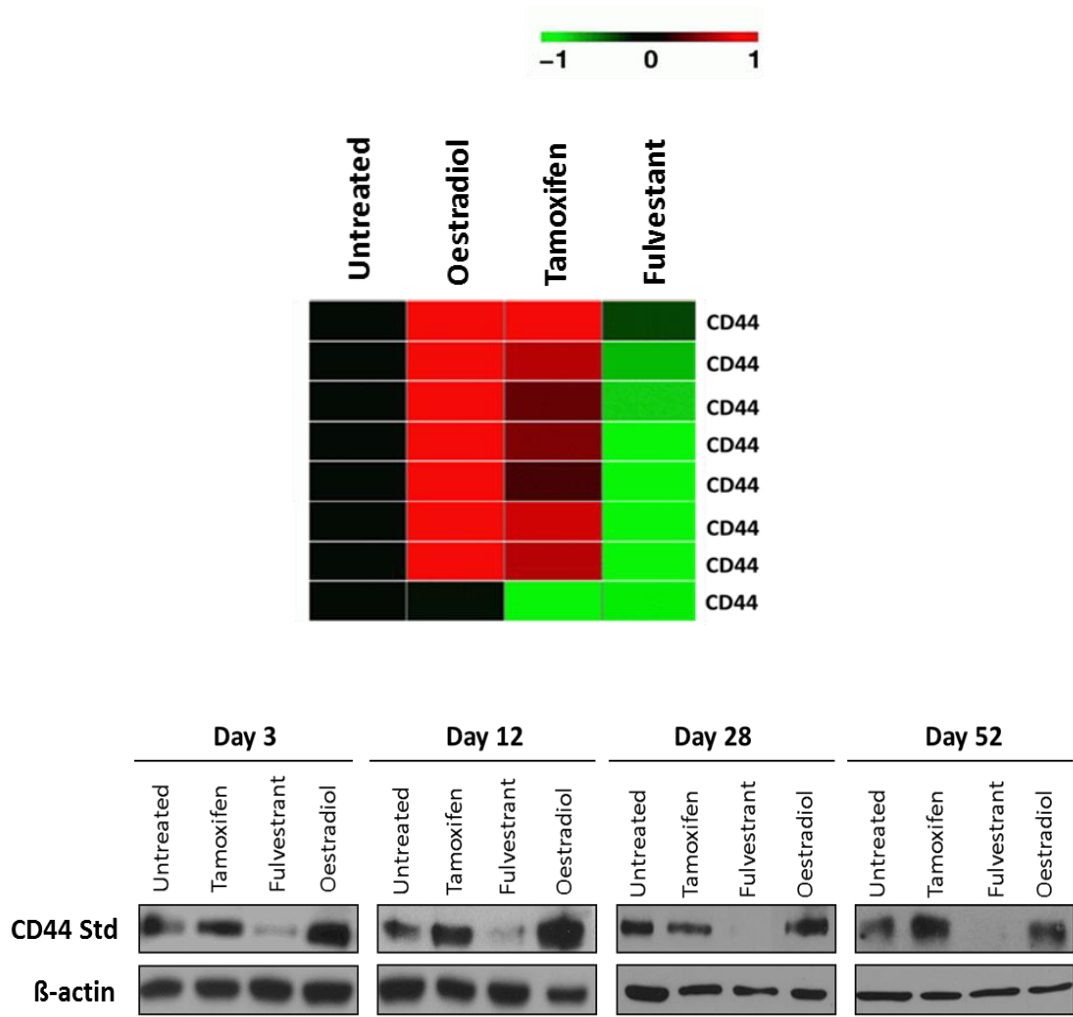


Figure 9.21. Effect of short-term endocrine treatment upon CD44 expression in MCF-7 cells. A heatmap profile was generated by AffymetrixU-133A gene microarray analysis from 3 independent experiments to show CD44 gene expression after 10 day exposure to tamoxifen (100 nM), fulvestrant (100 nM) and oestradiol (1 nM) in MCF-7 cells compared to the untreated control cells. Representative Western blotting images from 3 independent experiments showing CD44 Std expression in MCF-7 cells after exposure to tamoxifen (100 nM), fulvestrant (100 nM) and oestradiol (1 nM) between 3 – 52 days. β -actin was used as a loading control.